

# KC-135 Winglet Program Review

**FOR EARLY DOMESTIC DISSEMINATION**

Because of its significant early commercial potential, this information, which has been developed under a U.S. Government program, is being disseminated within the United States in advance of general publication. This information may be duplicated and used by the recipient with the express limitation that it not be published. Release of this information to other domestic parties by the recipient shall be made subject to these limitations.

Foreign release may be made only with prior NASA approval and appropriate export licenses. This legend shall be marked on any reproduction of this information in whole or in part.

Review for general release

January 31, 1984

*Proceedings of a symposium  
held at Dryden Flight Research Center  
Edwards, California  
September 16, 1981*

**NASA**

*NASA Conference Publication 2211*

# KC-135 Winglet Program Review

Proceedings of a symposium  
held at Dryden Flight Research Center  
Edwards, California  
September 16, 1981

**NASA**

National Aeronautics  
and Space Administration

**Scientific and Technical  
Information Branch**

1982



## PREFACE

A review of the results of a joint NASA/USAF program to develop and flight test winglets on a KC-135 aircraft was held at the Dryden Flight Research Center on September 16, 1981. This publication is a compilation of the results presented.

# CONTENTS

Preface . . . . .	iii	
1. KC-135 WINGLET PROGRAM OVERVIEW . . . . . Marvin R. Barber and David Selegan	1	✓✓
2. KC-135 WING AND WINGLET FLIGHT PRESSURE DISTRIBUTIONS, LOADS, AND WING DEFLECTION RESULTS WITH SOME WIND TUNNEL COMPARISONS . . . . . Lawrence Montoya, Peter Jacobs, Stuart Flechner, and Robert Sims	47	✓✓
3. IN-FLIGHT LIFT AND DRAG MEASUREMENTS ON A FIRST GENERATION JET TRANSPORT EQUIPPED WITH WINGLETS . . . . . David P. Lux	103	✓✓
4. MEASUREMENTS OF THE FUEL MILEAGE OF A KC-135 AIRCRAFT WITH AND WITHOUT WINGLETS . . . . . Gary E. Temanson	117	✓✓
5. COMPARISON OF FLIGHT MEASURED, PREDICTED AND WIND TUNNEL MEASURED WINGLET CHARACTERISTICS ON A KC-135 AIRCRAFT . . . . . Robert O. Dodson, Jr.	145	✓✓
6. KC-135A WINGLET FLIGHT FLUTTER PROGRAM . . . . . Michael W. Kehoe	171	✓✓

## KC-135 WINGLET PROGRAM OVERVIEW

Marvin R. Barber\* and David Selegan\*\*

### SUMMARY

A joint NASA/USAF program was conducted to accomplish the following objectives:

1. Evaluate the benefits that could be achieved from the application of winglets to KC-135 aircraft.
2. Determine the ability of wind tunnel tests and analytical analysis to predict winglet characteristics.

The program included wind-tunnel development of a test winglet configuration; analytical predictions of the changes to the aircraft resulting from the application of the test winglet; and finally, flight tests of the developed configuration.

Pressure distribution, loads, stability and control, buffet, fuel mileage, and flutter data were obtained to fulfill the objectives of the program.

### INTRODUCTION

This paper provides an overview of a joint NASA/USAF effort that resulted in full-scale flight tests of winglets on a KC-135 aircraft. Winglet evolution is traced from concept, through wind-tunnel testing and full-scale flight tests.

The details of the flight tests are emphasized in this paper and serve as an introduction for the flight test result papers that follow in this proceeding.

### SYMBOLS

L	Lift Force - lbs
D	Drag Force - lbs
W	Gross Weight - lbs
$\delta$	Ambient Pressure in Standard Atmospheres
M	Mach Number
hp	Pressure Altitude - ft.
$C_t$	Wing Tip Chord
CRT	Cathode Ray Tube

---

\*NASA Dryden Flight Research Center

\*\*USAF Wright Aeronautical Laboratory

NRT

Normal Rated Thrust

Keas

Knots Equivalent Airspeed - knots

## CONCEPT

Winglets are small, nearly vertical aerodynamic surfaces which are designed to be mounted at the tips of aircraft wings (see figure 1). Winglets are designed with the same careful attention to airfoil shape and local flow conditions as the wing itself. The primary component of the winglet configurations is a large winglet mounted rearward above the wing tip. The "upper surface" of this airfoil is the inboard surface. For some configurations an additional small winglet, mounted forward, below the wing tip, is necessary. The "upper surface" of the airfoil for this lower winglet is the outboard surface.

The winglets operate in the circulation field around the wing tip. Because of the pressure differential between the wing surfaces at the tip, the air flow tends to move outboard along the wing lower surface, around the tip, and inboard along the wing upper surface. This wing-tip vortex produces cross flows at each winglet. Thus the winglets produce large side forces even at low aircraft angles of attack. Since the side force vectors are approximately perpendicular to the local flow, the side forces produced by the winglets have forward (thrust) components (figure 1) which reduce the aircraft induced drag. This is the same principle that enables a sailboat to travel upwind by tacking. For winglets to be fully effective the side forces must be produced as efficiently as possible; therefore, advanced aerodynamic airfoil shapes are used. The side force produced by the winglets, and therefore the thrust produced, is dependent upon the strength of the circulation around the wing tip. Since the circulation strength is a function of the lift loads near the wing tip, winglets are more effective on those aircraft with higher wing loads near the tip.

The near vertical mounting of the winglets enables them to provide their thrust with very little increase in wing root bending. This can be an important design or retrofit consideration.

Theoretical calculations indicate that the aerodynamic benefit would be the same for a given size winglet in either the upper or lower position. However, ground clearance of low-wing jet transports limits the span of the lower winglet, and interference with the upper winglet flow limits the chord length of the lower winglet. Thus, from a practical standpoint for low-wing aircraft, the lower winglet must be relatively small. As a result, for the jet transports being discussed herein, the contributions of the lower winglet to the reduction of drag were relatively small.

As indicated in figure 1, the winglets tend to straighten the air flow thus slightly reducing the wing-tip vortex strength. However, the trailing vortex hazard still exists. The reduction is an indication of an increase in the aircraft efficiency. Winglets are not designed to improve flight safety for trailing aircraft, but to increase aerodynamic efficiency.

## FLIGHT PROGRAM DEVELOPMENT

### Program Inception and Motivation

The concept of winglets to reduce aircraft drag was developed by NASA/Langley. An empirical investigation of winglets on a DC-10 model was conducted in the NASA/Langley 8-foot transonic tunnel. Results of the investigation indicated a decrease in induced drag of about 15 percent and an overall drag decrease of about 5 percent. These preliminary results and fuel conservation interests were the motivation for application to military vehicles. Subsequently, a Boeing Company analysis of the effects of winglets on the 747 was correlated with wind tunnel data and indicated a drag reduction of approximately 4 percent on the full-scale 747 aircraft.

Based on these early results, a Memorandum of Understanding (MOU) for a joint USAF/NASA Winglet Development Program was developed. Under this MOU, NASA LaRC and the Flight Dynamics Laboratory coordinated the development of a wind tunnel data base relative to the application of winglets to selected Air Force aircraft.

The Boeing Company, under contract to the Air Force, performed an analytical investigation of winglet concepts for the KC-135 and C-141 aircraft and for the purpose of recommending winglet configurations. The analysis addressed the effect of winglets on vehicle aerodynamic characteristics and wing root bending moments. The feasibility of winglets on KC-135 aircraft and wing tip winglets interface moments were also addressed. This effort was supported by NASA/LaRC through wind tunnel tests of selected configurations.

Wind tunnel tests of a NASA/Langley constructed semi-span KC-135 model with winglets were conducted in the NASA/Langley 8-foot transonic tunnel. Results of these tests indicated an 8 percent total drag reduction at cruise flight conditions ( $M = 0.78$ ,  $h_p = 35,000$  ft.).

Subsequently, a full span KC-135 model with winglets was tested in the NASA/LaRC 8 foot transonic tunnel, indicating drag reductions of 6 percent at cruise. This series included off-nominal conditions. Low speed investigations of the winglets effects on the KC-135 with various flap and aileron configurations were completed during the months of July and August 1976.

The results of the wind tunnel tests and analytical studies are reported in references 1 through 11. In summary, these studies indicate that winglets would reduce KC-135 aircraft drag by 6 to 8 percent. This reduction translated into approximately 37 million gallons of fuel saved per year for the KC-135 fleet.

Based on these results, and the high priority fuel conservation effort within the United States in this time period, the Air Force initiated an Advanced Development Program to build and flight test a set of winglets on a KC-135 aircraft. NASA was eager to participate in a flight test program to obtain full-scale lift and drag data for comparison with the wind tunnel results. Reynolds number effects on the winglets aerodynamic performance was the primary concern in initiating flight and wind tunnel data comparisons. Both agencies objectives, though different, were compatible to a joint program and were formalized in another Memorandum of Understanding that formulated a flight program.

Obviously, both the USAF and NASA were interested in obtaining as much information as possible from the flight program. However, the specific data interests of each organization were slanted differently in some areas. A breakdown of the primary interest of each organization is provided in table I.

The responsibilities of the organizations participating in the joint program are defined in figure 2. The program was under the overall management of the Flight Dynamics Laboratory. They provided the test aircraft, a serviceable set of outer wing panels, and were technically and financially responsible for contracting with the Boeing Military Airplane Company for the design, fabrication and ground test of a set of winglets and modified outer wing panels.

NASA/Dryden was responsible for the flight phase of the program. They instrumented the aircraft, and provided funds, manpower and facilities required for this portion of the program.

The Air Force Flight Test Center provided flight crew and engineering support to the flight test program. They were also responsible for all flight flutter testing and were the onsite Air Force representative during flight testing.

NASA/Langley provided facilities, personnel, and data processing as required to support the winglet wind tunnel tests. They also provided technical support in the design of the flight winglet.

Boeing Military Airplane Company accomplished the design, fabrication, and ground testing of the winglets and provided onsite engineering support during the flight test phase.

The original flight program milestones are shown in figure 3. A contract was awarded to The Boeing Military Airplane Company, Wichita, Kansas, in September 1977. The effort included the design, fabrication and ground testing of a set of winglets and the modification of the outer wing panels to accept the winglets. Preliminary and final design reviews were held at Boeing in February and June 1978, respectively.

In conjunction with the design effort, a low speed flutter test was conducted in January 1978 in the Convair wind tunnel in San Diego. The test results are reported in reference 11. Also in support of the design effort, a limited amount of force and moment and pressure data was obtained in NASA/Langley facilities.

Prior to delivery of the winglets to NASA, Boeing conducted a ground vibration and proof load test on the outer wing panel and winglet. Included in the proof load test was a loads calibration test wherein 12 point loads were applied to the wing.

The winglets and outer wing panels were delivered to NASA/Dryden in May 1979. The outer wing panels were installed by NASA and instrument checkout was completed in July 1979. The first winglet flight was made 24 July 1979. The flight test program was interrupted several times for maintenance problems with the test aircraft. These problems are discussed later in the paper.

## Winglet Design and Construction

The winglet geometry was specified by the Government and conformed to Dr. Whitcomb's design criteria as shown in figure 4. The winglet airfoil was a general purpose airfoil and the same airfoil section was used from root to tip. No twist distribution was incorporated into the design. Airfoil coordinates are listed in table II.

The design philosophy was to provide a winglet and outboard wing modification for a flight research program and not oriented to production. The design included the capability to vary the winglet incidence and cant angle on the ground as illustrated in figure 5. A two-spar design was selected for the winglet. This design allowed for a positive positioning of the winglets using fittings with a total of four shear pins per side. The seven different cant/incidence combinations could be obtained by inserting bolts through designated holes in the fittings. Gap cover fairings were provided to assure aerodynamic sealing and smoothness for each setting. The structural arrangement is shown in figure 6.

A new internal structure was designed for the wing tip to transmit the loads from the winglet to the outboard wing. The principal load carrying paths were from the front spar of the winglet to the rear spar of the outboard wing and from the rear spar of the winglet to the outboard wing auxiliary spar. A thin doubler was added to the outboard portion of the outboard wing to prevent skin "oilcanning" in the fuel tank area. All areas were smoothed with aerodynamic sealer and/or fiber glass to maintain smooth contours on the wing and winglet (see figure 7).

The design also included provisions for total removal of the winglet so that baseline airplane data could be obtained. A new tip cap was manufactured for use in baseline testing.

The winglet skin was supported by ribs, placed at 10-inch intervals, from the front spar to the winglet trailing edge. The leading edge was manufactured by nesting two 0.050-inch thick skins bonded together with close out ribs at the winglet tip and root. This approach allowed for minimum tooling since the spars and ribs could be manufactured using numeric control procedures. This approach did require that all loads from the winglet be transferred to the wing tip through the fittings (no loads in skin at the winglet root). It was decided that skin "oilcanning" would be allowed at the limit load, with no "oilcanning" below 50 percent of limit load, which should have provided smooth airfoil contours during testing. The design was verified by proof load testing during which "oilcanning" of the skin was noted between 60 and 80 percent of limit load. Pillowing of the skins during flight testing was found. The pillowing was the result of a combination of the inboard pressure loading on the surface and the compressive loads in the skin. The inboard pressure loads were not considered in the design, nor were they simulated during the proof load testing. Because of pillowing, corrections were required to the aerodynamic drag; however, there was no concern from a loads standpoint as the spars were designed to carry the total load.



## Test Airplane

The airplane assigned to the flight test program was a very early model of the KC-135A which had been used for other than normal tanker missions (e.g., zero "g" training missions for the astronauts). It had not received the lower wing reskin (a fleet modification on KC-135 aircraft designed to extend the fatigue life of high time or highly stressed airplanes), and due to its relatively high and unusual usage, the Air Force determined that the airplane should be restricted per the criteria for high time airplanes without the reskin modification. This restriction did not appreciably impact the flutter or performance testing, but did require that all loads data be gathered within a constrained envelope, rather than testing at the limits of the V-n envelope.

To reduce concerns that arose from the lack of a lower wing reskin, splice plates were installed at the airplane's wing root. These splice plates are a standard USAF modification designed to extend an airplane's fatigue life until a lower wing reskin can be accomplished.

A photograph of the test airplane with the flight test nose boom installed is provided in figure 8.

## Instrumentation

A broad description of the instrumentation that was used for the various types of measurements that were made (i.e., drag, fuel mileage, loads, etc.) is provided in table III. A detailed definition of all the parameters that were measured as of the last flight is provided in the instrumentation line-up in appendix A. A noseboom was installed for the air data measurements. The boom is evident in figure 8 and the details of its head are shown in figure 9. Longitudinal and normal accelerometers were attached to the angle-of-attack vane to provide a measure of flight path acceleration.

A digital pulse code modulated data acquisition unit with a multiplexing capability was used to acquire the flight data. In its design configuration the data system provided a telemetry capability to Dryden and Air Force Flight Test Center ground stations for real-time data analysis, and an onboard recording capability as a backup in case of telemetry losses. This configuration was acceptable for the flutter testing but proved unacceptable for the performance testing. Tying the performance tests to the Edwards airspace complex in order to allow telemetry to the ground station resulted in constrained flight rates dependent on local weather and ground station scheduling conflicts, and constrained data gathering capability dependent on the length of the Edwards airspace complex. Therefore, after eight attempts to gather performance data via telemetry to the ground based station, the data system was modified to provide an onboard computational capability that enabled breaking the ground link.

A PDP-11 computer was installed on the airplane to provide the needed real-time calculations (i.e. W,  $W/\delta$ , M, and hp) for performance testing. A CRT and keyboard provided the display and programing capabilities for the computer. A simplified block diagram of the data system in final configuration is provided in figure 10.

## FLIGHT PROGRAM

### Test Plans

Initial planning laid out 35 flutter, performance, and envelope coverage flights to be conducted in the order of sequence specified in figure 11. Seven winglet configurations were to be tested in an attempt to define the configuration that would provide the best trade-off between winglet-induced performance gains and loads. The strategy was to clear the four configuration corners for flutter and thereby allow performance and envelope coverage flights for the remaining configurations without concern of flutter. The 15° can/4° incidence angle configuration included additional testing because it was the configuration at which wind-tunnel data had been obtained to evaluate stability and control characteristics and buffet boundaries.

A typical performance flight plan is shown in figure 12. Note that it includes not only performance maneuvers but loads and buffet boundaries as well. The scani-valve runs were to obtain pressure distribution data. A typical flutter flight plan is shown in figure 13. These plans nominally allowed for the coverage of two fuel configurations per flight. Envelope coverage flight plans included additional items as follows: roll response, minimum control speed, check climbs, check descents, missed approach characteristics, stability and control maneuvers, and 1g stall approaches.

Upon completion of the testing of the seven winglet configurations, it was planned to obtain data for a baseline configuration which was termed Modified Wing Tips (see figure 11). This terminology resulted from minor external modifications that were made to accommodate the winglet installation.

While the baseline tests were being conducted, it was planned that the USAF would have evaluated sufficient data from the seven winglet configuration tests to enable them to select a configuration that they would most desire to retrofit the KC-135 fleet with. That configuration then would be subjected to additional flutter and performance testing as well as envelope coverage tests.

### Test Accomplishments

Figure 14 presents a photograph of the test airplane with the winglets installed. A complete log of the test airplane's flight activity from the time it arrived at Dryden in December 1977 is provided in table IV. Flight crew checkout training was flown in the spring of 1978. Between May and September 1978, the aircraft was "laid up" while being instrumented. Upon completion of the instrumentation installation it was necessary to take the airplane to Tinker AFB, Oklahoma, for the installation of the wing root splice plates previously referred to. Some airspeed calibration and instrumentation checkout flying was accomplished prior to the delivery of the modified wing tips and winglets to Dryden in May 1979. The winglets were installed and the first winglet flight occurred on July 24, 1979. Per the plan laid out in figure 11, this winglet configuration was 15° cant angle/-2° incidence angle. This configuration required seven flights to complete rather than the planned four and uncovered a "pillowing" of the winglet skins as shown in figure 15. This "pillowing" caused sufficient concern, relative to its effect on the performance of the test

articles, and it was decided to deviate from the test plan and go to the 15° cant angle/-4° incidence angle configuration for the next tests. Wind tunnel, pressure distribution, and lift and drags measurements were available in the 15°/-4° configuration to provide some indication of the effect the pillowing might be causing. The 15°-4° tests were conducted and baseline tests (modified wing tips) immediately thereafter, still giving priority to the question of the effects of the "pillowing". Preliminary analysis indicated that the pillowing was having a small effect on the winglets' performance (approximately 10 percent of the expected gain) but was certainly not masking all of their expected benefit. (A detailed analysis of the winglet skin "pillowing", its causes and effects, is provided in reference 12.)

With the effects of the "pillowing" in hand, other considerations started driving the flight sequencing. The activity was behind schedule because of airplane fuel leaks and instrumentation problems. Therefore, it was decided to go to the 0° cant/-4° configuration and delete the 0°/-2° and 0°/-7.5° configurations. In testing this configuration, less than adequate structural damping occurred at airspeeds greater than the operational flight envelope speeds but less than the dive speeds. The low damping is discussed in detail in references 12 and 13. Also, while testing this configuration a large fuel leak developed that was the result of a crack in the front spar chord at the number 3 engine strut location. The crack in the spar chord has occurred on other airplanes and the source is a bad fatigue detail. Neither the fuel leaks nor the cracked spar cap were due to the installation of winglets. The repair of this wing spar required significant down time, January - July 1980. The need for the onboard computational capability discussed under Instrumentation had become evident and this down time was used to accomplish that modification.

Also during this down time the USAF selected the 15° cant/-4° incidence configuration as the best for fleet retrofit. This selection was primarily driven by the less than adequate structural damping that was found in the 0°/-4° configuration. The retrofit selection is discussed in reference 14.

Upon resuming flight testing in July 1980 the 0° cant/-4° incidence configuration was again checked for flutter to see if the cracked wing spar might have had some effect on that result. Verifying that the cracked wing spar had no effect, the 0°/-4° performance flights were resumed with the onboard computational capability.

During the spar crack repair downtime, a review of the performance data indicated that more data than planned for each configuration would be necessary to sufficiently define the winglet fuel mileage gains. Therefore, the performance data points in the plan were doubled in number. Scatter in the data resulting from weather disturbances was the prime driver of this conclusion. The remainder of the flight activity was devoted to obtaining the 0°/-4 baseline, and 15°/-4 performance data in acceptable quantity and quality as shown in table IV.

## CONCLUSIONS

A joint NASA/USAF program was conducted to accomplish the following objectives:

1. Evaluate the benefits that could be achieved from the application of winglets to KC-135 aircraft.
2. Determine the ability of wind tunnel tests and analytical analysis to predict winglet characteristics.

The program included wind-tunnel development of a test winglet configuration; analytical predictions of the changes to the aircraft resulting from the application of the test winglet; and finally, flight tests of the developed configuration.

The pressure distribution, loads, stability and control, buffet, fuel mileage, and flutter data produced fulfilled the objectives of the program.

#### REFERENCES

1. Whitcomb, Richard T.: A Design Approach and Selected Wind-Tunnel Results at High Subsonic Speeds for Wing-Tip Mounted Winglets. NASA TN D-8260, 1976.
2. Bartlett, Dennis W.; and Patterson, James C., Jr.: NASA Supercritical Wing Technology. CTOL Transport Technology - 1978, NASA CP-2036, Pt. II, 1978, pp. 533-552.
3. Ishimitsu, K. K.; VanDevender, N.; Dodson, R.: Design and Analysis of Winglets for Military Aircraft. USAF AFFDL Technical Report 76-6, 1976.
4. Jacobs, Peter F.; Flechner, Stuart G.; and Montoya, Lawrence C.: Effect of Winglets on a First-Generation Jet Transport Wing. I - Longitudinal Aero-dynamic Characteristics of a Semi-Span Model at Subsonic Speeds. NASA TN D-8473, 1977.
5. Ishimitsu, K. K.; Zanton, D. F.: Design and Analysis of Winglets for Military Aircraft; Phase II. USAF AFFDL Technical Report 77-23, 1977.
6. Montoya, Lawrence C.; Flechner, Stuart G.; and Jacobs, Peter F.: Effect of Winglets on a First-Generation Jet Transport Wing. II - Pressure and Spanwise Load Distributions for a Semi-Span Model at High Subsonic Speeds. NASA TN D-8474, 1977.
7. Montoya, Lawrence C.; Jacobs, Peter F.; and Flechner, Stuart G.: Effect of Winglets of a First-Generation Jet Transport Wing. III - Pressure and Spanwise Load Distributions for a Semi-Span Model at Mach 0.30. NASA TN D-8478, 1977.
8. Meyer, Robert R., Jr.: Effect of Winglets on a First-Generation Jet Transport Wing. IV - Stability Characteristics for a Full-Span Model at Mach 0.30. NASA TP-1119, 1978.
9. Jacobs, Peter F.: Effect of Winglets on a First-Generation Jet Transport Wing. V - Stability Characteristics of a Full-Span Wing with a Generalized Fuselage at High Subsonic Speeds. NASA TP-1163, 1978.

10. Flechner, Stuart G.: Effect of Winglets on a First-Generation Jet Transport Wing. VI - Stability Characteristics for a Full-Span Model at Subsonic Speeds. NASA TP-1330, 1979.
11. Schneider, F. C.; and Shoup, G. S.: "KC-135A Winglet Flutter Model Test", Boeing Document D3-11353-1, Boeing Wichita Company, Wichita, Kansas, May 5, 1978.
12. Dodson, R. O.; Ayala, J.; Shurtz, R. M.; and Temanson, G.: KC-135 Winglet Flight Research and Demonstration Program. AFWAL-TR-81-3115; July 1981.
13. Kehoe, Michael W.: KC-135A Winglet Flight Flutter Test Program. USAF, AFFTC-TR-81-4; June 1981.
14. Dodson, R. O.; Ayala, J.; Shurtz, R. M.; et al: KC-135 Winglet Flight Research and Demonstration Program - Trade Study Results. AFWAL-TR-81-3031; May 1981.

TABLE I. - PRIMARY FLIGHT DATA INTERESTS

Data	USAF	NASA
Lift and Drag		X
Fuel Mileage	X	
Loads	X	X
Flutter	X	
Stability and Control	X	
Buffet	X	
Handling Qualities	X	

TABLE II. - AIRFOIL COORDINATES FOR WINGLETS

x/c	z/c for -	
	Upper Surface	Lower Surface
0	0	0
.0020	.0077	-.0032
.0050	.0119	-.0041
.0125	.0179	-.0060
.0250	.0249	-.0077
.0375	.0296	-.0090
.0500	.0333	-.0100
.0750	.0389	-.0118
.1000	.0433	-.0132
.1250	.0469	-.0144
.1500	.0499	-.0154
.1750	.0525	-.0161
.2000	.0547	-.0167
.2500	.0581	-.0175
.3000	.0605	-.0176
.3500	.0621	-.0174
.4000	.0628	-.0168
.4500	.0627	-.0158
.5000	.0618	-.0144
.5500	.0599	-.0122
.5750	.0587	-.0106
.6000	.0572	-.0090
.6250	.0554	-.0071
.6500	.0533	-.0052
.6750	.0508	-.0033
.7000	.0481	-.0015
.7250	.0451	.0004
.7500	.0419	.0020
.7750	.0384	.0036
.8000	.0349	.0049
.8250	.0311	.0060
.8500	.0270	.0065
.8750	.0228	.0064
.9000	.0184	.0059
.9250	.0138	.0045
.9500	.0089	.0021
.9750	.0038	-.0013
1.0000	-.0020	-.0067

TABLE III. - KC-135 WINGLET TEST AIRPLANE INSTRUMENTATION

1. <u>DRAG:</u>	Engine-Pressures, and RPM's Flight Path and Body Axis Accelerometers Air Data ( $M, h_p, \alpha$ )	5. <u>BUFFET BOUNDARIES:</u>	Accelerometers Air Data ( $M, h_p, \alpha$ )
2. <u>RANGE:</u>	Fuel Flows Accelerometers Air Data ( $M, h_p, \alpha$ )	6. <u>STABILITY AND CONTROL:</u>	Control Positions Accelerometers Angular - Attitudes, Rates and Accelerations Air Data ( $M, h_p, \alpha, \beta$ )
3. <u>LOADS:</u>	Load and Strain Gages Accelerometers Air Data ( $M, h_p, \alpha, \beta$ )	7. <u>FLUTTER:</u>	Accelerometers Air Data ( $M, h_p, \alpha, \beta$ ) Control Positions
4. <u>PRESSURE DISTRIBUTIONS:</u>	Scanning Pressure Valves Reference Pressures Air Data ( $M, h_p, \alpha, \beta$ )		



TABLE IV. - KC-135 (3129) FLIGHT LOG

FLIGHT NO.	FLIGHT TIME	DATE	CONFIGURATION	OBJECTIVE
1	1.2	11 Apr 78	Baseline	Crew Checkout
2	2.2	11 Apr 78	Baseline	Crew Checkout
3	2.1	12 Apr 78	Baseline	Crew Checkout
4	1.8	12 Apr 78	Baseline	Crew Checkout
5	2.2	14 Apr 78	Baseline	Crew Checkout
6	2.7	20 Apr 78	Baseline	Crew Checkout
7	3.7	24 Apr 78	Baseline	Crew Checkout
8	4.3	28 Apr 78	Baseline	Crew Checkout
9	2.4	21 Sep 78	Baseline	Airspeed Calibration and Flutter
10	2.5	25 Sep 78	Baseline	Ferry to Tinker AFB
11	0.6	22 Dec 78	Baseline	Check Flight
12	3.3	17 Jan 79	Baseline	Ferry to Edwards AFB
13	3.0	14 Mar 79	Baseline	Airspeed Calibration and Flutter
14	3.8	23 Apr 79	Baseline	Flutter and Instrumentation Checkout
15	3.0	26 Apr 79	Baseline	Instrumentation Checkout
16	2.8	30 Apr 79	Baseline	Instrumentation Checkout
17	2.3	24 Jul 79	15/-2	Airspeed Calibration and Flutter
18	3.5	1 Aug 79	15/-2	Flutter
19	3.8	2 Aug 79	15-2	Airspeed Calibration and Flutter
20	3.8	10 Aug 79	15/-2	Flutter
21	5.4	24 Aug 79	15/-2	Performance
22	2.9	19 Sep 79	15/-2	Performance
23	5.4	21 Sep 79	15/-2	Airspeed Calibration and Performance
24	5.0	26 Oct 79	15/-4	Flutter
25	6.4	2 Nov 79	15/-4	Performance

TABLE IV. - KC-135 (3129) FLIGHT LOG (cont'd)

FLIGHT NO.	FLIGHT TIME	DATE	CONFIGURATION	OBJECTIVE
26	4.0	9 Nov 79	Baseline (Mod Wing Tips)	Flutter
27	6.8	16 Nov 79	Baseline (Mod Wing Tips)	Performance
28	3.6	28 Nov 79	0/-4	Flutter
29	3.3	13 Dec 79	0/-4	Flutter and Performance
30	2.3	16 Jan 80	0/-4	Performance*
31	2.3	17 Jan 80	0/-4	Performance*
32	1.8	31 Jan 80	0/-4	Inflight Fuel Leak Check
33	1.4	15 Jul 80	0/-4	Functional Check Flight
34	2.0	22 Jul 80	0/-4	Flutter
35	7.7	29 Jul 80	0/-4	Performance
36	1.9	1 Aug 80	0/-4	Performance*
37	2.6	4 Aug 80	0/-4	Performance*
38	6.7	8 Aug 80	0/-4	Performance
39	5.0	14 Aug 80	0/-4	Performance
40	1.5	21 Aug 80	Baseline (Mod Wing Tips)	Performance**
41	7.0	25 Aug 80	Baseline (Mod Wing Tips)	Performance
42	6.9	28 Aug 80	Baseline (Mod Wing Tips)	Performance
43	6.3	5 Sep 80	Baseline (Mod Wing Tips)	Performance
44	7.0	9 Sep 80	Baseline (Mod Wing Tips)	Performance
45	6.7	11 Sep 80	Baseline (Mod Wing Tips)	Performance
46	6.9	17 Sep 80	15/-4	Performance
47	7.1	23 Sep 80	15/-4	Performance
48	4.6	25 Sep 80	15/-4	Performance*
49	5.3	3 Oct 80	15/-4	Performance

TABLE IV. - KC-135 (3129) FLIGHT LOG (cont'd)

FLIGHT NO.	FLIGHT TEST	DATE	CONFIGURATION	OBJECTIVE
50	2.7	15 Oct 80	15/-4	Performance*
51	4.6	17 Oct 80	15/-4	Performance
52	7.0	19 Dec 80	15/-4	Performance
53	3.0	23 Dec 80	15/-4	Performance
54	2.0	24 Dec 80	15/-4	Performance**
55	4.8	8 Jan 81	15/-4	Performance
*Flight aborted due to rough air.				
**Flight aborted due to computer malfunction.				

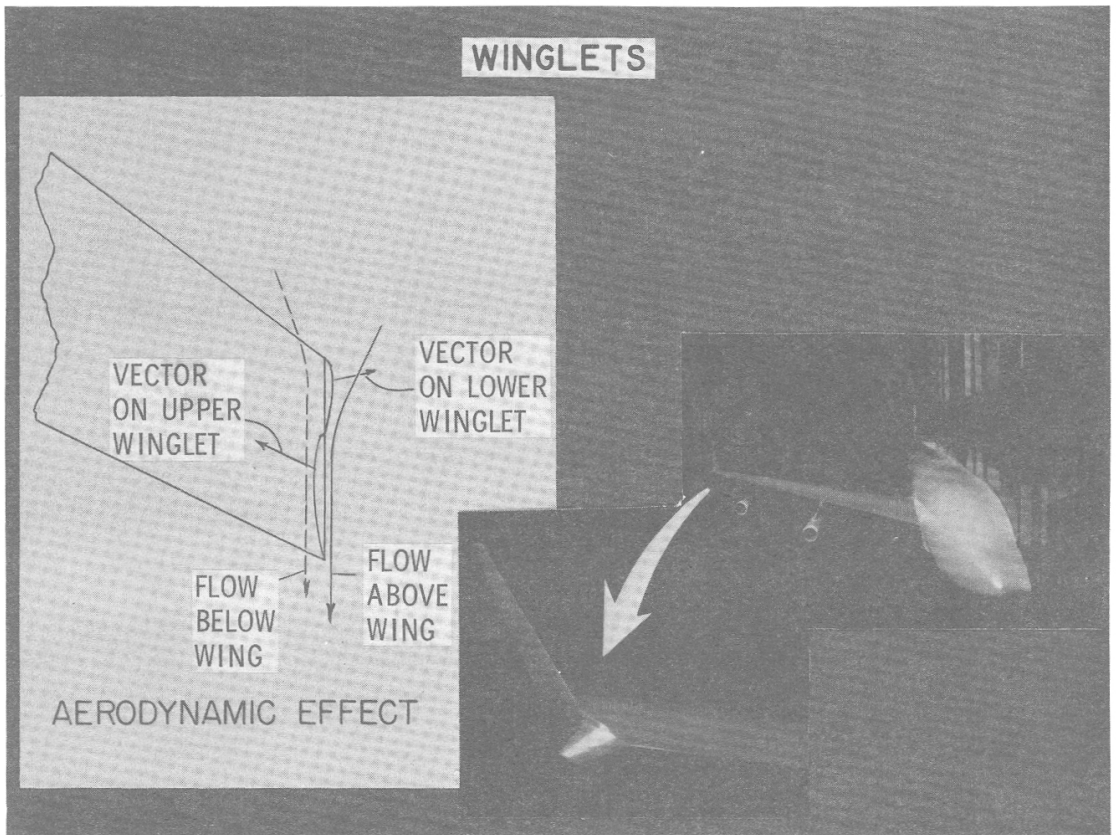


Figure 1. - Aerodynamic effect of winglet

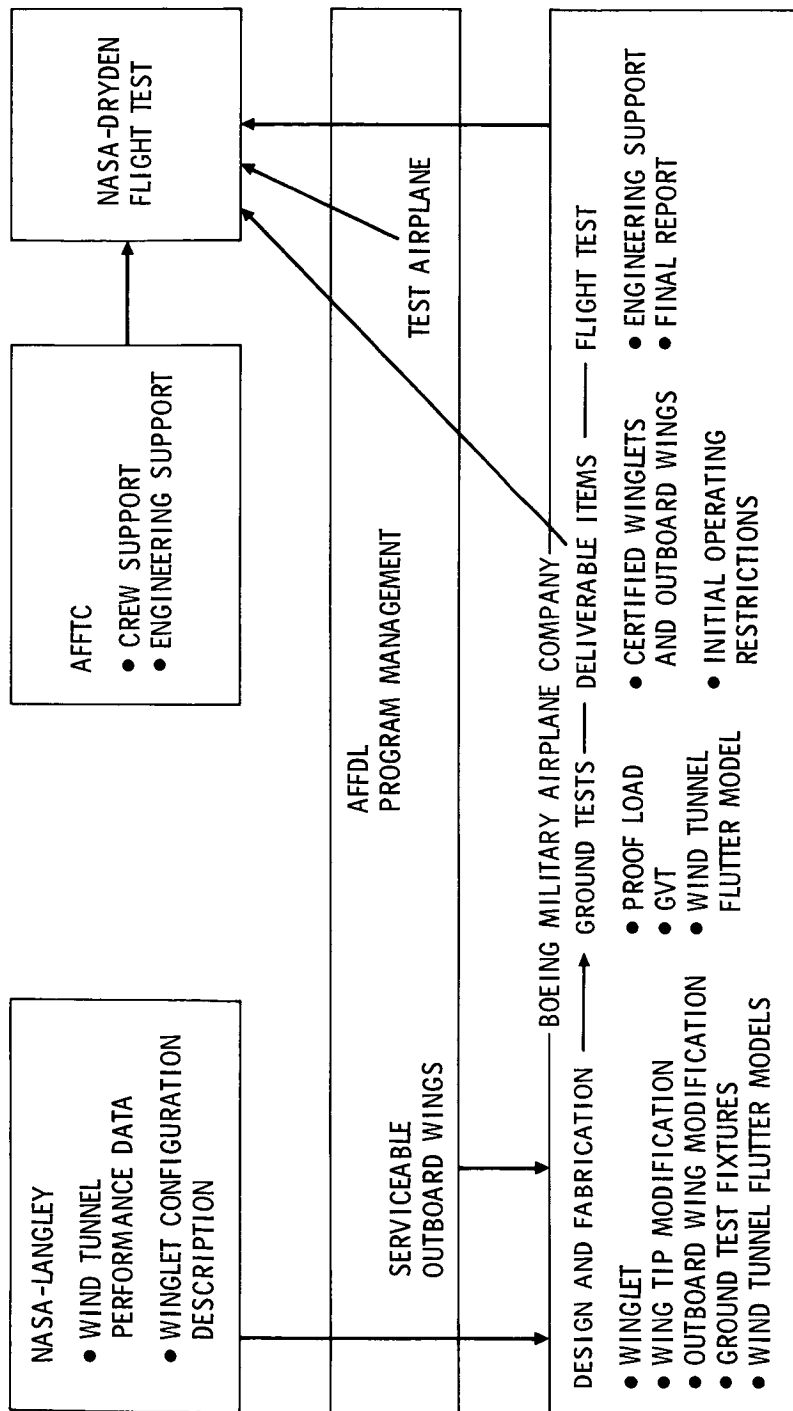


Figure 2. - KC-135 winglet flight research and demonstration program  
(joint program responsibilities)

	CALENDAR YEAR															
	77				78				79				80			
	1	2	3	4	1	2	3	4	1	2	3	4	1	2	3	4
CONTRACT AWARD				△												
DESIGN PHASE				△	△	△	△									
DESIGN REVIEWS					△		△									
FABRICATION					△	△										
GROUND TEST					△		△△									
FLIGHT TEST									△	△						
REPORTS													△			

Figure 3. - KC-135 winglet flight research and demonstration program milestones

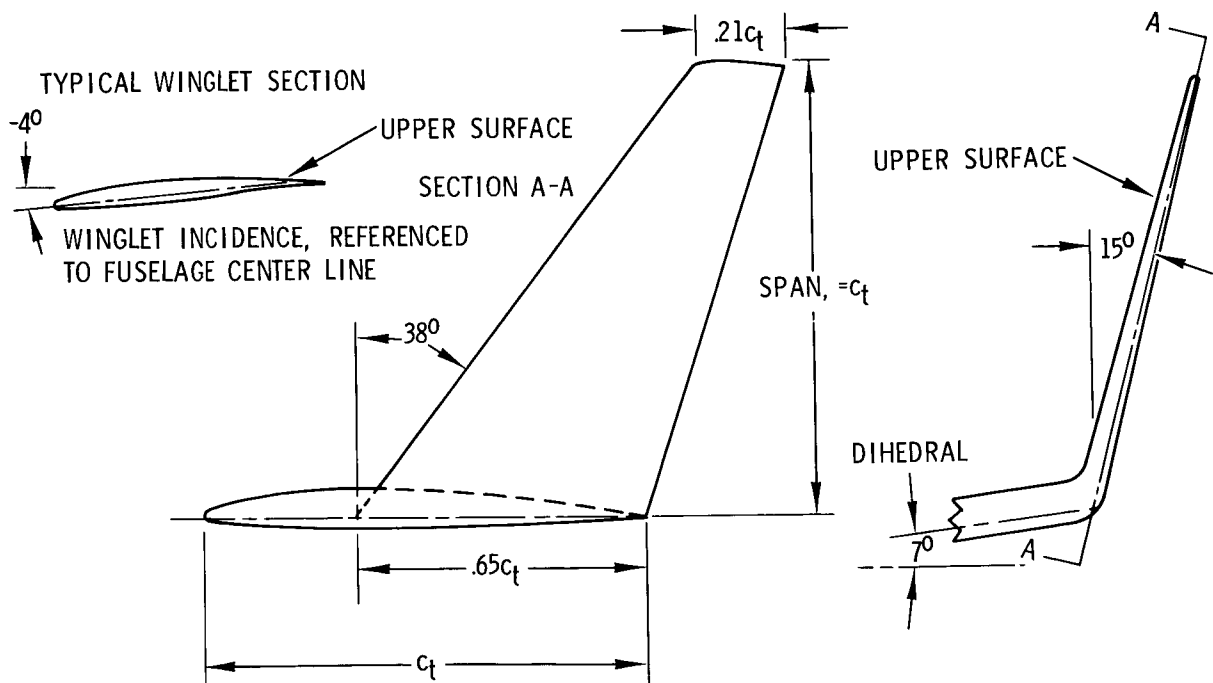


Figure 4. - KC-135 winglet design

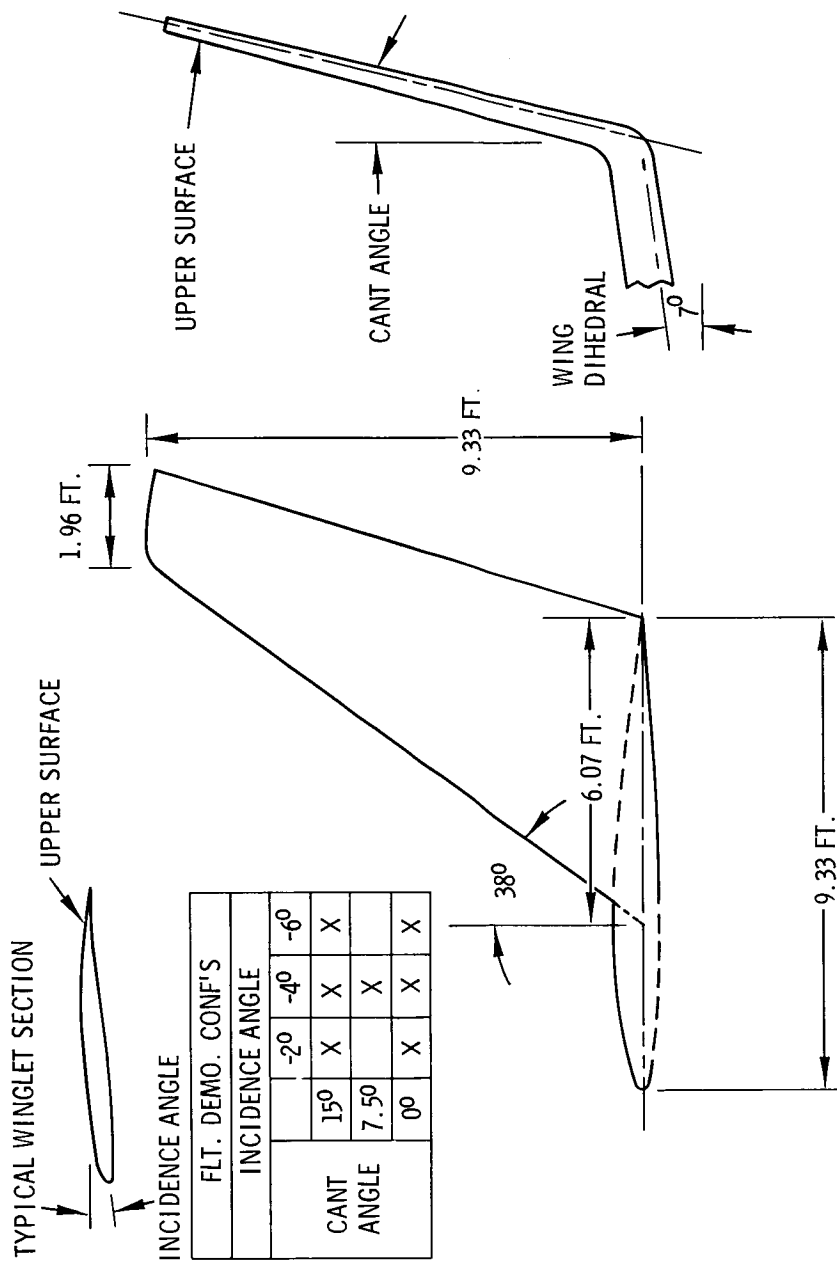


Figure 5. - Winglet geometry



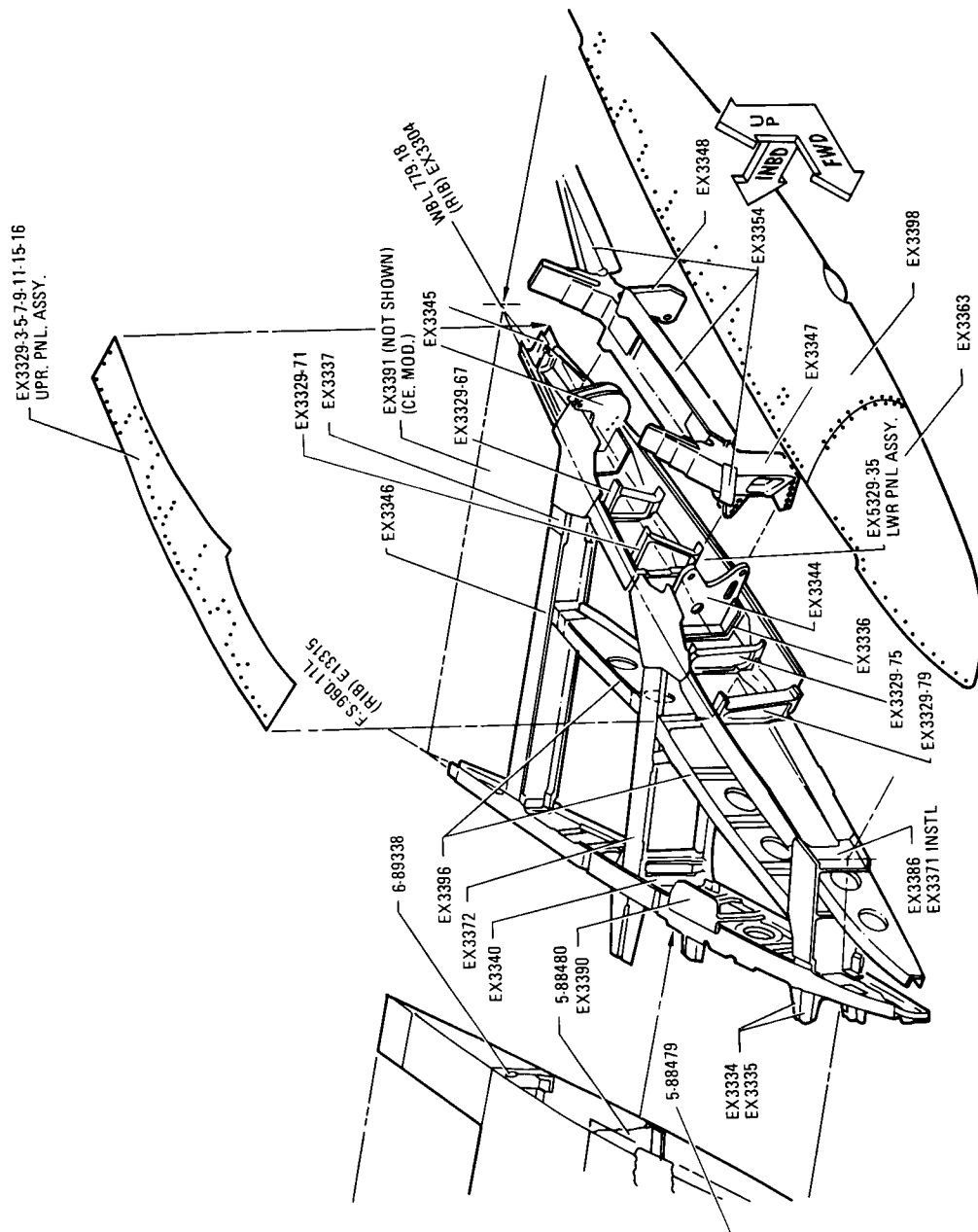


Figure 6. - KC-135 test wingtip structure

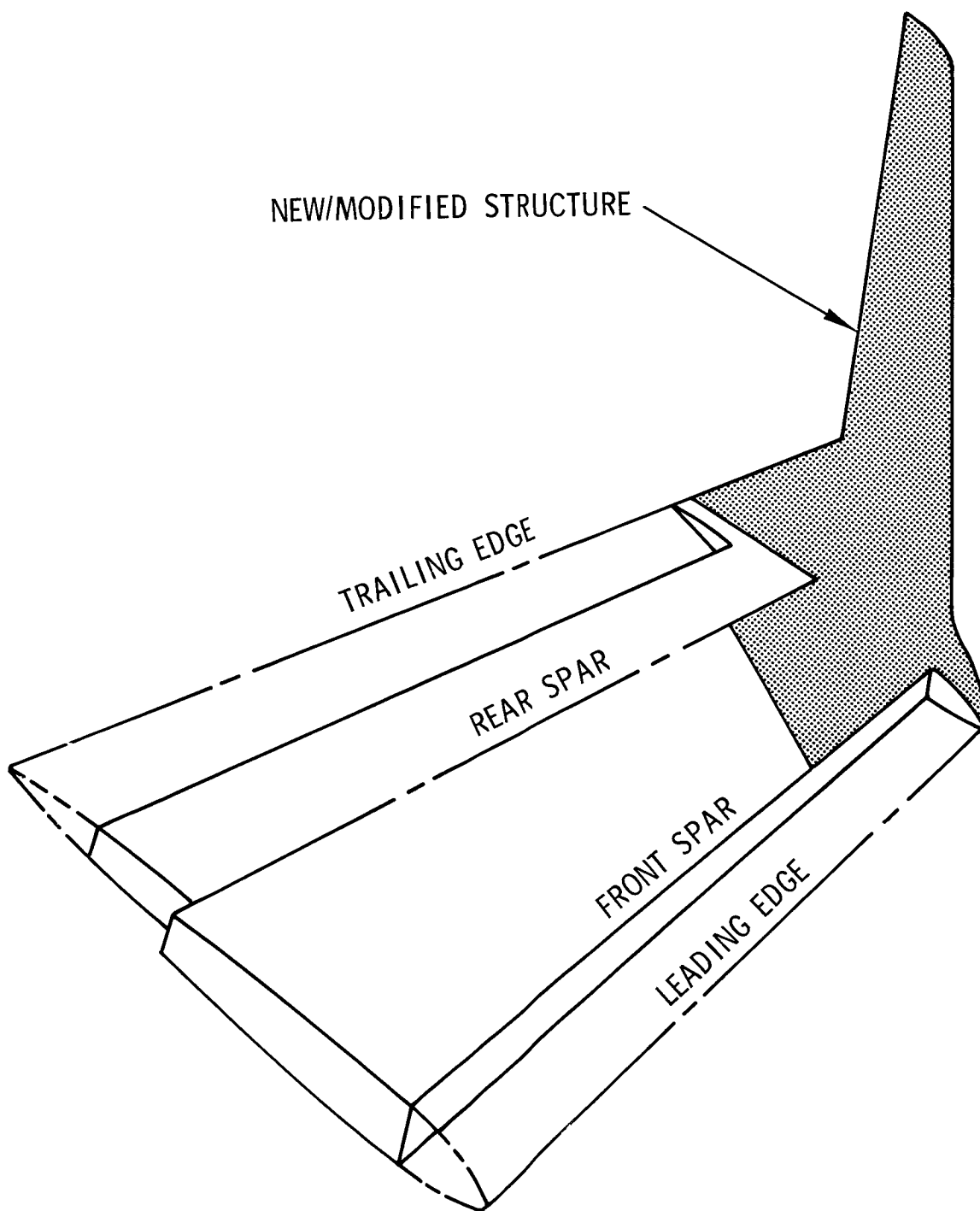


Figure 7. - Outboard wing/winglet arrangements



Figure 8. - KC-135 aircraft in flight

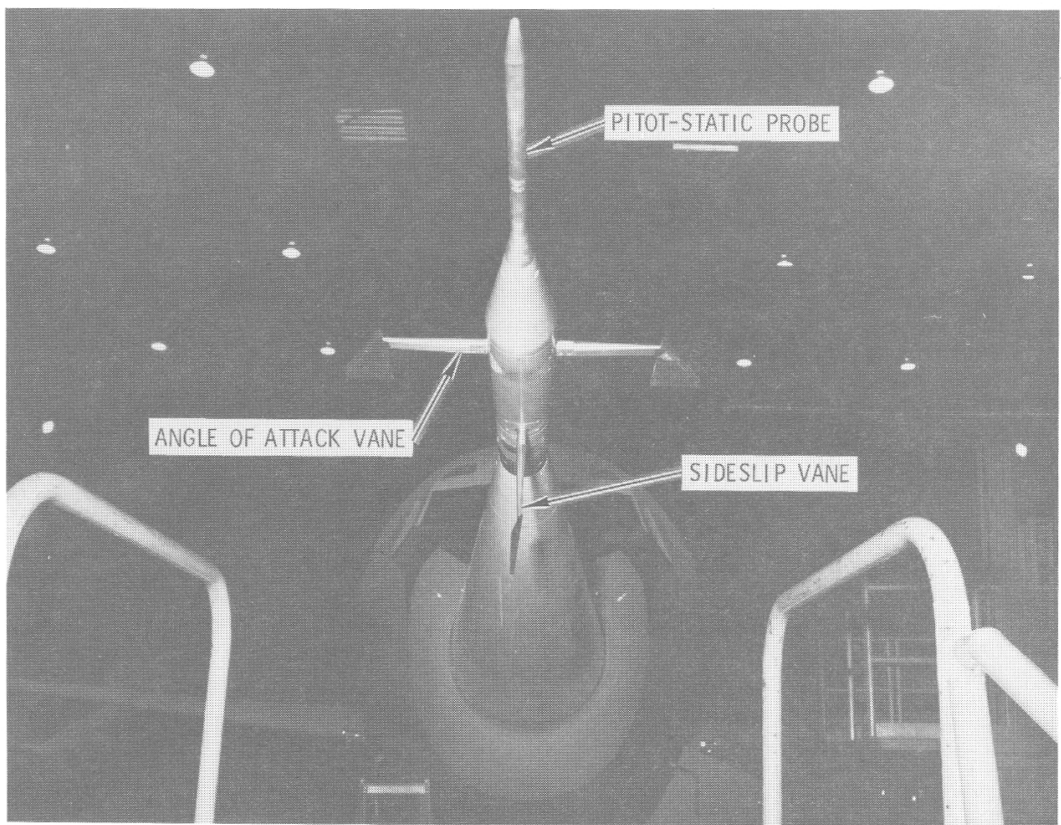


Figure 9. Noseboom instrumentation unit

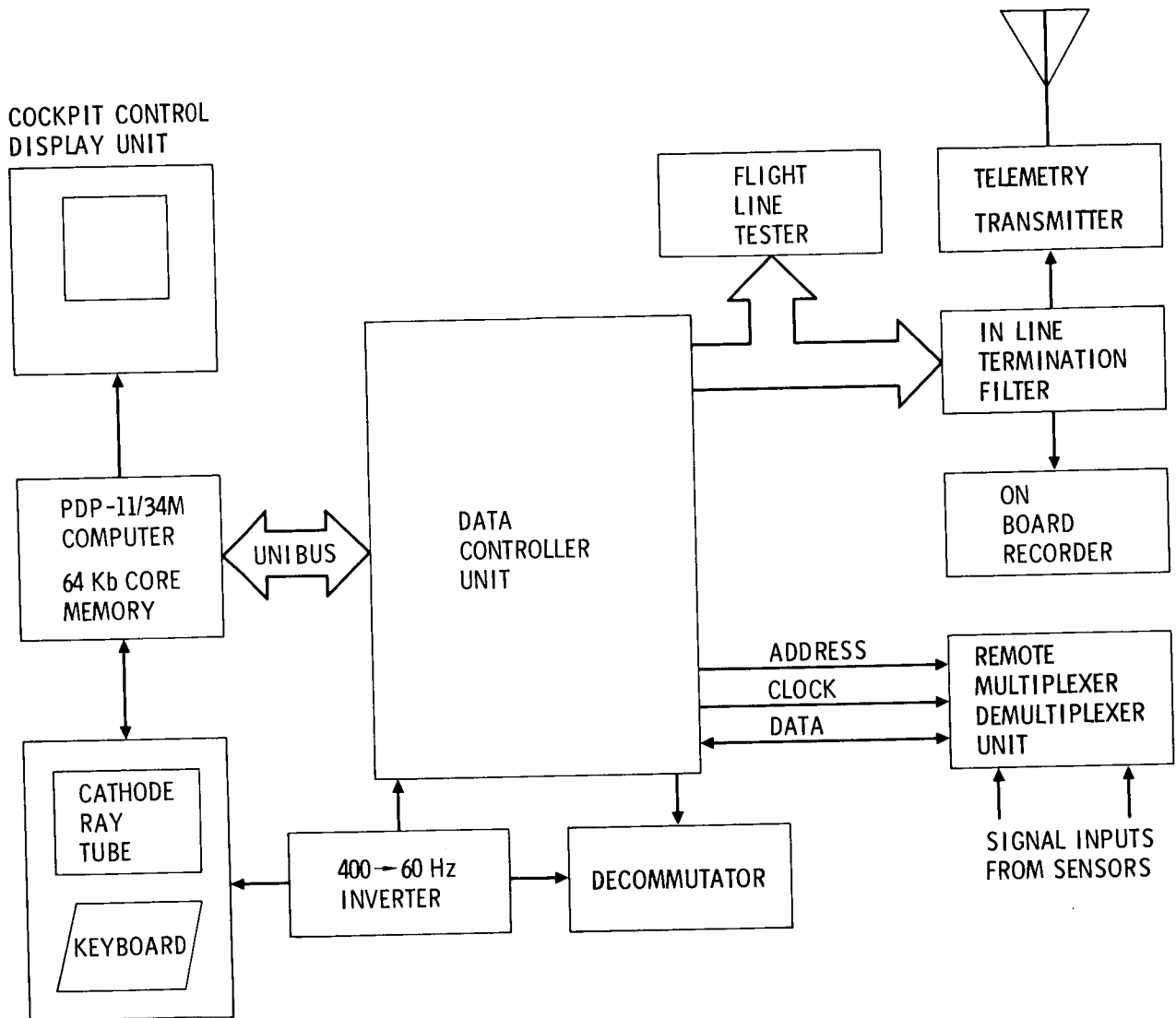


Figure 10. - Computer interactive data system  
(simplified block diagram)

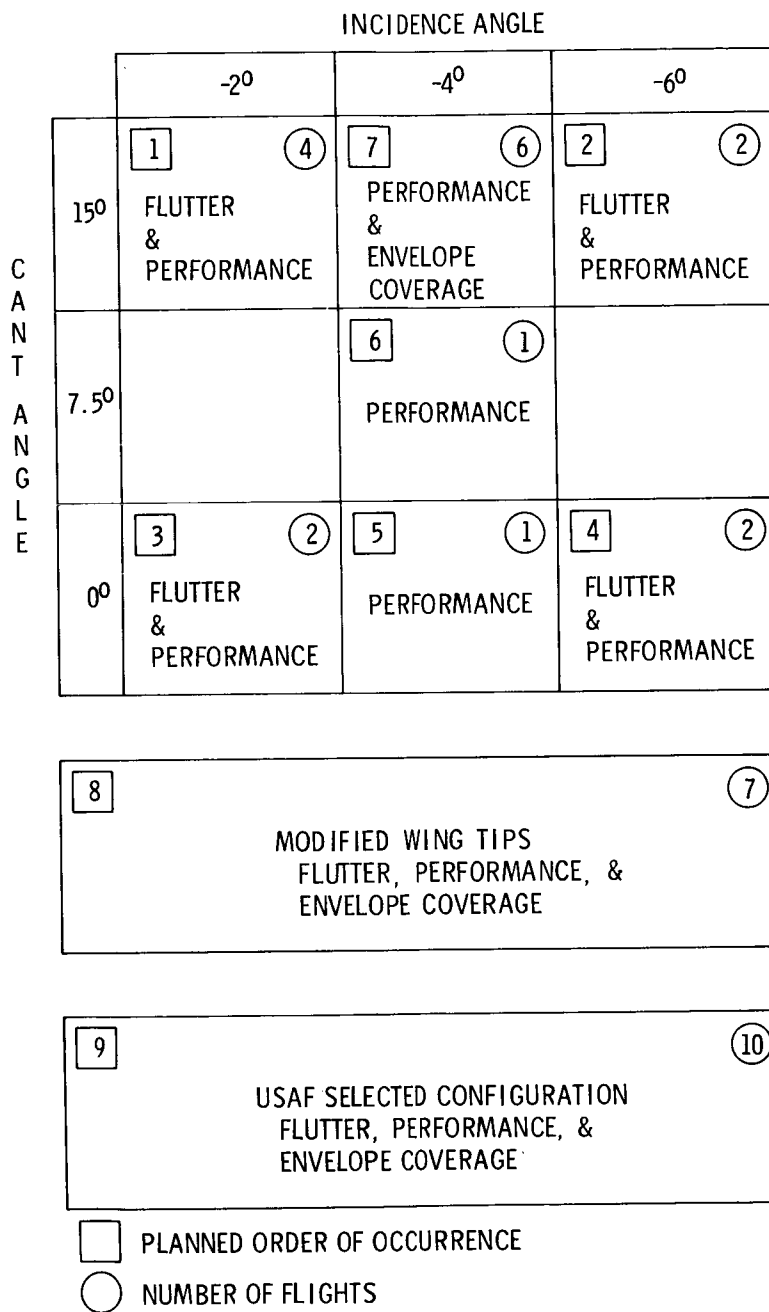


Figure 11. - Planned KC-135 winglet flight sequence

## KC-135 WINGLET FLIGHT SEQUENCE

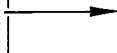
FLIGHT NO. _____		CANT / _____		INCIDENCE / _____	
OBJECTIVE	MANEUVER	A/S, M, ALT	WEIGHT	COMMENTS	
TAKE OFF PERFORMANCE	HANDBOOK TAKEOFF	FIELD ELEVATION	265,000 LBS, INCLUDING 5,600# WATER	THEODOLITE MEAS. FROM BRAKE RELEASE TO 50 FT.	
CRUISE PERFORMANCE W/ $\delta$ = 1,050,000	SPEED POWER, ACCEL	.82, .80, .78, .75, .72, .70, ACCEL .70, .82, .80, .78 $\approx$ 35.5K FT.	240,000 LBS	3 MIN STABILIZED POINTS WITH 1 MIN OF SCANI-VALVE AT END OF EACH RUN. WING DEFLECTION PHOTOS DURING RUN ACCEL AT NRT.	
CRUISE PERFORMANCE W/ $\delta$ = 900,000	SPEED POWER, PUSH OVER, PULLUP, AND ACCEL	.82, .80, .78, .75, .72, .70, ACCEL .70 - .82, .80, .78 $\approx$ 34.5K FT.	220,000 LBS		
LOADS	TRIM POINT, STEADY STATE SIDESLIPS (NOISE LEFT AND RIGHT), AND PULLUP-PUSHOVER PULLUP (1.5- 5-1.5g)	220, 250, 280, 320, 350 KEAS @ 15K	200,000 LBS	SCANI-VALVE DATA AT TRIM POINT AND SIDESLIPS	
CRUISE PERFORMANCE W/ $\delta$ = 800,000	SPEED POWER, AND ACCEL	.82, .80, .78, .75, .72, .70, ACCEL .70 - .82, .80, .78 $\approx$ 35K FT.	188,000 LBS	3 MIN STABILIZED POINTS WITH 1 MIN OF SCANI-VALVE AT END OF EACH RUN. WING DEFLECTION PHOTOS DURING RUN ACCEL AT NRT.	
BUFFET BOUNDARIES	WIND UP TURN TO INITIAL BUFFET ( $\approx$ 15 SEC DURATION)	40K @ .60, .70, .80, .84 33K' @ .50 24K' @ .40 15K' @ .33	LESS THAN 170K LBS FWD AND AFT BODY EMPTY		

Figure 12. - KC-135 winglet flight sequence



# KC-135 WINGLET FLIGHT SEQUENCE

FLIGHT NO. _____		CANT _____		INCIDENCE _____	
OBJECTIVE	MANEUVER	A/S, M, ALT	WEIGHT	COMMENTS	
TAKE OFF PERFORMANCE	HANDBOOK TAKEOFF	FIELD ELEVATION	252,600 LBS. INCLUDING WATER	THEODOLITE MEAS. FROM BRAKE RELEASE TO 50 FT	
FLUTTER CHECKS FUEL CONDITION	2 EACH - ELEV., RUDDER, AND AILERON RAPS	300/67* 320/712 340/754, 350/775* 360/795, 370/815 380/835, 390/857*	MAIN AND RESERVE TANKS FULL	*3 AXIS AUTO-PILOT ON AND OFF (ALL OTHER CONDITIONS - AUTO PILOT OFF).	
		395/867, 400/876 405/887, 410/897 413/903, 416/911 CAS/M @ 21,500'			
FLUTTER CHECKS FUEL CONDITION	2 EACH ELEV., RUDDER, AND AILERON RAPS	300/67* 320/712 340/754, 350/775 360/795, 370/815 380/885, 390/857*	10,000 LBS EACH MAIN TANK RESERVE TANKS EMPTY	*3 AXIS AUTO PITOT ON AND OFF (ALL OTHER CONDITIONS AUTO PILOT OFF).	
		395/867, 400/876 405/887, 410/897 413/903, 416/911 CAS/M @ 21,500'			

Figure 13. - KC-135 winglet flight sequence



Figure 14. - Test airplane with winglets installed

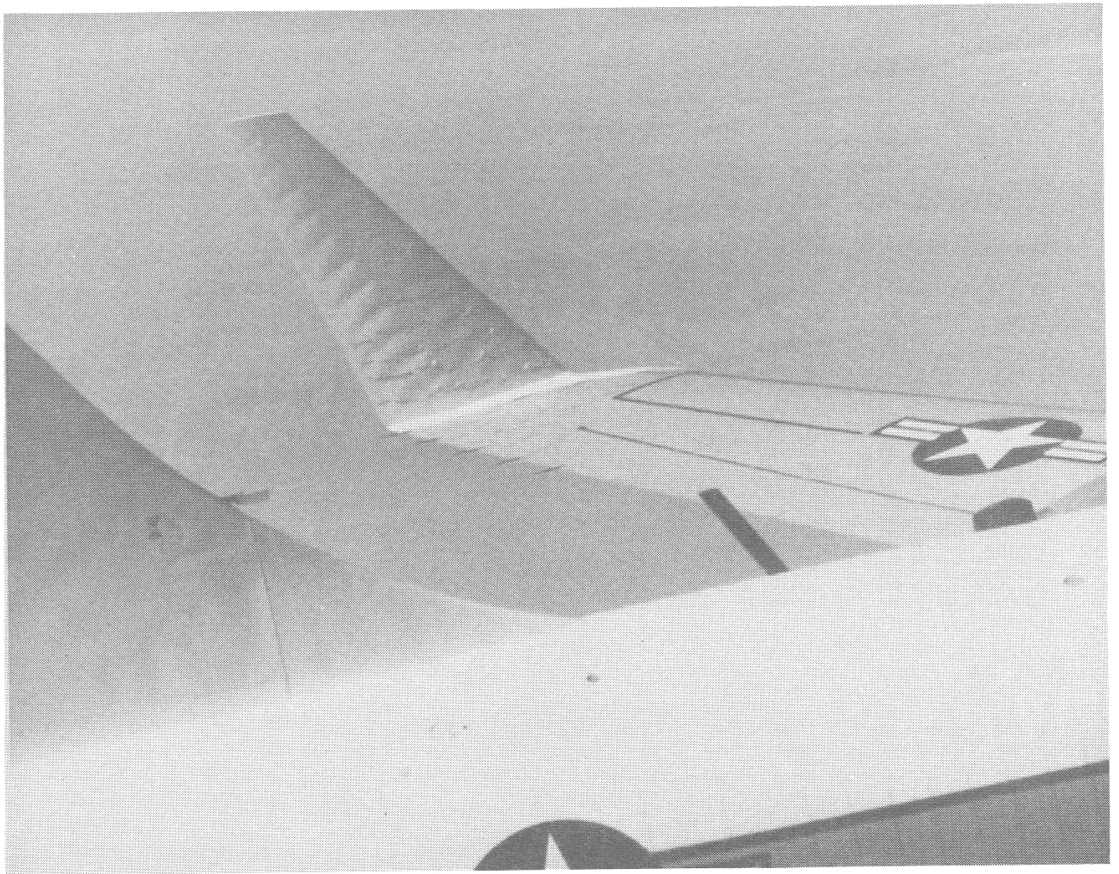


Figure 15. - Winglet inflight with skin "pillowing"

# APPENDIX A

777777: 01/07/91

FLIGHT INSTRUMENTATION PARAMETER LIST  
REV: 0 DATE: 7/24/79

PAGE 1 OF COPY 1

VEHICLE: KC-135 WINGLET PROGRAM  
FLT NO: 054  
SCHED FLT DATE: 12/24/80  
TM FREQ: 447 S/N  
PCM SYS/CDR NO: 1-00 FJRMAT NO: 1  
PCM SYS MODEL: RMDU

PROJ INSTR ENG: GENE KENNER

PCM BIT RATE: 125 KHZ  
BITS/WORD: 10  
WORDS/FRAME: 64  
FR/DATA CY: 10  
F8T-BIT1-MSR

MAIN FRAME SYNC WORDS: 00, 01, 02

ITEM NO.	PARAMETER	NAME	DATE	RANGE	UNITS	ENG	FRAM:FRAM	SAMP:CMPT	REF	VP/TP	FILTER	ITEM
NO.	NAME	NAME	DATE	RANGE	UNITS	ENG	FRAM:FRAM	SAMP:CMPT	REF	VP/TP	FILTER	ITEM
NO.	NAME	NAME	DATE	RANGE	UNITS	ENG	FRAM:FRAM	SAMP:CMPT	REF	VP/TP	FILTER	ITEM
114451***	1311 00 000	MAIN FRAME SYNC NO.1	0045 OCT				0	200:2000				1
214452***	1311 00 001	MAIN FRAME SYNC NO.2	0134 OCT				1	200:2000				2
314453***	1311 00 002	MAIN FRAME SYNC NO.3	1677 OCT				2	200:2000				3
417011***	1311 00 003	SUR FRAME I.D.COUNTFR					3	200:2000				4
51AC51LFL	1311 05 009 C	L/H WINGLET LE LONG ACCEL	108/11/80	-5	5/G		4	195:4000				33:18: 5
61AC51LEN	1311 05 008 R	L/H WINGLET LE NORM ACCEL	106/16/80	-10	10/G		5	195:4000				33:18: 6
71SV1P	1311 02 010 R	SCANIVALVE NO 1 PRESS	106/16/80	-3	3:PSID		6	195:4000	SVRPIB			40: 6: 7
81SV1DI	1311 00 107 C	SCANIVALVE NO 1 ID	103/14/79	1	48:CODE		7	195:4000				1: 1: 8
91AC19WFM	1311 02 021 O	VERT STM LAT ACCEL	102/23/79	-5	5/G		8	195:4000				1: 1: 9
101AC19HM	1311 02 022 A	HOPIT STAR ACCEL	111/17/80	-5	5/G		9	195:4000				1: 1: 10
111AC19AN	1311 02 015 R	ENGINE 4 NORMAL ACCEL	108/16/80	-5	5/G		10	195:4000				18:18: 11
121AC19AL	1311 02 020 R	ENGINE 4 LATERAL ACCEL	108/16/80	-5	5/G		11	195:4000				18:18: 12
131AC19LAT	1311 05 012 A	AFT BODY LATERAL ACCEL	106/16/80	-1	1/G		12	195:4000				20:18: 13
141AC19WPM	1311 05 014 A	AFT BODY NORMAL ACCEL	106/16/80	-5	5/G		13	195:4000				35:18: 14
151AC19LL	1311 04 019 C	L/H OUTDR AILEXON POS	106/16/80	-15	15:DEG		14	195:4000				1: 1: 15
161AC19LR	1311 04 020 R	R/H OUTDR AILEXON POS	106/16/80	-17	17:5:DEG		15	195:4000				1: 1: 16
171SV2P	1311 02 011 R	SCANIVALVE NO 2 PRESS	106/16/80	-3	3:PSID		16	195:4000	SVRPIB	1VM002		55: 6: 17
181SV2R	1311 02 012 R	SCANIVALVE NO 3 PRESS	106/16/80	-3	3:PSID		17	195:4000	SVRPIB	1VM002		55: 6: 18
191SV4P	1311 02 013 R	SCANIVALVE NO 4 PRESS	106/16/80	-3	3:PSID		18	195:4000	SVRPIB	1VM002		55: 6: 19
201SV4R	1311 02 014 R	SCANIVALVE NO 5 PRESS	106/16/80	-3	3:PSID		19	195:4000	SVRPIB	1VM002		55: 6: 20
211SV1D2	1311 10 101 O	SCANIVALVE NO 2 ID	107/15/79	1	48:PORT ID		20	200:4000				1: 1: 21
221SV1R3	1311 10 102 A	SCANIVALVE NO 3 ID	107/15/79	1	48:PORT ID		21	200:4000				1: 1: 22
231SV1R4	1311 09 104 C	SCANIVALVE NO 4 ID	107/15/79	1	48:PORT ID		22	200:4000				1: 1: 23
241SV1D5	1311 09 102 O	SCANIVALVE NO 5 ID	107/15/79	1	48:PORT ID		23	200:4000				1: 1: 24
251AC7LFL	1311 05 001 R	R/H WINGTIP LE NORM ACCEL	106/16/80	-10	10/G		24	195:4000				55:18: 25
261AC7TEN	1311 05 002 A	R/H WINGTIP TE NORM ACCEL	106/16/80	-10	10/G		25	195:4000				55:18: 26
271AC7LEL	1311 05 003 A	R/H WINGTIP LE LONG ACCEL	106/16/80	-2	2/G		26	195:4000				55:18: 27
281AC7LEN	1311 05 004 R	L/H WINGTIP LE NORM ACCEL	106/16/80	-10	10/G		27	195:4000				55:18: 28
291AC7LEN	1311 05 005 A	R/H WINGLET LE NORM ACCEL	106/16/80	-10	10/G		28	195:4000				55:18: 29
301AC7LEL	1311 05 006 R	R/H WINGLET LE LONG ACCEL	108/12/80	-5	5/G		29	195:4000				37:18: 30
311AC7TEN	1311 05 007 A	R/H WINGLET TE NORM ACCEL	106/16/80	-10	10/G		30	195:4000				55:18: 31
321TCRFF	1311 02 016 O	THRMNO PFF OVEN TEMP	110/01/80	100	100:DEG F		31	195:4000				1: 1: 32
331NULL	1311 00 032						32	200:2000				1: 1: 33
341PMT	1311 03 015 A	ROLL ANGLE	106/16/80	-30	30:DEG		33	195:4000				1: 1: 34
351SVR0TB	1311 03 001 A	SCANIVALVE REF PRESS - INRD	106/16/80	0	15:PSIA		34	195:4000				40: 6: 35
361SVR0PB	1311 03 002 R	SCANIVALVE REF PRESS - OUTBD	106/16/80	0	15:PSIA		35	195:4000				55: 6: 36
371AC9MM	1311 05 015 O	NGSE 800M NORM ACCEL	102/27/79	-15	15/G		36	200:4000				40: 6: 37
381AC7WPM	1311 05 016 A	WING PANFL ACCEL	111/20/79	-80	80/G		37	195:4000				100:18: 38
391ACE3M	1311 07 019 R	ENGINE 3 NORMAL ACCEL	109/08/80	-3	3/G		38	195:4000				18:18: 39
401ACE3L	1311 07 020 A	ENGINE 3 LATERAL ACCEL	108/16/80	-5	5/G		39	195:4000				18:18: 40
411NULL	1311 00 040						40	200:2000				1: 1: 41
421SIF001*	1311 00 041	SUBFRAME 01					41	195:1000				1: 1: 42
431SIF002*	1311 00 042	SUBFRAME 02					42	195:1000				1: 1: 43
441SIF003*	1311 00 043	SUBFRAME 03					43	195:1000				1: 1: 44
451SIF004*	1311 00 044	SUBFRAME 04					44	195:1000				1: 1: 45
461SIF005*	1311 00 045	SUBFRAME 05					45	195:1000				1: 1: 46
471SIF006*	1311 00 046	SUBFRAME 06					46	195:1000				1: 1: 47
481SIF007*	1311 00 047	SUBFRAME 07					47	195:1000				1: 1: 48

TODAY: 01/07/81

FLIGHT INSTRUMENTATION PARAMETER LIST  
REV: D DATE: 7/24/79

PAGE 2 OF COPY 1

VEHICLE: KC-135 WINGLET PROGRAM  
FLT NO: 054  
SCHED FLT DATE: 12/24/80  
TM REF: 4H7 J/N  
PCM SYS/CJM NO: L-00 FJRHAT NO. 1  
PCM SYS MUEL: RMDU

PROJ INST ENGR: GENE KENNER

PCM BIT RATE: 125 KHZ  
BITS/WORD: 10  
WORDS/FRAME: 64  
FR/CATA CY: 10  
FBT-BIT1=MSB

MAIN FRAME SYNC WORDS: 00, 01, 02

TTM	NO.	PARAMETER	CALIB	NAME	DATE	RANGE	UNITS	ENG	FRAM	FRAM	SAMP	COMP	REF	VM/TP	FILTER	TTM
						LOW	HIGH		WORD	NO.	RATE	ALG	PRESS	KP		INC.
SYS									POS				PARMID	PARMID	IEBEG	DBICOM
40	151F0099	311 00 048		SUBFRAME 08					48		195	1000				40
50	151F0099	311 00 049		SUBFRAME 09					49		195	1000				50
51	151F0100	311 00 050		SUBFRAME 10					50		195	1000				51
52	151F0101	311 00 051		SUBFRAME 11					51		195	1000				52
53	151F0102	311 00 052		SUBFRAME 12					52		195	1000				53
54	151F0103	311 00 053		SUBFRAME 13					53		195	1000				54
55	151F0104	311 00 054		SUBFRAME 14					54		195	1000				55
56	151F0105	311 00 055		SUBFRAME 15					55		195	1000				56
57	151F0106	311 00 056		SUBFRAME 16					56		195	1000				57
58	151F0107	311 00 057		SUBFRAME 17					57		195	1000				58
59	151F0108	311 00 058		SUBFRAME 18					58		195	1000				59
60	151F0109	311 00 059		SUBFRAME 19					59		195	1000				60
61	151F0110	311 00 060		SUBFRAME 20					60		195	1000				61
62	151F0111	311 00 061		SUBFRAME 21					61		195	1000				62
63	151F0112	311 00 062		SUBFRAME 22					62		195	1000				63
64	151F0113	311 00 063		SUBFRAME 23					63		195	1000				64

TRAY: 01/07/71

# FLIGHT INSTRUMENTATION PARAMETER LIST REV: D DATE: 7/24/79

PAGE 3 OF COPY 1

VEHICLE: KC-135 WINGLET PROGRAM  
FLT NO: 254  
SCHED FLT DATE: 12/24/80  
TM FREQ: MHZ S/N  
PCM SYS/COM NO. 1-00 FORMAT NO. 1  
PCM SYS MODEL: RMDU

PROJ INSTR ENGR: GENE KENNER

PCM BIT RATE: 125 KHZ  
BITS/WORD: 10  
WORDS/FRAME: 64  
FR/DATA CY: 1C  
FBT=BIT1=MSB

MAIN FRAME SYNC WORDS: 00 , 01 , 02

S/V PRESSURE PARMID SVIP		SCANIVALVE NO. 1		S/V REF PRESSURE PARMID SVRPIB		S/V PORT IO		SVID1	
SYS ITEM NO/FR NO POS		SYS ITEM NO/FR NO POS		SYS ITEM NO/FR NO POS		SYS ITEM NO/FR NO POS		R	
ITEM	PARAMETER	PORT	IO DEC	PARAMETERS AFFECTED	PORT	IO DEC	PARAMETERS AFFECTED	PORT	IO DEC
NO.	NAME	NO.	IO DEC	NO.	IO DEC	NO.	IO DEC	NO.	IO DEC
7	S1REF01	REF PRESS PORT 01	26% SV 1	10	PORTS PER SEC	1			
7	R1U00	26 PCT PORT U00		2		2			
7	R1U03	26 PCT PORT 03		3		3			
7	R1U05	26 PCT PORT 05		4		4			
7	R1U15	26 PCT PORT 15		5		5			
7	R1U25	26 PCT PORT 25		6		6			
7	R1U35	26 PCT PORT 35		7		7			
7	R1U45	26 PCT PORT 45		8		8			
7	R1U55	26 PCT PORT 55		9		9			
7	R1U65	26 PCT PORT 65		10		10			
7	R1U75	26 PCT PORT 75		11		11			
7	R1U85	26 PCT PORT 85		12		12			
7	R1U95	26 PCT PORT 95		13		13			
7	R1L03	26 PCT PORT L03		14		14			
7	R1L05	26 PCT PORT L05		15		15			
7	R1L15	26 PCT PORT L15		16		16			
7	R1L25	26 PCT PORT L25		17		17			
7	R1L35	26 PCT PORT L35		18		18			
7	R1L45	26 PCT PORT L45		19		19			
7	R1L55	26 PCT PORT L55		20		20			
7	R1L65	26 PCT PORT L65		21		21			
7	R1L75	26 PCT PORT L75		22		22			
7	R1L85	26 PCT PORT L85		23		23			
7	S1REC24	REF PRESS PORT 24		24		24			
7	S1SP25	SPARE S.V. PORTS AT 25 PCT		25		25			
7	S1SP26	SPARE S.V. PORTS AT 26 PCT		26		26			
7	S1SP27	SPARE S.V. PORTS AT 26 PCT		27		27			
7	S1SP28	SPARE S.V. PORTS AT 26 PCT		28		28			
7	S1SP29	SPARE S.V. PORTS AT 26 PCT		29		29			
7	S1SP30	SPARE S.V. PORTS AT 26 PCT		30		30			
7	S1SP31	SPARE S.V. PORTS AT 26 PCT		31		31			
7	S1SP32	SPARE S.V. PORTS AT 26 PCT		32		32			
7	S1SP33	SPARE S.V. PORTS AT 26 PCT		33		33			
7	S1SP34	SPARE S.V. PORTS AT 26 PCT		34		34			
7	S1SP35	SPARE S.V. PORTS AT 26 PCT		35		35			
7	S1SP36	SPARE S.V. PORTS AT 26 PCT		36		36			
7	S1SP37	SPARE S.V. PORTS AT 26 PCT		37		37			
7	S1SP38	SPARE S.V. PORTS AT 26 PCT		38		38			
7	S1SP39	SPARE S.V. PORTS AT 26 PCT		39		39			
7	S1SP40	SPARE S.V. PORTS AT 26 PCT		40		40			
7	S1SP41	SPARE S.V. PORTS AT 26 PCT		41		41			
7	S1SP42	SPARE S.V. PORTS AT 26 PCT		42		42			
7	S1SP43	SPARE S.V. PORTS AT 26 PCT		43		43			
7	S1SP44	SPARE S.V. PORTS AT 26 PCT		44		44			
7	S1SP45	SPARE S.V. PORTS AT 26 PCT		45		45			
7	S1SP46	SPARE S.V. PORTS AT 26 PCT		46		46			
7	S1SP47	SPARE S.V. PORTS AT 26 PCT		47		47			
7	S1SP48	SPARE S.V. PORTS AT 26 PCT		48		48			

TODAY: 01/07/81

FLIGHT INSTRUMENTATION PARAMETER LIST

PAGE 4 OF COPY 1

VEHICLE: KC-135 WINGLET PROGRAM  
 FLT NO: 054  
 SCHED FLT DATE: 12/24/80  
 TM FREQ: MH7 S/M  
 PCM SYS/CDM NO. 1-00 FJPPAT NO. 1  
 PCM SYS MODFL: RMDU

REF: D DATE: 7/24/79  
 PROJ INSTR ENGR: GENE KENNER

PCM BIT RATE: 125 KHZ  
 BITS/WORD: 10  
 WORDS/FRAME: 64  
 FR/DATA CY: 10  
 FBT-RT1-MSB

MAIN FRAME SYNC WORDS: 00 , 01 , 02

S/V PRESSURE PARMID SV2P		SCANIVALVE NO. 2		S/V REF PRESSURE PARMID SVRPOA		S/V PORT ID		SVID2	
SYS IIFM NO/FR NO POS 17 16		SYS IIFM NO/FR NO POS 36 35		SYS IIFM NO/FR NO POS		SYS IIFM NO/FR NO POS		21 20	
ITEM	PARAMETER	PORT	PARAMETERS AFFECTED	PORT	PARAMETERS AFFECTED	PORT	PARAMETERS AFFECTED	PORT	PARAMETERS AFFECTED
NO.	NAME	NO.	NAME	NO.	NAME	NO.	NAME	NO.	NAME
17	*REF01	REF PRESSURE PORT 1	1	10 PORTS / SECOND	1				
17	*2100	77 % PORT U00	2		2				
17	*2103	77 % PORT U03	3	20 SAMPLES / PORT	3				
17	*2105	77 % PORT U05	4		4				
17	*2110	77 % PORT U10	5		5				
17	*2115	77 % PORT U15	6		6				
17	*2120	77 % PORT U20	7		7				
17	*2125	77 % PORT U25	8		8				
17	*2130	77 % PORT U30	9		9				
17	*2135	77 % PORT U35	10		10				
17	*2140	77 % PORT U40	11		11				
17	*2145	77 % PORT U45	12		12				
17	*2150	77 % PORT U50	13		13				
17	*2155	77 % PORT U55	14		14				
17	*2160	77 % PORT U60	15		15				
17	*2165	77 % PORT U65	16		16				
17	*2170	77 % PORT U70	17		17				
17	*2175	77 % PORT U75	18		18				
17	*2180	77 % PORT U80	19		19				
17	*2185	77 % PORT U85	20		20				
17	*2190	77 % PORT U90	21		21				
17	*2195	77 % PORT U95	22		22				
17	*2200	77 % PORT L00	23		23				
17	*2205	77 % PORT L05	24		24				
17	*2210	77 % PORT L10	25		25				
17	*2215	77 % PORT L15	26		26				
17	*2220	77 % PORT L20	27		27				
17	*2225	77 % PORT L25	28		28				
17	*2230	77 % PORT L30	29		29				
17	*2235	77 % PORT L35	30		30				
17	*2240	77 % PORT L40	31		31				
17	*2245	77 % PORT L45	32		32				
17	*2250	77 % PORT L50	33		33				
17	*2255	77 % PORT L55	34		34				
17	*2260	77 % PORT L60	35		35				
17	*2265	77 % PORT L65	36		36				
17	*2270	77 % PORT L70	37		37				
17	*2275	77 % PORT L75	38		38				
17	*2280	77 % PORT L80	39		39				
17	*2285	77 % PORT L85	40		40				
17	*2290	77 % PORT L90	41		41				
17	*2295	77 % PORT L95	42		42				
17	*2300	77 % PORT L00	43		43				
17	*2305	77 % PORT L05	44		44				
17	*2310	77 % PORT L10	45		45				
17	*2315	77 % PORT L15	46		46				
17	*2320	77 % PORT L20	47		47				
17	*2325	77 % PORT L25	48		48				
17	*2330	77 % PORT L30	49		49				
17	*2335	77 % PORT L35	50		50				
17	*2340	77 % PORT L40	51		51				
17	*2345	77 % PORT L45	52		52				
17	*2350	77 % PORT L50	53		53				
17	*2355	77 % PORT L55	54		54				
17	*2360	77 % PORT L60	55		55				
17	*2365	77 % PORT L65	56		56				
17	*2370	77 % PORT L70	57		57				
17	*2375	77 % PORT L75	58		58				
17	*2380	77 % PORT L80	59		59				
17	*2385	77 % PORT L85	60		60				
17	*2390	77 % PORT L90	61		61				
17	*2395	77 % PORT L95	62		62				
17	*2400	77 % PORT L00	63		63				
17	*2405	77 % PORT L05	64		64				
17	*2410	77 % PORT L10	65		65				
17	*2415	77 % PORT L15	66		66				
17	*2420	77 % PORT L20	67		67				
17	*2425	77 % PORT L25	68		68				
17	*2430	77 % PORT L30	69		69				
17	*2435	77 % PORT L35	70		70				
17	*2440	77 % PORT L40	71		71				
17	*2445	77 % PORT L45	72		72				
17	*2450	77 % PORT L50	73		73				
17	*2455	77 % PORT L55	74		74				
17	*2460	77 % PORT L60	75		75				
17	*2465	77 % PORT L65	76		76				
17	*2470	77 % PORT L70	77		77				
17	*2475	77 % PORT L75	78		78				
17	*2480	77 % PORT L80	79		79				
17	*2485	77 % PORT L85	80		80				
17	*2490	77 % PORT L90	81		81				
17	*2495	77 % PORT L95	82		82				
17	*2500	77 % PORT L00	83		83				
17	*2505	77 % PORT L05	84		84				
17	*2510	77 % PORT L10	85		85				
17	*2515	77 % PORT L15	86		86				
17	*2520	77 % PORT L20	87		87				
17	*2525	77 % PORT L25	88		88				
17	*2530	77 % PORT L30	89		89				
17	*2535	77 % PORT L35	90		90				
17	*2540	77 % PORT L40	91		91				
17	*2545	77 % PORT L45	92		92				
17	*2550	77 % PORT L50	93		93				
17	*2555	77 % PORT L55	94		94				
17	*2560	77 % PORT L60	95		95				
17	*2565	77 % PORT L65	96		96				
17	*2570	77 % PORT L70	97		97				
17	*2575	77 % PORT L75	98		98				
17	*2580	77 % PORT L80	99		99				
17	*2585	77 % PORT L85	100		100				
17	*2590	77 % PORT L90	101		101				
17	*2595	77 % PORT L95	102		102				
17	*2600	77 % PORT L00	103		103				
17	*2605	77 % PORT L05	104		104				
17	*2610	77 % PORT L10	105		105				
17	*2615	77 % PORT L15	106		106				
17	*2620	77 % PORT L20	107		107				
17	*2625	77 % PORT L25	108		108				
17	*2630	77 % PORT L30	109		109				
17	*2635	77 % PORT L35	110		110				
17	*2640	77 % PORT L40	111		111				
17	*2645	77 % PORT L45	112		112				
17	*2650	77 % PORT L50	113		113				
17	*2655	77 % PORT L55	114		114				
17	*2660	77 % PORT L60	115		115				
17	*2665	77 % PORT L65	116		116				
17	*2670	77 % PORT L70	117		117				
17	*2675	77 % PORT L75	118		118				
17	*2680	77 % PORT L80	119		119				
17	*2685	77 % PORT L85	120		120				
17	*2690	77 % PORT L90	121		121				
17	*2695	77 % PORT L95	122		122				
17	*2700	77 % PORT L00	123		123				
17	*2705	77 % PORT L05	124		124				
17	*2710	77 % PORT L10	125		125				
17	*2715	77 % PORT L15	126		126				
17	*2720	77 % PORT L20	127		127				
17	*2725	77 % PORT L25	128		128				
17	*2730	77 % PORT L30	129		129				
17	*2735	77 % PORT L35	130		130				
17	*2740	77 % PORT L40	131		131				
17	*2745	77 % PORT L45	132		132				
17	*2750	77 % PORT L50	133		133				
17	*2755	77 % PORT L55	134		134				
17	*2760	77 % PORT L60	135		135				
17	*2765	77 % PORT L65	136		136				
17	*2770	77 % PORT L70	137		137				
17	*2775	77 % PORT L75	138		138				
17	*2780	77 % PORT L80	139		139				
17	*2785	77 % PORT L85	140		140				
17	*2790	77 % PORT L90	141		141				
17	*2795	77 % PORT L95	142		142				
17	*2800	77 % PORT L00	143		143				
17	*2805	77 % PORT L05	144		144				
17	*2810	77 % PORT L10	145		145				
17	*2815	77 % PORT L15	146		146				
17	*2820	77 % PORT L20	147		147				
17	*2825	77 % PORT L25	148		148				
17	*2830	77 % PORT L30	149		149				
17	*2835	77 % PORT L35	150		150				
17	*2840	77 % PORT L40	151		151				
17	*2845	77 % PORT L45	152		152				
17	*2850	77 % PORT L50	153		153				
17	*2855	77 % PORT L55	154		154				
17	*2860	77 % PORT L60	155		155				
17	*2865	77 % PORT L65	156		156				
17	*2870	77 % PORT L70	157		157				
17	*2875	77 % PORT L75	158		158				
17	*2880	77 % PORT L80	159		159				
17	*2885	77 % PORT L85	160		160				
17	*2890	77 % PORT L90	161		161				
17	*2895	77 % PORT L95	162		162				
17	*2900	77 % PORT L00	163		163				
17	*2905	77 % PORT L05	164		164				
17	*2910	77 % PORT L10	165		165				
17	*2915	77 % PORT L15	166		166				
17	*2920	77 % PORT L20	167		167				
17	*2925	77 % PORT L25	168		168				
17	*2930	77 % PORT L30	169		169				
17	*2935	77 % PORT L35	170		170				
17	*2940	77 % PORT L40	171		171				
17	*2945	77 % PORT L45							

TODAY: 01/07/81

FLIGHT INSTRUMENTATION PARAMETER LIST

PAGE 2 OF COPY 1

VHICLE: KC-135 WINGLET PROGRAM  
 FLT NO: 354  
 SCHED FLT DATE: 12/24/79  
 TM FREQ: MHZ S/N  
 PCN SYS/CUM NO: 1-00 FORMAT NO: 1  
 PCN SYS MODFL: RMDU

PROJ INSTN ENGR: GENE KENNER

PCP BIT RATE: 125 KHZ  
 BITS/WORD: 10  
 WORDS/FRAME: 64  
 FR/DATA CY: 10  
 FBT-RIT1-MSR

MAIN FRAME SYNC WORDS: 00, 01, 02

S/V PRESSURE PARMID		SV3P		SCANIVALVE NO. 3		S/V REF PRESSURE PARMID SVRPOB		S/V PORT ID		SVI03	
SYS ITEM NUMBER NO POS		18 17		SYS ITEM NUMBER NO POS		36 25		SYS ITEM NO/FR WP POS		22 21	
PARAMETER		PORT		PARAMETERS AFFECTED		PORT		NC			
NO.	NAME	ID	DEF	REMARKS							
18	330FF01	1	REF PRESS PPORT C1	10 PORTS PER SEC							
18	031075	02	PCT PPORT U75								
18	031080	02	PCT PPORT 80								
18	031085	02	PCT PPORT 85								
18	031090	02	PCT PPORT 90								
18	031095	02	PCT PPORT 95								
18	031100	02	PCT PPORT 100								
18	031105	02	PCT PPORT 105								
18	031110	02	PCT PPORT 110								
18	031115	02	PCT PPORT 115								
18	031120	02	PCT PPORT 120								
18	031125	02	PCT PPORT 125								
18	031130	02	PCT PPORT 130								
18	031135	02	PCT PPORT 135								
18	031140	02	PCT PPORT 140								
18	031145	02	PCT PPORT 145								
18	031150	02	PCT PPORT 150								
18	031155	02	PCT PPORT 155								
18	031160	02	PCT PPORT 160								
18	031165	02	PCT PPORT 165								
18	031170	02	PCT PPORT 170								
18	031175	02	PCT PPORT 175								
18	031180	02	PCT PPORT 180								
18	031185	02	PCT PPORT 185								
18	031190	02	PCT PPORT 190								
18	031195	02	PCT PPORT 195								
18	031200	02	PCT PPORT 200								
18	031205	02	PCT PPORT 205								
18	031210	02	PCT PPORT 210								
18	031215	02	PCT PPORT 215								
18	031220	02	PCT PPORT 220								
18	031225	02	PCT PPORT 225								
18	031230	02	PCT PPORT 230								
18	031235	02	PCT PPORT 235								
18	031240	02	PCT PPORT 240								
18	031245	02	PCT PPORT 245								
18	031250	02	PCT PPORT 250								
18	031255	02	PCT PPORT 255								
18	031260	02	PCT PPORT 260								
18	031265	02	PCT PPORT 265								
18	031270	02	PCT PPORT 270								
18	031275	02	PCT PPORT 275								
18	031280	02	PCT PPORT 280								
18	031285	02	PCT PPORT 285								
18	031290	02	PCT PPORT 290								
18	031295	02	PCT PPORT 295								
18	031300	02	PCT PPORT 300								
18	031305	02	PCT PPORT 305								
18	031310	02	PCT PPORT 310								
18	031315	02	PCT PPORT 315								
18	031320	02	PCT PPORT 320								
18	031325	02	PCT PPORT 325								
18	031330	02	PCT PPORT 330								
18	031335	02	PCT PPORT 335								
18	031340	02	PCT PPORT 340								
18	031345	02	PCT PPORT 345								
18	031350	02	PCT PPORT 350								
18	031355	02	PCT PPORT 355								
18	031360	02	PCT PPORT 360								
18	031365	02	PCT PPORT 365								
18	031370	02	PCT PPORT 370								
18	031375	02	PCT PPORT 375								
18	031380	02	PCT PPORT 380								
18	031385	02	PCT PPORT 385								
18	031390	02	PCT PPORT 390								
18	031395	02	PCT PPORT 395								
18	031400	02	PCT PPORT 400								
18	031405	02	PCT PPORT 405								
18	031410	02	PCT PPORT 410								
18	031415	02	PCT PPORT 415								
18	031420	02	PCT PPORT 420								
18	031425	02	PCT PPORT 425								
18	031430	02	PCT PPORT 430								
18	031435	02	PCT PPORT 435								
18	031440	02	PCT PPORT 440								
18	031445	02	PCT PPORT 445								
18	031450	02	PCT PPORT 450								
18	031455	02	PCT PPORT 455								
18	031460	02	PCT PPORT 460								
18	031465	02	PCT PPORT 465								
18	031470	02	PCT PPORT 470								
18	031475	02	PCT PPORT 475								
18	031480	02	PCT PPORT 480								
18	031485	02	PCT PPORT 485								
18	031490	02	PCT PPORT 490								
18	031495	02	PCT PPORT 495								
18	031500	02	PCT PPORT 500								
18	031505	02	PCT PPORT 505								
18	031510	02	PCT PPORT 510								
18	031515	02	PCT PPORT 515								
18	031520	02	PCT PPORT 520								
18	031525	02	PCT PPORT 525								
18	031530	02	PCT PPORT 530								
18	031535	02	PCT PPORT 535								
18	031540	02	PCT PPORT 540								
18	031545	02	PCT PPORT 545								
18	031550	02	PCT PPORT 550								
18	031555	02	PCT PPORT 555								
18	031560	02	PCT PPORT 560								
18	031565	02	PCT PPORT 565								
18	031570	02	PCT PPORT 570								
18	031575	02	PCT PPORT 575								
18	031580	02	PCT PPORT 580								
18	031585	02	PCT PPORT 585								
18	031590	02	PCT PPORT 590								
18	031595	02	PCT PPORT 595								
18	031600	02	PCT PPORT 600								
18	031605	02	PCT PPORT 605								
18	031610	02	PCT PPORT 610								
18	031615	02	PCT PPORT 615								
18	031620	02	PCT PPORT 620								
18	031625	02	PCT PPORT 625								
18	031630	02	PCT PPORT 630								
18	031635	02	PCT PPORT 635								
18	031640	02	PCT PPORT 640								
18	031645	02	PCT PPORT 645								
18	031650	02	PCT PPORT 650								
18	031655	02	PCT PPORT 655								
18	031660	02	PCT PPORT 660								
18	031665	02	PCT PPORT 665								
18	031670	02	PCT PPORT 670								
18	031675	02	PCT PPORT 675								
18	031680	02	PCT PPORT 680								
18	031685	02	PCT PPORT 685								
18	031690	02	PCT PPORT 690								
18	031695	02	PCT PPORT 695								
18	031700	02	PCT PPORT 700								
18	031705	02	PCT PPORT 705								
18	031710	02	PCT PPORT 710								
18	031715	02	PCT PPORT 715								
18	031720	02	PCT PPORT 720								
18	031725	02	PCT PPORT 725								
18	031730	02	PCT PPORT 730								
18	031735	02	PCT PPORT 735								
18	031740	02	PCT PPORT 740								
18	031745	02	PCT PPORT 745								
18	031750	02	PCT PPORT 750								
18	031755	02	PCT PPORT 755								
18	031760	02	PCT PPORT 760								
18	031765	02	PCT PPORT 765								
18	031770	02	PCT PPORT 770								
18	031775	02	PCT PPORT 775								
18	031780	02	PCT PPORT 780								
18	031785	02	PCT PPORT 785								
18	031790	02	PCT PPORT 790								
18	031795	02	PCT PPORT 795								
18	031800	02	PCT PPORT 800								
18	031805	02	PCT PPORT 805								
18	031810	02	PCT PPORT 810								
18	031815	02	PCT PPORT 815								
18	031820	02	PCT PPORT 820								



TODAY: 01/07/81

FLIGHT INSTRUMENTATION PARAMETER LIST  
REV: D DATE: 7/24/79

PAGE 6 OF COPY 1

VEHICLE: KC-135 WINGLIFT PROGRAM  
FLT NO: 054  
SCHED FLT DATE: 12/24/80  
TM FREQ: 447 S/M  
PCM SYS/CJM NO: 1-00 FORMAT NO: 1  
PCM SYS MODEL: RMDU

PROJ INSTR ENGR: GENE KENNER

PCM BIT RATE: 125 KHZ  
BITS/WOPD: 1C  
WORDS/FRAME: 64  
FR/DATA CY: 1C  
FBT=BIT1=MSB

MAIN FRAME SYNC WCFDS: 00, 01, 02

S/V PRESSURE PARMID SV40  
SYS ITEM NO/REF NO POS 19 18  
SCANIVALVE NO: 4  
S/V REF PRESSURE PARMID SVRPOB

S/V PORT ID SVID4  
SYS ITEM NO/FR WD POS 23 22

ITEM	PARAMETER	PORT	PARAMETERS AFFECTED	PORT
NO.	NAME	ID DEC	NO.	NO.
SYS 1	PARMID 1	NAME	REMARKS	
19	SATEFO1	REFERENCE PRESSURE PORT 1	1C PORTS / SECOND	1
19	R5U00	101 Y PORT U00		2
19	R5U02	101 Y PORT 02		3
19	R5U05	101 Y PORT 05	20 SAMPLES / PORT	4
19	R5U15	101 Y PORT 15		5
19	R5U25	101 Y PORT 25		6
19	R5U35	101 Y PORT 35		7
19	R5U45	101 Y PORT 45		8
19	R5U55	101 Y PORT 55		9
19	R5U65	101 Y PORT 65		10
19	R5U75	101 Y PORT 75		11
19	R5U85	101 Y PORT 85		12
19	R5U95	101 Y PORT 95		13
19	R5L02	101 Y PORT L02		14
19	R5L05	101 Y PORT L05		15
19	R5L15	101 Y PORT L15		16
19	R5L25	101 Y PORT L25		17
19	R5L35	101 Y PORT L35		18
19	R5L45	101 Y PORT L45		19
19	R5L55	101 Y PORT L55		20
19	R5L65	101 Y PORT L65		21
19	R5L75	101 Y PORT L75		22
19	R5L85	101 Y PORT L85		23
19	R5L95	101 Y PORT L95		24
19	R6U00	103 Y PORT U00		25
19	R6U02	103 Y PORT U02		26
19	R6U05	103 Y PORT U05		27
19	R6U15	103 Y PORT U15		28
19	R6U25	103 Y PORT U25		29
19	R6U35	103 Y PORT U35		30
19	R6U45	103 Y PORT U45		31
19	R6U55	103 Y PORT U55		32
19	R6U65	103 Y PORT U65		33
19	R6U75	103 Y PORT U75		34
19	R6U85	103 Y PORT U85		35
19	R6U95	103 Y PORT U95		36
19	R6L02	103 Y PORT L02		37
19	R6L05	103 Y PORT L05		38
19	R6L15	103 Y PORT L15		39
19	R6L25	103 Y PORT L25		40
19	R6L35	103 Y PORT L35		41
19	R6L45	103 Y PORT L45		42
19	R6L55	103 Y PORT L55		43
19	R6L65	103 Y PORT L65		44
19	R6L75	103 Y PORT L75		45
19	R6L85	103 Y PORT L85		46
19	R6L95	103 Y PORT L95		47
19	S4REF49	REFERENCE PRESSURE PORT 46		48

TODAY: 01/07/81

# FLIGHT INSTRUMENTATION PARAMETER LIST

PAGE 7 OF COPY 1

VEHICLE: KC-135 WINGLFT PROGRAM  
 FLT NO: 054  
 SCHED FLT DATE: 12/24/80  
 TM FREQ: MHZ S/M  
 PCM SYS/CJM NO: 1-00 FOPHAT NO: 1  
 PCM SYS MODEL: R4DU

REV: 0 DATE: 7/24/79  
 PROJ INST: ENGR: GENE KENNER

PCM BIT RATE: 125 KHZ  
 BITS/WORD: 10  
 WORDS/FRAME: 64  
 FR/DATA CY: 10  
 FBT-BIT1=MSB

MAIN FRAME SYNC WORDS: 00, 01, 02

S/V PRESSURE PARMID		SV5P		SCANIVALVE NO. 5		S/V REF PRESSURE PARMID SVRPOB		S/V PORT ID		SVI05	
SYS_ITEM_ND/REF_WD_POS		22 19		SYS_ITEM_ND/REF_WD_POS		36 35		SYS_ITEM_ND/REF_WD_POS		24 23	
PARAMETER		PORT 1		PARAMETERS AFFECTED		PORT 1		PORT 1		PORT 1	
NO.	NAME	NO.	NAME	NO.	NAME	NO.	NAME	NO.	NAME	NO.	NAME
20	SVRPOB1	105	% PORT U00	1	10 PORTS / SECOND	1		1		1	
20	SVRPOB2	105	% PORT U02	2		2		2		2	
20	SVRPOB3	105	% PORT U05	3	20 SAMPLES / PORT	3		3		3	
20	SVRPOB4	105	% PORT U15	4		4		4		4	
20	SVRPOB5	105	% PORT L25	5		5		5		5	
20	SVRPOB6	105	% PORT L35	6		6		6		6	
20	SVRPOB7	105	% PORT L45	7		7		7		7	
20	SVRPOB8	105	% PORT L55	8		8		8		8	
20	SVRPOB9	105	% PORT L65	9		9		9		9	
20	SVRPOB10	105	% PORT L75	10		10		10		10	
20	SVRPOB11	105	% PORT L85	11		11		11		11	
20	SVRPOB12	105	% PORT L95	12		12		12		12	
20	SVRPOB13	105	% PORT L02	13		13		13		13	
20	SVRPOB14	105	% PORT L05	14		14		14		14	
20	SVRPOB15	105	% PORT L15	15		15		15		15	
20	SVRPOB16	105	% PORT L25	16		16		16		16	
20	SVRPOB17	105	% PORT L35	17		17		17		17	
20	SVRPOB18	105	% PORT L45	18		18		18		18	
20	SVRPOB19	105	% PORT L55	19		19		19		19	
20	SVRPOB20	105	% PORT L65	20		20		20		20	
20	SVRPOB21	105	% PORT L75	21		21		21		21	
20	SVRPOB22	105	% PORT L85	22		22		22		22	
20	SVRPOB23	105	% PORT L95	23		23		23		23	
20	SVRPOB24	105	% PORT L02	24		24		24		24	
20	SVRPOB25	105	% PORT L05	25		25		25		25	
20	SVRPOB26	105	% PORT L15	26		26		26		26	
20	SVRPOB27	105	% PORT L25	27		27		27		27	
20	SVRPOB28	105	% PORT L35	28		28		28		28	
20	SVRPOB29	105	% PORT L45	29		29		29		29	
20	SVRPOB30	105	% PORT L55	30		30		30		30	
20	SVRPOB31	105	% PORT L65	31		31		31		31	
20	SVRPOB32	105	% PORT L75	32		32		32		32	
20	SVRPOB33	105	% PORT L85	33		33		33		33	
20	SVRPOB34	105	% PORT L95	34		34		34		34	
20	SVRPOB35	105	% PORT L02	35		35		35		35	
20	SVRPOB36	105	% PORT L05	36		36		36		36	
20	SVRPOB37	105	% PORT L15	37		37		37		37	
20	SVRPOB38	105	% PORT L25	38		38		38		38	
20	SVRPOB39	105	% PORT L35	39		39		39		39	
20	SVRPOB40	105	% PORT L45	40		40		40		40	
20	SVRPOB41	105	% PORT L55	41		41		41		41	
20	SVRPOB42	105	% PORT L65	42		42		42		42	
20	SVRPOB43	105	% PORT L75	43		43		43		43	
20	SVRPOB44	105	% PORT L85	44		44		44		44	
20	SVRPOB45	105	% PORT L95	45		45		45		45	
20	SVRPOB46	105	% PORT L02	46		46		46		46	
20	SVRPOB47	105	% PORT L05	47		47		47		47	
20	SVRPOB48	105	% PORT L15	48		48		48		48	

TODAY: 01/07/81

FLIGHT INSTRUMENTATION PARAMETER LIST

PAGE 8 OF COPY 1

VEHICLE: KC-135 WINGLET PROGRAM  
 FLT NO: 054  
 SCHED FLT DATE: 12/24/80  
 TM FREQ: MMZ 5/M  
 PCM SYS/CTM NO. 1-01 FUPMAT NO. 1  
 PCM SYS MODFL: RMDU

PROJ INSTR ENGR: GENE KENNER

PCM BIT RATE: 125 KHZ  
 BITS/WORD: 10  
 WORDS/FRAME: 64  
 FR/DATA CY: 10  
 FRT=RTI=MSB

MAIN FRAME SYNC WORDS: 00, 01, 02

ITEM NO.	PARAMETER	NAME	DATE	RANGE	UNITS	FRAME NO.	SAMPLE RATE	COMP	REF	VP/TP	FILTER	ITEM
NO.	CALID			LOW	HIGH					KP		INC.
65:FTOT2F	1311 07 101	FUEL TOTALIZER ENG 2		0	512:COUNTS	421	0	39:1000				1
66:FTOT2F	1311 07 102 OK	FUEL TOTALIZER ENG 2	08/28/78	512	65535:COUNTS	421	0	39:1000			FTOT2F	2
67:RUDD	1311 04 017 8*	RUDDER POSITION	06/16/80	-25	25:DEG	431	0	39:1000				3
68:RUDD	1311 04 018 8*	RUDDER TRIM TAB POSITION	06/16/80	-21	22.5:DEG	441	0	39:1000				4
69:FFWD	1311 08 301 0*	FUEL FLOW RATE CIG. ENG. 1	06/16/80	0	40:GPM	451	0	39:1000				5
70:SFRT1	1311 02 323	FRONT SPAR BENDING UP SURF				461	0	119.5:4000				6
71:SFRT2	1311 02 324	FRONT SPAR SHEAR UP SURF				471	0	119.5:4000				7
72:SFRT3	1311 02 025	FRONT SPAR BENDING UP SURF				481	0	119.5:4000				8
73:SFRT4	1311 02 026	FRONT SPAR SHEAR UP SURF				491	0	119.5:4000				9
74:SFRT5	1311 02 327	FRONT SPAR BENDING UP SURF				501	0	119.5:4000				10
75:SFRT6	1311 02 328	AFT SPAR SHEAR UP SURF				511	0	119.5:4000				11
76:SFRT7	1311 02 329	AFT SPAR BENDING UP SURF				521	0	119.5:4000				12
77:PT2E1P1	1311 01 001 AP	PT-2 ENGINE 1 PORT 1	06/16/80	-4	4:PSID	531	0	119.5:4000:OPR01C				13
78:PT2E1P2	1311 01 002 AP	PT-2 ENGINE 1 PORT 2	06/16/80	-4	4:PSID	541	0	119.5:4000:OPR01C				14
79:PT2E1P3	1311 01 003 AP	PT-2 ENGINE 1 PORT 3	06/16/80	-4	4:PSID	551	0	119.5:4000:OPR01C				15
80:PT2E1P4	1311 01 004 AP	PT-2 ENGINE 1 PORT 4	06/16/80	-4	4:PSID	561	0	119.5:4000:OPR01C				16
81:PT2E1P5	1311 01 005 AP	PT-2 ENGINE 1 PORT 5	06/16/80	-4	4:PSID	571	0	119.5:4000:OPR01C				17
82:PT2E1P6	1311 01 006 AP	PT-2 ENGINE 1 PORT 6	06/16/80	-4	4:PSID	581	0	119.5:4000:OPR01C				18
83:PT2E1P7	1311 01 007 AP	PT-2 ENGINE 1 PORT 7	11/21/79	-4	4:PSID	591	0	20:4000:OPR01C				19
84:PT2E1P8	1311 01 008 AP	PT-2 ENGINE 1 PORT 8	07/19/80	-4	4:PSID	601	0	119.5:4000:OPR01C				20
85:PT2E2P1	1311 01 009 AP	PT-2 ENGINE 2 PORT 1	06/16/80	-4	4:PSID	611	0	119.5:4000:OPR01C				21
86:PT2E2P2	1311 01 010 AP	PT-2 ENGINE 2 PORT 2	06/16/80	-4	4:PSID	621	0	119.5:4000:OPR01C				22
87:PT2E2P3	1311 01 011 AP	PT-2 ENGINE 2 PORT 3	06/16/80	-4	4:PSID	631	0	119.5:4000:OPR01C				23
88:FTOT3F	1311 07 103	FUEL TOTALIZER ENG 3		0	512:COUNTS	431	0	39:1000				24
89:FTOT3F	1311 08 101 OK	FUEL TOTALIZER ENG 3	08/28/78	512	65535:COUNTS	431	0	39:1000			FTOT3F	25
90:DALLY	1311 04 021 0*	L/H INAD AILFRON POS	06/16/80	-19.4	16.5:DEG	441	0	39:1000				26
91:DALLY	1311 04 022 6*	R/H INAD AILFRON POS	10/30/80	-18.2	19.5:DEG	441	0	39:1000				27
92:AC19CN	1311 05 010 8*	COCKPIT NORMAL ACCFL	08/11/80	-1	3:G	451	0	39:1000				28
93:SFRT8	1311 02 030	AFT SPAR SHEAR UP SURF				461	0	119.5:4000				29
94:SFRT9	1311 02 031	AFT SPAR BENDING UP SURF				471	0	119.5:4000				30
95:SFRT10	1311 02 032	AFT SPAR SHEAR UP SURF				481	0	119.5:4000				31
96:SFRT11	1311 06 013	AFT BENDING UP SURF				491	0	119.5:4000				32
97:SFRT12	1311 06 014	FRONT SPAR BENDING UP SURF				501	0	119.5:4000				33
98:SFRT13	1311 06 015	FRONT SPAR SHEAR UP SURF				511	0	119.5:4000				34
99:SFRT14	1311 06 016	FRONT SPAR BENDING UP SURF				521	0	119.5:4000				35
100:PT2E2P4	1311 01 012 AP	PT-2 ENGINE 2 PORT 4	06/16/80	-4	4:PSID	531	0	119.5:4000:OPR01C				36
101:PT2E2P5	1311 01 013 AP	PT-2 ENGINE 2 PORT 5	06/16/80	-4	4:PSID	541	0	119.5:4000:OPR01C				37
102:PT2E2P6	1311 01 014 AP	PT-2 ENGINE 2 PORT 6	06/16/80	-4	4:PSID	551	0	119.5:4000:OPR01C				38
103:PT2E2P7	1311 01 015 AP	PT-2 ENGINE 2 PORT 7	06/16/80	-4	4:PSID	561	0	119.5:4000:OPR01C				39
104:PT2E2P8	1311 01 016 AP	PT-2 ENGINE 2 PORT 8	06/16/80	-4	4:PSID	571	0	119.5:4000:OPR01C				40
105:PT2E3P1	1311 01 017 AP	PT-2 ENGINE 3 PORT 1	06/16/80	-4	4:PSID	581	0	119.5:4000:OPR01C				41
106:PT2E3P2	1311 01 018 AP	PT-2 ENGINE 3 PORT 2	06/16/80	-4	4:PSID	591	0	119.5:4000:OPR01C				42
107:PT2E4P1	1311 01 019 AP	PT-2 ENGINE 4 PORT 1	06/16/80	-4	4:PSID	601	0	119.5:4000:OPR01C				43
108:PT2E4P2	1311 01 020 AP	PT-2 ENGINE 4 PORT 2	06/16/80	-4	4:PSID	611	0	119.5:4000:OPR01C				44
109:PT2E1P8	1311 01 021 AP	PT-2 ENGINE 1 PORT 8	06/16/80	-4	4:PSID	621	0	119.5:4000:OPR01C				45
110:PT2E1P8	1311 01 022 AP	PT-2 ENGINE 1 PORT 8	06/16/80	-4	4:PSID	631	0	119.5:4000:OPR01C				46
111:FTOT4F	1311 08 102	FUEL TOTALIZER ENG 4		0	512:COUNTS	441	0	39:1000				47
112:FTOT4F	1311 08 103 OK	FUEL TOTALIZER ENG 4	08/28/78	512	65535:COUNTS	441	0	39:1000			FTOT4F	48

TODAY: 01/07/81

FLIGHT INSTRUMENTATION PARAMETER LIST  
REV: D DATE: 7/24/79

PAGE 9 OF COPY 1

VEHICLE: KC-135 WINGLET PROGRAM  
FLT NO: 754  
SCHED FLT DATE: 12/24/80  
TH FREQ: 447 S/M  
PCM SYS/COMP NO: 1-01 FJRMAT NO. 1  
PCM SYS MODEL: RMFU

PROJ INSTR ENGR: GENE KENNER

PCM BIT RATE: 125 KBZ  
BITS/WORD: 10  
WORDS/FRAME: 64  
FR/DATA CY: 10  
FRT-RIT1=MSB

MAIN FRAME SYNC WORDS: 00, 01, 02

ITEM	PARAMETER	UNIT	NAME	DATE	LOW	HIGH	UNITS	FRAME	FRAME	FRAME	COMP	REF	VM/TP	FILTER	ITEM
NO.	PARAMETER	UNIT	NAME	DATE	LOW	HIGH	UNITS	FRAME	FRAME	FRAME	COMP	REF	VM/TP	FILTER	ITEM
11700ALLCT	1311 04 023 RM	L/H INNR ALL CONTROL TAR	106/16/RC	-21.5	19.5	DEG	431	21	3914000	1	1	551	61	49	
11610ALLPCT	1311 04 024 RM	R/H INNR ALL CONTROL TAR	106/16/RC	-20	21.5	DEG	441	21	3914000	1	1	551	61	50	
11610ALL	1311 04 025 RM	C.G. NORMAL ACCEL	106/16/RC	-1	31G		451	21	3914000	1	1	3118	51		
11610GRT16	1311 04 017	FRONT SPAR	LO SURF	1	1		461	219.5	514000	1	1	551	61	52	
11710GRT16	1311 04 018	FRONT SPAR	LO SURF	1	1		471	219.5	514000	1	1	551	61	53	
11810GRT17	1311 04 019	AFT SPAR SHEAR	LO SURF	1	1		481	219.5	514000	1	1	551	61	54	
11910GRT18	1311 04 020	AFT SPAR BENDING	LO SURF	1	1		491	219.5	514000	1	1	551	61	55	
12010GRT19	1311 04 021	AFT SPAR SHEAR	LO SURF	1	1		501	219.5	514000	1	1	551	61	56	
12110GRT20	1311 04 022	AFT SPAR BENDING	LO SURF	1	1		511	219.5	514000	1	1	551	61	57	
12210GRT21	1311 04 023	AFT SPAR SHEAR	LO SURF	1	1		521	219.5	514000	1	1	551	61	58	
12310GRT22	1311 04 024	ENG 1 WAKE PORT C	106/16/RC	-6	61PSID		531	219.5	514000	OPR01C	1	1	51	61	59
12410GRT23	1311 04 025	ENG 1 WAKE PORT D	106/16/RC	-6	61PSID		541	219.5	514000	OPR01C	1	1	51	61	60
12510GRT24	1311 04 026	ENG 2 WAKE PORT A	106/16/RC	-6	61PSID		551	219.5	514000	OPR01C	1	1	51	61	61
12610GRT25	1311 04 027	ENG 2 WAKE PORT B	106/16/RC	-6	61PSID		561	219.5	514000	OPR01C	1	1	51	61	62
12710GRT26	1311 04 028	ENG 2 WAKE PORT C	106/16/RC	-6	61PSID		571	219.5	514000	OPR01C	1	1	51	61	63
12810GRT27	1311 04 029	ENG 2 WAKE PORT D	106/16/RC	-6	61PSID		581	219.5	514000	OPR01C	1	1	51	61	64
12910GRT28	1311 04 030	ENG 3 WAKE PORT A	106/16/RC	-6	61PSID		591	219.5	514000	OPR01C	1	1	51	61	65
13010GRT29	1311 04 031	ENG 3 WAKE PORT B	106/16/RC	-6	61PSID		601	219.5	514000	OPR01C	1	1	51	61	66
13110GRT30	1311 04 032	ENG 3 WAKE PORT C	106/16/RC	-6	61PSID		611	219.5	514000	OPR01C	1	1	51	61	67
13210GRT31	1311 04 033	ENG 3 WAKE PORT D	106/16/RC	-6	61PSID		621	219.5	514000	OPR01C	1	1	51	61	68
13310GRT32	1311 04 034	VOLTAG MONITOR 10 V	102/16/79	0	101COUNTS		631	21	2014000	1	1	51	61	69	
13410GRT33	1311 04 035	PORT KFF PRESS	1	1	1PSIA		641	31	3914000	1	1	1	1	70	
13510GRT34	1311 04 036	PORT KFF PRESS	106/16/RC	0	401PSIA		651	31	3914000	OPR01F	1	1	1	71	
13610GRT35	1311 04 037	R/H ELEVATOR POSITION	106/16/RC	-24.5	151DEG		661	31	3914000	1	1	551	61	72	
13710GRT36	1311 04 038	ELEVATOR CONTROL TAR PJS	102/20/79	-17.5	23.5	DEG	671	31	3914000	1	1	551	61	73	
13810GRT37	1311 04 039	WING STAB POSITION	106/16/RC	-13.5	51DEG		681	31	3914000	1	1	551	61	74	
13910GRT38	1311 04 040	AFT SPAR BENDING	LO SURF	1	1		691	319.5	514000	1	1	551	61	75	
14010GRT39	1311 04 041	O/B WING REAR SPAR 779 MAIN	1	1	1		701	319.5	514000	1	1	551	61	76	
14110GRT40	1311 04 042	O/B WING REAR SPAR 779 SPARE	1	1	1		711	319.5	514000	1	1	551	61	77	
14210GRT41	1311 04 043	O/B WING AUX SPAR 779 MAIN	1	1	1		721	319.5	514000	1	1	551	61	78	
14310GRT42	1311 04 044	O/B WING AUX SPAR 779 SPARE	1	1	1		731	319.5	514000	1	1	551	61	79	
14410GRT43	1311 04 045	O/B WING FR SPAR 745 MAIN	1	1	1		741	319.5	514000	1	1	551	61	80	
14510GRT44	1311 04 046	O/B WING FR SPAR 745 SPARE	1	1	1		751	319.5	514000	1	1	551	61	81	
14610GRT45	1311 04 047	PT-7 ENG 1 DIFF PRESS	110/21/RC	0	401PSID		761	319.5	514000	OPR01C	1	1	51	61	82
14710GRT46	1311 04 048	PT-7 ENG 2 DIFF PRESS	110/21/RC	0	401PSID		771	319.5	514000	OPR01C	1	1	51	61	83
14810GRT47	1311 04 049	PT-7 ENG 3 DIFF PRESS	110/21/RC	0	401PSID		781	319.5	514000	OPR01C	1	1	51	61	84
14910GRT48	1311 04 050	PT-7 ENG 4 DIFF PRESS	106/16/RC	0	401PSID		791	319.5	514000	OPR01C	1	1	51	61	85
15010GRT49	1311 04 051	PT-7 ENG 1 DIFF PRESS	106/16/RC	-30	301PSID		801	319.5	514000	OPR01C	1	1	51	61	86
15110GRT50	1311 04 052	PT-7 ENG 2 DIFF PRESS	106/16/RC	-30	301PSID		811	319.5	514000	OPR01C	1	1	51	61	87
15210GRT51	1311 04 053	PT-7 ENG 3 DIFF PRESS	106/16/RC	-30	301PSID		821	319.5	514000	OPR01C	1	1	51	61	88
15310GRT52	1311 04 054	PT-7 ENG 4 DIFF PRESS	106/16/RC	-30	301PSID		831	319.5	514000	OPR01C	1	1	51	61	89
15410GRT53	1311 04 055	PT-7 ENG 2 DIFF PRESS	110/21/RC	0	401PSID		841	319.5	514000	OPR01C	1	1	51	61	90
15510GRT54	1311 04 056	FUEL TEMP ENGINE 1	110/01/80	0	1351DEG F		851	319.5	514000	1	1	101	61	91	
15610GRT55	1311 04 057	FUEL TEMP ENGINE 2	110/01/80	0	1351DEG F		861	319.5	514000	1	1	101	61	92	
15710GRT56	1311 04 058	AIRSPEC	1	1	1KNOTS		871	41	3914000	1	1	1	1	93	
15810GRT57	1311 04 059	AIRSPEC	108/09/79	0	1000KNOTS		881	41	3914000	1	1	1	1	94	
15910GRT58	1311 04 060	C.G. LONG ACCEL SENSITIVE	106/16/RC	-0.25	0.251G		891	41	3914000	1	1	3118	51	95	
16010GRT59	1311 04 061	C.G. LONG ACCEL	106/16/RC	-1	11G		901	41	3914000	1	1	3118	51	96	

TIME: 01/07/81

# FLIGHT INSTRUMENTATION PARAMETER LIST

PAGE 10 OF COPY 1

VEHICLE: KC-135 WINGLET PROGRAM  
 FLT NO: 354  
 SCHED FLT DATE: 12/24/80  
 TM FREQ: MH7 J/N  
 PCM SYS/CDR NO: 1-01 CDR MAT NO: 1  
 PCM SYS MODEL: RMDU

REV: 0 DATE: 7/24/79  
 PROJ INSTR ENGR: GENF KENNER

PCM BIT RATE: 125 KHZ  
 BITS/WORD: 10  
 WORDS/FRAME: 64  
 FR/DATA CY: 10  
 FRT=RT1=MSB

MAIN FRAME SYNC WORDS: 00, 01, 02

TIME	PARAMETER	NAME	DATE	UNIT	WORD NO.	FRAME	SAMP	COMP	REF	VM/TF	FILTER	ITH
NO.	PARAMETER	NAME	DATE	UNIT	WORD NO.	FRAME	SAMP	COMP	REF	VM/TF	FILTER	ITH
1611AY	1311 04 030 A	C.G. LAT ACCEL	06/16/80	1/G	45	41	3914000					
1621SGW3	1311 07 001	U/R WING SHR FR SPAR 745-1			46	41	19.514000					551 61 98
1631SGW4	1311 07 002	U/R WING SHR FR SPAR 745-2			47	41	19.514000					551 61 99
1641SGW5	1311 07 003	U/R WING REAR SPAR 745 MAIN			48	41	19.514000					551 61 100
1651SGW6	1311 07 004	U/R WING REAR SPAR 745 SPARE			49	41	19.514000					551 61 101
1661SGW7	1311 07 005	U/R WING SHR REAR SPAR 745-1			50	41	19.514000					551 61 102
1671SGW8	1311 07 006	U/R WING SHR REAR SPAR 745-2			51	41	19.514000					551 61 103
1681SGW9	1311 06 001	R/H OUTDR WING PANEL			52	41	19.514000					551 61 104
1691FTW3	1311 03 008 C	FUEL TEMP ENGINE 3	10/01/80	0 135 DEG F	53	41	19.514000					551 61 105
1701FTW4	1311 03 014 C	FUEL TEMP ENGINE 4	10/01/80	0 135 DEG F	54	41	19.514000					551 61 106
1711FVFTC	1311 02 017 J	EVENT-DEFLECTION CAMERA	08/30/79	OFF	55	41	19.514000					101 61 107
1721THFTA	1311 03 016 A	PITCH ANGLE	06/16/80	-30	56	41	19.514000					101 61 108
1731DFL3L	1311 05 021 R	L/H OUTDR FLAP POSITION	06/16/80	0 50 DEG	57	41	19.514000					101 61 109
1741DFL3R	1311 05 022 J	R/H OUTDR FLAP POSITION	06/16/80	0 50 DEG	58	41	19.514000					101 61 110
1751DFLVL	1311 05 023 C	L/H ELEVATOR POSITION	06/16/80	-23.5	59	41	19.514000					551 61 111
1761VVE1	1311 03 009 O	BLEED VALVE ENG NO 1	02/20/79	0 500 PSIA	60	41	19.514000					551 61 112
1771VVE2	1311 03 010 O	BLEED VALVE ENG NO 2	02/20/79	0 500 PSIA	61	41	19.514000					551 61 113
1781VVE3	1311 03 011 J	BLEED VALVE ENG NO 3	02/20/79	0 500 PSIA	62	41	19.514000					551 61 114
1791VVE4	1311 03 012 J	BLEED VALVE ENG NO 4	02/20/79	0 500 PSIA	63	41	19.514000					551 61 115
1801SGWR2	1311 06 002	WINGLET MOMENT FR SPAR SPARE			46	51	19.514000					551 61 116
1811SGWR3	1311 06 005	WINGLET SHEAR FR SPAR MAIN			47	51	19.514000					551 61 117
1821SGWR4	1311 06 006	WINGLET SHEAR FR SPAR SPARE			48	51	19.514000					551 61 118
1831SGWR5	1311 06 003	WINGLET MOM REAR SPAR MAIN			49	51	19.514000					551 61 119
1841SGWR6	1311 06 004	WINGLET MOM REAR SPAR SPARE			50	51	19.514000					551 61 120
1851SGWR7	1311 06 007	WINGLET SHR REAR SPAR MAIN			51	51	19.514000					551 61 121
1861SGWR8	1311 06 008	WINGLET SHR REAR SPAR SPARE			52	51	19.514000					551 61 122
1871FVFT1	1311 03 013 J	PILIT EVENT	02/15/79	OFF	53	51	19.514000					551 61 123
1881ACF0AL	1311 05 011 E	FLIGHT PATH LONG ACCEL	06/16/80	-25	54	51	19.514000					318 61 124
1891ACF0AN	1311 05 012 A	FLIGHT PATH NORM ACCEL	06/16/80	-3	55	51	19.514000					318 61 125
1901DFLL3	1311 05 024 R	L/H LF FLAP POS OUTDR	06/16/80	0 100 PERCENT	56	51	19.514000					101 61 126
1911DFLL3	1311 05 025 B	R/H LF FLAP POS OUTDR	06/16/80	0 100 PERCENT	57	51	19.514000					101 61 127
1921TTP001	1311 03 019 J	TOTAL TEMPERATURE	03/02/79	-70	58	51	19.514000					551 61 128
1931FRT1	1311 03 020 J	EXHAUST TOTAL TEMP ENG 1	03/05/79	0 1200 DEG F	59	51	19.514000					551 61 129
1941FRT2	1311 03 021 O	EXHAUST TOTAL TEMP ENG 2	03/05/79	0 1200 DEG F	60	51	19.514000					551 61 130
1951FRT3	1311 03 022 O	EXHAUST TOTAL TEMP ENG 3	03/05/79	0 1200 DEG F	61	51	19.514000					551 61 131
1961FRT4	1311 03 023 O	EXHAUST TOTAL TEMP ENG 4	03/05/79	0 1200 DEG F	62	51	19.514000					551 61 132
1971VW002	1311 05 018	VOLTAGE MONITOR 5V XCR PWR			63	51	19.514000					551 61 133
1981SGWR9	1311 06 009	WINGLET SHR I/R SKIN MAIN			46	61	19.514000					551 61 134
1991SGWR10	1311 06 010	WINGLET SHR I/R SKIN SPARE			47	61	19.514000					551 61 135
2001SGF2	1311 07 021	FATIGUE STRESS GAGE 2			48	61	19.514000					551 61 136
2011SGF2A	1311 07 022	FATIGUE STRESS GAGE 2A			49	61	19.514000					551 61 137
2021SGF3	1311 07 023	FATIGUE STRESS GAGE 3			50	61	19.514000					551 61 138
2031VFF15	1311 07 020 C	LG FUSELAGE LONG ACCEL	06/16/80	-1	51	61	19.514000					318 61 139
2041AC11FL	1311 07 030 C	CLOCKFIT LONG ACCEL	06/16/80	-1	52	61	19.514000					318 61 140
2051RPM1	1311 03 025 A	RPM ENG NO 1 N1	06/16/80	C10000RPM	53	61	19.514000					551 61 141
2061RPM2	1311 03 026 A	RPM ENG NO 2 N1	06/16/80	C10000RPM	54	61	19.514000					551 61 142
2071RPM3	1311 03 027 A	RPM ENG NO 3 N1	06/16/80	C10000RPM	55	61	19.514000					551 61 143
2081RPM4	1311 03 028 A	RPM ENG NO 4 N1	06/16/80	C10000RPM	56	61	19.514000					551 61 144

TPDAY: 01/07/81

FLIGHT INSTRUMENTATION PARAMETER LIST  
REV: D DATE: 7/24/79

PAGE 11 OF COPY 1

VF41CLF: KC-135 WINGLET PROGPAM  
FLT NO: 054  
SCHED FLT DATE: 12/24/80  
TM FRQ: 4MHZ S/M  
PCM SYS/CDM NO. 1-01 FJPMAT NO. 1  
PCM SYS MODEL: RMLU

PCM BIT RATE: 125 KHZ  
BITS/WORD: 10  
WORDS/FRAME: 64  
FR/DATA CY: 10  
FBT-BIT1-HSR

MAIN FRAME SYNC WORDS: 00, 01, 02

YTM	NO.	PARAM	NAME	DATE	RANGE	UNITS	WORD	NO.	RATE	ALG	REF	VM/TH	FILTER	ITEM
					LOW	HIGH								
200	FFR1	1311 03 029	FUEL FLOW RATE ENG NO 1	106/16/80	0	30 GAL/MIN	57	619.514000						1145
210	FFR2	1311 03 030	FUEL FLOW RATE ENG NO 2	106/16/80	0	30 GAL/MIN	58	619.514000						1146
211	FFR3	1311 03 031	FUEL FLOW RATE ENG NO 3	106/16/80	0	30 GAL/MIN	59	619.514000						1147
212	FFR4	1311 03 032	FUEL FLOW RATE ENG NO 4	106/16/80	0	30 GAL/MIN	60	619.514000						1148
213	PPS4FL	1311 05 020	SAF TAB POSITION LEFT	107/25/79	-22.0	23.0 DEG	61	619.514000						1149
214	PLA1	1311 04 005	POWER LEVER ANGLE ENG NO 1	106/16/80	0	100 PERCENT	62	619.514000						1150
215	PLA2	1311 04 006	POWER LEVER ANGLE ENG NO 2	106/16/80	0	100 PERCENT	63	619.514000						1151
216	GRSSW	1310 RC 001	GRSS WEIGHT (ANALOG COARSE)	106/16/80	100K	300K LB	46	719.514000						1152
217	GRSSWF	1310 RC 002	GRSS WEIGHT (ANALOG FINE)	106/16/80	100K	300K LB	47	719.514000						1153
218	WTDIG	1310 RC 003	GRSS WEIGHT (DIG COARSE)	106/16/80	100K	300K LB	48	719.514000						1154
219	WTDIGF	1310 RC 004	GRSS WEIGHT (DIG FINE)	106/16/80	100K	300K LB	49	719.514000						1155
220	NIHL	1311 00 507					50	120000						1156
221	ACDOLN	1311 07 031	AFT BODY LONG ACCEL	106/16/80	-1	1 G	51	719.514000						1157
222	FFR2	1311 03 030	FUEL FLOW RATE DIG. ENG. 2	111/13/80	0	30 GAL/MIN	52	719.514000						1158
223	PSPL7	1311 04 001	L/H SPOILER OUTBD POS	106/16/80	0	60 DEG	53	719.514000						1159
224	PSPL7	1311 04 002	L/H SPOILER INBD POS	106/16/80	0	60 DEG	54	719.514000						1160
225	PSPL7	1311 04 003	R/H SPOILER OUTBD POS	106/16/80	0	60 DEG	55	719.514000						1161
226	PSPL7	1311 04 004	R/H SPOILER INBD POS	106/16/80	0	60 DEG	56	719.514000						1162
227	DFLLFT	1311 04 004	L/H LF FLAP POS INPD	106/16/80	0	100 PERCENT	57	719.514000						1163
228	DFRLFT	1311 04 010	R/H LF FLAP POS INPD	106/16/80	0	100 PERCENT	58	719.514000						1164
229	DFLRLT	1311 04 015	L/H FLAP POS INPD	106/16/80	0	50 DEG	59	719.514000						1165
230	DFLRLT	1311 04 016	R/H FLAP POS INPD	106/16/80	0	50 DEG	60	719.514000						1166
231	FFR03	1311 08 303	FUEL FLOW RATE DIG. ENG. 3	106/16/80	0	40 GPM	61	719.514000						1167
232	PLA3	1311 04 007	POWER LEVER ANGLE ENG NO 3	106/16/80	0	100 PERCENT	62	719.514000						1168
233	PLA4	1311 04 008	POWER LEVER ANGLE ENG NO 4	106/16/80	0	100 PERCENT	63	719.514000						1169
234	SGM15	1311 06 025	O/R WING FR SPAR #12 MAIN				46	819.514000						1170
235	SGM15	1311 06 026	O/R WING FR SPAR #12 SPARE				47	819.514000						1171
236	SGM17	1311 06 027	O/R WING REAR SPAR FOR MAIN				48	819.514000						1172
237	SGM19	1311 06 028	O/R WING REAR SPAR FOR SPARE				49	819.514000						1173
238	CTG01	1311 11 401	FUEL TEMP DIG. ENG. 1	107/24/80	0	212 F	50	819.514000						1174
239	CTG02	1311 11 402	FUEL TEMP DIG. ENG. 2	107/24/80	0	212 F	51	819.514000						1175
240	CTG03	1311 11 403	FUEL TEMP DIG. ENG. 3	107/24/80	0	212 F	52	819.514000						1176
241	NIHL	1311 01 538					53	120000						1177
242	NIHL	1311 01 539					54	120000						1178
243	PPS4FR	1311 04 011	SAF TAB POS RIGHT	107/15/79	-22	18 DEG	55	619.514000						1179
244	PPS4FR	1311 04 012	PPS4 POSITION	106/16/80	-3.5	3.5 IN	56	619.514000						1180
245	WHL	1311 04 013	WHEEL POSITION	106/16/80	-90	90 DEG	57	619.514000						1181
246	NCCLM	1311 04 014	CGNTAL COLUMN POSITION	106/16/80	-10.5	17.0 DEG	58	619.514000						1182
247	TD	1311 03 003	PITCH RATE	102/28/79	-40	40 DEG/SEC	59	619.514000						1183
248	TD	1311 03 004	ROLL RATE	102/28/79	-40	40 DEG/SEC	60	619.514000						1184
249	TD	1311 03 005	YAW RATE	102/28/79	-10	10 DEG/SEC	61	619.514000						1185
250	PPMAT	1311 03 017	ANGLE OF ATTACK (BDDM)	106/16/80	-5	18 DEG	62	619.514000						1186
251	PPMAT	1311 03 018	ANGLE OF SIDESLIP (BDDM)	106/16/80	-8	9 DEG	63	619.514000						1187
252	FFR1F5	1311 05 026	FUEL FLOW RATE SENS ENG 1	106/16/80	0	15 GPM	46	919.514000						1188
253	FFR2F5	1311 05 027	FUEL FLOW RATE SENS ENG 2	106/16/80	0	15 GPM	47	919.514000						1189
254	FFR3F5	1311 05 028	FUEL FLOW RATE SENS ENG 3	106/16/80	0	15 GPM	48	919.514000						1190
255	FFR4F5	1311 05 029	FUEL FLOW RATE SENS ENG 4	106/16/80	0	15 GPM	49	919.514000						1191
256	CTG04	1311 11 404	FUEL TEMP DIG. ENG. 4	107/24/80	0	212 F	50	919.514000						1192

TDAY: 01/07/81

FLIGHT INSTRUMENTATION PARAMETER LIST  
REV: D DATE: 7/24/79

PAGE 12 OF COPY 1

VEHICLE: KC-135 WINGLET PROGRAM  
FLT NO: 354  
SCHED FLT DATE: 12/24/80  
TM FREQ: 447.3/M  
PCM SYS/COM NO: 1-01 FUPHAT NO. 1  
PCM SYS MODEL: RMDI

PMOJ INSTR ENGR: GENE KENNER

PCM BIT RATE: 125 KHZ  
RTS/WORD: 10  
WORDS/FRAME: 64  
FR/CATA CY: 10  
FRT=BIT1=MSB

MAIN FRAME SYNC WORDS: 00, 01, 02

TTM	NO.	PARMTH	CALC	PARAMETER	NAME	DATE	RANGE	UNITS	FRAME	FRAME	SAMP	COMP	REF	VM/TM	FILTER	TTM
SYS							LOW	HIGH	WORD	NO.	RATE	ALG	PRESS	KP		INC.
257	NULL	1311	00	519					51	9	12000					1193
258	NULL	1311	00	529					52	9	12000					1194
259	FTOTIF	1311	11	102	FUEL TOTALIZER ENG 1		0	511	COUNTS	53	9	2011000				1195
260	FTOTIF	1311	11	103	FUEL TOTALIZER ENG 1	108/28/78	512	65535	COUNTS	54	9	2011000			FTOTIF	1196
261	PCMLLC	1311	00	559	PCM LOW LEVEL CAL				55	9	11000					1197
262	PCMHLC	1311	00	569	PCM HI LEVEL CAL				56	9	11000					1198
263	PCMSA	1311	00	579	GPA TERT				57	9	11000					1199
264	PCMPS	1311	00	589	PCM PWR SUPPLY				58	9	11000					1200
265	NULL	1311	00	609					59	9	119.5	12000				1201
266	FFR04	1311	08	304	FUEL FLOW RATE DIG. ENG. 4	106/16/80	0	40	GPM	60	9	119.5	14000			1202
267	401	1311	11	101	ALTITUDE	164/04/79	0	8000	FEET	62	9	119.5	11000		HPIF	1203
269	401	1311	10	103	ALTITUDE				61	9	119.5	11000				1204
269	TAPE04	1311	00	963	TAPE ON		0	1		63	9	119.5	14000			1205

TODAY: 01/07/81

FLIGHT INSTRUMENTATION PARAMETER LIST  
REV: D DATE: 7/24/79

PAGE 13 OF COPY 1

VEHICLE: KC-135 WINGLET PROGRAM  
FLT NO: 054  
SCHED FLT DATE: 12/24/80  
TM FREQ: 447.5 MHz  
PCM SYS/CUM NO: 1-01 FORMAT NO: 1  
PCM SYS MODEL: RMDU

PROJ INSTR ENGR: GENE KENNER

PCM BIT RATE: 125 KHZ  
BITS/WORD: 16  
WORDS/FRAME: 64  
FR/DATA CY: 10  
FRT-BIT1=MSB

MAIN FRAME SYNC WORDS: 00, 01, 02

DIGITAL WORD INFORMATION										MAIN FRAME SYNC WORDS	
ITEM NO.	PARAMETER	FRAME	FRAME BIT	BIT DESIGNATION	PARAMETERS AFFECTED	ITEM NO.	PARAMETER	FRAME	FRAME BIT	BIT DESIGNATION	PARAMETERS AFFECTED
260	FTJT1C FUEL TOTALIZER ENG NO 1	54	0	1	32768	1	FTJT1C FUEL TOTALIZER ENG NO 1	54	0	1	32768
260				2	16384	2					
260				3	8191	3					
260				4	4096	4					
260				5	2048	5					
260				6	1024	6					
260				7	512	7					
260				8		8					
260				9		9					
260				10		10					
259	FTOT1F FUEL TOTALIZER ENG NO 1	53	0	1	256	11	FTOT1F FUEL TOTALIZER ENG NO 1	53	0	1	256
259				2	128	12					
259				3	64	13					
259				4	32	14					
259				5	16	15					
259				6	8	16					
259				7	4	17					
259				8	2	18					
259				9	1	19					
259				10		20					
66	FTJT2C FUEL TOTALIZER ENG NO 2	42	0	1	32768	21	FTJT2C FUEL TOTALIZER ENG NO 2	42	0	1	32768
66				2	16384	22					
66				3	8191	23					
66				4	4096	24					
66				5	2048	25					
66				6	1024	26					
66				7	512	27					
66				8		28					
66				9		29					
66				10		30					
65	FTOT2F FUEL TOTALIZER ENG NO 2	41	0	1	256	31	FTOT2F FUEL TOTALIZER ENG NO 2	41	0	1	256
65				2	128	32					
65				3	64	33					
65				4	32	34					
65				5	16	35					
65				6	8	36					
65				7	4	37					
65				8	2	38					
65				9	1	39					
65				10		40					
80	FTJT3C FUEL TOTALIZER ENG NO 3	42	1	1	32768	41	FTJT3C FUEL TOTALIZER ENG NO 3	42	1	1	32768
80				2	16384	42					
80				3	8191	43					
80				4	4096	44					
80				5	2048	45					
80				6	1024	46					
80				7	512	47					
80				8		48					



TODAY: 01/07/81

FLIGHT INSTRUMENTATION PARAMETER LIST

PAGE 14 OF COPY 1

VEHICLE: KC-135 WINGLET PROGRAM  
 FLT NO: 054  
 SCHED FLT DATE: 12/24/80  
 TM FREQ: 447.5/M  
 PCM SYS/COM NO. 1-01 FJRMAT NO. 1  
 PCM SYS MODEL: RMDU

KEV: D DATE: 7/24/79  
 PROJ INSTR ENGR: GENE KENNER

PCM BIT RATE: 125 KHZ  
 BITS/WORD: 10  
 WORDS/FRAME: 64  
 FR/DATA CY: 10  
 FBT=BIT1=MSB

MAIN FRAME SYNC WORDS: 00, 01, 02

ITEM		PARAMETER		DIGITAL WORD INFORMATION		BIT DESIGNATION		PARAMETERS AFFECTED		ITEM
NO.				WORD	NO.	NO.				NO.
SYS	PARMID1	PARMID2	NAME	POSH	1	2	3	4	5	6
89										49
89										50
89										51
89										52
89										53
89										54
89										55
89										56
89										57
89										58
89										59
112										60
112										61
112										62
112										63
112										64
112										65
112										66
112										67
112										68
112										69
111										70
111										71
111										72
111										73
111										74
111										75
111										76
111										77
111										78
111										79
135										80
135										81
135										82
135										83
135										84
135										85
135										86
135										87
135										88
135										89
134										90
134										91
134										92
134										93
134										94
134										95
134										96

TODAY: 01/07/81

FLIGHT INSTRUMENTATION PARAMETER LIST

PAGE 15 OF COPY 1

VEHICLE: KC-135 WINGLET PROGRAM  
 FLT NO: 054  
 SCHED FLT DATE: 12/24/80  
 TW FREQ: MHZ S/N  
 PCM SYS/CJM NO. 1-01 EUPPAT NJ. 1  
 PCM SYS MODEL: KMDH

PRD INSTP ENGR: GENE KENNER

PCM BIT RATE: 125 KHZ  
 BITS/WORD: 10  
 WORDS/FRAME: 64  
 FR/DATA CY: 10  
 FBT=RTT=MSP

MAIN FRAME SYNC WORDS: 00 , 01 , 02

DIGITAL WORD INFORMATION									
ITEM NO.	PARAMETER				FRAME: FRAME: BIT: BIT DESIGNATION:	PARAMETERS AFFECTED		ITEM NO.	
SYS	134	134	134	134	134	134	134	134	
SYS	134	134	134	134	134	134	134	134	
SYS	134	134	134	134	134	134	134	134	
SYS	134	134	134	134	134	134	134	134	
SYS	134	134	134	134	134	134	134	134	
SYS	134	134	134	134	134	134	134	134	
SYS	134	134	134	134	134	134	134	134	
SYS	134	134	134	134	134	134	134	134	
SYS	134	134	134	134	134	134	134	134	
SYS	134	134	134	134	134	134	134	134	
SYS	134	134	134	134	134	134	134	134	
SYS	134	134	134	134	134	134	134	134	
SYS	134	134	134	134	134	134	134	134	
SYS	134	134	134	134	134	134	134	134	
SYS	134	134	134	134	134	134	134	134	
SYS	134	134	134	134	134	134	134	134	
SYS	134	134	134	134	134	134	134	134	
SYS	134	134	134	134	134	134	134	134	
SYS	134	134	134	134	134	134	134	134	
SYS	134	134	134	134	134	134	134	134	
SYS	134	134	134	134	134	134	134	134	
SYS	134	134	134	134	134	134	134	134	
SYS	134	134	134	134	134	134	134	134	
SYS	134	134	134	134	134	134	134	134	
SYS	134	134	134	134	134	134	134	134	
SYS	134	134	134	134	134	134	134	134	
SYS	134	134	134	134	134	134	134	134	
SYS	134	134	134	134	134	134	134	134	
SYS	134	134	134	134	134	134	134	134	
SYS	134	134	134	134	134	134	134	134	
SYS	134	134	134	134	134	134	134	134	
SYS	134	134	134	134	134	134	134	134	
SYS	134	134	134	134	134	134	134	134	
SYS	134	134	134	134	134	134	134	134	
SYS	134	134	134	134	134	134	134	134	
SYS	134	134	134	134	134	134	134	134	
SYS	134	134	134	134	134	134	134	134	
SYS	134	134	134	134	134	134	134	134	
SYS	134	134	134	134	134	134	134	134	
SYS	134	134	134	134	134	134	134	134	
SYS	134	134	134	134	134	134	134	134	
SYS	134	134	134	134	134	134	134	134	
SYS	134	134	134	134	134	134	134	134	
SYS	134	134	134	134	134	134	134	134	
SYS	134	134	134	134	134	134	134	134	
SYS	134	134	134	134	134	134	134	134	
SYS	134	134	134	134	134	134	134	134	
SYS	134	134	134	134	134	134	134	134	
SYS	134	134	134	134	134	134	134	134	
SYS	134	134	134	134	134	134	134	134	
SYS	134	134	134	134	134	134	134	134	
SYS	134	134	134	134	134	134	134	134	
SYS	134	134	134	134	134	134	134	134	
SYS	134	134	134	134	134	134	134	134	
SYS	134	134	134	134	134	134	134	134	
SYS	134	134	134	134	134	134	134	134	
SYS	134	134	134	134	134	134	134	134	
SYS	134	134	134	134	134	134	134	134	
SYS	134	134	134	134	134	134	134	134	
SYS	134	134	134	134	134	134	134	134	
SYS	134	134	134	134	134	134	134	134	
SYS	134	134	134	134	134	134	134	134	
SYS	134	134	134	134	134	134	134	134	
SYS	134	134	134	134	134	134	134	134	
SYS	134	134	134	134	134	134	134	134	
SYS	134	134	134	134	134	134	134	134	
SYS	134	134	134	134	134	134	134	134	
SYS	134	134	134	134	134	134	134	134	
SYS	134	134	134	134	134	134	134	134	
SYS	134	134	134	134	134	134	134	134	
SYS	134	134	134	134	134	134	134	134	
SYS	134	134	134	134	134	134	134	134	
SYS	134	134	134	134	134	134	134	134	
SYS	134	134	134	134	134	134	134	134	
SYS	134	134	134	134	134	134	134	134	
SYS	134	134	134	134	134	134	134	134	
SYS	134	134	134	134	134	134	134	134	
SYS	134	134	134	134	134	134	134	134	
SYS	134	134	134	134	134	134	134	134	
SYS	134	134	134	134	134	134	134	134	
SYS	134	134	134	134	134	134	134	134	
SYS	134	134	134	134	134	134	134	134	
SYS	134	134	134	134	134	134	134	134	
SYS	134	134	134	134	134	134	134	134	
SYS	134	134	134	134	134	134	134	134	
SYS	134	134	134	134	134	134	134	134	
SYS	134	134	134	134	134	134	134	134	
SYS	134	134	134	134	134	134	134	134	
SYS	134	134	134	134	134	134	134	134	
SYS	134	134	134	134	134	134	134	134	
SYS	134	134	134	134	134	134	134	134	
SYS	134	134	134	134	134	134	134	134	
SYS	134	134	134	134	134	134	134	134	
SYS	134	134	134	134	134	134	134	134	
SYS	134	134	134	134	134	134	134	134	
SYS	134	134	134	134	134	134	134	134	
SYS	134	134	134	134	134	134	134	134	
SYS	134	134	134	134	134	134	134	134	
SYS	134	134	134	134	134	134	134	134	
SYS	134	134	134	134	134	134	134	134	
SYS	134	134	134	134	134	134	134	134	
SYS	134	134	134	134	134	134	134	134	
SYS	134	134	134	134	134	134	134	134	
SYS	134	134	134	134	1				

770AY: 01/07/91

FLIGHT INSTRUMENTATION PARAMETER LIST  
REV: D DATE: 7/24/79

PAGE 16 OF COPY 1

VEHICLE: KC-135 WINGLET PROGRAM  
FLT NO: 354  
SCHED FLT DATE: 12/24/80  
TM FREQ: 447 S/N  
PCM SYS/COM NO: 1-01 FJFFAT NO: 1  
PCM SYS MODEL: RMDU

PRD INSTR ENGR: GENE KENNER

PCM BIT RATE: 125 KHZ  
BITS/WORD: 10  
WORDS/FRAME: 64  
FR/DATA CY: 10  
FBT-RIT1-MSB

MAIN FRAME SYNC WORDS: 00 , 01 , 02

ITEM		DIGITAL WORD INFORMATION										PARAMETERS AFFECTED		ITEM
NO.	PARAMETER	FRAME NO.	FRAME NO.	BIT	BIT	DESIGNATION							NO.	
SYS	LRASHMID1	PARMID1	NAME	LRASHMID1	PARMID1	NAME	LRASHMID1	PARMID1	NAME	LRASHMID1	PARMID1	NAME	LRASHMID1	PARMID1
218														145
218														146
218														147
218														148
218														149
218														150
219			WT0IGF GROSS WEIGHT (PIG FINE)	49	7	1								151
219														152
219														153
219														154
219														155
219														156
219														157
219														158
219														159
219														160
267			HPI ALTITUDE	62	9	1								161
267														162
267														163
267														164
267														165
267														166
267														167
267														168
267														169
267														170
268			HPIF ALTITUDE	61	9	1								171
268														172
268														173
268														174
268														175
268														176
268														177
268														178
268														179
268														180

END OF INFORMATION

\*\*\*\*\* \*IDENT FLT054  
 ///// \*DELETE FLT053.1  
 C L101 KC-135 WINGLET PROGRAM 125 054 GENE KENNER 12/24/EJ 10  
 ///// \*DELETE FLT053.2  
 C L102 64 10 1 KMDU 00 01 02 01 K135054 00

MODIFICATIONS / CONTROL CARDS

WINGLET	C L101 KC-135 WINGLET PROGRAM	125 053	GENE KENNER	12/23/80 10	FLT053	1	D
WINGLET	C L101 KC-135 WINGLET PROGRAM	125 054	GENE KENNER	12/24/80 10	FLT054	1	I
WINGLET	C L102 64	10 1	KMDU	00 01	02 01 K135053	00	FLT053
WINGLET	C L102 64	10 1	KMDU	00 01	02 01 K135054	00	FLT054

CORRECTION IDENTs ARE LISTED IN CHRONOLOGICAL ORDER OF INSERTION

YANKSSS	WINGLET	FLT007	FLT013	THRUST	FLT014	FLT015	FLT016
FLT017	FLT018	FLT019	FLT020	FLT021	FLT022	FLT023	FLT024
FLT025	FLT026	FLT027	FLT028	FLT029	FLT030	FLT031	FLT032
FLT033	FLT034	FLT035	FLT036	FLT037	FLT038	FLT039	FLT040
FLT041	FLT042	FLT043	FLT044	FLT045	FLT046	FLT047	FLT048
FLT049	FLT050	FLT051	FLT052	FLT053	FLT054		

17 PURGED IDENTs WERE FOUND

DECKs ARE LISTED IN THE ORDER OF THEIR OCCURRENCE ON A NEW PROGRAM LIBRARY IF ONE IS CREATED BY THIS UPDATE

YANKSSS WINGLET DIGITAL

KC-135 WING AND WINGLET FLIGHT PRESSURE  
DISTRIBUTIONS, LOADS, AND WING DEFLECTION RESULTS  
WITH SOME WIND TUNNEL COMPARISONS

Lawrence Montoya\*, Peter Jacobs\*\*,  
Stuart Flechner\*\*, and Robert Sims\*

SUMMARY

A full-scale winglet flight test on a KC-135 airplane with an upper winglet was conducted in a joint NASA/USAF flight project. Data were taken at Mach numbers from 0.70 to 0.82 at altitudes from 34,000 feet to 39,000 feet at stabilized flight conditions for wing/winglet configurations of basic wing tip,  $15^\circ/-4^\circ$ ,  $15^\circ/-2^\circ$ , and  $0^\circ/-4^\circ$  winglet cant/incidence.

An analysis of selected pressure distribution and data showed that with the basic wing tip, the flight and wind tunnel wing pressure distribution data showed good agreement. With winglets installed, the effects on the wing pressure distribution were mainly near the tip. Also, the flight and wind tunnel winglet pressure distributions had some significant differences primarily due to the "oilcanning" in flight. However, in general, the agreement was good.

For the winglet cant and incidence configuration presented, the incidence had the largest effect on the winglet pressure distributions.

The incremental flight wing deflection data showed that the semispan wind tunnel model did a reasonable job of simulating the aeroelastic effects at the wing tip.

The flight loads data showed good agreement with predictions at the design point and also substantiated the predicted structural penalty (load increase) of the  $15^\circ$  cant/ $-2^\circ$  incidence winglet configuration.

INTRODUCTION

The NASA Langley Research Center has conducted extensive experimental wind tunnel investigations on the effects of winglets on jet transports at various subsonic Mach numbers, references 1 through 8. Winglets, as described in reference 1, have shown significant performance improvements on the KC-135 airplane. To confirm these wind tunnel predictions, a joint NASA/USAF full-scale winglet flight evaluation on a KC-135 was conducted at the NASA Dryden Flight Research Center. The flight measurements consisted of total airplane lift and drag, loads, buffet, stability and control, range factor, and wing/winglet pressure distributions. These measurements were taken with the winglets on and off for various winglet cant and incident angles to determine the incremental effect of winglets on the airplane performance.

\*NASA Dryden Flight Research Center

\*\*NASA Langley Research Center

This paper presents selected wing and winglet pressure distributions, loads and wing deflection results with some wind tunnel comparisons. The data presented are for Mach numbers of 0.70, 0.78, 0.80 and 0.82 for altitudes between 34,000 feet to 39,000 feet. The configuration tested in flight consisted of the basic wingtip (winglets off) and wing/winglet with winglet variations of cant/incidence of 15°/-4°, 15°/-2°, and 0°/-4°. The design conditions for this study are the 15° cant/-4° incidence winglet configuration at a Mach number of 0.78 and lift coefficient of 0.42.

## SYMBOLS

$b'$	Exposed Semispan of Wing with Basic Tip, 55.2 ft
$c$	Local Chord
$\bar{c}$	Mean Geometric Chord of Exposed Basic Wing, 18.73 ft
$c_{av}$	Average Chord of Exposed Basic Wing, $s/b'$ , 17.52 ft
$c_L$	Lift Coefficient
$c_n$	Section Normal-Force Coefficient, Integration of Pressure Measurements
$c_{n_A}$	Airplane Normal Force Coefficient
$C_p$	Pressure Coefficient, $(P_\ell - P_\infty)/q_\infty$
$g$	Gravitational Acceleration, $\text{ft/sec}^2$
$i$	Incidence of Winglet Measured from Free-Stream Direction, Positive with Leading Edge Inward for Upper Winglet, deg (see figure 3).
$M_\infty$	Free-Stream Mach Number
$P_d$	Differential Static Pressure, psi
$P_\ell$	Local Static Pressure, psi
$P_r$	Reference Static Pressure, psi
$P_\infty$	Free-Stream Static Pressure, psf
$q_\infty$	Free-Stream Dynamic Pressure, psf
$R$	Reynolds Number per Unit Length, per ft
$w/\delta$	Airplane Weight Divided by Ratio of Pressure at Test Altitude to Standard Sea Level Pressure

x	Chordwise Distance from Leading Edge, Positive Aft
y	Spanwise Distance from Wing-Fuselage Juncture, Positive Outboard
z	Vertical Coordinate of Airfoil
z'	Distance Along Winglet Span from Chord Plane of Wing, in.
$\alpha$	Angle of Attack, deg
$\eta$	Exposed Wing Semispan Station (based on basic-wing panel), $y/b'$

#### SUBSCRIPT

basic	Reference Configuration, Basic Wing Tip
-------	---

#### ABBREVIATION

L.S.	Lower Surface
U.S.	Upper Surface
G.W.	Gross Weight
B.M.	Bending Moment

#### AIRPLANE DESCRIPTION

A Boeing KC-135 airplane, figure 1, with modified outboard wing panels was used for this study. The modifications were primarily to the internal structure near the wing tips for installing the winglets with the capability to allow winglet cant/incidence changes on the ground. Provisions were also made so that a "basic" KC-135 wing tip configuration with the winglets removed could be installed.

The other major aerodynamic differences from a standard KC-135 was the addition of the nose boom for obtaining airspeed and flow direction, and the absence of the refueling boom.

Wing. The basic wing is a typical first generation transport configuration with a quarter-chord sweep of 35°, 7° dihedral and 2° of incidence at the root chord. The wing has no geometric twist and the thickness varies nonlinearly from 15 percent at the wing-fuselage juncture to 9 percent at the trailing edge break and then remains constant at 9 percent to the wing tip. A typical outboard wing airfoil section is shown in figure 2 with the coordinates presented in table I.

Winglets. The winglet configuration used in this investigation is presented in figure 3. The winglets employed an 8-percent-thick general aviation airfoil. Winglet airfoil coordinates are presented in table II.

The winglet has a span approximately equal to the wing tip chord, a root chord equal to about 65 percent of the wing tip chord, a leading-edge sweep of 38°, a taper ratio of 0.32, and an aspect ratio of 2.33. The planform area of the upper winglet is 3.8 percent of the exposed trapezoidal planform area of the basic wing. The upper winglet is canted outboard 15° from vertical (75° dihedral) and incidence (toed out) of 4° (leading edge outboard) relative to the fuselage center line. The upper winglet is untwisted and therefore has constant negative geometric incidence across its span. The "upper surface" of the upper winglet is the inboard surface. This geometry was derived from the wind-tunnel model coordinates with the exception of some slight wing/winglet juncture fairing differences which result from the method used to allow cant/incidence variations for the flight test.

## TEST CONDITIONS

Flight data were obtained over a range of angles of attack at speeds from Mach 0.70 to Mach 0.82, for altitudes between 34,000 feet to 39,000 feet and dynamic pressures from about 129 psf to 240 psf. All the wing and winglet pressure data presented were taken at steady state trim conditions. The loads data are for cruise conditions and  $\pm 0.5g$  roller coaster maneuvers from trim conditions.

## INSTRUMENTATION

Wing/Winglet Pressures. The flight wing/winglet pressure measurements were obtained on the right side from seven rows of orifices on the top and bottom surface at the span stations and locations shown in figure 4. Both the span and chordwise location of the orifices were essentially the same as the wind-tunnel model of reference 5.

All the wing orifices except the leading-edge orifices were externally mounted using the method similar to that found in reference 9. The external tubing size was 3/16 inch A.D. multibore (strip-a-tubing) tubing. All the winglet orifices were flush mounted with an inside diameter of 1/8 inch.

The wing/winglet pressures were transmitted to instrument bays, where the pressures were measured with scanivalves. The locations were chosen so that the pressure sensors could be as close as practical to the orifices.

Differential transducers were used on all scanivalves and referenced to a compartment source which was measured by precision absolute pressure transducer.

Wing Deflection Measurement. A medium format camera was mounted on the fuselage door looking out over the right wing upper surface toward the tip, figure 5. Two deflection targets were installed at the wing tip with reference



targets installed on the inboard portion of the wing to establish a plane from which the flight deflections were measured.

Wing/Winglet Load and Stress. The load and stress stations where strain gages were installed are shown in figure 6. The winglet, wing-winglet inter-section, and outboard wing station gages were installed during the wing tip modification and after construction. These gages were calibrated for loads measurements during proof tests. The wing root station gages were installed chordwise on both the upper and lower surfaces strictly for stress measurements.

Air Data. Air data measurements were obtained from a standard NACA air-speed head mounted on the nose boom. The airspeed system was calibrated using the techniques described in reference 10. Flow direction was obtained from a flight path accelerometer (F.P.A.) system (reference 11), also mounted on the nose boom aft of the NACA head.

Accuracy. The pressure range for the scanivalve transducers was scaled on the basis of the wind tunnel pressure coefficients for flight conditions near the winglet design of Mach 0.78 and altitude of 35,000 feet. The scanivalve zero pressure differential was checked during each flight by connecting both sides of the differential transducer to the same pressure.

The average error in  $C_p$  based on the flight data was determined to be about 0.01, which is similar to that of the wind tunnel data.

The estimated error in each of the following measurements at  $M = 0.78$  and at 35,000 feet altitude is as follows:

$P_d$ , psi	$\pm 0.6$
$P_r$ , psi	$\pm 0.3$
$P_\infty$ , psf	$\pm 0.02$
$M_\infty$	$\pm 0.01$
$\alpha$	$\pm 0.25^\circ$
$q_\infty$ , psf	$\pm 0.08$

For the loads and stress measurements presented in this paper, the estimated accuracies are as follows:

<u>Location</u>	<u>Type</u>	<u>Accuracy</u>
Wing-Winglet Juncture	Bending	$\pm 6\%$
Outboard Wing	Bending	$\pm 2\%$
Wing Root	Stress	$\pm 250$ psi

## RESULTS AND DISCUSSION

The discussion presented herein will be limited to a few cases which are considered generally representative of the trends for the various configurations tested. Comparisons with wind tunnel results are also included for the  $15^\circ/-4^\circ$  winglet cant/incidence configuration.

In figure 7, flight and wind tunnel pressure coefficient data are presented for the basic wing tip configuration. In general, the comparisons show good agreement at all four wing span stations, Mach numbers, and angles of attack. Some small differences do exist at some locations and test conditions which, in part, could be attributed to the airplane surface conditions and externally mounted orifices.

Figure 8 presents flight and wind tunnel wing and winglet pressure distributions comparisons for the  $15^\circ$  cant/ $-4^\circ$  incidence winglet configuration. The wing pressure distributions comparisons, in general, show good agreement at all span stations and test conditions, while the winglet data have some significant differences. At semispan station 1.01 the main differences between flight and wind tunnel occur on the upper surface near the leading edge at all test conditions. These large differences at the leading edge are attributed to "oilcanning" (skin deflections) which occurred in flight. Observations of the "oilcanning" during flight showed that the existence of a large "oilcan" occurred in this region. A photograph of the "oilcanning" on the left winglet is shown in figure 9.

At semispan stations 1.03 and 1.05 the winglet flight and wind tunnel data in figure 8 generally show good agreement for the lower surface while the flight upper surface data tend to be more positive on the forward chord regions and more negative on the aft portion. These differences are in part attributed to the "oilcanning"; however, the trends and levels show good agreement.

In figure 10, flight wing pressure distributions for the basic wing tip and with the  $15^\circ$  cant/ $-4^\circ$  incidence winglet configuration are presented. The data show that at all test conditions the effects of the winglet on the wing pressure distributions are mainly at the wing tip upper surface (semispan station 0.99). At this span station, the wing upper surface pressure distributions with the winglet tend to be more negative on the aft region with good trailing edge pressure recovery. The more negative pressure coefficients begin at about  $X/C = 0.4$  which is where the winglet leading edge intersects the wing upper surface. These results are similar to those predicted by the wind tunnel data of reference 5. The other wing semispan stations (0.26, 0.77, and 0.92) along with the lower surface of semispan station 0.99 in general do not show significant effects due to the winglet.

Figure 11 presents wing tip and winglet pressure distribution comparisons for the  $15^\circ/-4^\circ$ ,  $15^\circ/-2^\circ$ , and  $0^\circ/-4^\circ$  winglet cant/incident configurations. The wing tip data ( $\eta = 0.99$ ) in general show good agreement except for the  $15^\circ$  cant/ $-2^\circ$  incidence data which have slightly more negative coefficients on the upper surface at the higher Mach numbers.

The winglet pressure distributions in figure 11 show that  $15^\circ/-4^\circ$  and  $0^\circ/-4^\circ$  data generally agree while the  $15^\circ/-2^\circ$  data tend to be more negative on forward portion of the upper surface and more positive on the lower surface. This indicates that for the test conditions presented, the winglet incidence had a stronger effect on the pressure distribution than did cant.

Wing and winglet flight and wind tunnel span load distributions for the  $15^\circ$  cant/ $-4^\circ$  incidence winglet configuration are presented in figure 12. Some differences exist at some of the test conditions presented. These differences are due to the airplane surface conditions; i.e., externally mounted pressure

tubing for the wing flight data and winglet "oilcanning," and the method used in the model construction to get the proper outboard wing deflections. With the above taken into account, agreement is considered good.

Figure 13 presents schematics of both the construction method used in the semispan model of reference 5, to get the predicted wing tip deflections along with the type of deflections which would be expected in actual flight and from the model. As is shown, the model deflections occur primarily outboard of the fill area while the actual flight deflections occur more uniformly throughout the span; although the total wing tip deflection may be similar. Therefore the wing span loads as shown in figure 12 may differ due to this effect.

Flight and wind tunnel measured deflections at the design cruise Mach number of 0.78 are compared in figure 14 for the winglets off and  $15^\circ$  cant/ $-4^\circ$  incidence configurations. Because of the different reference planes, comparisons of absolute deflection cannot be made. However, comparing the incremental deflection from winglets off to  $15^\circ$  cant/ $-4^\circ$  incidence at a given  $C_L$ , the wind tunnel and flight data are fairly close. The increment for the flight data appears to be slightly higher than the wind tunnel increment. From this and other data, the overall assessment is that the flexible wind tunnel model did a reasonable job of simulating the aeroelastic effects at the wing tip where it is important to get the winglet in the right environment.

The overall character of the winglet loading is shown in figure 15 where the center of pressure location outboard of the load station is plotted for the  $15^\circ/-2^\circ$  and  $15^\circ/-4^\circ$  configurations. The data were obtained from  $\pm 0.5g$  roller coaster maneuvers performed at the 0.78 design Mach number. Of particular note is the fairly aft chordwise locations, especially at the lower angle-of-attack points.

The effective center of pressure location for the total outboard wing loads is shown in figure 16 for the same maneuvers. The load penalty at this station for both winglet configurations is quite evident from the outboard shift in center of pressure. It is also interesting to note that for all three configurations the chordwise center of pressure remains virtually unchanged, with the data centering around the elastic (torque) axis.

In figure 17 the flight measured winglet intersection bending moment, as a function of airplane normal force coefficient, is compared with Boeing aeroelastic prediction data at the design test condition. The airload at  $1g$  for the  $15^\circ$  cant/ $-2^\circ$  incidence winglet configuration is about 34 percent higher than the  $15^\circ/-4^\circ$  configuration, indicating the desirability of the  $15^\circ/-4^\circ$  configuration. A comparison of the flight data with the predicted data shows good agreement at the  $1g$  condition, but predictions are somewhat higher than flight data at the  $1.5g$  condition.

The flight measured bending moment at the outboard wing station, as a function of airplane normal force coefficient, is shown in figure 18 for the design test condition. At  $1g$ , the  $15^\circ$  cant/ $-4^\circ$  incidence configuration shows a 32 percent increase in airload over the basic wing while the  $15^\circ/-2^\circ$  configuration exceeds the basic wing by 50 percent. Comparison between the measured flight loads and the Boeing predicted data is considered quite good at both  $1g$  and  $1.5g$ .

The flight measured bending stress distribution at the wing root station is shown in figure 19 for the design cruise condition at 1g. As predicted from the flexible wind tunnel tests, the flight data for the 15° cant/-4° incidence winglet configuration show only a slight increase compared to the basic wing without winglets. The average stress increment is approximately 2.5 percent.

#### SUMMARY OF RESULTS

A full scale winglet flight program on a KC-135 airplane with an upper winglet was conducted. An analysis of selected wing and winglet pressure distribution data for the basic wing tip, 15°/-4°, 15°/-2°, and 0°/-4° winglet cant/incident configurations indicated the following:

1. The flight wing pressure distributions with the basic tip in general showed good agreement with the wind tunnel data.
2. Winglet configuration effects on the wing pressure distribution were mainly near the wing tip. The winglet made the aft upper surface pressure distributions more negative.
3. The flight and wind tunnel winglet pressure distributions had some significant differences primarily due to the "oilcanning" (skin deflections) in flight; however, in general the agreement was good.
4. For the winglet cant and incidence configurations presented the incidence had the largest effect on the winglet pressure distributions.

Also, the loads and deflection data showed the following:

5. The incremental flight wing deflection data showed that the semispan wind tunnel model did a reasonable job of simulating the aeroelastic effects at the wing tip.
6. At the design conditions the flight loads agreed with predictions.
7. The flight loads substantiated the predicted structural penalty (load increase) of the 15° cant/-2° incidence winglet configuration.

#### REFERENCES

1. Whitcomb, Richard T.: A Design Approach and Selected Wind-Tunnel Results at High Subsonic Speeds for Wing-Tip Mounted Winglets. NASA TN D-8260, 1976.
2. Flechner, Stuart G.; Jacobs, Peter F.; and Whitcomb, Richard T.: A High Subsonic Speed Wind-Tunnel Investigation of Winglets on a Representative Second-Generation Jet Transport Wing. NASA TN D-8264, 1976.
3. Jacobs, Peter F.; and Flechner, Stuart G.: The Effect of Winglets on the Static Aerodynamic Stability Characteristics of a Representative Second Generation Jet Transport Model. NASA TN D-8267, 1976.

4. Jacobs, Peter F.; Flechner, Stuart G.; and Montoya, Lawrence C.: Effect of Winglets on a First-Generation Jet Transport Wing. I - Longitudinal Aerodynamic Characteristics of a Semispan Model at Subsonic Speeds. NASA TN D-8473, 1977.
5. Montoya, Lawrence C.; Flechner, Stuart G.; and Jacobs, Peter F.: Effect of Winglets on a First-Generation Jet Transport Wing. II - Pressure and Spanwise Load Distributions for a Semispan Model at High Subsonic Speeds. NASA TN D-8474, 1977.
6. Montoya, Lawrence C.; Jacobs, Peter F.; and Flechner, Stuart G.: Effect of Winglets on a First-Generation Jet Transport Wing. III - Pressure and Spanwise Load Distributions for a Semispan Model at Mach 0.30. NASA TN D-8478, 1977.
7. Meyer, Robert R., Jr.: Effect of Winglets on a First-Generation Jet Transport Wing. IV - Stability Characteristics for a Full-Span Model at Mach 0.30. NASA TP-1119, 1978.
8. Jacobs, Peter F.: Effect of Winglets on a First-Generation Jet Transport Wing. V - Stability Characteristics of a Full-Span Wing With a Generalized Fuselage at High Subsonic Speeds. NASA TP-1163, 1978.
9. Montoya, Lawrence C.; and Lux, David P.: Comparison of Wing Pressure Distribution from Flight Tests of Flush and External Orifices for Mach Numbers from 0.50 to 0.97. NASA TM X-56032, April 1975.
10. Larson, Terry J.; and Ehernberger, L. J.: Techniques Used for Determination of Static Source Position Error of a High Altitude Supersonic Airplane. NASA TM X-3152, 1975.
11. Final Report Flight Path Accelerometer System AFFTC Report FTC-TR-68-28, December 1968.

TABLE I. - COORDINATES OF TYPICAL OUTBOARD WING SECTION

Wing Section at 2° Incidence			
Upper Surface		Lower Surface	
x/c	z/c	x/c	z/c
0	0	0	0
.0011	.0042	.0020	-.0054
.0022	.0056	.0035	-.0063
.0034	.0071	.0061	-.0073
.0058	.0090	.0092	-.0081
.0095	.0116	.0201	-.0097
.0132	.0136	.0391	-.0116
.0180	.0161	.0631	-.0139
.0234	.0186	.0950	-.0168
.0324	.0221	.1016	-.0174
.0415	.0253	.1445	-.0212
.0536	.0291	.1826	-.0245
.0716	.0338	.2235	-.0284
.0897	.0377	.2597	-.0314
.0990	.0394	.2950	-.0341
.1132	.0417	.3326	-.0366
.1408	.0454	.3726	-.0391
.1589	.0471	.4276	-.0418
.1740	.0483	.4690	-.0429
.1861	.0492	.5110	-.0433
.2011	.0501	.5560	-.0430
.2192	.0510	.5967	-.0424
.2342	.0516	.6386	-.0414
.2584	.0522	.6818	-.0406
.3432	.0522	.7243	-.0397
.3729	.0524	.7620	-.0389
.4090	.0513	.7951	-.0381
.4572	.0489	.8308	-.0377
.5054	.0454	.8662	-.0371
.5416	.0420	.9029	-.0363
.6379	.0304	.9790	-.0348
.6862	.0226	.9999	-.0350
.7343	.0513		
.7582	.0108		
.7823	.0065		
.8040	.0027		
.8344	-.0023		
.8642	-.0076		
.8874	-.0119		
.9223	-.0810		
.9492	-.0229		
.9718	-.0269		
.9920	-.0308		
1.0001	-.0347		

TABLE II. - AIRFOIL COORDINATES FOR WINGLETS

x/c	z/c for -	
	Upper Surface	Lower Surface
0	0	0
.0020	.0077	-.0032
.0050	.0119	-.0041
.0125	.0179	-.0060
.0250	.0249	-.0077
.0375	.0296	-.0090
.0500	.0333	-.0100
.0750	.0389	-.0118
.1000	.0433	-.0132
.1250	.0469	-.0144
.1500	.0499	-.0154
.1750	.0525	-.0161
.2000	.0547	-.0167
.2500	.0581	-.0175
.3000	.0605	-.0175
.3500	.0621	-.0174
.4000	.0628	-.0168
.4500	.0627	-.0158
.5000	.0618	-.0144
.5500	.0599	-.0122
.5750	.0587	-.0106
.6000	.0572	-.0090
.6250	.0554	-.0071
.6500	.0533	-.0053
.6750	.0508	-.0033
.7000	.0481	-.0015
.7250	.0451	.0004
.7500	.0419	.0020
.7750	.0384	.0036
.8000	.0349	.0049
.8250	.0311	.0060
.8500	.0270	.0065
.8750	.0228	.0064
.9000	.0184	.0059
.9250	.0138	.0045
.9500	.0089	.0021
.9750	.0038	-.0013
1.0000	-.0020	-.0067

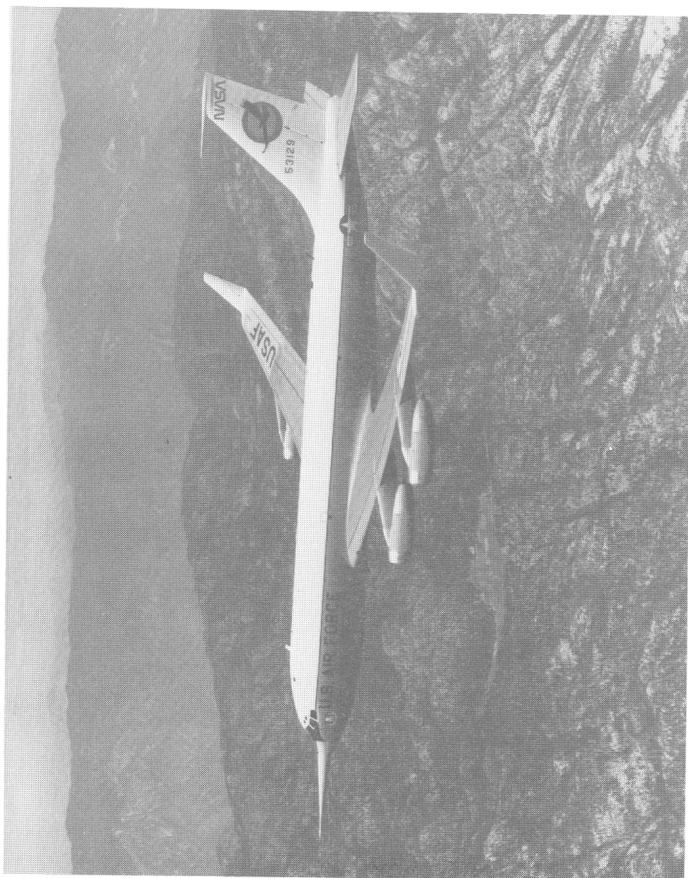


Figure 1. - Inflight photograph of KC-135 with winglets.





Figure 2. - Typical outboard wing airfoil section

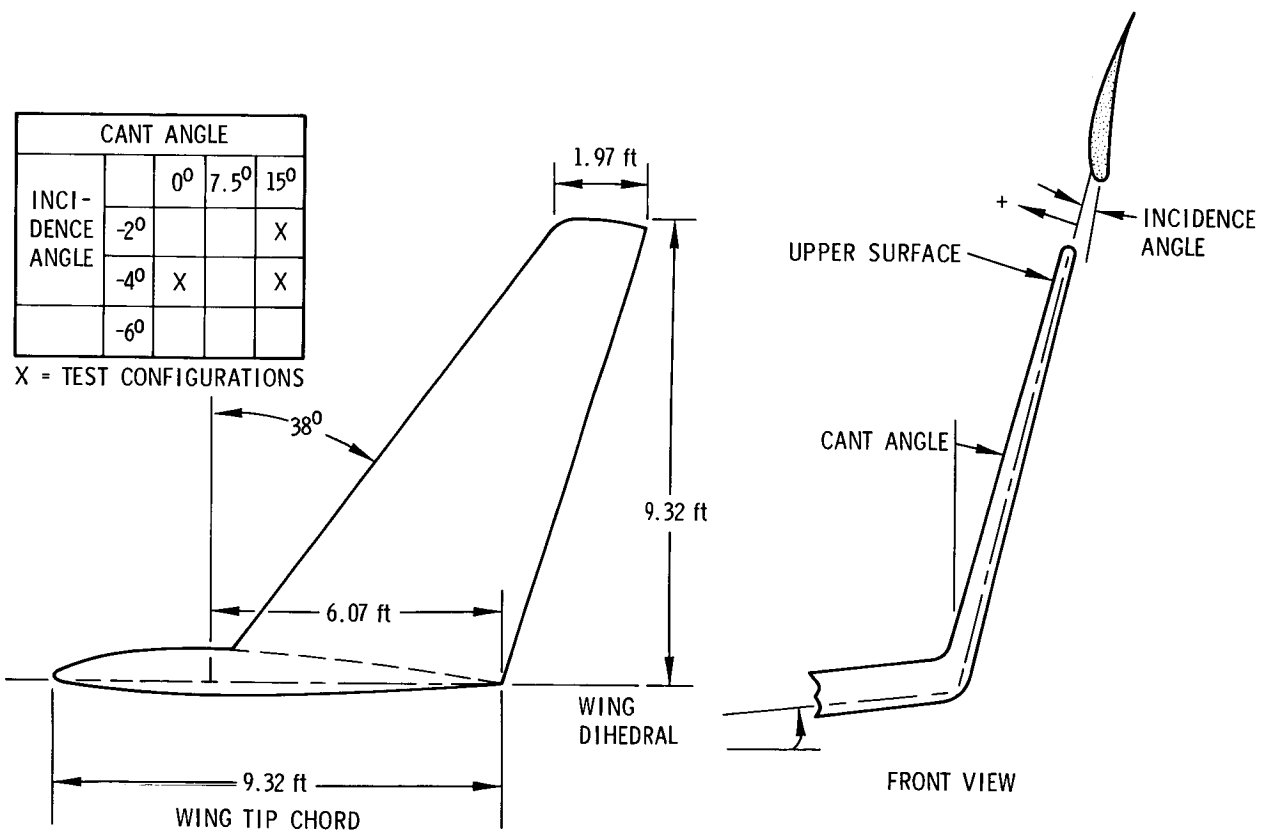


Figure 3. - KC-135 winglet geometry

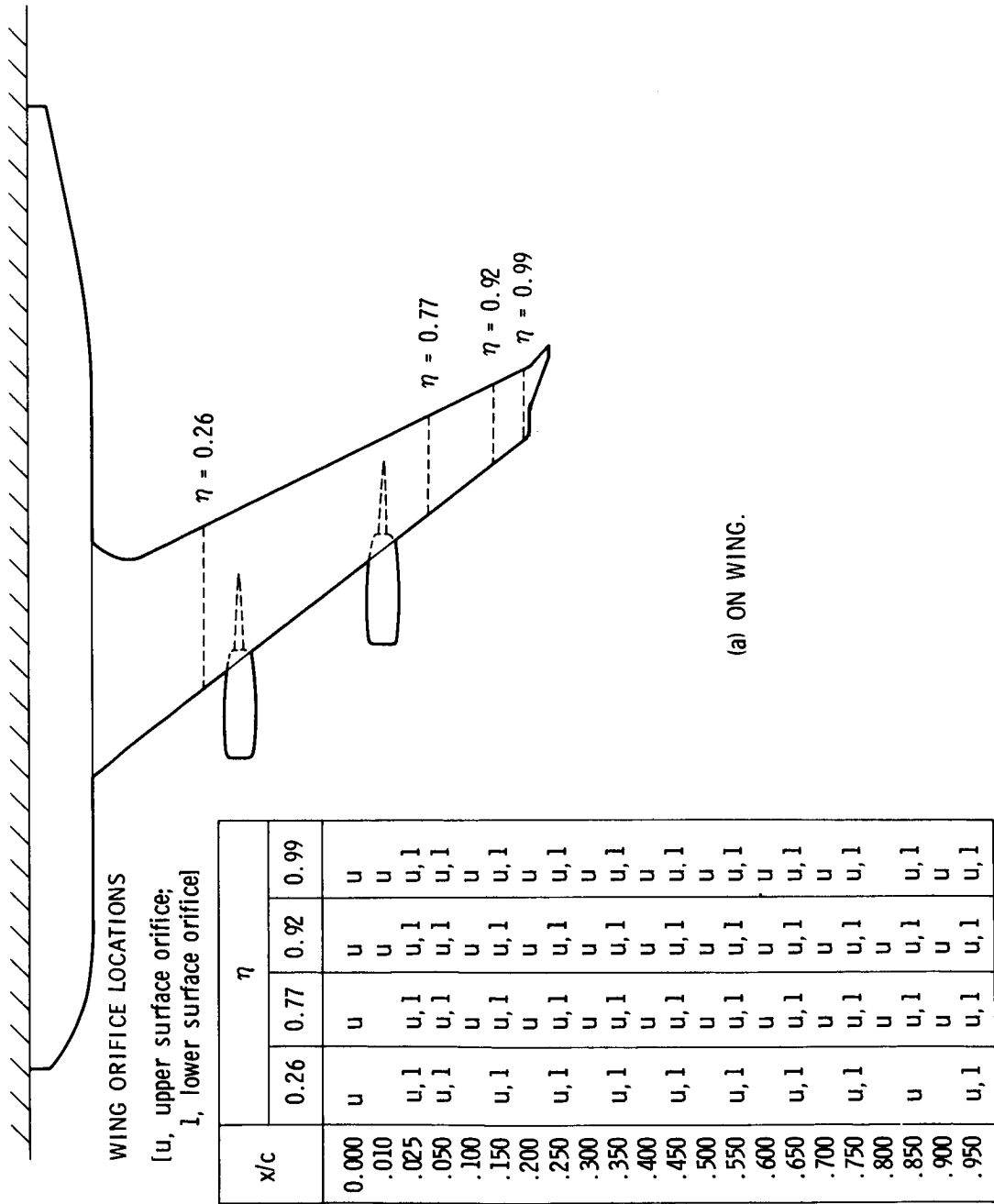
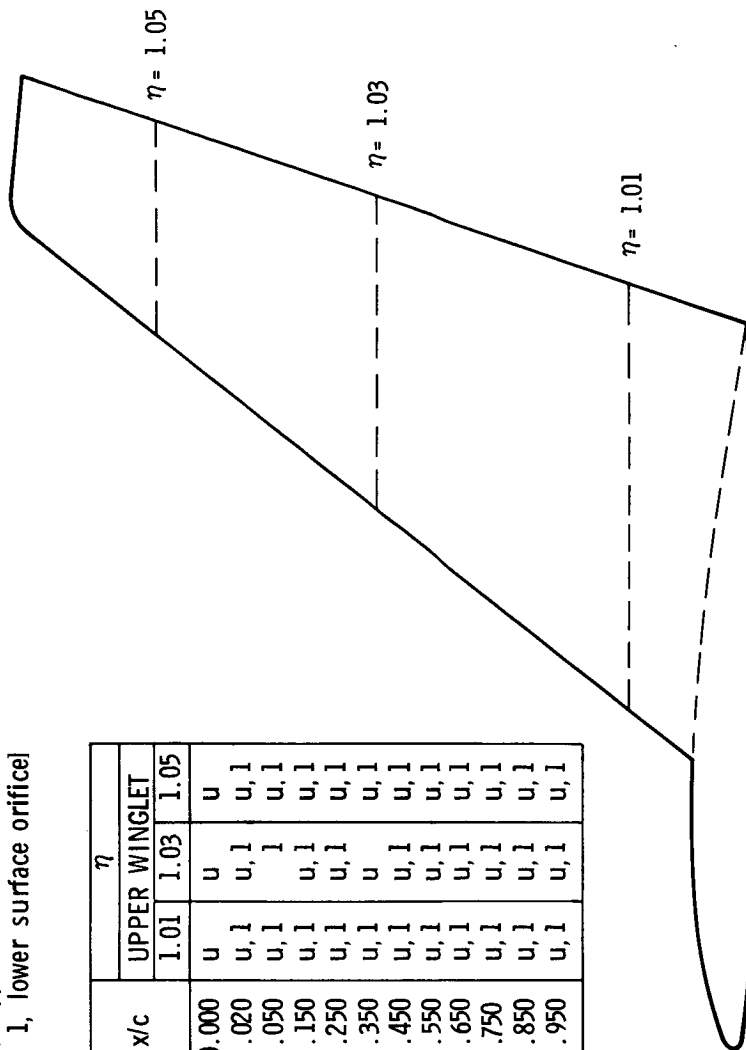


Figure 4. - Wing and winglet static-pressure orifice locations

# WINGLET ORIFICE LOCATIONS

[u, upper surface orifice;  
1, lower surface orifice]

x/c	$\eta$		
	UPPER WINGLET		
	1.01	1.03	1.05
0.000	u	u	u
.020	u, 1	u, 1	u, 1
.050	u, 1	1	u, 1
.150	u, 1	u, 1	u, 1
.250	u, 1	u, 1	u, 1
.350	u, 1	u	u, 1
.450	u, 1	u, 1	u, 1
.550	u, 1	u, 1	u, 1
.650	u, 1	u, 1	u, 1
.750	u, 1	u, 1	u, 1
.850	u, 1	u, 1	u, 1
.950	u, 1	u, 1	u, 1



(b) ON WINGLETS.

Figure 4. - Concluded

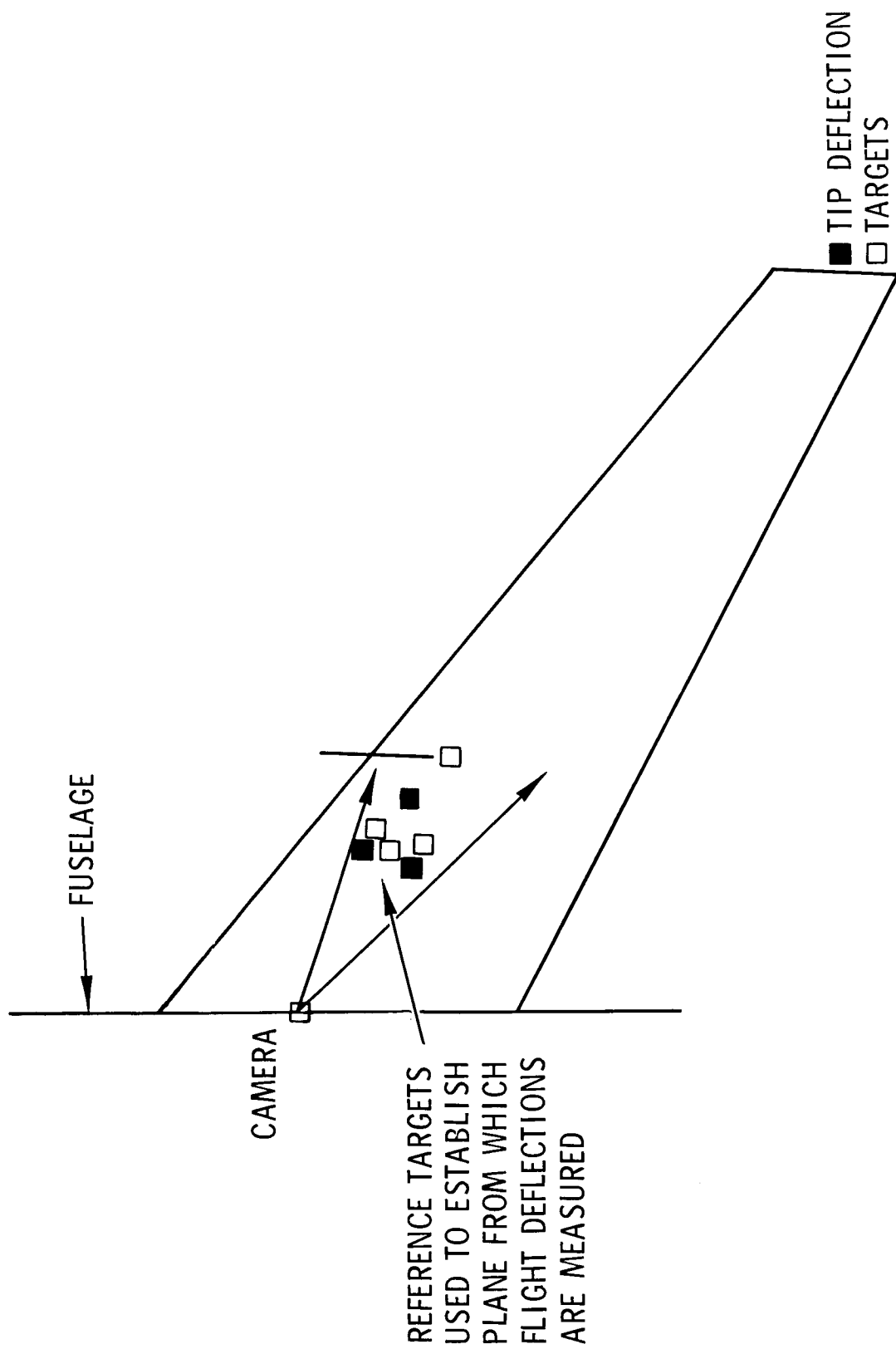


Figure 5. - Schematic of flight wing deflection camera and wing targets

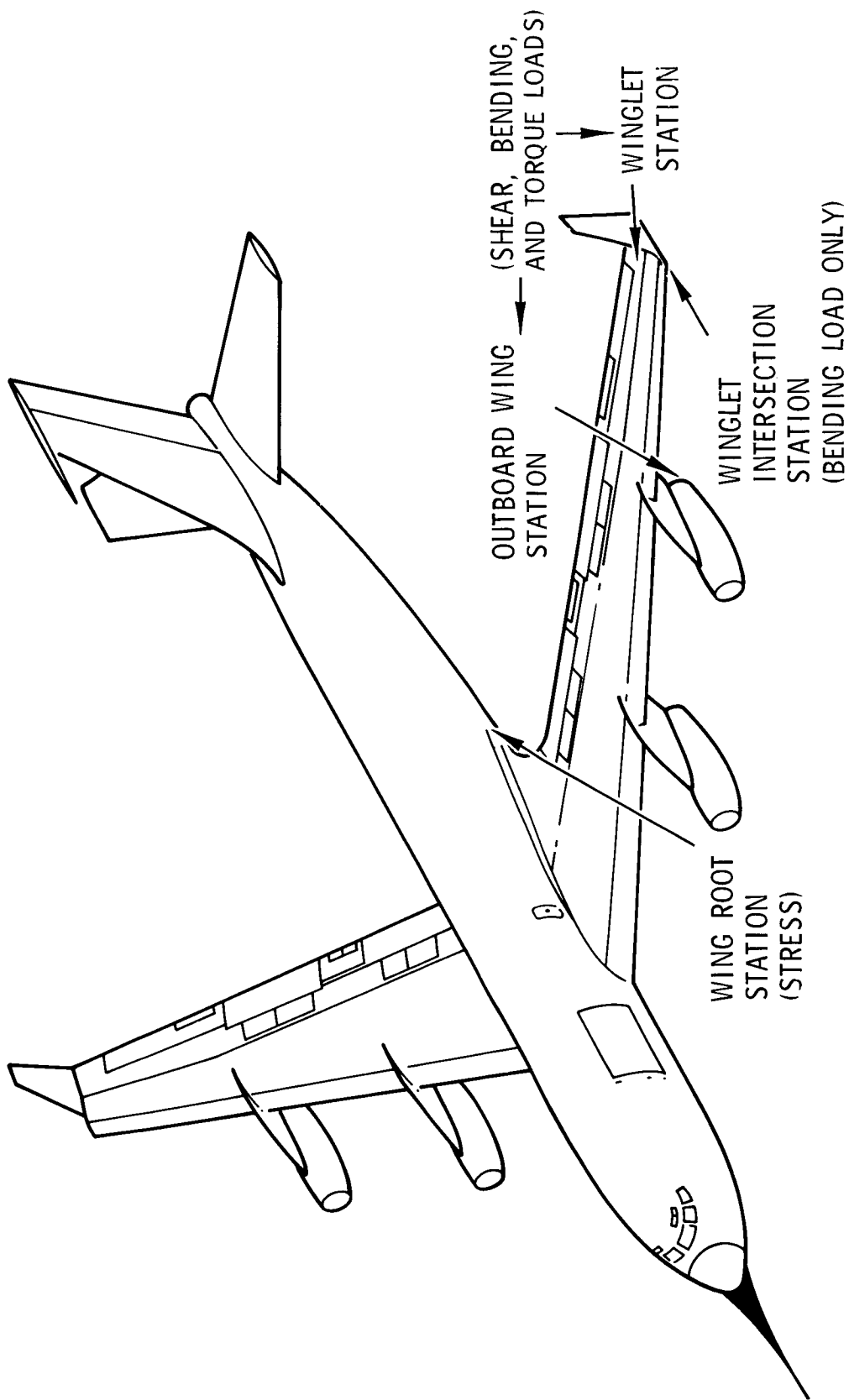


Figure 6. - KC-135 strain gage stations

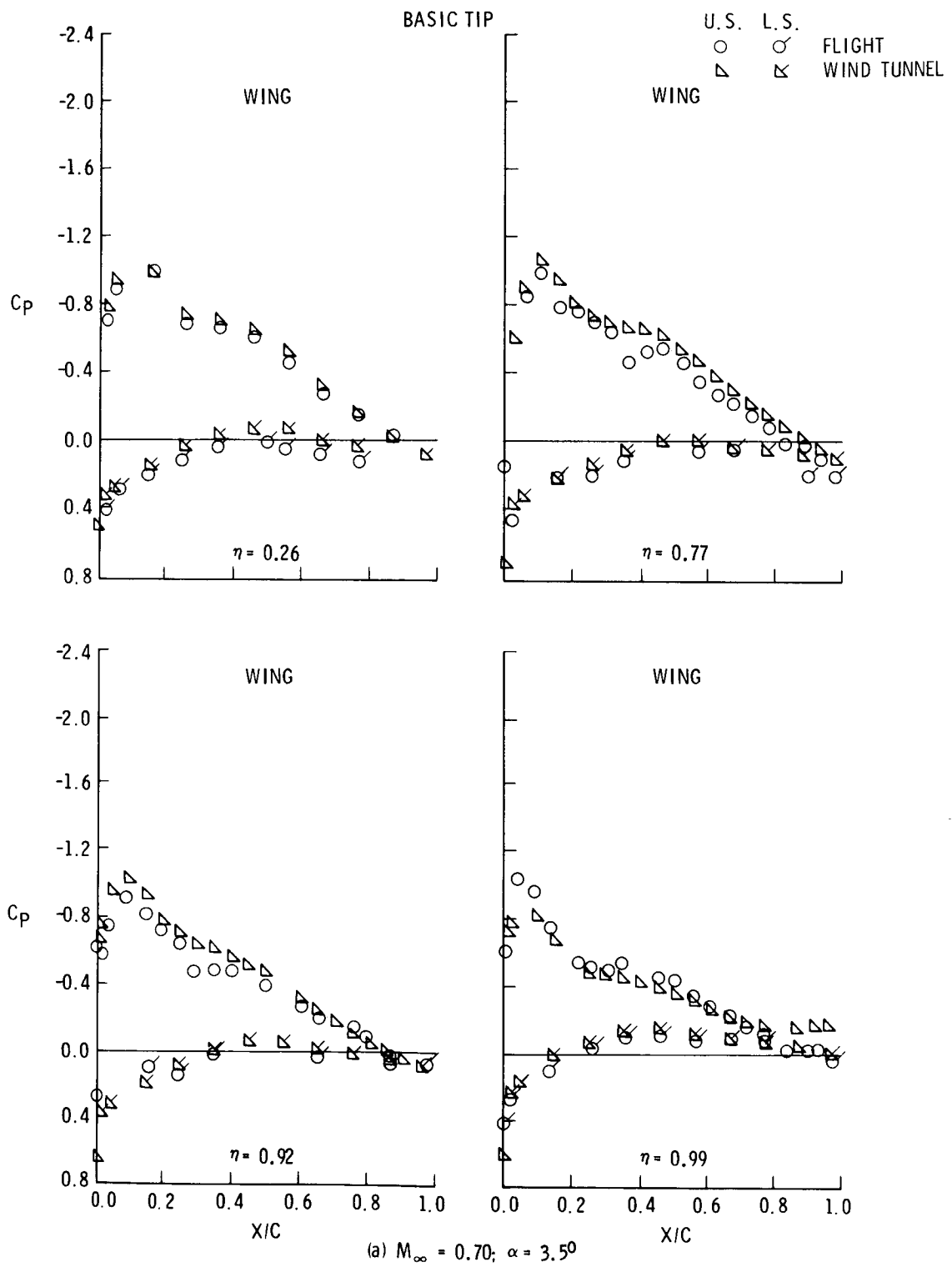


Figure 7. - Flight and wind tunnel wing pressure distribution comparisons

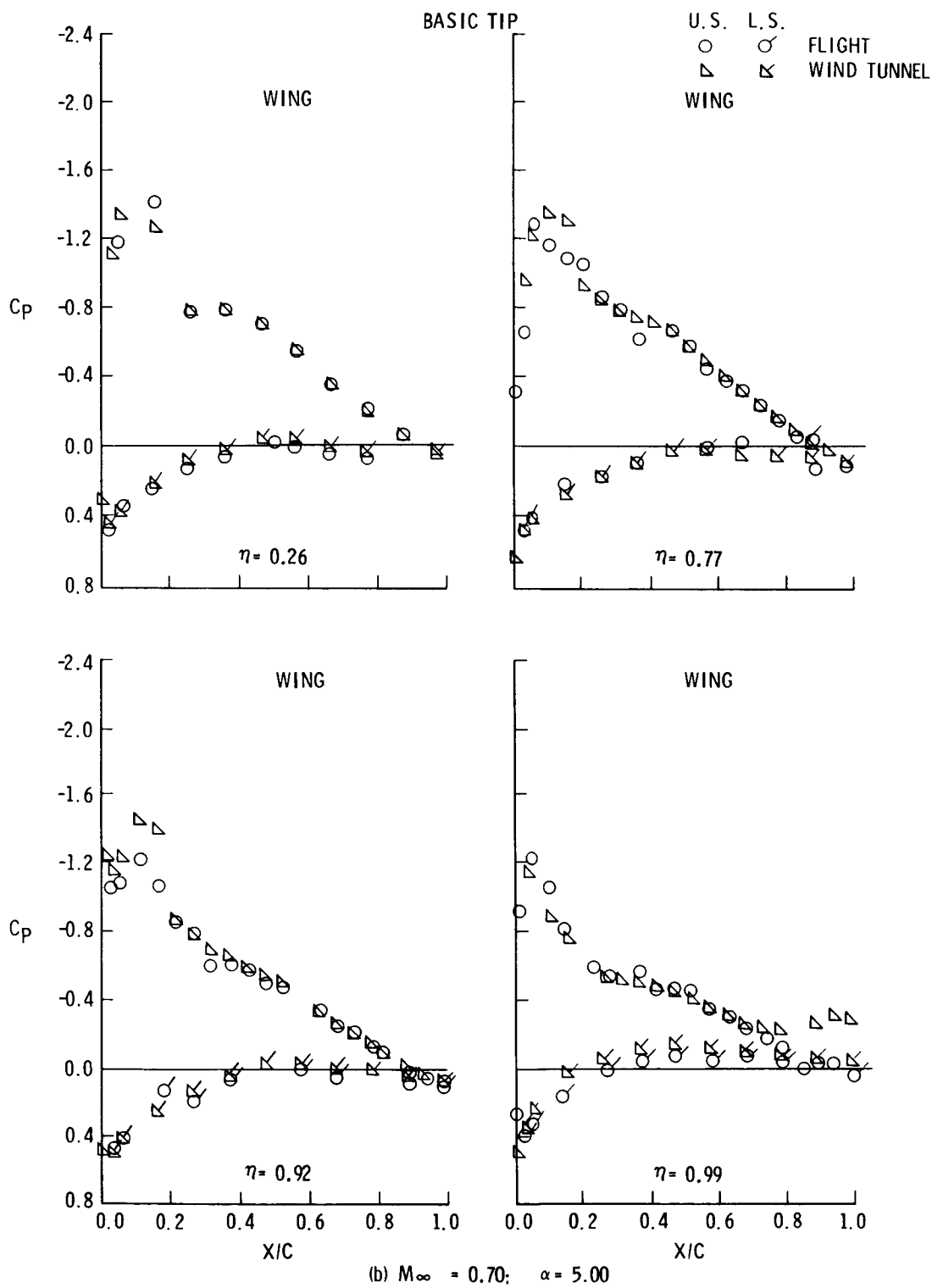


Figure 7. - Continued

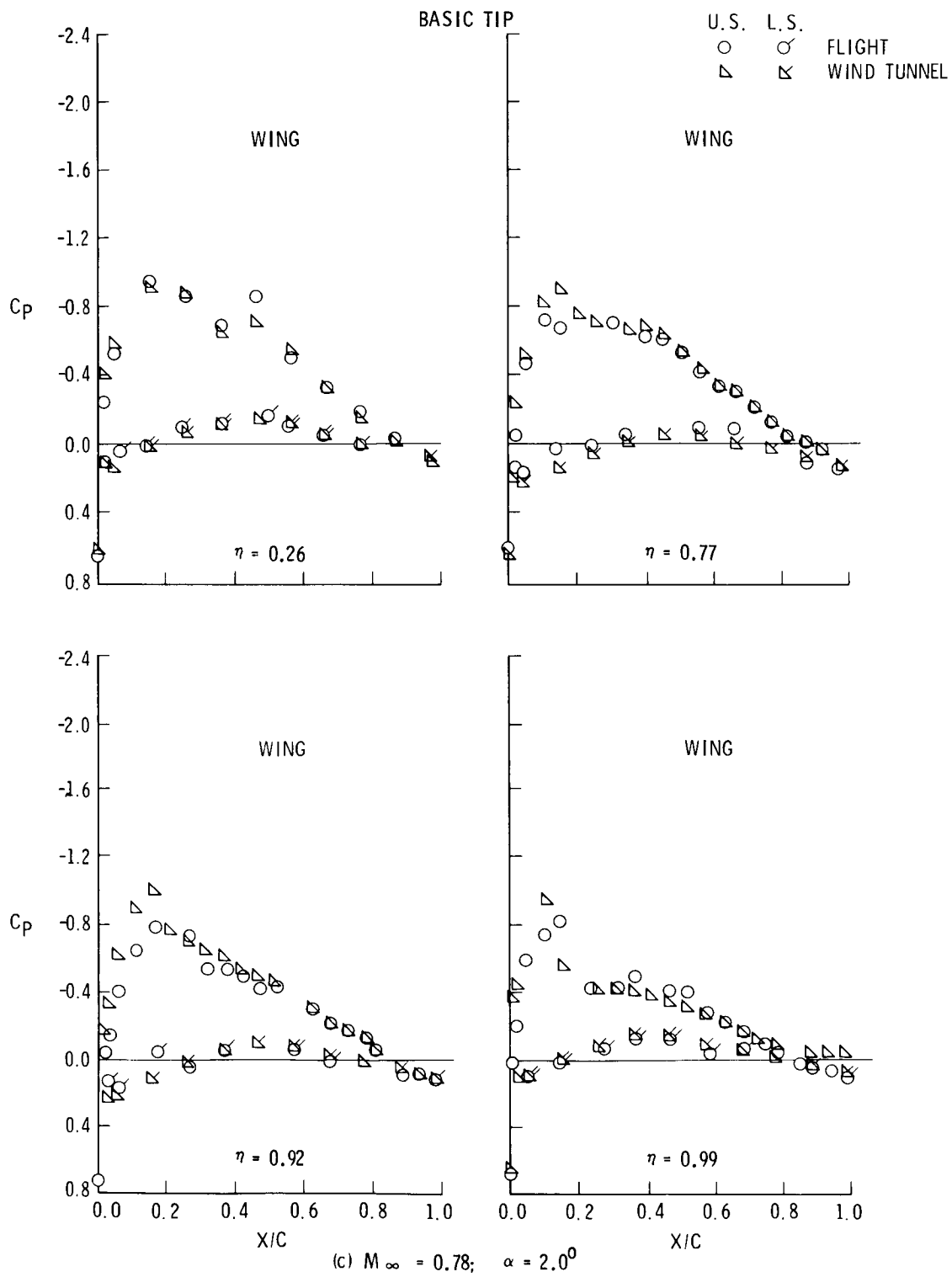


Figure 7. - Continued



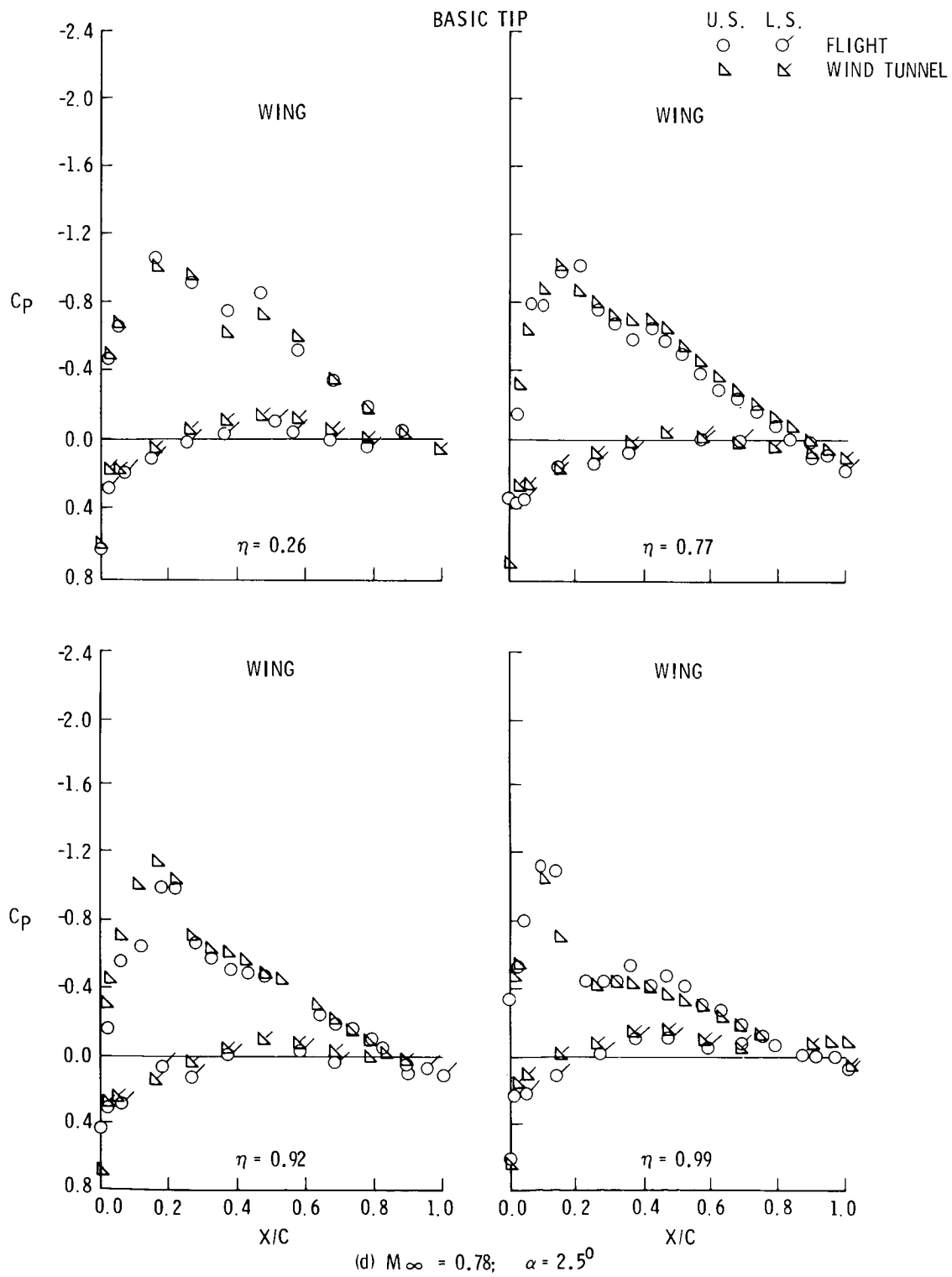


Figure 7. - Continued

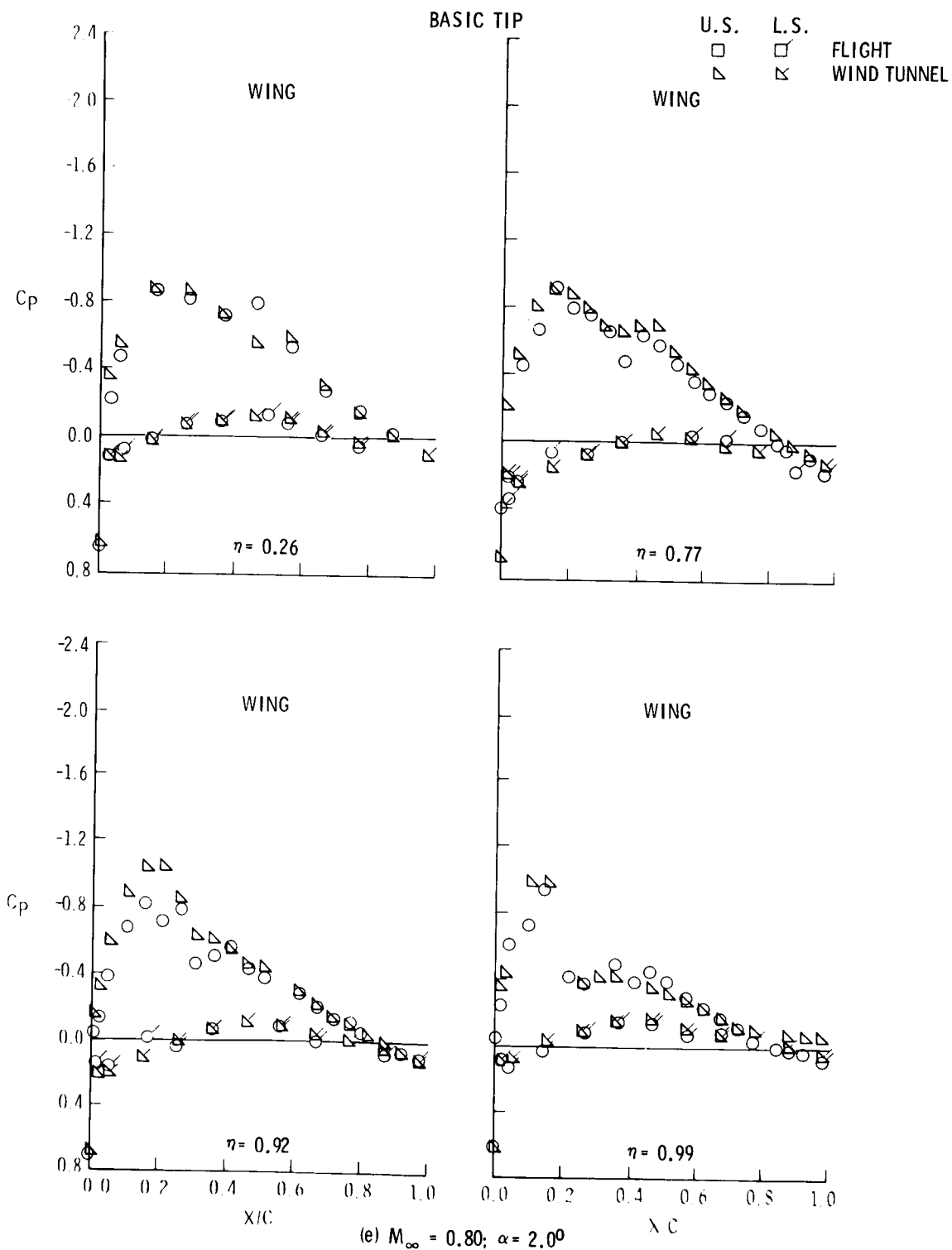


Figure 7. - Continued

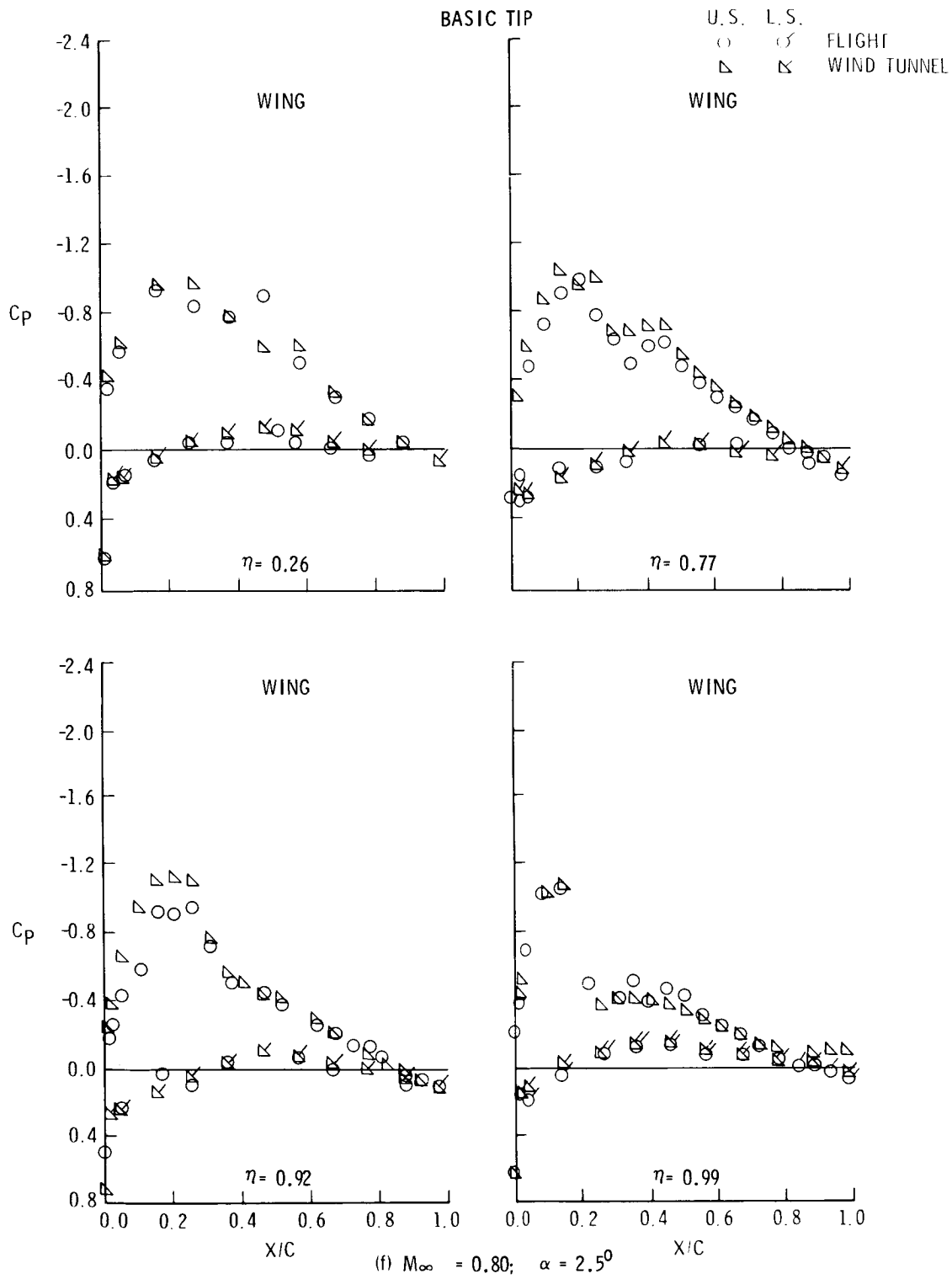


Figure 7. - Concluded

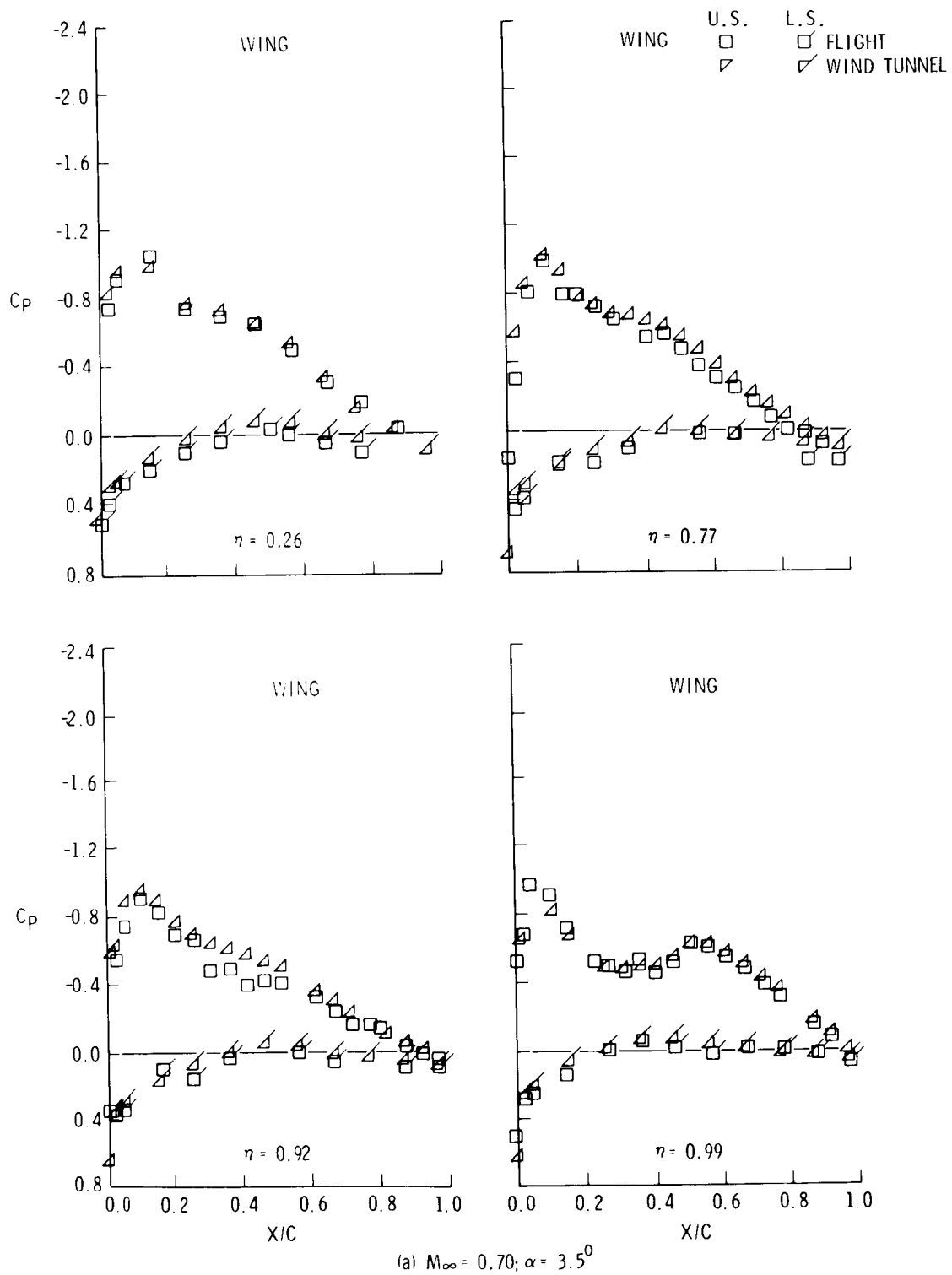
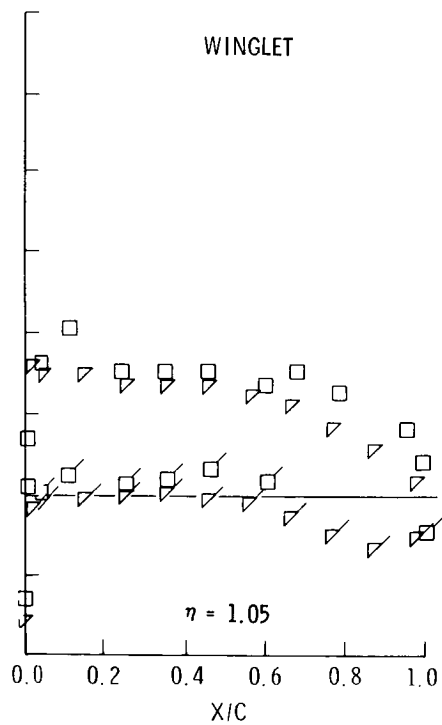
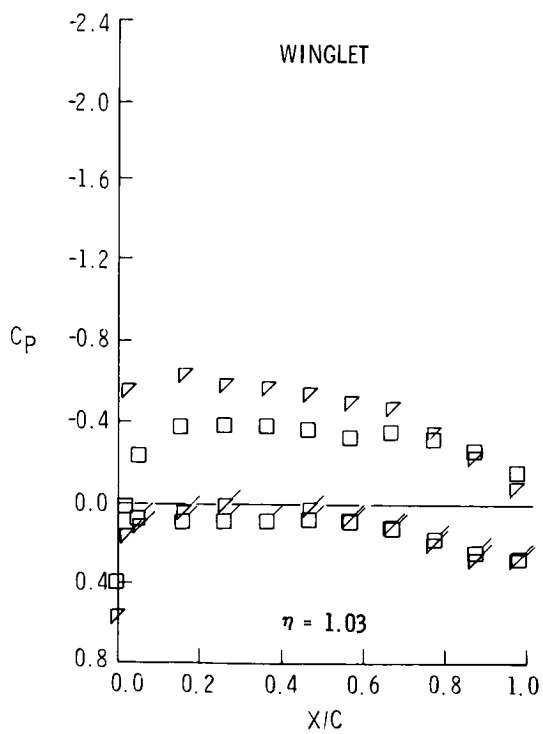
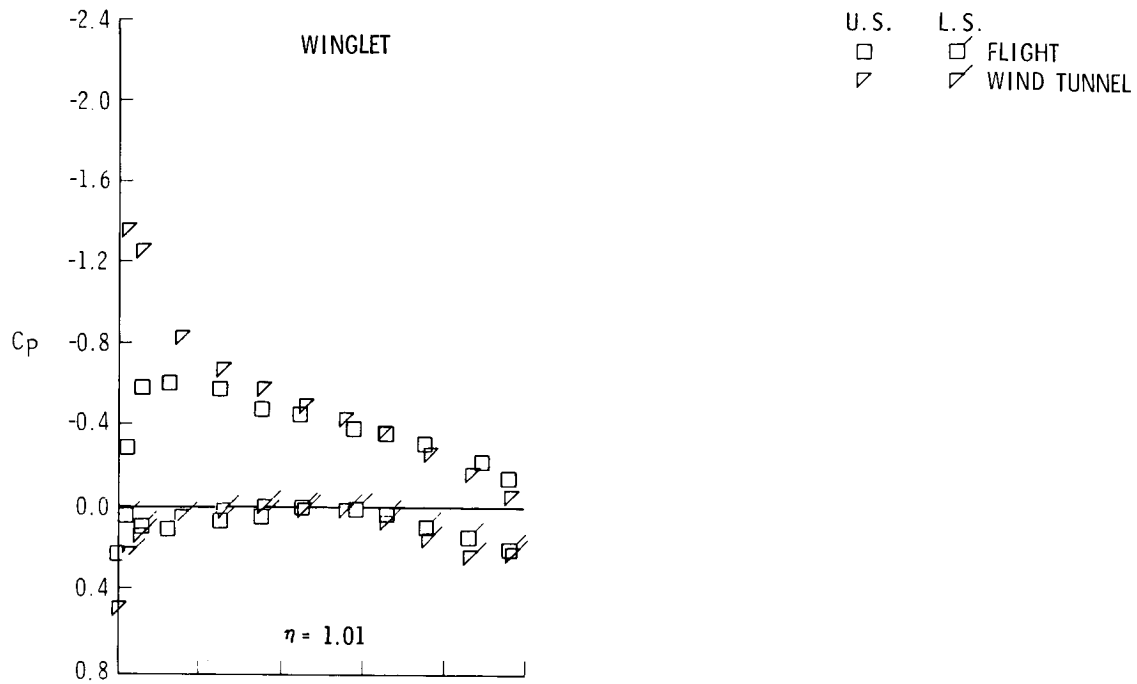
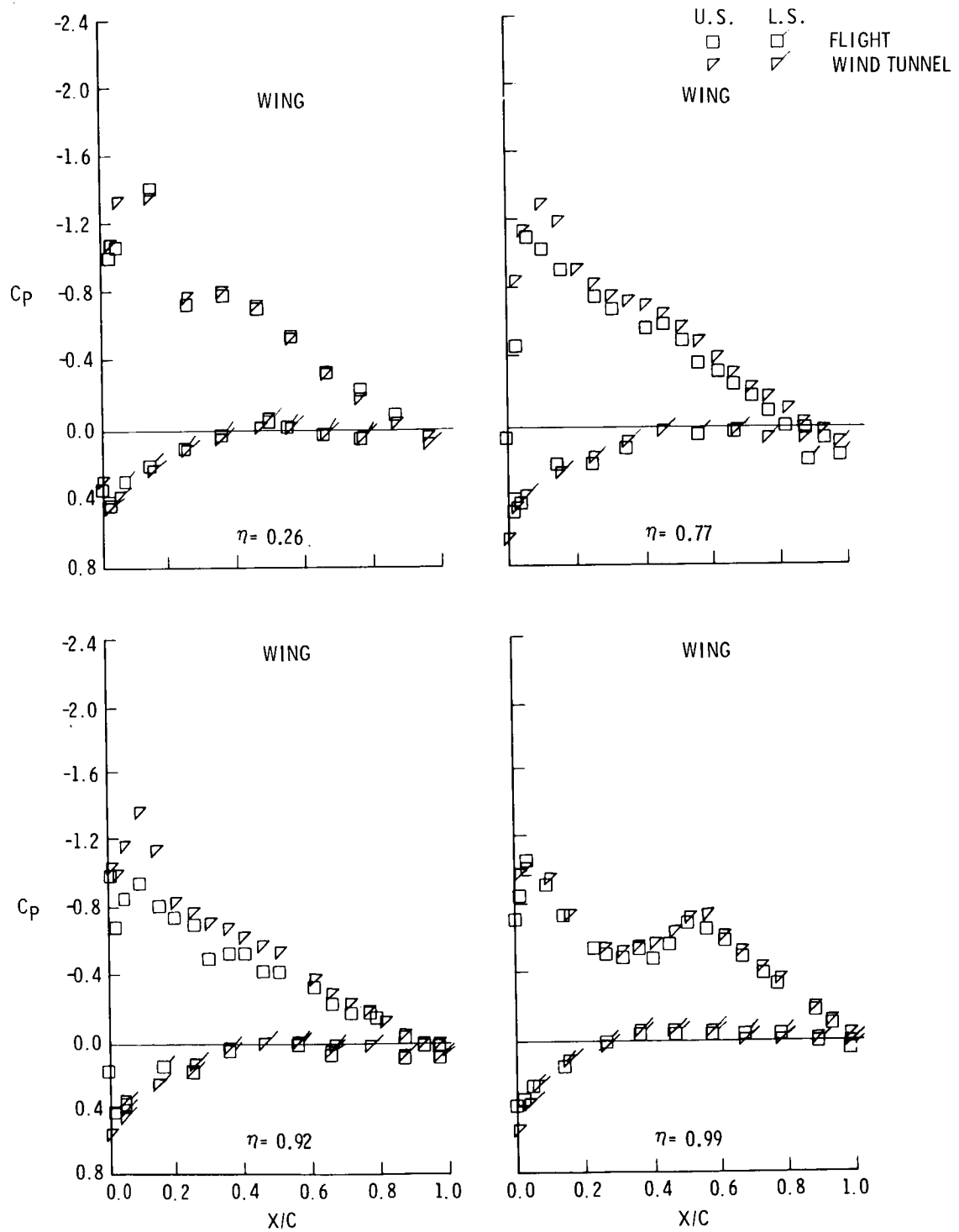


Figure 8. - Comparison of flight and windtunnel wing and winglet pressure distribution for the  $15^\circ/-4^\circ$  winglet configuration



(a)  $M_\infty = 0.70$ ;  $\alpha = 3.5^\circ$  CONCLUDED

Figure 8. - Continued



(b)  $M_\infty = 0.70$ ;  $\alpha = 5.0^\circ$

Figure 8. - Continued

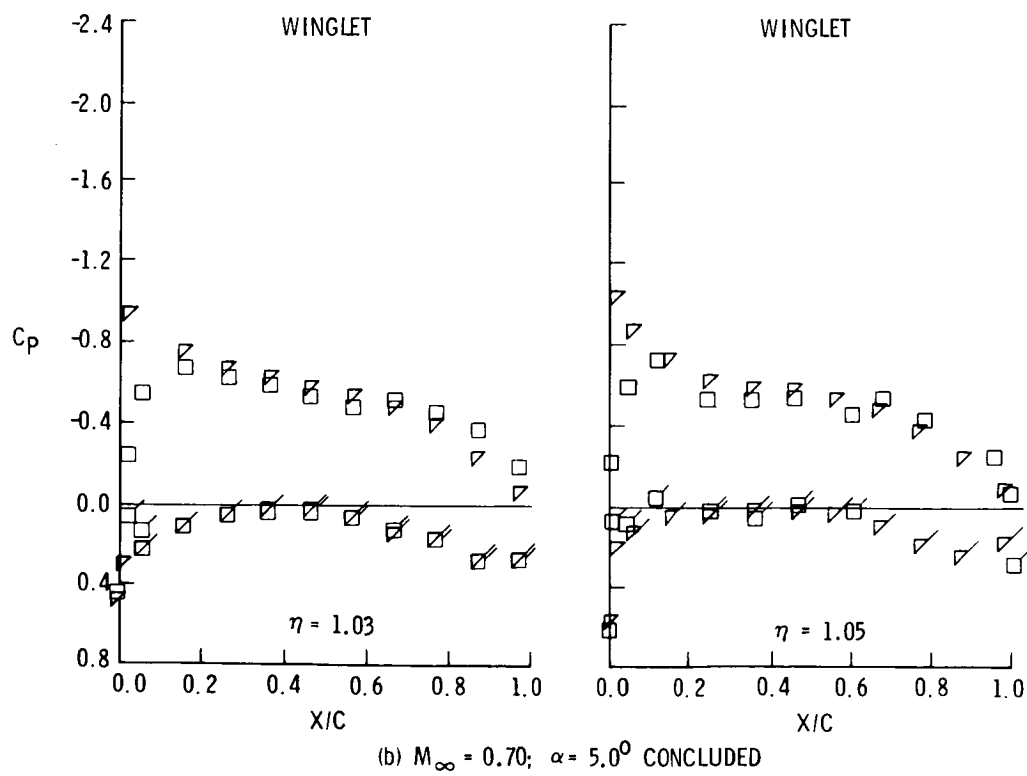
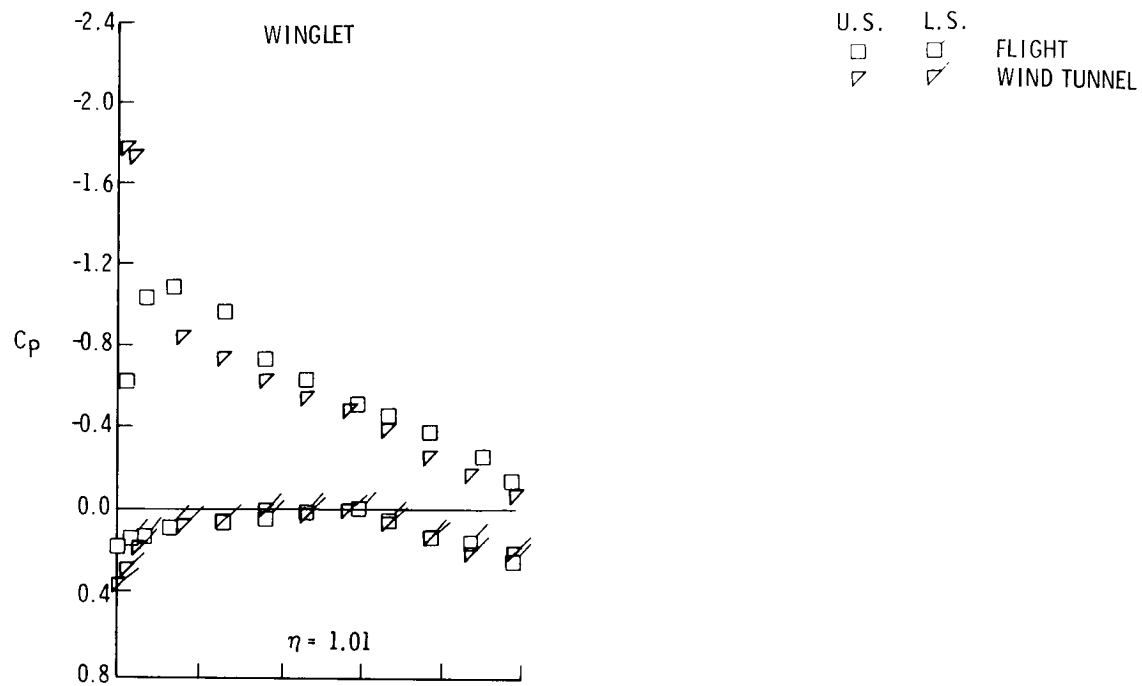


Figure 8. - Continued

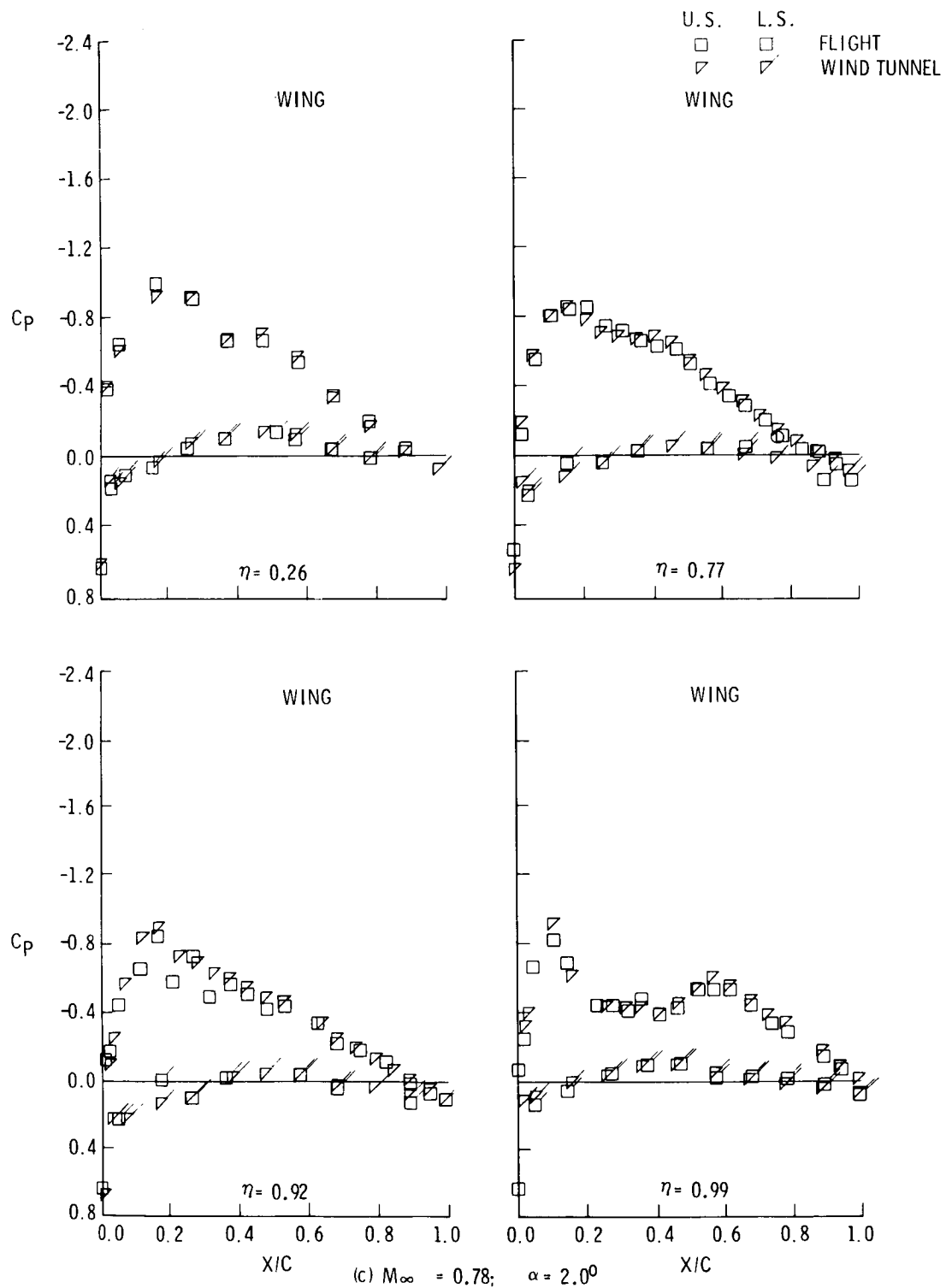


Figure 8. - Continued



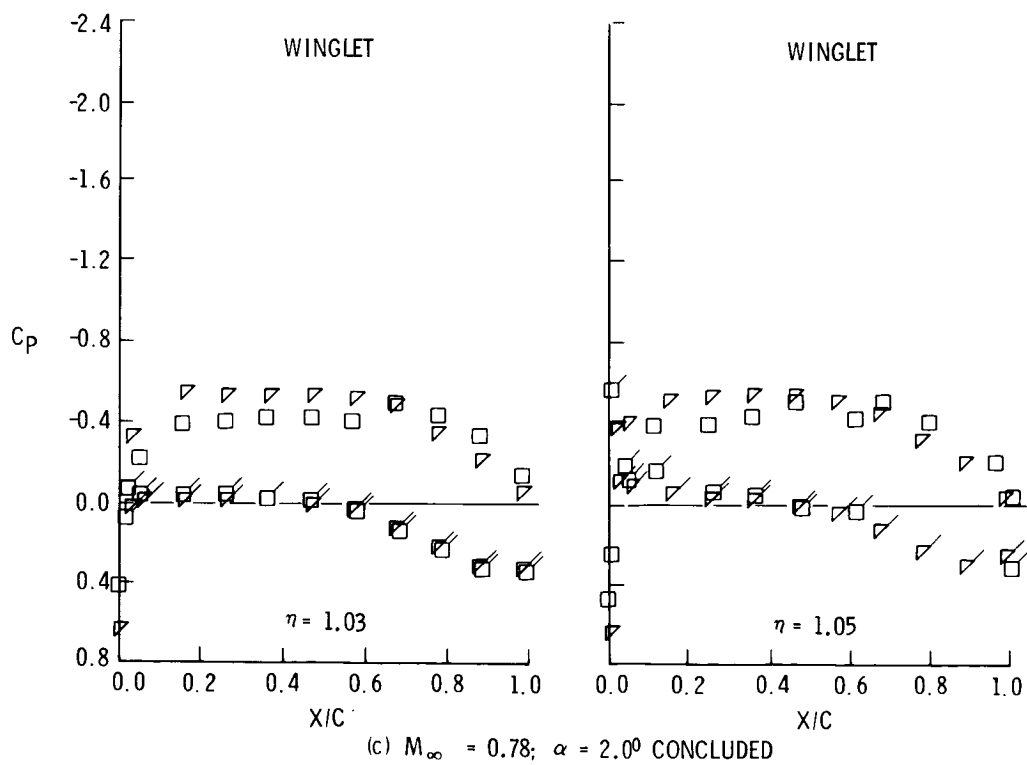
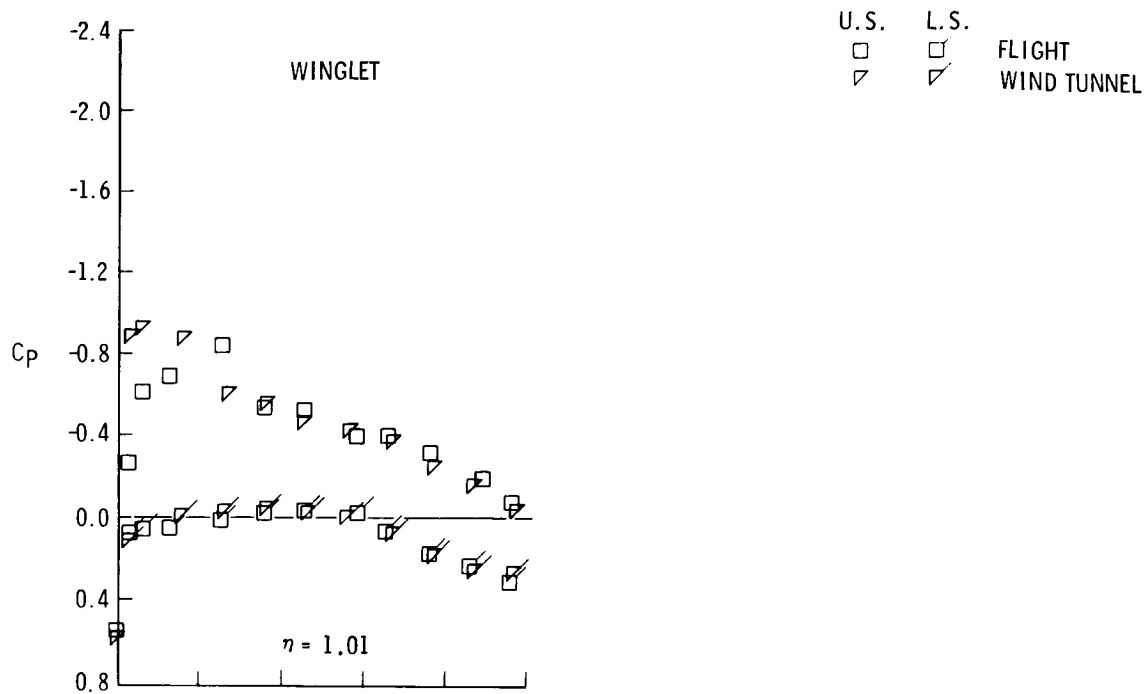


Figure 8. - Continued

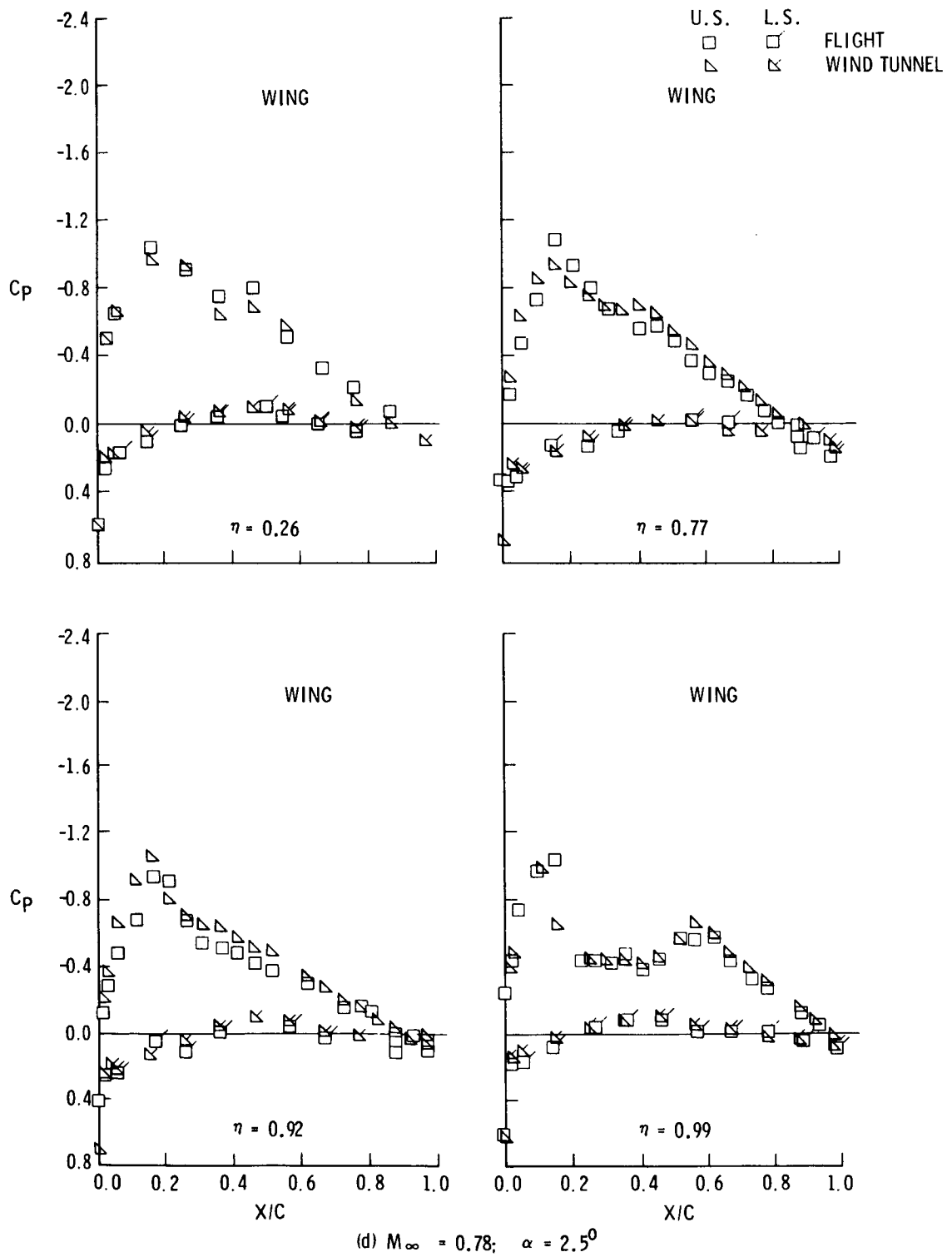


Figure 8. - Continued

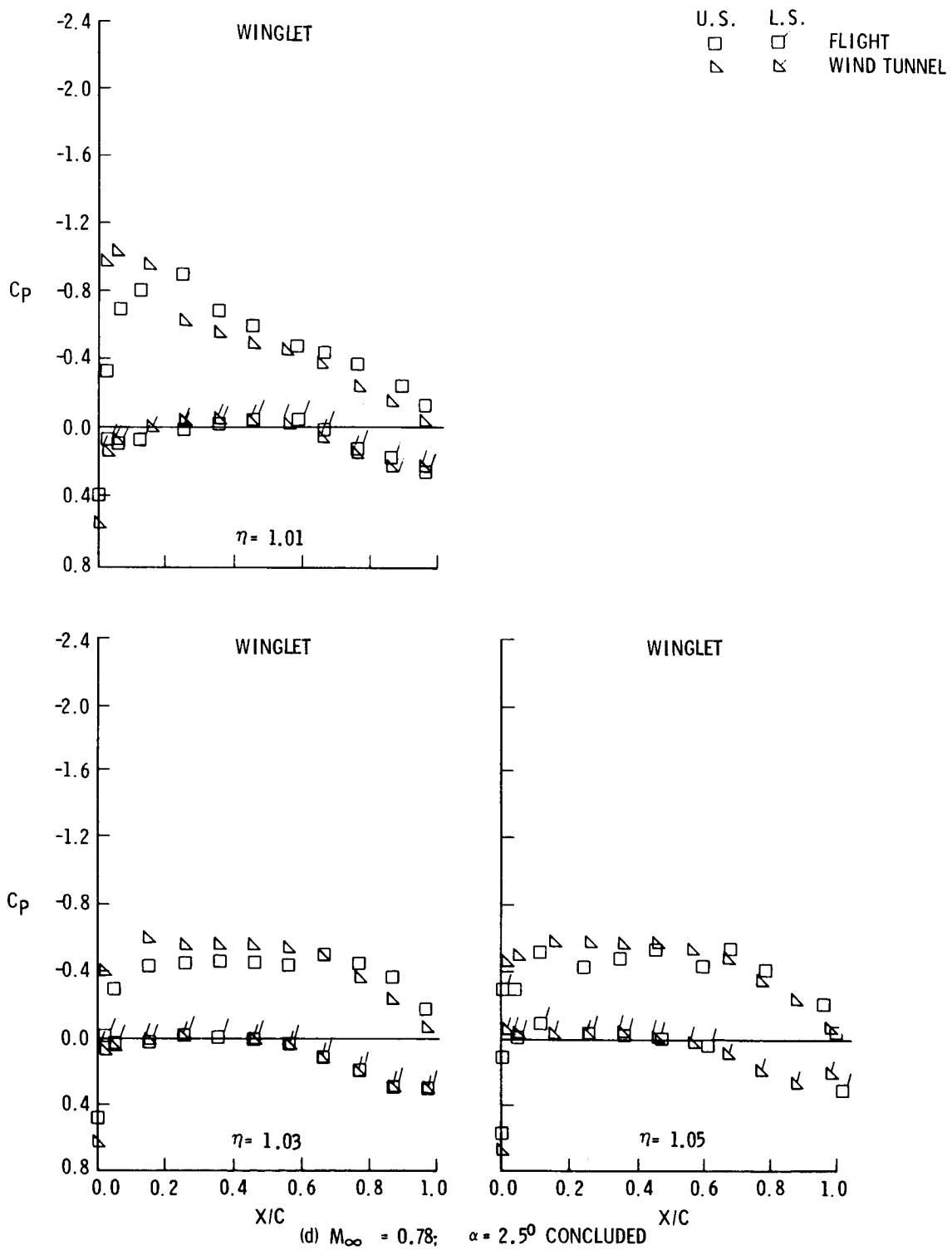


Figure 8. - Continued

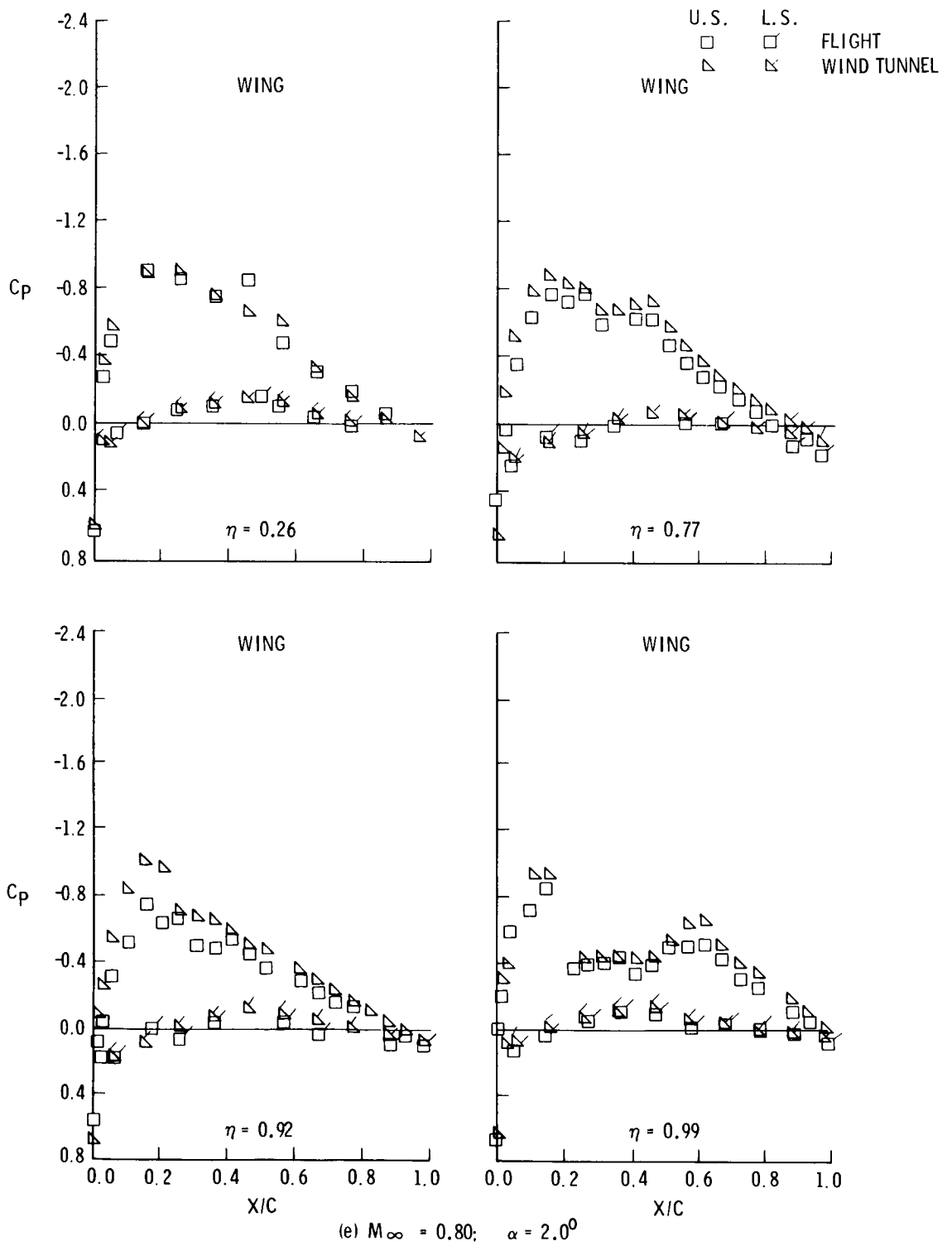
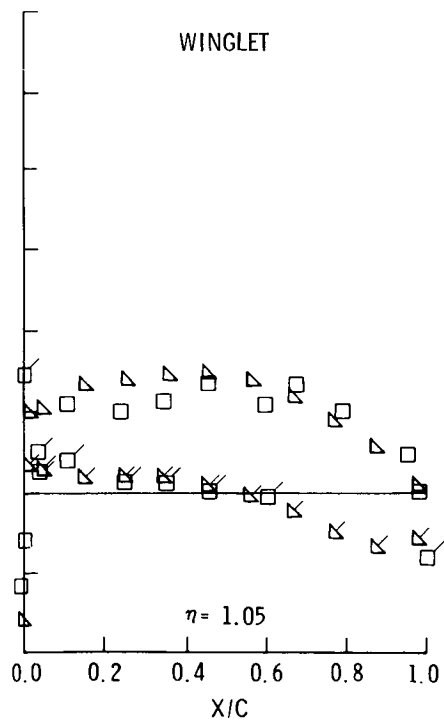
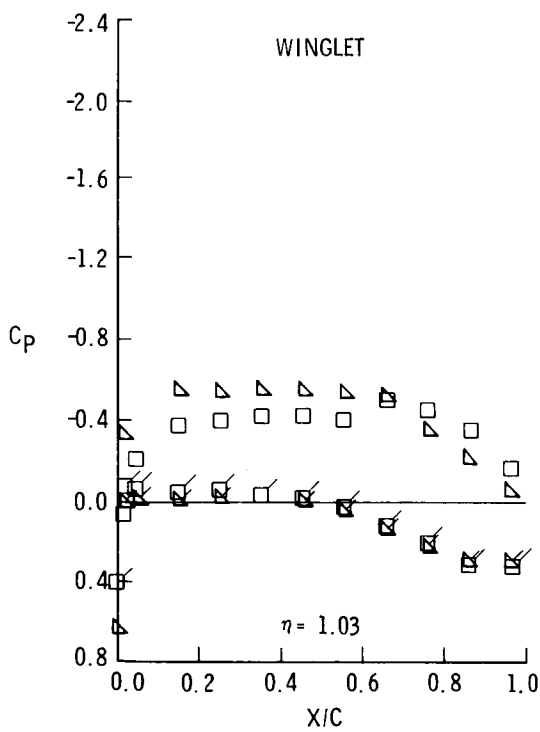
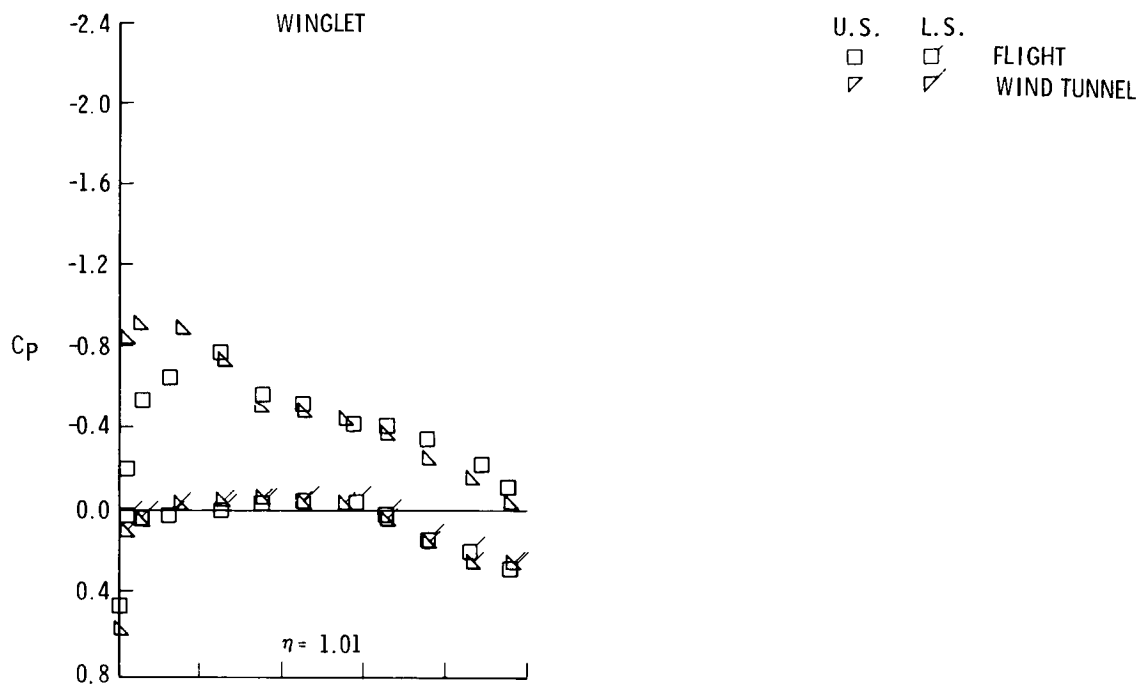


Figure 8. - Continued



(e)  $M_\infty = 0.80$ ;  $\alpha = 2.0^\circ$  CONCLUDED

Figure 8. - Continued

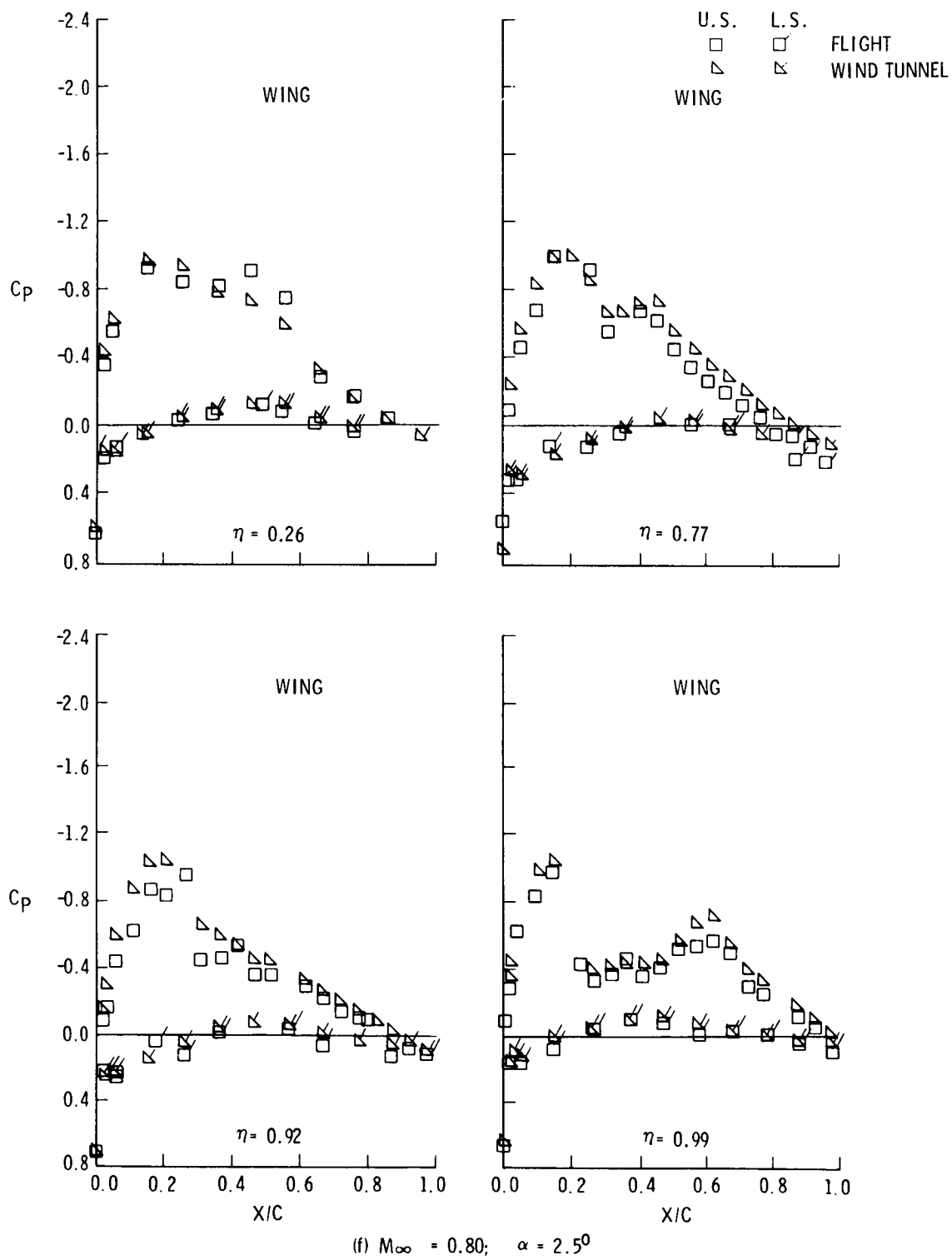


Figure 8. - Continued

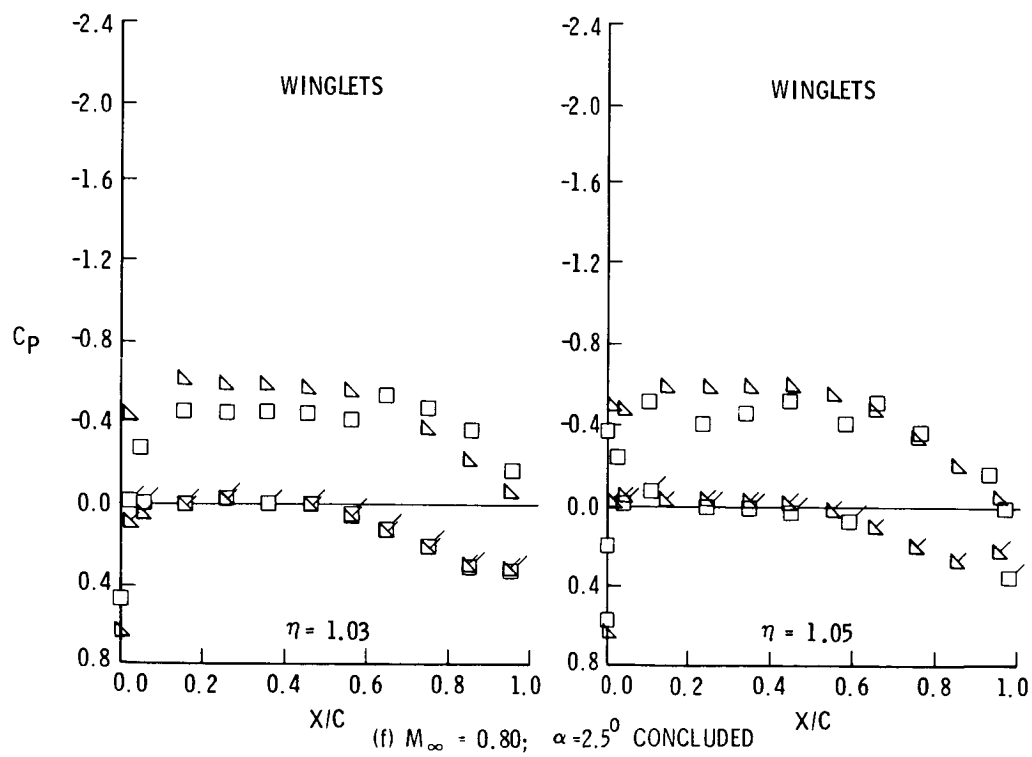
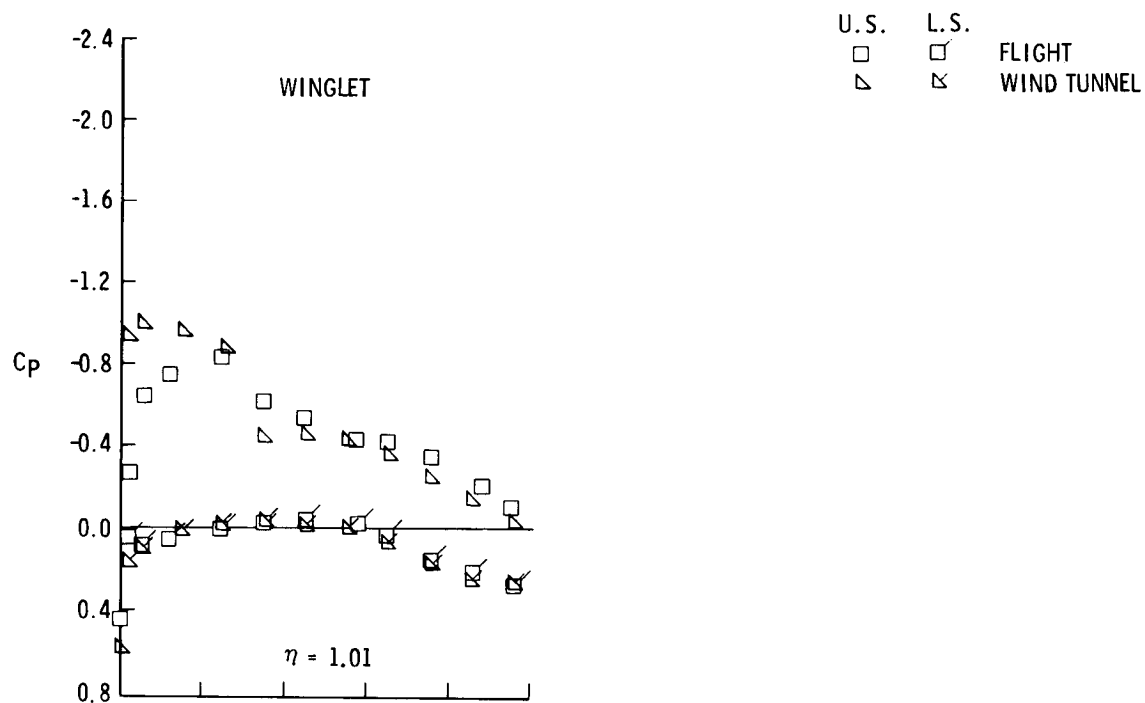


Figure 8. - Concluded

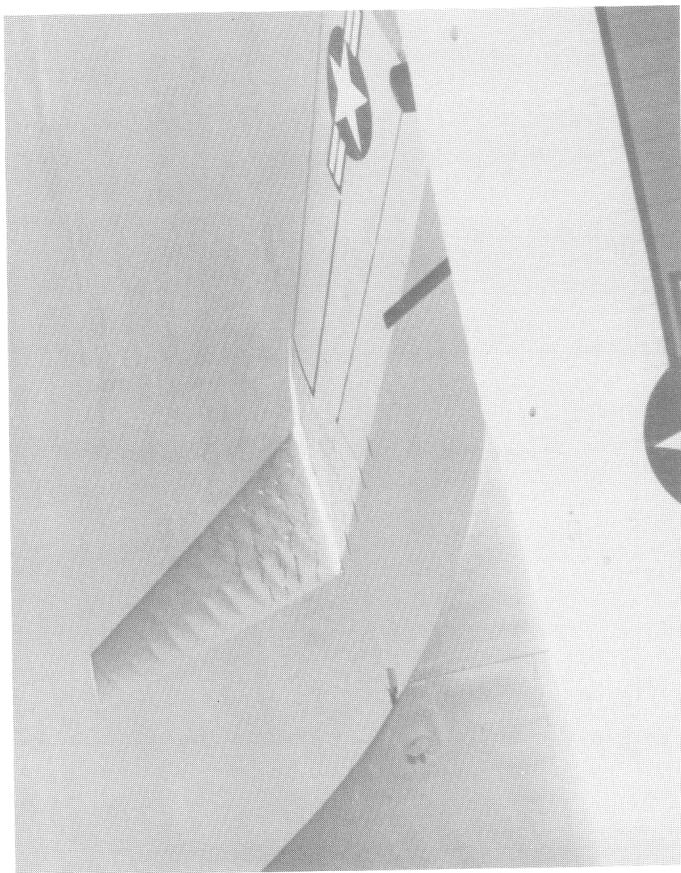


Figure 9. - Inflight photo of winglet "oilcanning"



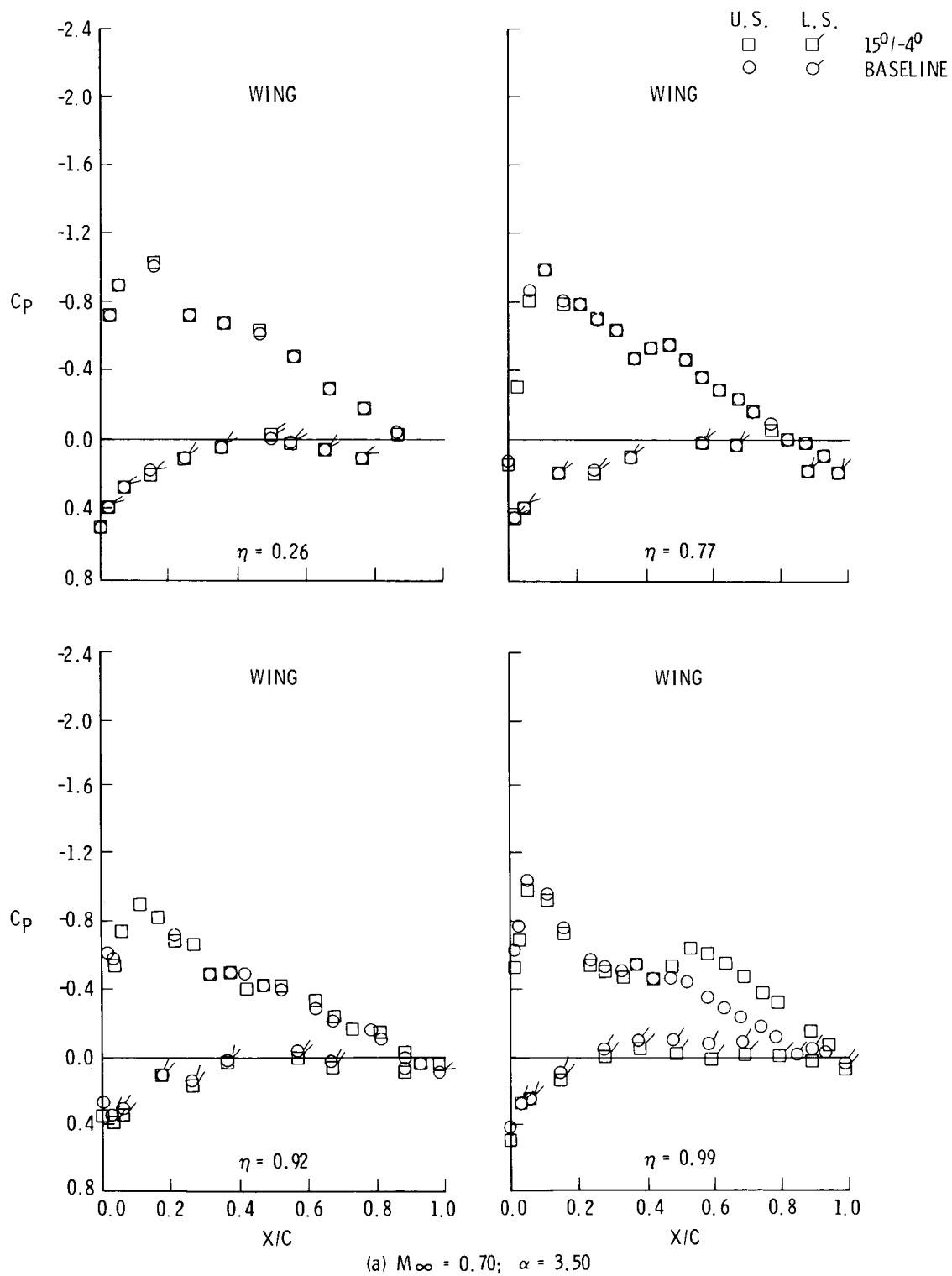


Figure 10. - Flight wing pressure distribution comparisons with the basic wing tip and 15°/-4° winglet configuration

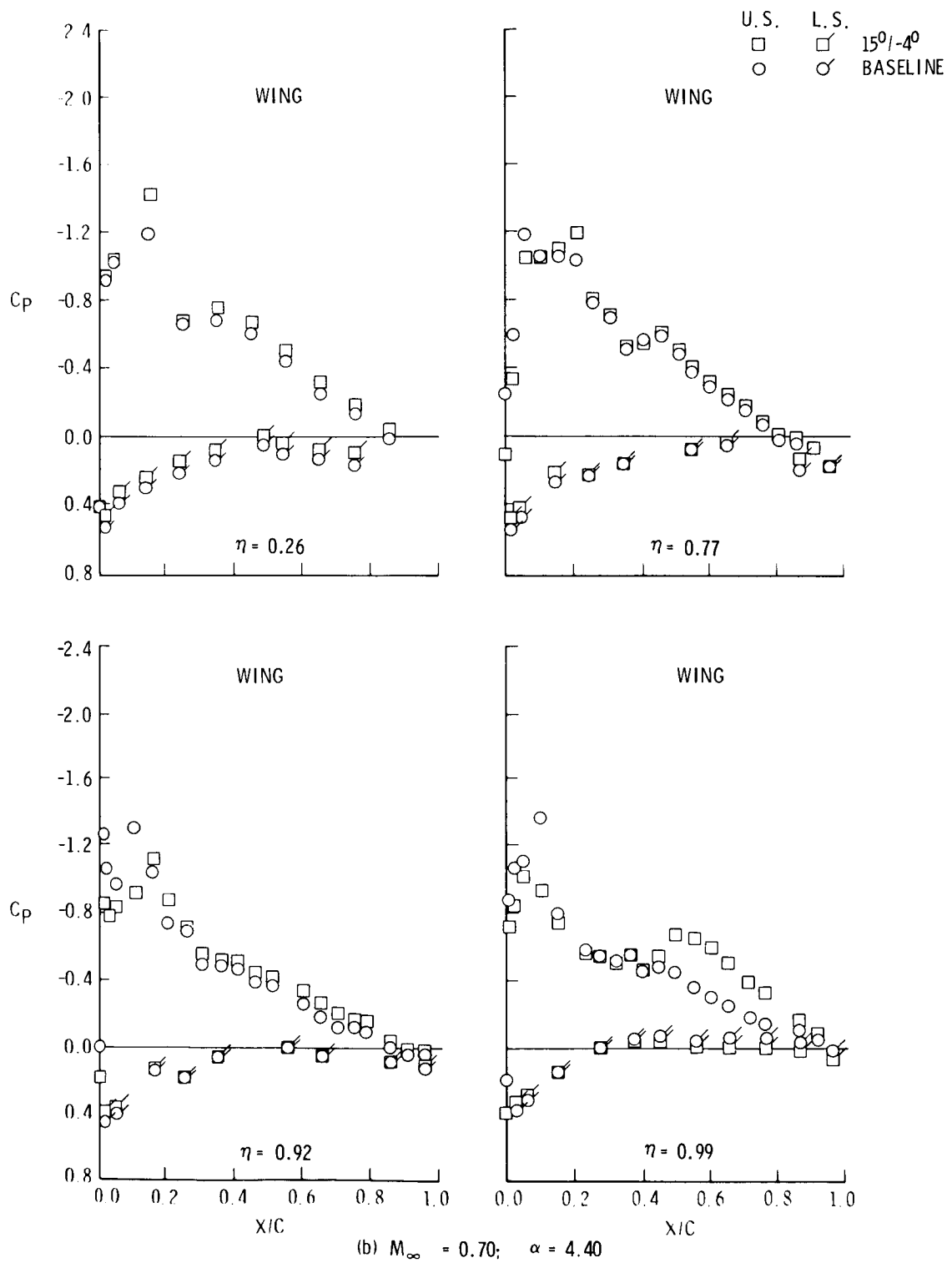


Figure 10. - Continued

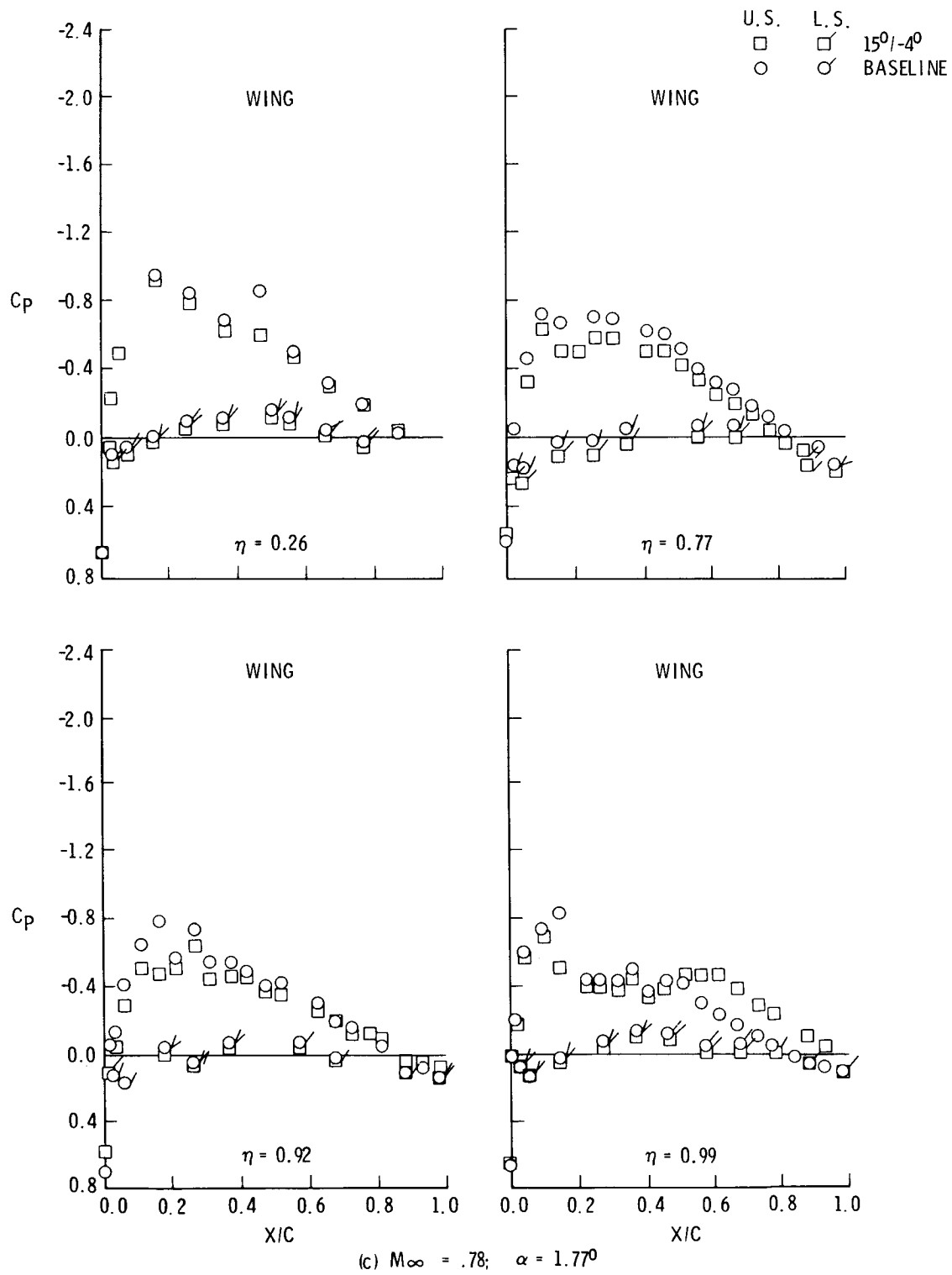


Figure 10. - Continued

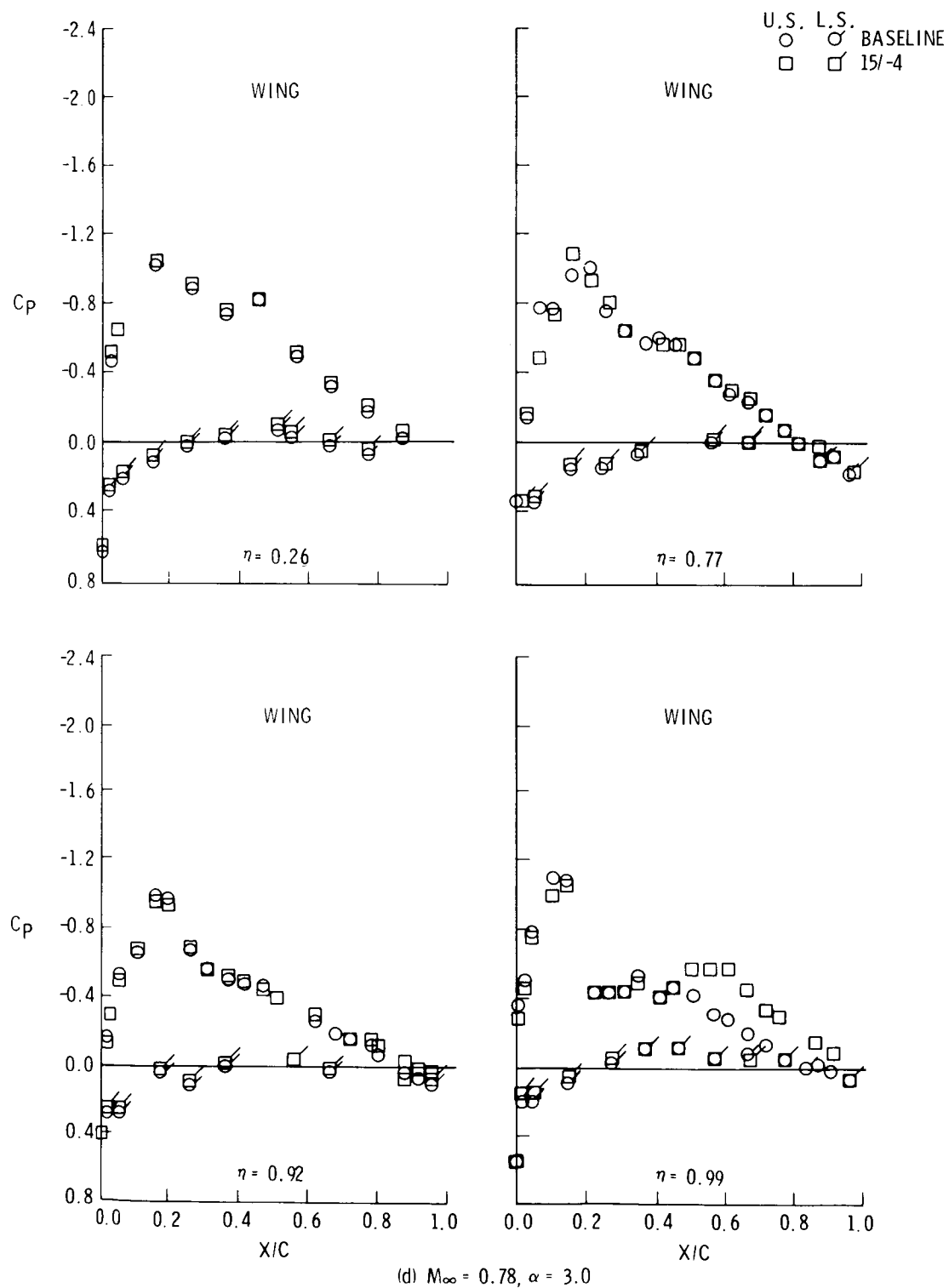


Figure 10. - Continued

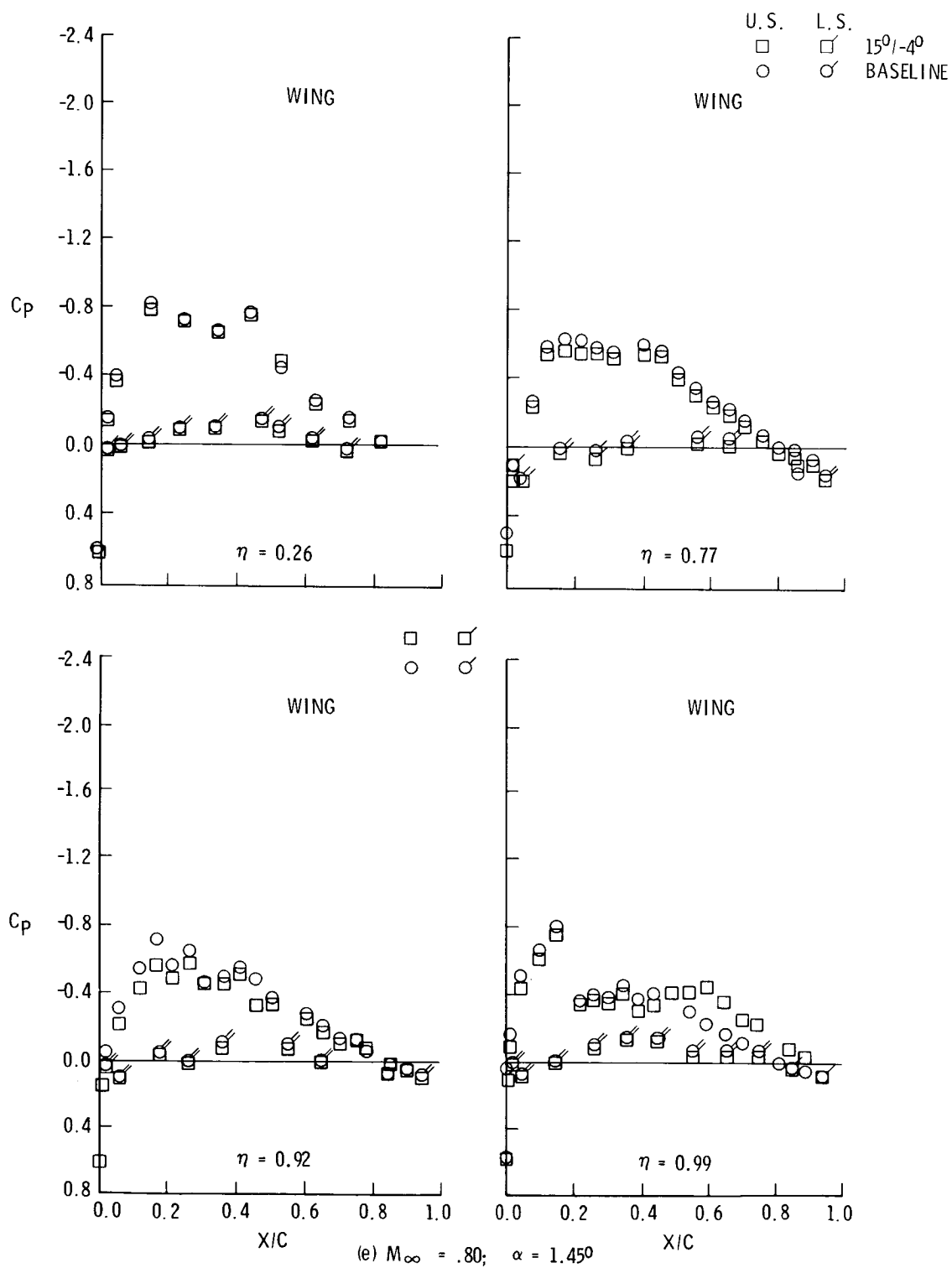


Figure 10. - Continued

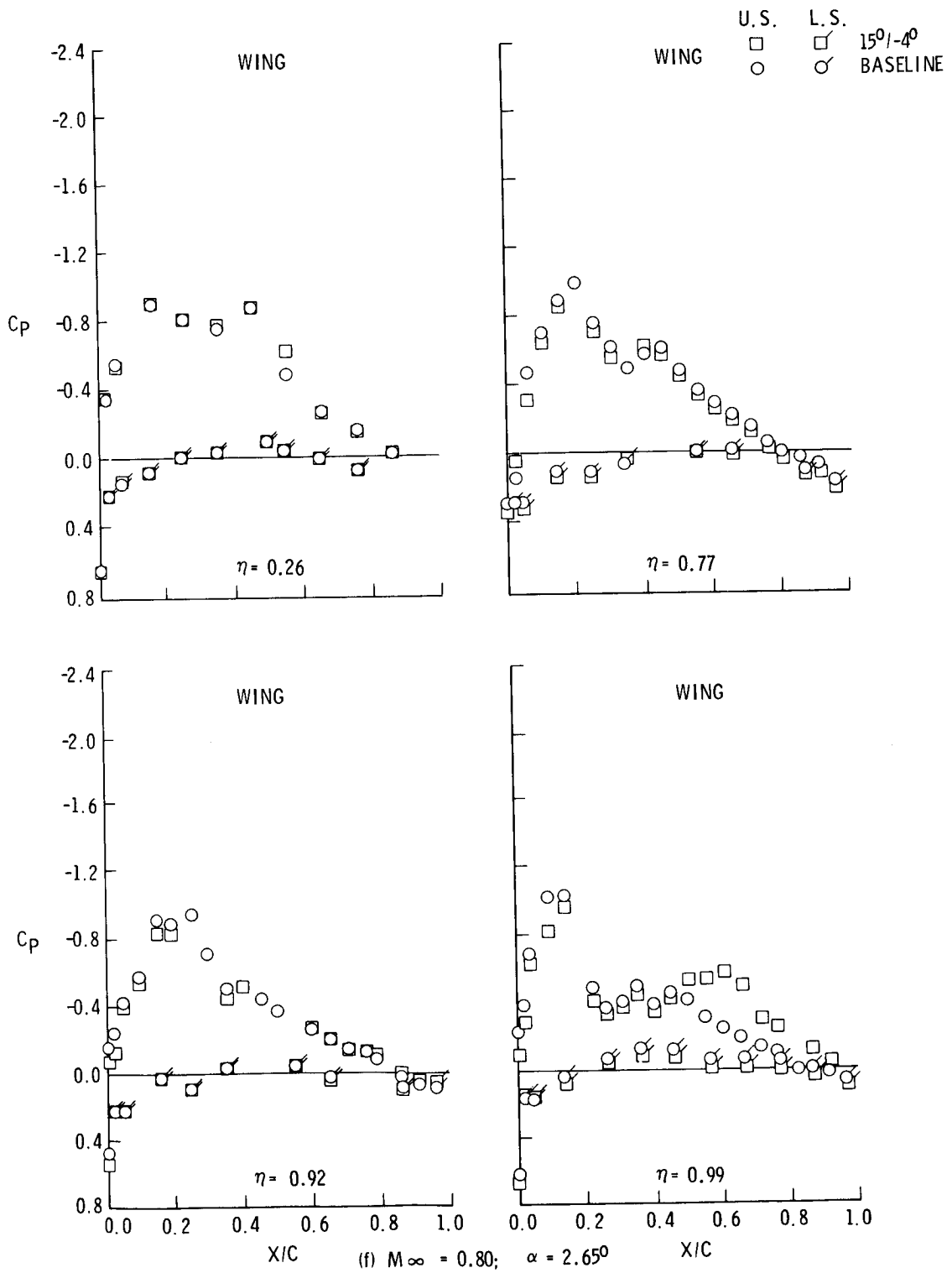


Figure 10. - Continued

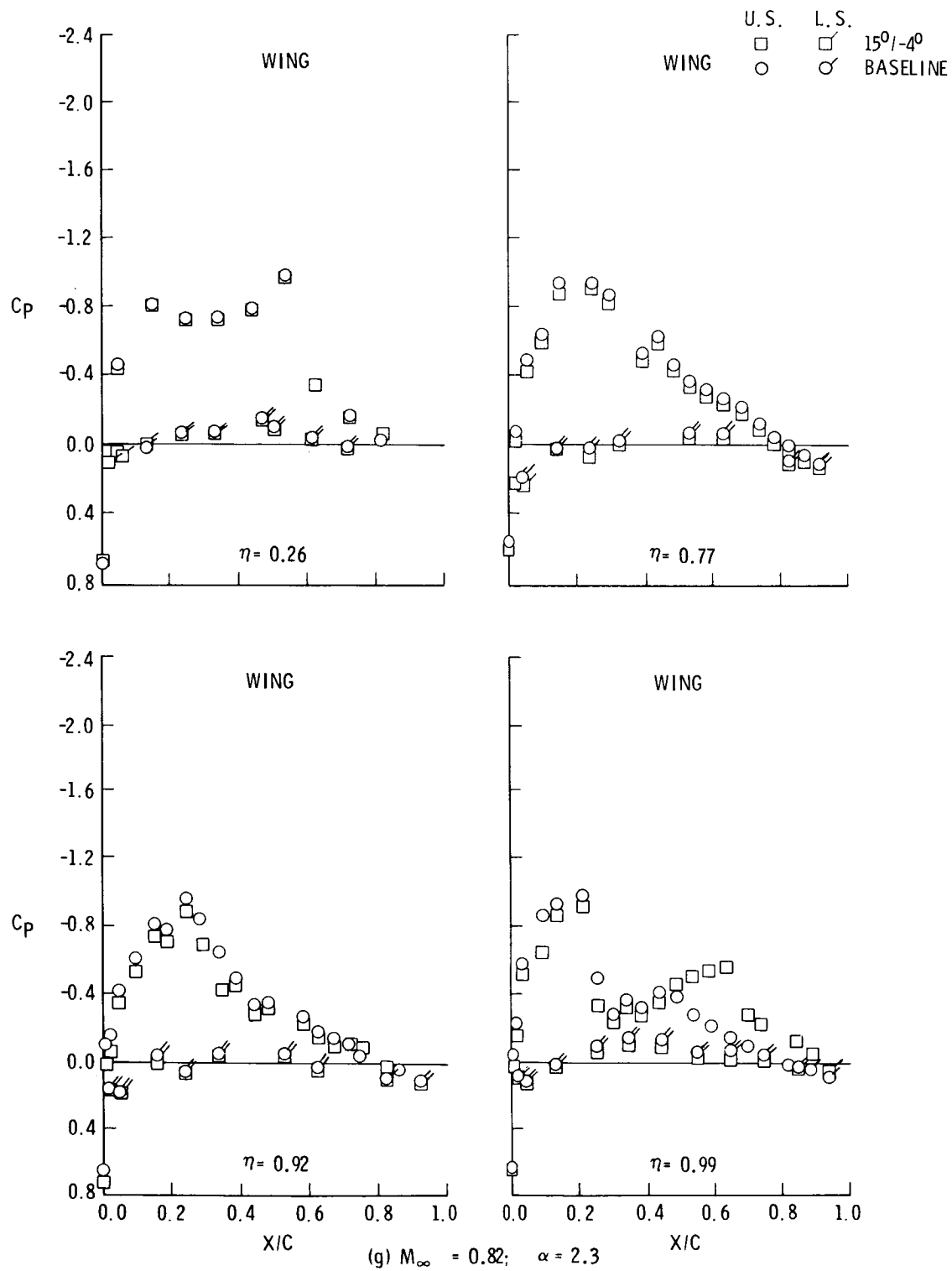


Figure 10. - Concluded

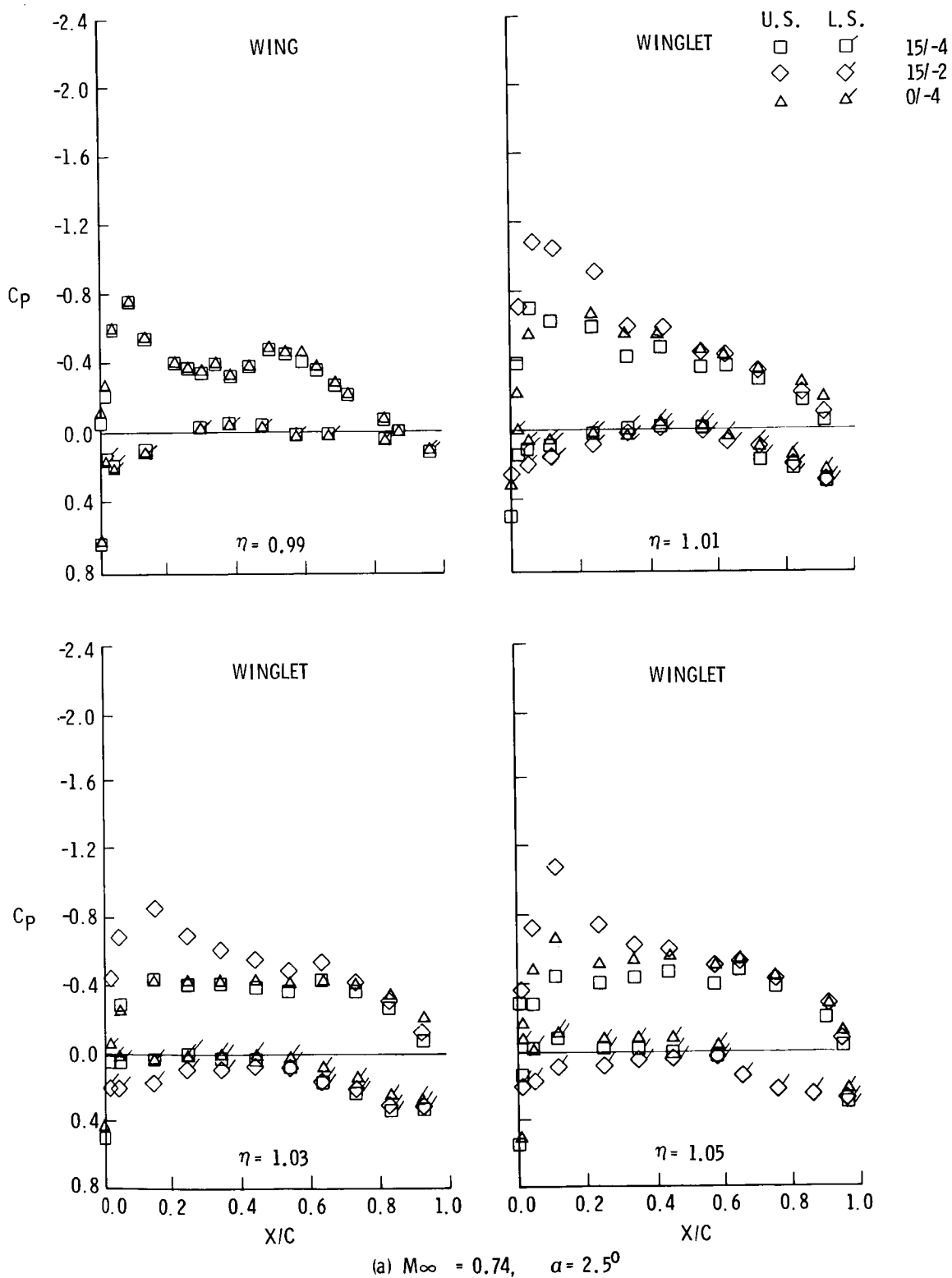
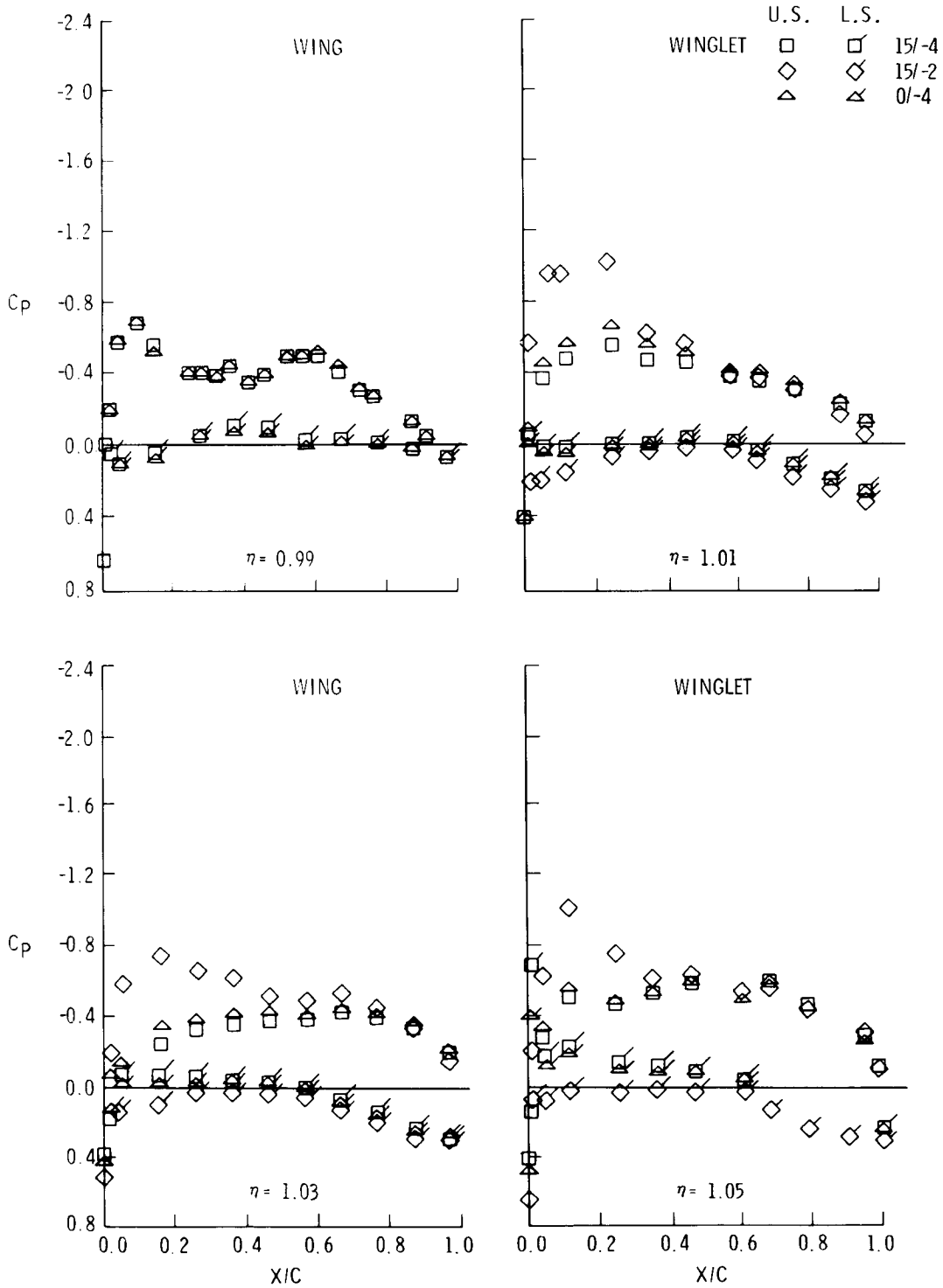


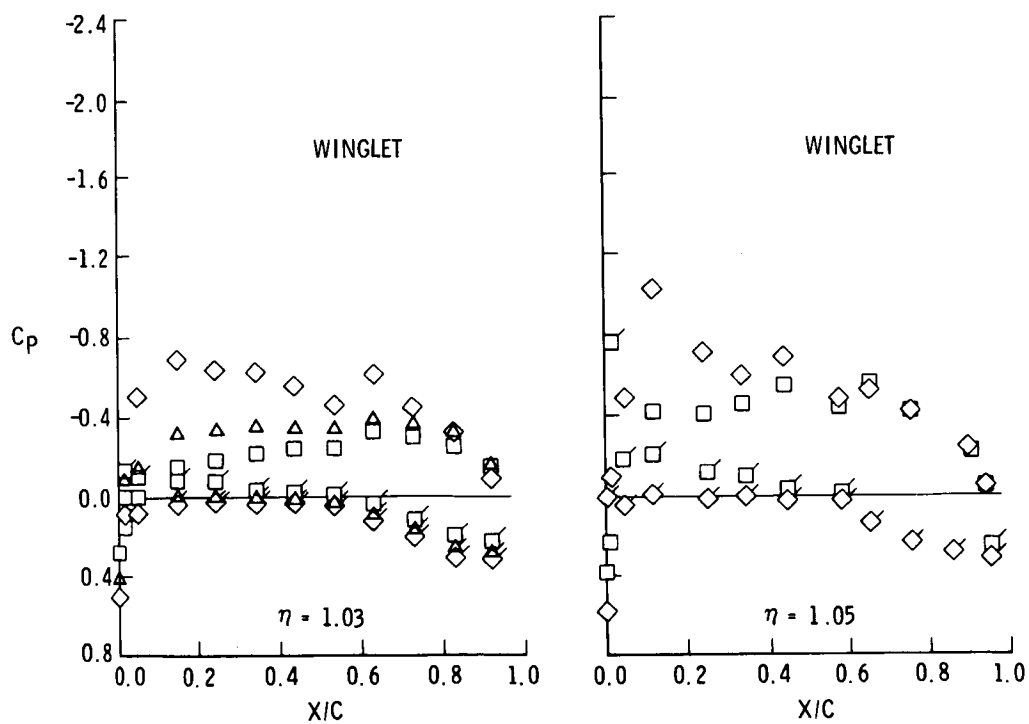
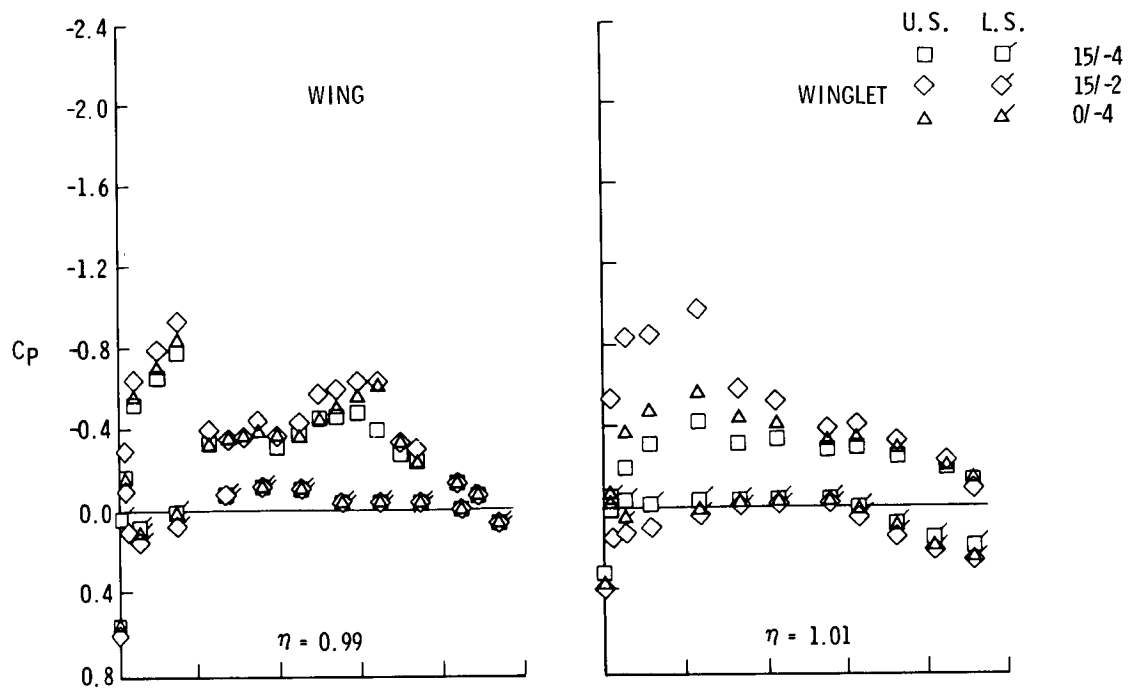
Figure 11. - Flight wing tip and winglet pressure distributions for the 15°/-4°, 15°/-2°, and 0°/-4° winglet cant/incidence configurations





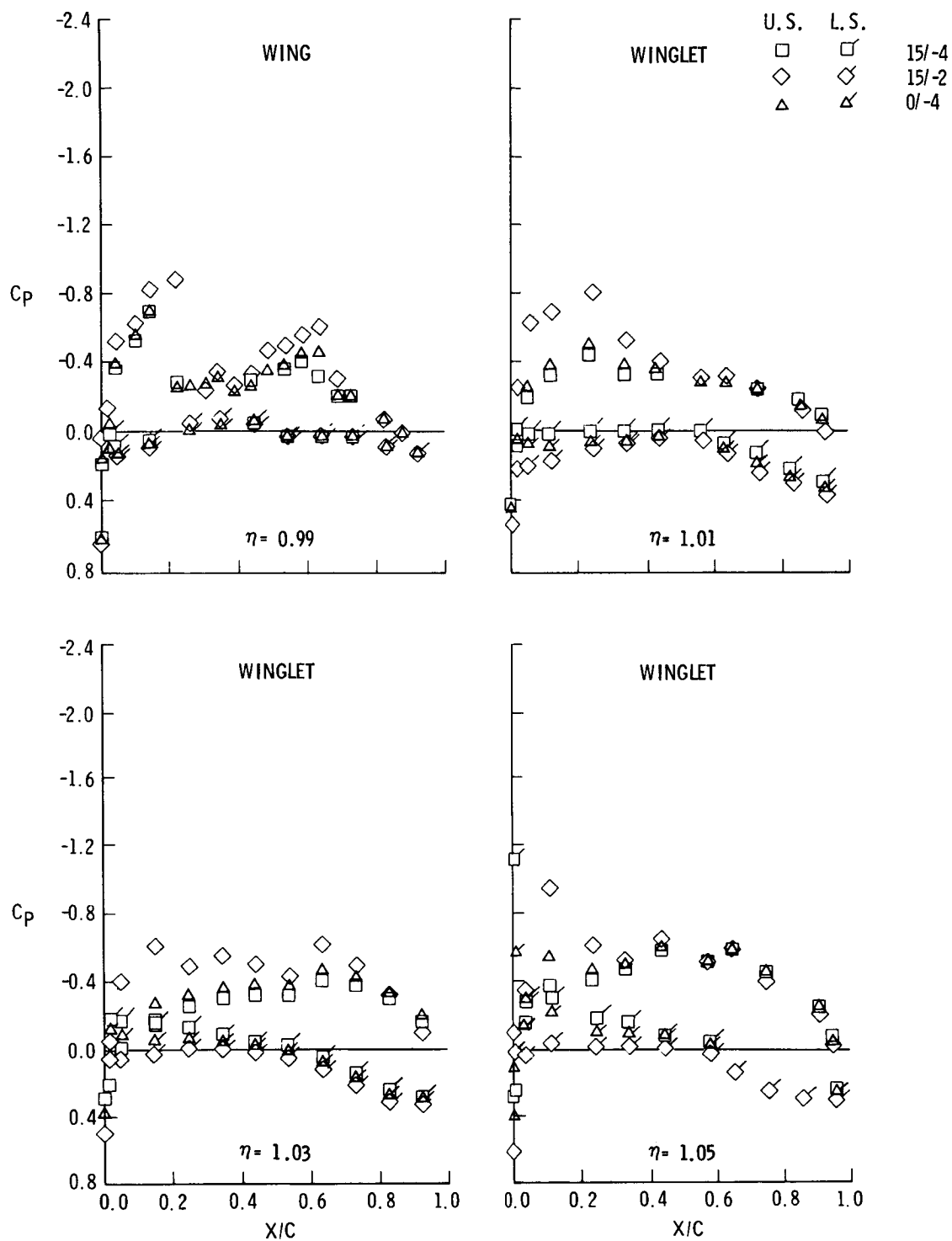
(b)  $M_\infty = 0.78$ ,  $\alpha = 1.90$

Figure 11. - Continued



(c)  $M_\infty = 0.80, \alpha = 1.80$

Figure 11. - Continued



(d)  $M_\infty = 0.82$ ;  $\alpha = 1.30$

Figure 11. - Concluded

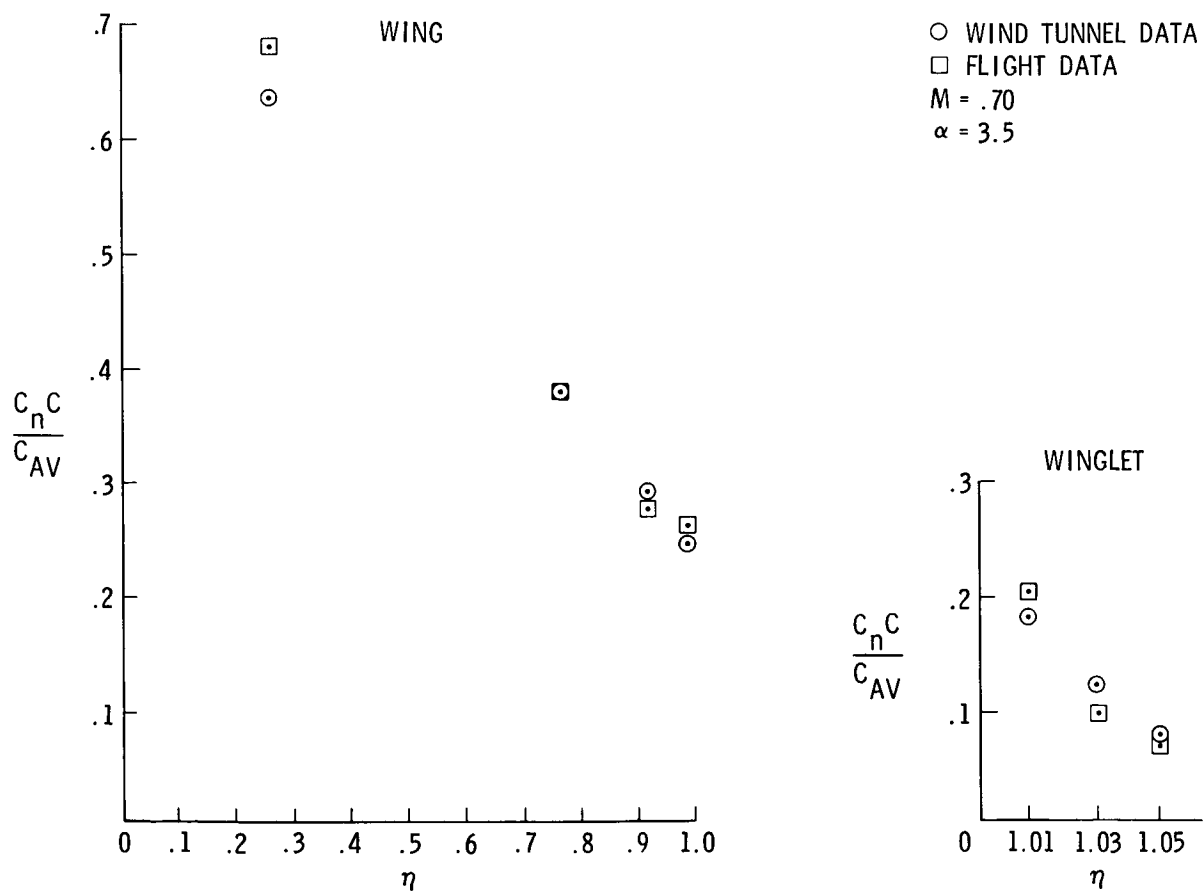


Figure 12. - Comparison of flight and windtunnel wing and winglet span load

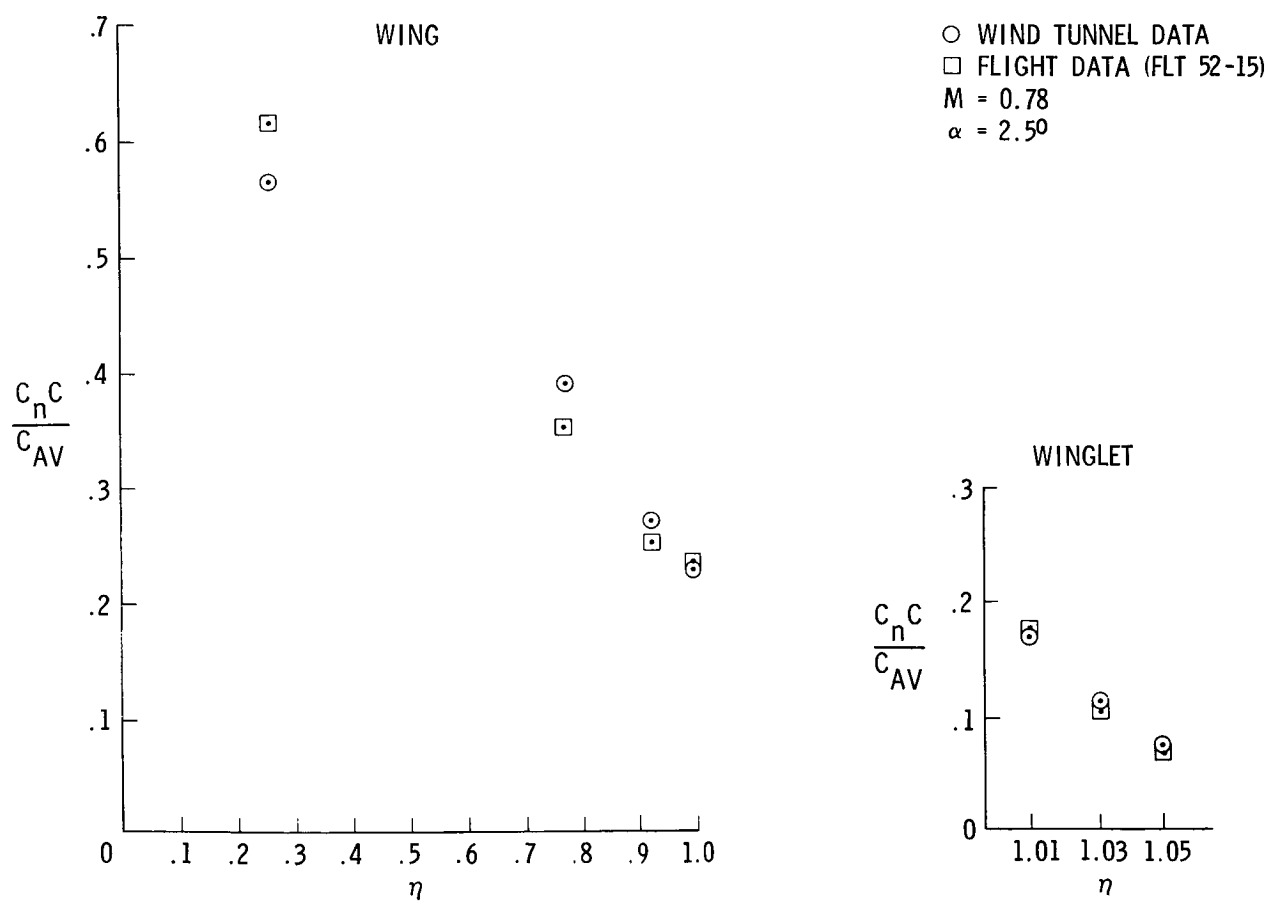


Figure 12. - Continued

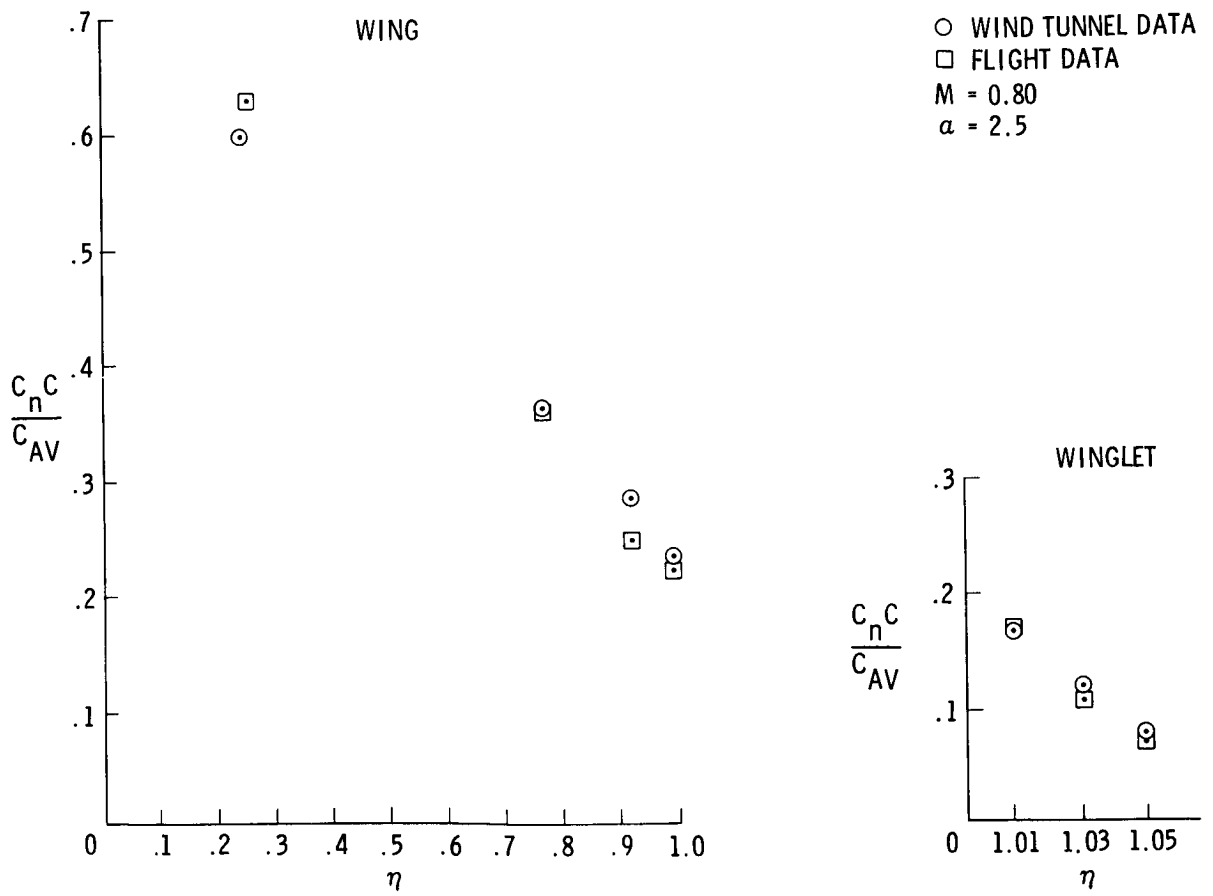


Figure 12. - Concluded

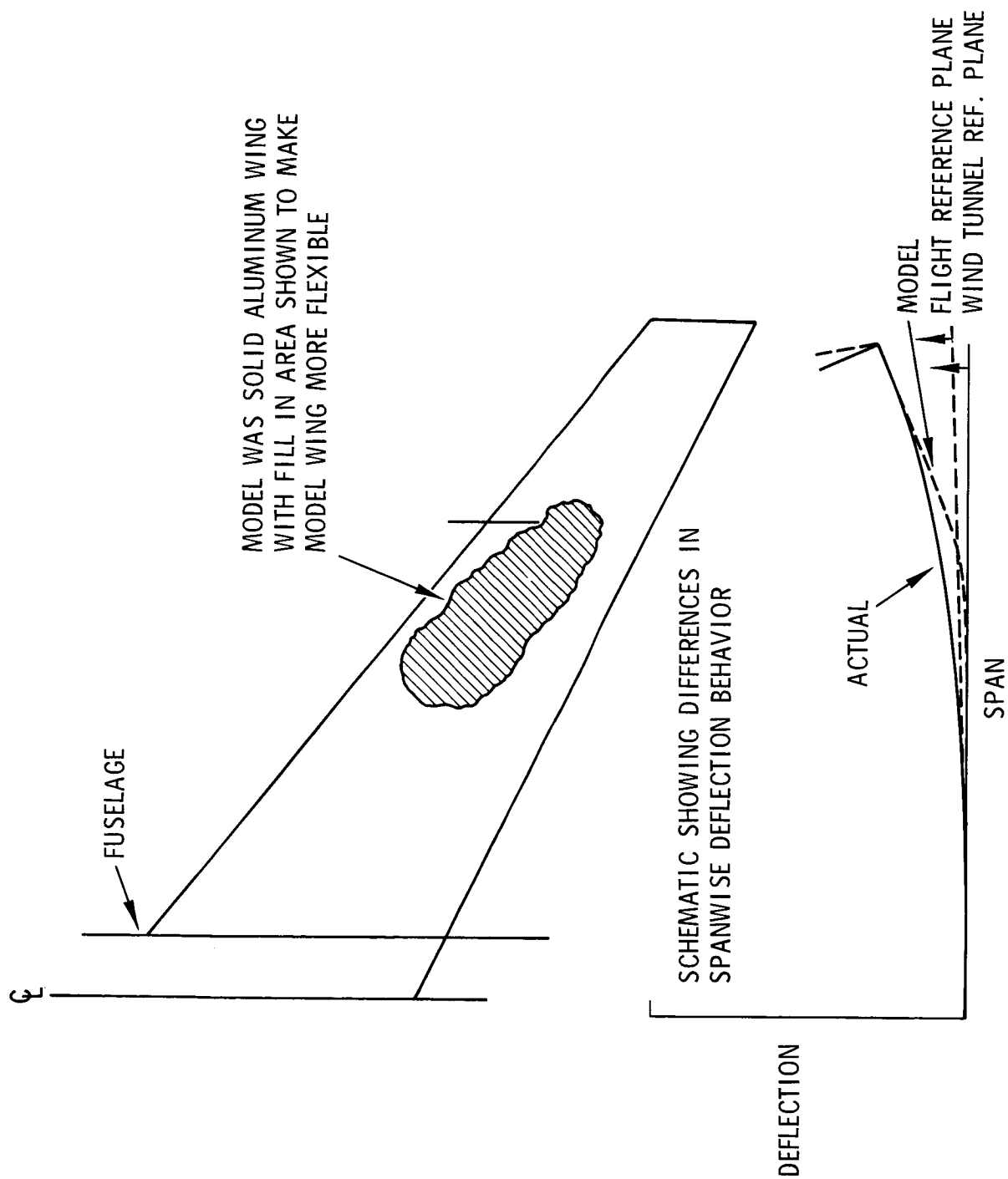


Figure 13. - Schematics of the semispan model wing construction flight versus wind tunnel model deflection measurements

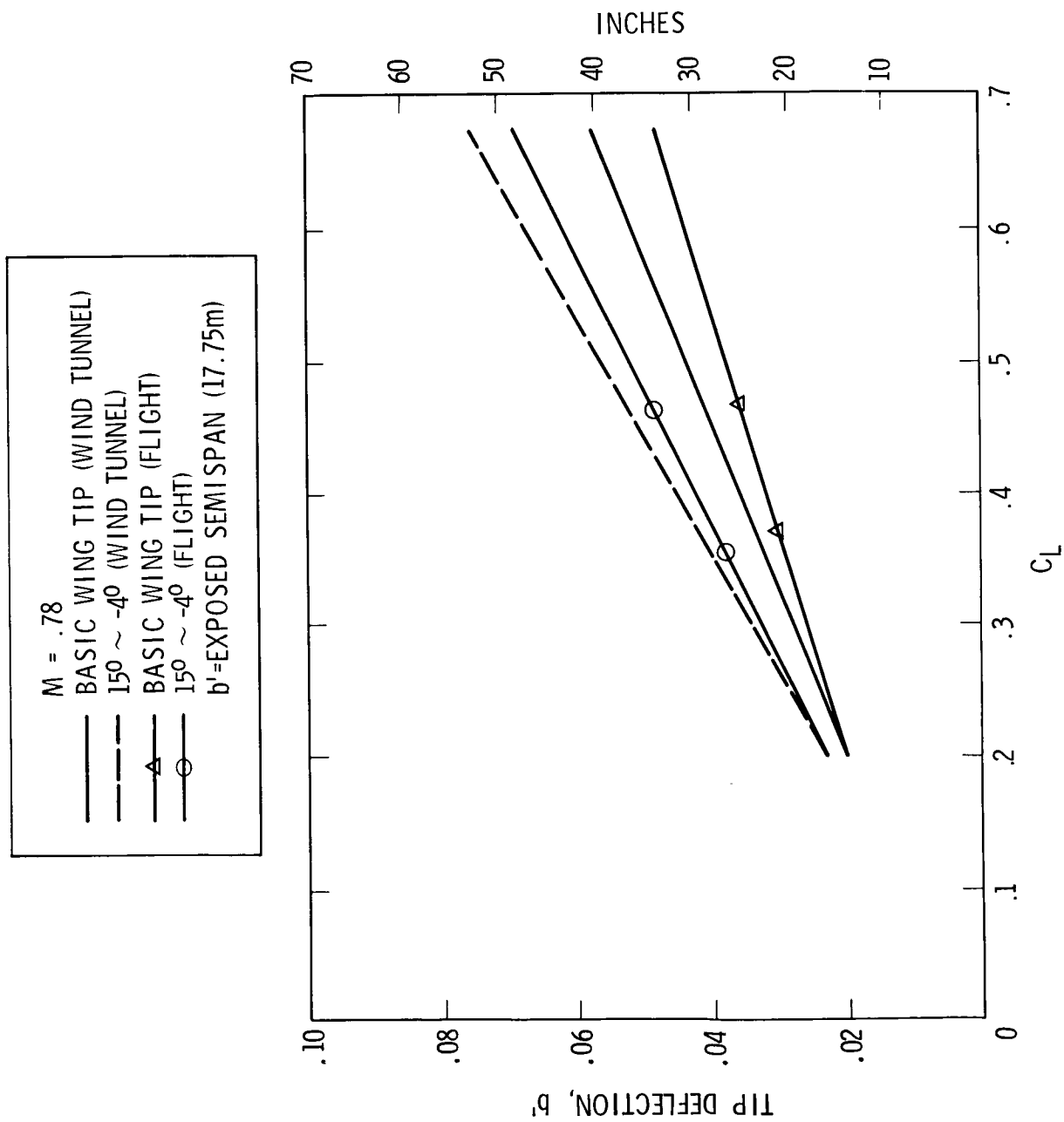


Figure 14. - Flight versus wind tunnel deflections at the design cruise condition



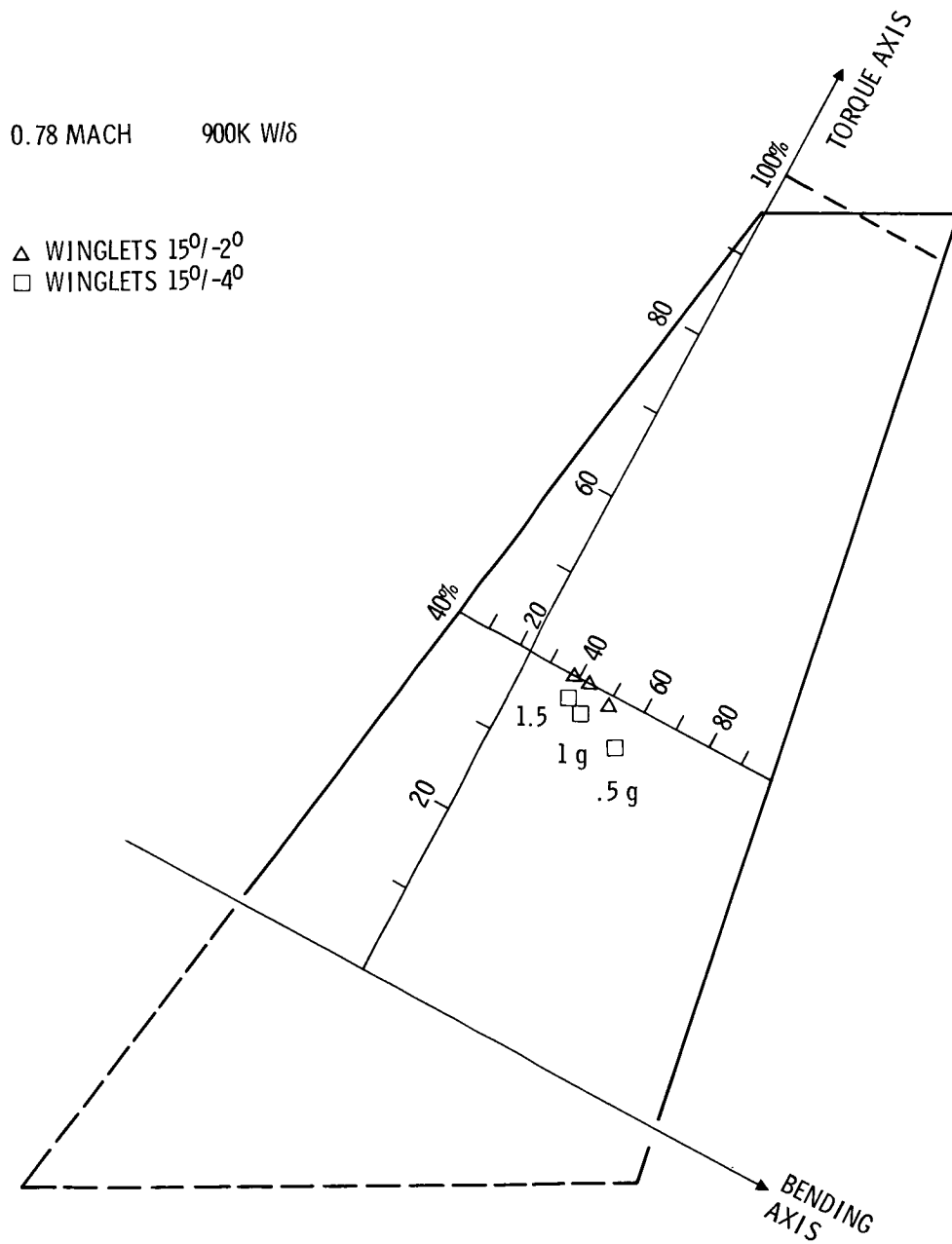


Figure 15. - Winglet center of pressure location

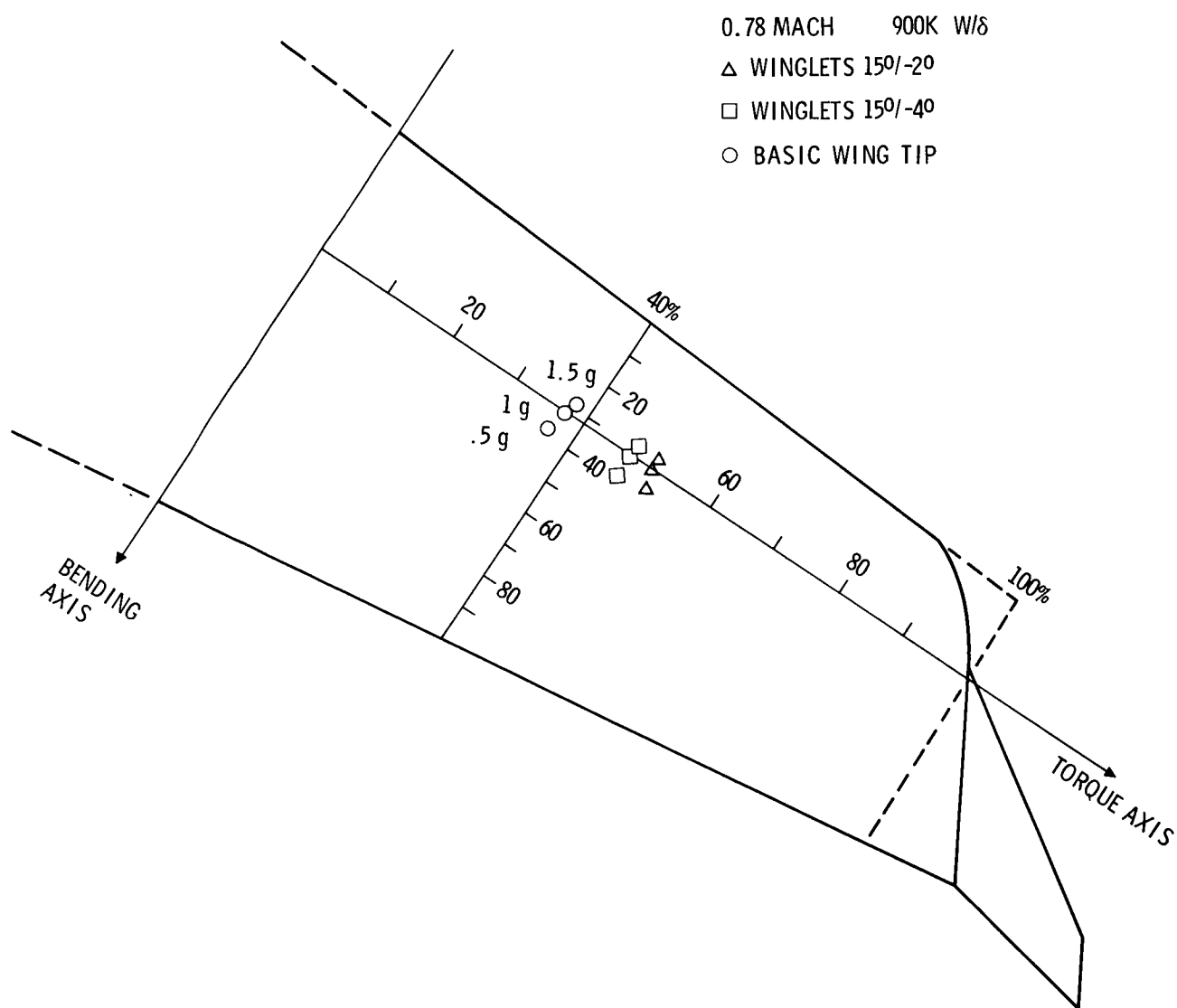


Figure 16. - Outboard wing center of pressure location

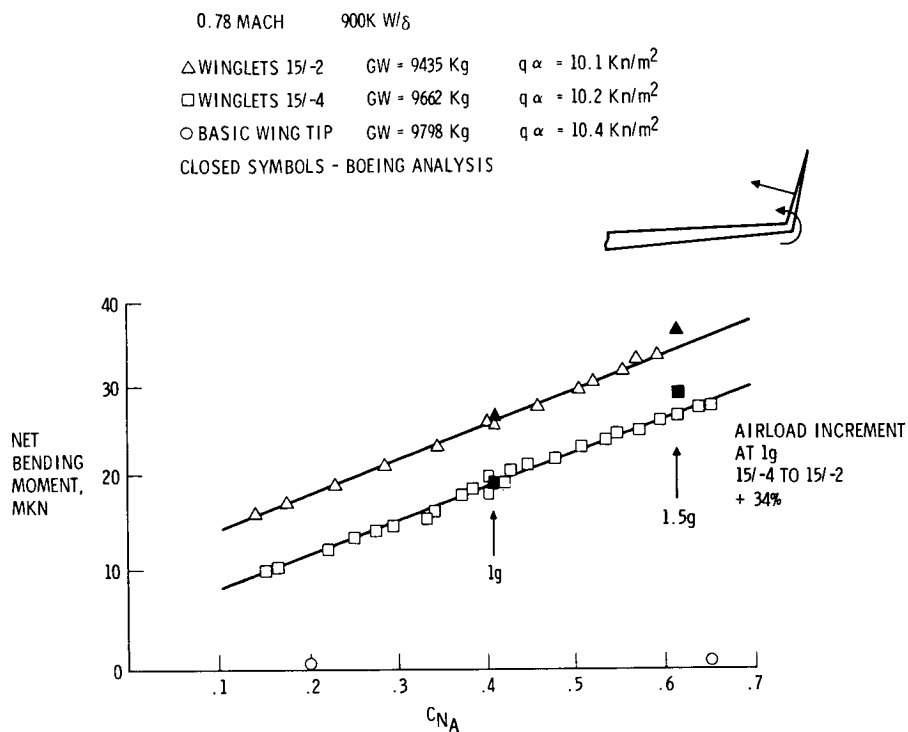


Figure 17. - Winglet intersection bending moment loads

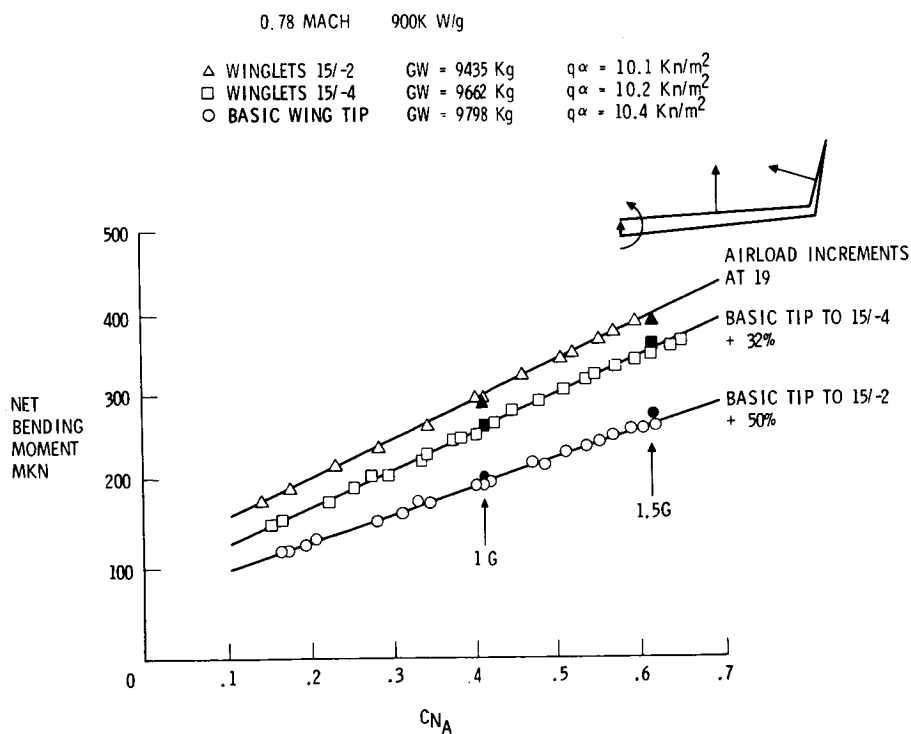


Figure 18. - Outboard wing bending moment loads

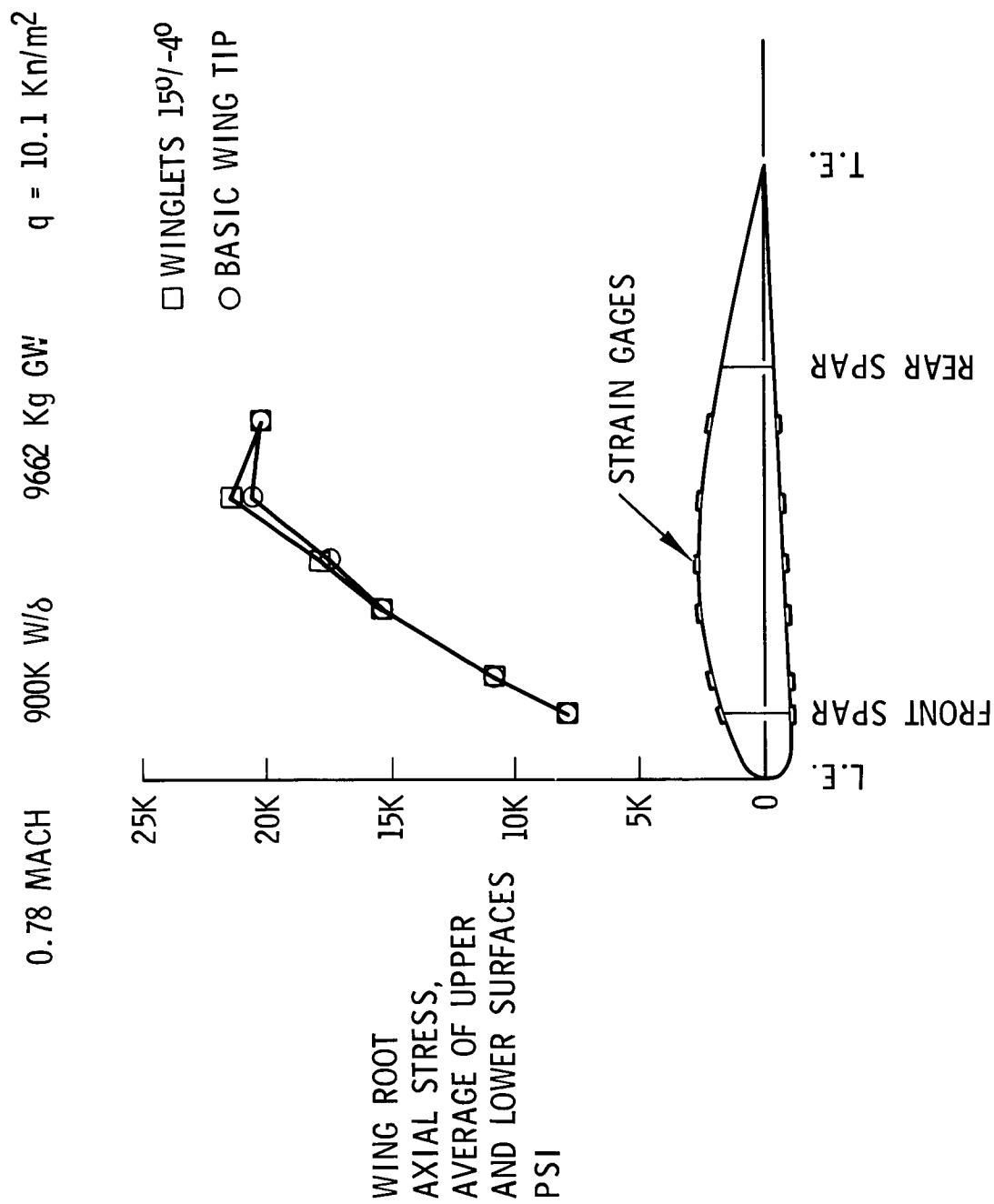


Figure 19. - Wing root bending stress distribution

IN-FLIGHT LIFT AND DRAG MEASUREMENTS  
ON A FIRST GENERATION JET TRANSPORT  
EQUIPPED WITH WINGLETS

David P. Lux  
NASA Dryden Flight Research Center

SUMMARY

NASA in a joint project with the USAF flight tested a KC-135A aircraft equipped with wing tip winglets to demonstrate and validate the potential performance gain of the winglet concept as predicted from analytical and wind tunnel data. Flight data were obtained at cruise conditions for Mach numbers of 0.70, 0.75, and 0.80 at a nominal altitude of 36,000 ft. and winglet configurations of 15° cant/-4° incidence, 0° cant/-4° incidence, and baseline.

For the Mach numbers tested the data show that the addition of winglets did not affect the lifting characteristics of the wing. However, both winglet configurations showed a drag reduction over the baseline configuration, with the best winglet configuration being the 15° cant/-4° incidence configuration. This drag reduction due to winglets also increased with increasing lift coefficient.

It was also shown that a small difference ( $\Delta C_D = 0.00045$ ) exists between the 15° cant/-4° incidence flight and wind tunnel predicted data. This difference was attributed to the pillowing of the winglet skins in flight which would decrease the winglet performance.

INTRODUCTION

With the advent of the 1973 fuel crisis, the fuel efficiency of transport type aircraft has become of paramount importance to all operators of this type of aircraft, including the Federal Government. To improve the fuel efficiency of these aircraft, Dr. Richard T. Whitcomb developed wing tip mounted winglets which reduce the drag of the wing lifting system. Many analytical studies and wind tunnel tests have been conducted (references 1, 2, 3), to show the decreased drag of the wing/winglet system and it was determined that a flight evaluation of this concept was in order. Therefore, the USAF, in a joint project with NASA, contracted for the design and fabrication of winglets to be attached to a KC-135A aircraft as shown in figure 1.

The objective of the NASA/USAF flight project was to demonstrate the incremental performance gains, predicted from analytical and wind tunnel studies, by installing winglets on an aircraft without degrading aircraft stability. This was accomplished by making measurements to obtain lift, drag and pressure distributions on both right wing and winglet, and to obtain fuel mileage data.

This report presents the lift and drag data for a Mach number range of 0.70 to 0.80 for the cruise flight condition at one altitude (36,000 feet nominal). Angle of attack and lift coefficient were varied by varying weight (fuel burn). The aircraft center of gravity was maintained at 25% mean

aerodynamic chord. Flights were made with winglets off (baseline) and winglets on for several cant and incidence conditions. The data presented in this report are for the baseline, 0° cant/-4° incidence, and 15° cant/-4° incidence.

#### SYMBOLS

$A_d$	Area of Engine Inlet Duct, $\text{ft}^2$
$A_e$	Area of Engine Nozzle, $\text{ft}^2$
$A_x$	Longitudinal Acceleration, g
$A_z$	Normal Acceleration, g
$\bar{c}$	Mean Aerodynamic Chord
$C_d$	Drag Coefficient, $\frac{\text{Drag}}{q_s}$
$C_f$	Nozzle Efficiency Coefficient
$C_L$	Lift Coefficient, $\frac{\text{Lift}}{q_s}$
$F_g$	Gross Thrust, lbs
$F_r$	Ram Drag, lbs
$M_\infty$	Freestream Mach Number
$M_d$	Inlet Duct Mach Number
$P_t$	Total Pressure, psi
$P_s$	Static Pressure, psi
$P_\infty$	Free Stream Static Pressure, psi
$q$	Dynamic Pressure, $0.7M_\infty^2 P_\infty$ , psf
$s$	Wing Reference Area, $\text{ft}^2$
$w$	Aircraft Gross Weight, lb
$\alpha_i$	Indicated Angle of Attack, deg
$\alpha_t$	True Angle of Attack, deg
$\delta$	Ambient Pressure Ratio
$\gamma$	Ratio of Specific Heats

## DESCRIPTION OF TEST AIRCRAFT

The test aircraft used for this study was a KC-135A aerial refueling tanker modified to allow the installation of wing tip mounted winglets. Also, an air data boom was added with provisions for measuring free stream impact pressure, static pressure, angle of attack, and angle of sideslip. Incorporated into the angle of attack and sideslip vanes were flight path accelerometers; however, these were not used in this study.

The configuration of the winglets, as tested in this study, is shown in figure 2. The winglets, as manufactured by the Boeing Military Aircraft Company (BMAC), were constructed to accommodate changing the angle of cant and incidence on the ground. This allowed flight testing to determine the optimum winglet configuration.

## FLIGHT TEST INSTRUMENTATION

In order to obtain the necessary parameters to allow calculation of lift and drag, the KC-135 aircraft had to be instrumented to accurately obtain aircraft weight, thrust, angle of attack, freestream impact and static pressures, and normal and longitudinal accelerations.

Each of the four engines' inlet ducts was instrumented to measure total pressure ( $P_{t_2}$ ) and static pressure ( $P_{s_2}$ ) for determining inlet momentum and with total pressure probes after the turbine ( $P_{t_7}$ ) to obtain gross thrust. As can be seen from figure 3, engine 1 and 2 used inlet rakes to obtain  $P_{t_2}$  while engines 3 and 4 used two  $P_{t_2}$  probes. All of the engine pressures were measured using differential pressure transducers located in the aircraft cabin. These transducers were all referenced to a single reference pressure taken from a  $P_{t_2}$  probe of engine 2. This reference pressure was measured by a very accurate absolute pressure transducer also located in the aircraft cabin.

Other instrumentation pertinent to the engines were fuel flow meters located in the fuel supply lines of all the engines to enable aircraft weight to be determined and instrumentation of the engine bleed doors. For all test points the engine bleed doors were closed.

As previously mentioned, an air data noseboom was installed on the flight test aircraft. The angle of attack that was used in this study was taken from the angle-of-attack vanes mounted on the noseboom. Freestream impact and static pressures were obtained from the noseboom pitot-static system. This system is described in detail in reference 4.

Normal and longitudinal accelerations were obtained from accelerometers mounted at the aircraft center of gravity. Alignment of this accelerometer package was checked periodically throughout the flight test program to ensure that the accelerometer mount plate was not shifting from flight to flight.

Other parameters that were measured which concern this study were ambient air temperature, engine rotor speeds, and all control surface deflections.

All data parameters were recorded through a pulse code modulation (PCM) system onto magnetic tape. In postflight processing the magnetic flight tape was formatted and processed to allow follow-on data programs to access the data and perform all pertinent calculations.

#### FLIGHT TEST PROCEDURE

Of all the tasks that were to be flown during the flight test, by far the most difficult task was to obtain good fuel mileage data. Since these data were of primary concern to the USAF, the requirements for this task dictated the manner in which the lift and drag task were to be performed. A discussion of how the data points were obtained and the manner in which the data was reduced follows.

Data were obtained at Mach numbers of 0.70, 0.75, 0.78, and 0.80 at three  $W/\delta$  conditions for each winglet configuration. By varying  $W/\delta$  it was possible to obtain a  $C_L$  range that was representative of the aircraft envelope. For each data point the aircraft was flown to the desired Mach number and altitude to obtain the proper  $W/\delta$ . This condition would be held for a minimum of three minutes. An onboard flight test engineer would determine if the aircraft/airmass was stable enough during the data run for the run to be acceptable. If not, the data run would be repeated. It was found that in most cases where the data runs were deemed unacceptable for fuel mileage data, the data was most adequate for lift and drag data.

One of the critical aspects of the flight program was the stability of the airmass required for data acquisition. Many times this required that the mission be flown at extreme distances from Base precluding real time ground monitoring of flight parameters. As a result a real time onboard computation capability was provided to allow both monitoring of instrumentation and computation of aircraft weight.

Throughout any given flight, a crew member would monitor the fuel status of the aircraft. Fuel would be transferred either forward or aft to maintain the aircraft's center of gravity at 25%  $\bar{c}$ . The accuracy to which this could be maintained is about  $\pm 1\%$ .

#### LIFT/DRAG DATA REDUCTION

The following are the equations for  $C_L$  and  $C_D$  used in this investigation:

$$C_L = \frac{1}{qS} \left[ w(A_z \cos \alpha_t + A_x \sin \alpha_t) - F_g \sin \alpha_t \right]$$

and

$$C_D = \frac{1}{qS} \left[ w(A_z \sin \alpha_t - A_x \cos \alpha_t) + F_g \cos \alpha_t - F_r \right]$$

These equations and their derivations can be found in reference 5. From these equations it can be seen that the important parameters are weight,



dynamic pressure, gross thrust and ram drag, longitudinal and normal accelerations, and true angle of attack. Each of these will be briefly discussed below.

Aircraft weight was determined by fueling and weighing the aircraft and crew prior to flight. From engine start to engine shutdown fuel flow meters on each engine supplied the information necessary to allow the integration of the fuel weight burned, which determined the weight of the aircraft at any given time. This calculation was checked after each flight by a postflight weighing of the aircraft.

Thrust and ram drag of the aircraft were determined from total and static pressures in the inlet duct and total pressures after the engine turbine. A very simple method of calculating thrust and ram drag was used for this investigation since the real interest was the incremental performance of winglets over a baseline configuration. For this investigation the following equations were used to determine gross thrust and ram drag per engine.

$$F_g = A_e C_f \left[ \left( \frac{2}{\gamma+1} \right)^{\frac{\gamma}{\gamma-1}} (\gamma+1) P_{t_7} - P_\infty \right] = C_f A_e \left( 1.259 P_{t_7} - P_\infty \right)$$

where  $\gamma$  is taken to be 1.33.  $C_f$  is the nozzle efficiency coefficient and is obtained from thrust stand runs.  $C_f$  for this investigation is shown in figure 4.

$$F_r = 1.4 A_d M_\infty M_d P_{s_2} \left( \frac{1 + 0.2 M_d^2}{1 + 0.2 M_\infty^2} \right)$$

where

$$M_d = 2.236 \left[ \left( \frac{P_{s_2}}{P_{t_2}} \right)^{\frac{-2}{7}} - 1 \right]^{1/2}$$

For a more indepth discussion of this technique of determining  $F_g$  and  $F_r$  see reference 6.

Longitudinal and normal accelerations were obtained from the center of gravity accelerometer package. The accelerometer package consisted of a -1.0/+3g normal accelerometer, -1.0/+1.0g longitudinal accelerometer, and a  $\pm 0.25g$  sensitive longitudinal accelerometer. When longitudinal accelerations were small the sensitive longitudinal accelerometer was used in the lift, drag calculations. All accelerometers were filtered at 3 hertz.

True angle of attack proved the most difficult parameter to determine. The KC-135 is a large, flexible aircraft and the angle of attack as measured

from the noseboom vanes and the c.g. accelerometers changes with changing flight conditions. Since all data points during this study were to be taken at 1g cruise conditions it was felt that the best method of determining true angle of attack was to calibrate  $\alpha$  in flight by relating true  $\alpha$  to the longitudinal accelerometer by the expression

$$\alpha_t = \sin^{-1} A_x$$

Indicated angle of attack was plotted against  $\alpha_t$  for each flight and a polynomial regression curve fit was made of this data (figure 5). This curve then became the calibration of angle of attack. It should be noted that this curve takes into account upwash effects, noseboom misalignment, and fuselage deflection effects. This is true only because the data was flown at cruise conditions, i.e. 1g stabilized flight.

## RESULTS AND DISCUSSION

The effect of the addition of winglets on the KC-135 aircraft aerodynamic parameters can be seen in figure 6 as lift coefficient versus angle of attack and lift coefficient versus drag coefficient.

The addition of winglets had little or no effect upon the  $C_L$  vs  $\alpha$  curve for either the 15/-4 or 0/-4 configuration. This was anticipated since the wind tunnel data of reference 1 also predicted little or no effect on  $C_{L\alpha}$  with the addition of winglets.

The addition of winglets, however, did affect the drag data as seen in figure 6. For every Mach number and lift coefficient tested, the addition of winglets to the aircraft reduced the total aircraft drag. Also the 15/-4 configuration is seen to be more effective at reducing the drag than the 0/-4 configuration for all Mach numbers and lift coefficients. This also was anticipated as a result of the wind tunnel tests which showed the 15/-4 configuration to be the optimum winglet configuration for the KC-135 aircraft.

Figure 7 shows the drag increment,  $\Delta C_D$ , plotted versus lift coefficient for each of the test Mach numbers. These data were obtained by computing the difference in  $C_D$  at a given  $C_L$  between the baseline data fairing and the fairing of the 15/-4 and 0/-4 data. These data show that the  $C_D$  reduction due to winglets increases with increasing lift coefficient for both winglet configurations. Also, the 15/-4 configuration is increasingly more effective in reducing drag than is the 0/-4 configuration, as  $C_L$  is increased. The data also show that, for the most part, the effect of the winglets is independent of Mach number for the small range of Mach numbers tested. ( $M = 0.70$  to  $0.80$ .)

Also shown in figure 7 as the dashed line is the wind tunnel predicted decrease in drag due to winglets for the 15/-4 configuration at a Mach number of 0.78. These data were taken from Langley test 754 and do not incorporate corrections for Reynolds number and trim drag which were considered to be small. The wind tunnel data show a decrease of approximately  $0.00045 C_D$  more than the flight data over the entire  $C_L$  range. There are several factors that could contribute to the miscomparison of the two sets of data, such as model

aeroelasticity, as compared to the flight vehicle, or angle of attack definition. However, the single most probable cause would be the existence of winglet skin pillowing as shown in figure 8. This pillowing, caused by a structural deficiency of the skin, would increase the drag of the winglet and not allow it to perform as predicted in the wind tunnel data. Further discussion of the effect of the winglet skin pillowing on the winglet performance can be found in reference 7.

#### CONCLUDING REMARKS

NASA in a joint project with the USAF flight tested a KC-135A aircraft equipped with wing tip winglets to demonstrate and validate the potential performance gain of the winglet concept as predicted from analytical and wind tunnel data. Flight data were obtained at cruise conditions for Mach numbers of 0.70, 0.75, 0.78, and 0.80 at a nominal altitude of 36,000 ft and winglet configurations of 15/-4, 0/-4 and baseline. The data show the following:

- No change was observed in the lift curve slope between the baseline (winglets off) configuration and winglets on configuration at any Mach number tested.
- Both the 15/-4 and 0/-4 winglet configuration reduced the airplane drag as compared with the baseline configuration for all Mach numbers and lift coefficients tested. The 15/-4 configuration had the highest drag reduction.
- The drag reduction due to winglets increased with increasing  $C_L$  and appeared to be independent of Mach number for the Mach number range tested.

Also observed was that the 15/-4 flight data and wind tunnel predicted  $C_D$  reduction disagreed by a small amount ( $\Delta C_D = 0.00045$ ). This difference was attributed to pillowing of the winglet skins in flight which would decrease winglet performance.

#### REFERENCES

1. Jacobs, Peter F.; Flechner, Stuart G.: Effect of Winglets on a First-Generation Jet Transport Wing, I-Longitudinal Aerodynamic Characteristics of a Semispan Model at Subsonic Speeds. NASA TN D-8473, 1977.
2. Whitcomb, Richard T.: A Design Approach and Selected Wind-Tunnel Results at High Subsonic Speeds for Wing-Tip Mounted Winglets. NASA TN D-8260, 1976.
3. Flechner, Stuart G.; Jacobs, Peter F.; and Whitcomb, Richard T.: A High Subsonic Speed Wind-Tunnel Investigation of Winglets on a Representative Second-Generation Jet Transport Wing. NASA TN D-8264, 1976.
4. Sakamoto, Glenn M.: Aerodynamic Characteristics of a Vane Flow Angularity Sensor System Capable of Measuring Flightpath Accelerations for the Mach Number Range from 0.40 to 2.54. NASA TN D-8242, 1976.

5. Arnaiz, Henry H.: Flight-Measured Lift and Drag Characteristics of a Large, Flexible, High Supersonic Cruise Airplane. NASA TM X-3532, 1977.
6. Beeler, De B.; Bellman, Donald R.; and Saltzman, Edwin J.: Flight Techniques for Determining Airplane Drag at High Mach Numbers. NACA TN 3821, 1956.
7. Dodson, Robert O.: Comparison of Flight Measured, Predicted and Wind Tunnel Measured Winglet Characteristics on a KC-135 Aircraft.



Figure 1. - KC-135A aircraft modified with winglets

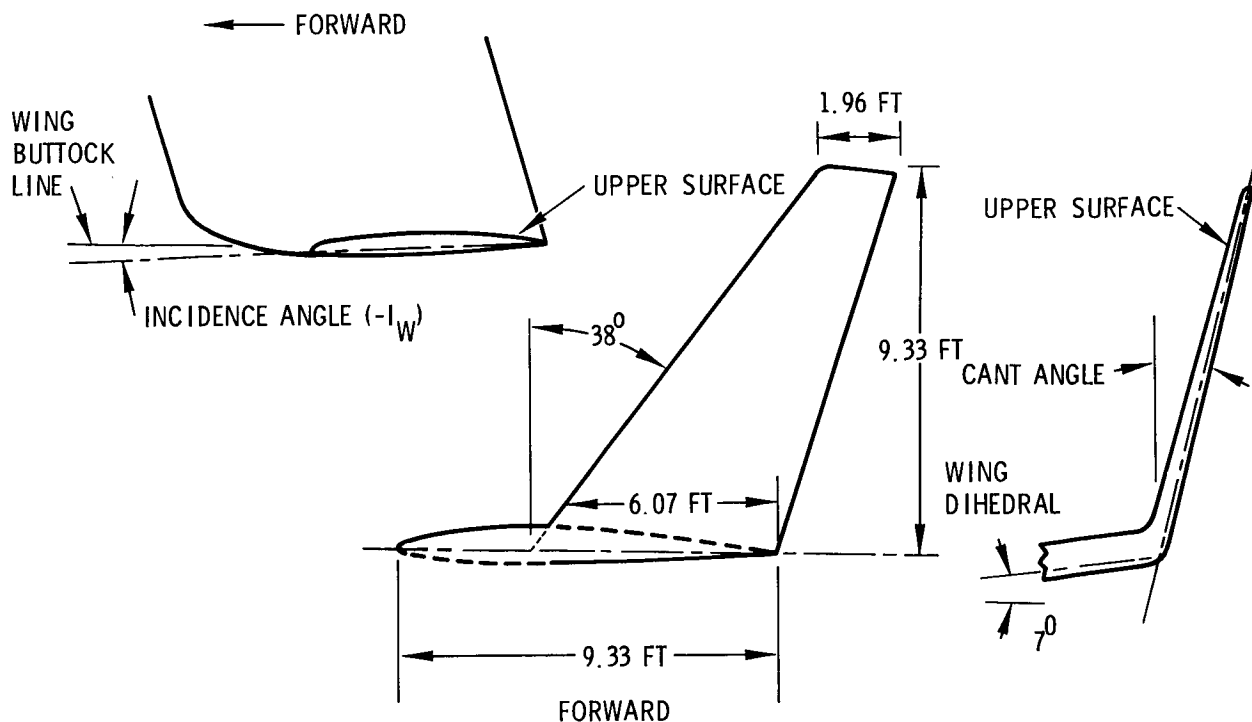


Figure 2. - Definition of winglet cant and incidence angles

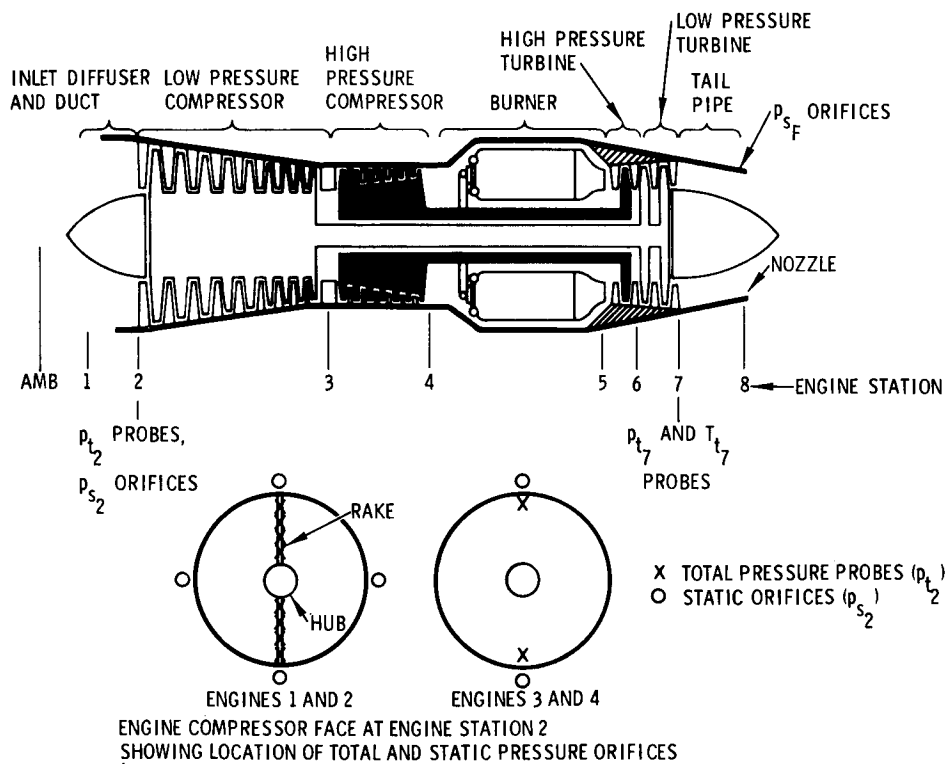


Figure 3. - J57-P-43W turbofan engine with station designations and measured parameter locations

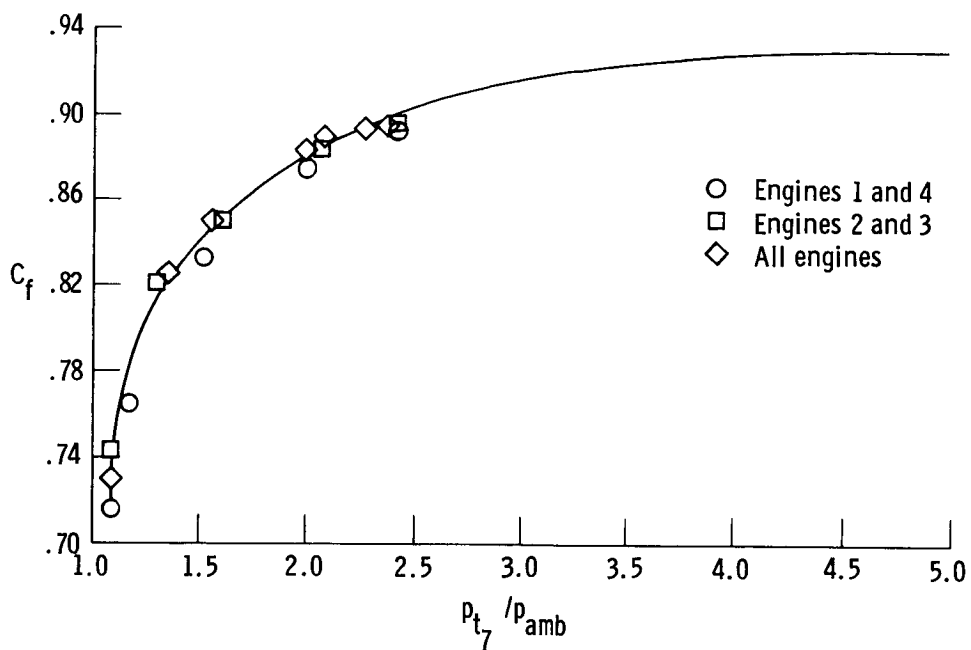


Figure 4. - Nozzle coefficient determined by ground thrust calibration

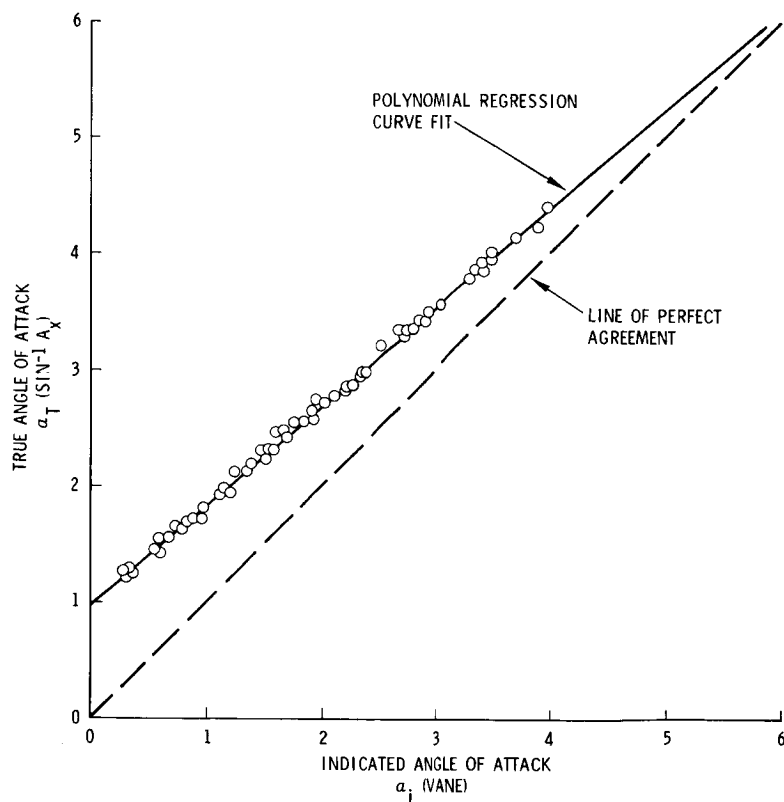


Figure 5. - Angle of attack calibration

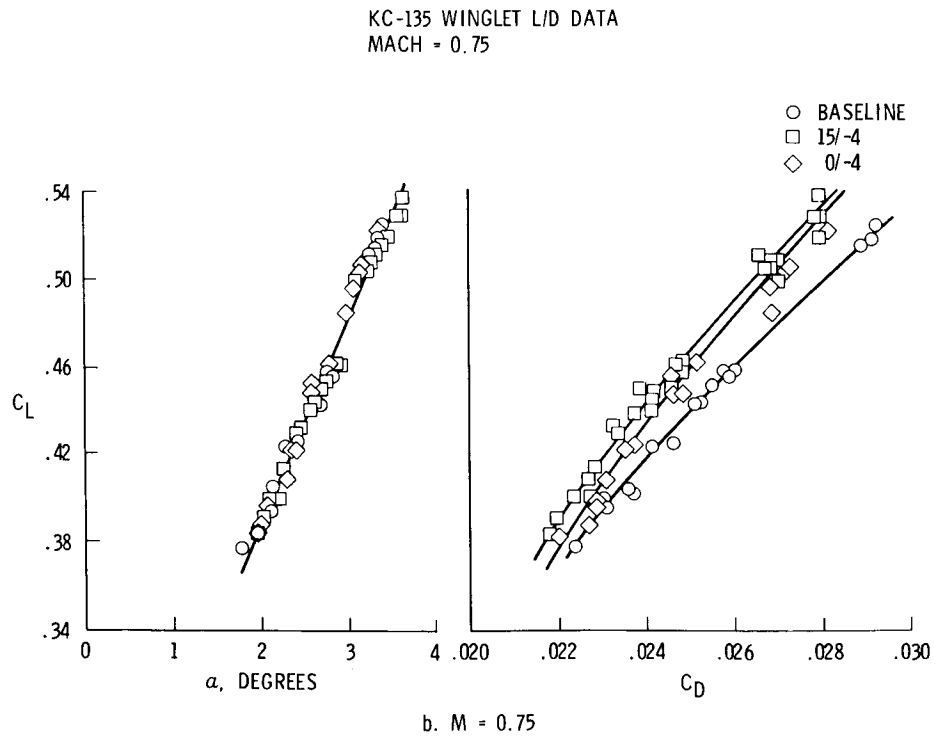
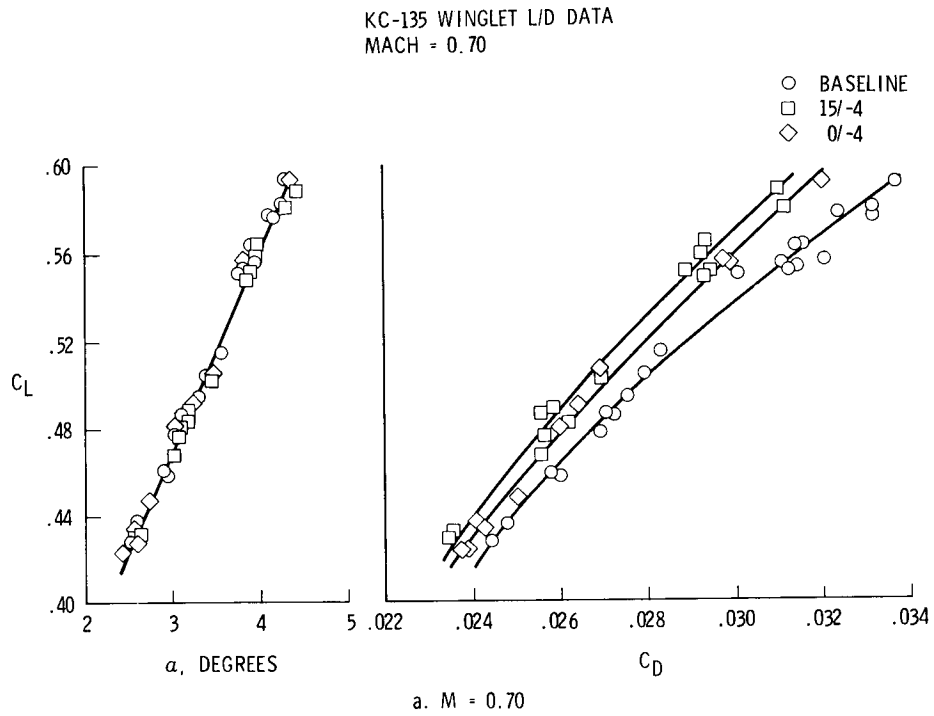


Figure 6. -  $C_L$  vs.  $\alpha$  and  $C_L$  vs.  $C_D$  for baseline, 15/-4, and 0/-4 configurations for KC-135 airplane



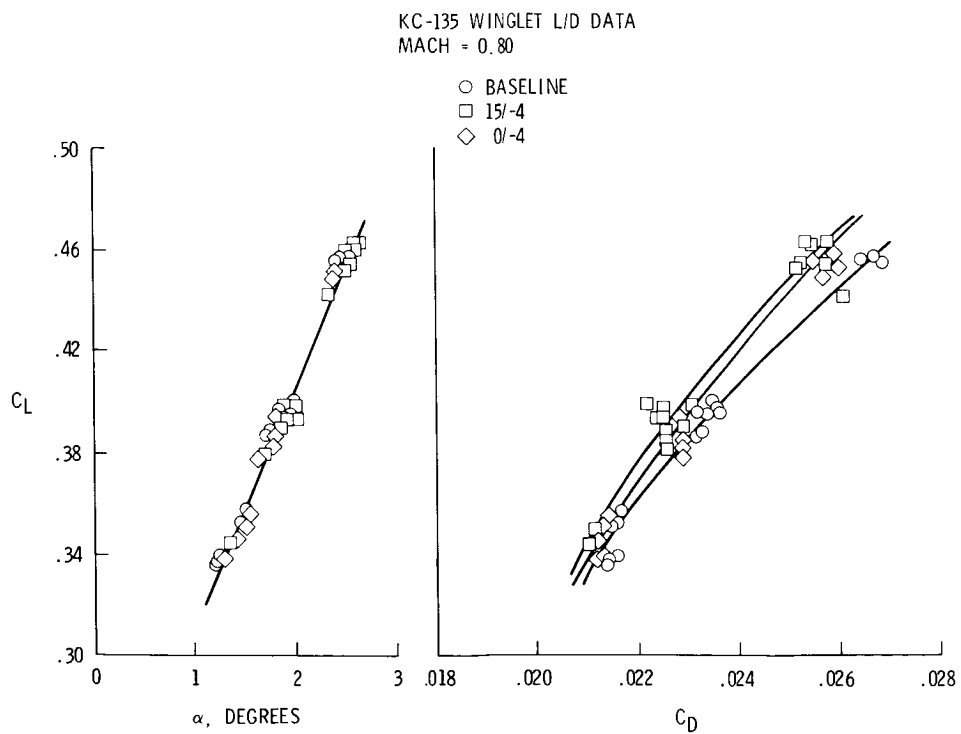
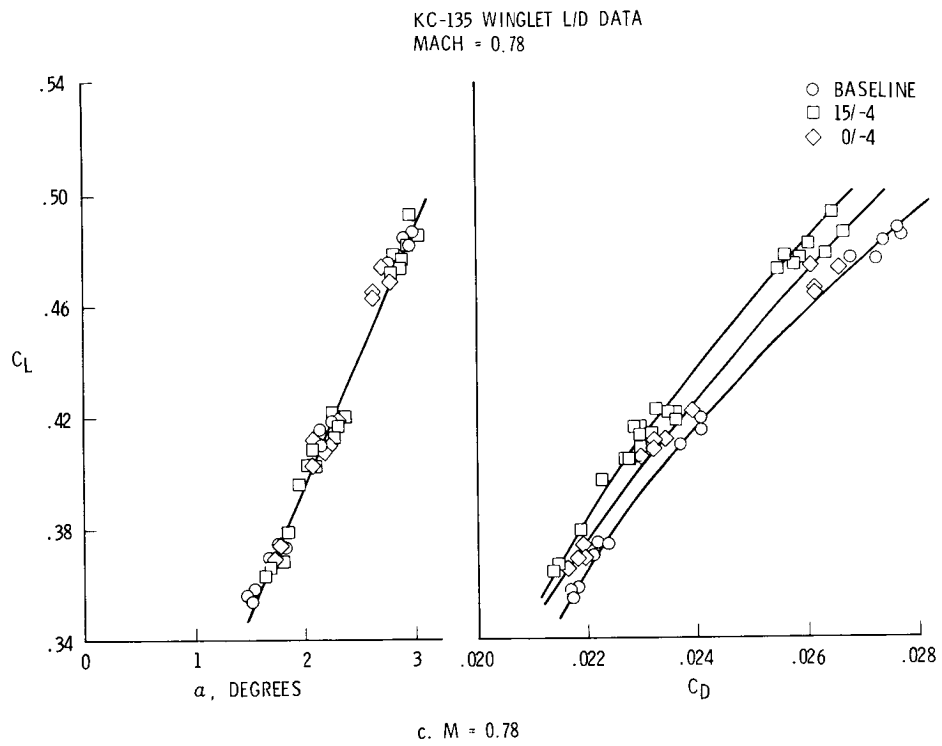


Figure 6. - concluded

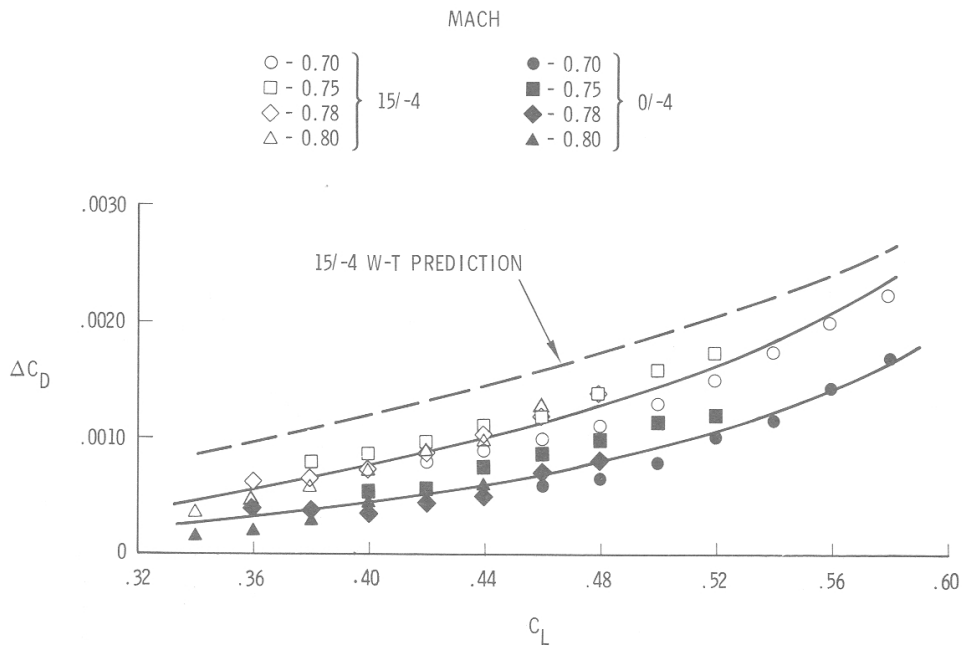


Figure 7. - Summary of drag results

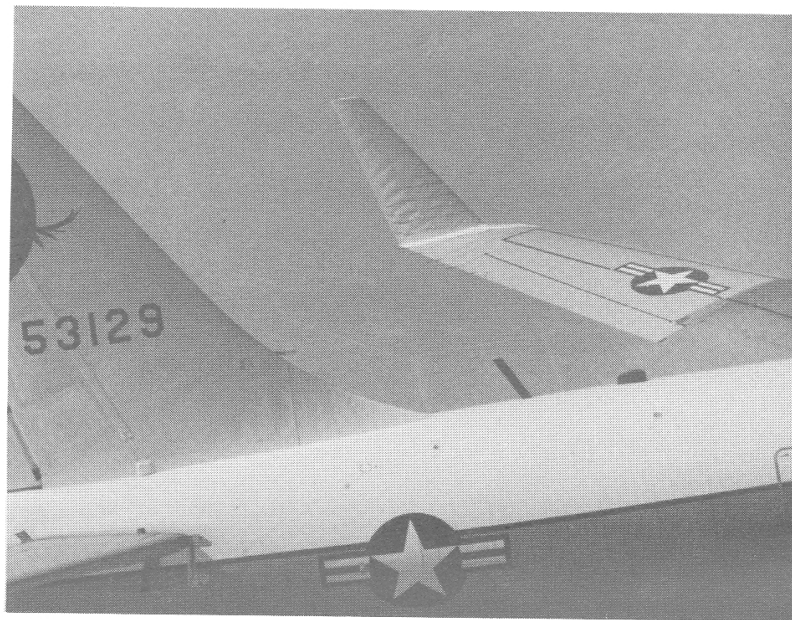


Figure 8. - Winglet in flight with skin "pillowing"

MEASUREMENTS OF THE FUEL MILEAGE  
OF A KC-135 AIRCRAFT WITH AND  
WITHOUT WINGLETS

Gary E. Temanson  
Boeing Military Airplane Company

SUMMARY

The KC-135A Winglet Flight Research and Demonstration Program was a joint effort of the Air Force, NASA and the Boeing Military Airplane Company to flight test winglets on the KC-135A. The primary objective of the program was to verify the cruise performance improvements predicted by analysis and wind tunnel tests. Flight test data were obtained for winglets positioned at 15° cant/-2° incidence, 0° cant/-4° incidence, 15° cant/-4° incidence and for winglets off (baseline). Both fuel mileage and drag measurements were obtained.

The 15° cant/-4° incidence winglet configuration provided the greatest performance improvement. The flight test measured fuel mileage improvement for a 0.78 Mach number was 3.1 percent at  $8 \times 10^5$  pounds  $W/\delta$  and 5.5 percent at  $1.05 \times 10^6$  pounds  $W/\delta$ . Correcting the flight measured data for surface pressure differences between wind tunnel and flight resulted in a fuel mileage improvement of 4.4 percent at  $8 \times 10^5$  pounds  $W/\delta$  and 7.2 percent at  $1.05 \times 10^6$  pounds  $W/\delta$ . The agreement between the fuel mileage and drag data was excellent.

INTRODUCTION

Analytical and experimental investigation indicated that a significant drag reduction could be realized on large transport aircraft through the incorporation of winglets. Winglets were projected to reduce the KC-135's cruise drag between 6 and 8 percent, which translates into a significant fuel savings for the KC-135 fleet. As a result the KC-135 Winglet Flight Research and Demonstration Program was developed to design, fabricate and flight test a set of winglets to verify the cruise performance improvement predicted by analysis and by wind tunnel tests (references 1 through 6). Three specific areas of performance were investigated:

- Fuel mileage performance obtained from fuel flow and airspeed measurements.
- Drag determined from engine thrust measurements.
- Pressure distributions on the wing and winglet.

This paper discusses the cruise performance testing and results obtained from the first two areas of investigation. The pressure distributions are discussed in reference 7. A detailed analysis of the final results of the overall program is presented in reference 8.

# SYMBOLS

$A_D$	Inlet Duct Area
$A_j$	Jet Nozzle Area
Alt	Altitude
$A_x$	Longitudinal Acceleration in g's
$A_z$	Normal Acceleration in g's
$C_D$	Drag Coefficient
$C_L$	Lift Coefficient
$C_f$	Jet Nozzle Coefficient
CF	Correction Factor
D	Drag
$F_g$	Gross Thrust
FM	Fuel Mileage
$F_R$	Ram Drag
$H_e$	Energy Altitude
$H_P$	Pressure Altitude
INS	Inertial Navigation System
KCAS	Knots Calibrated Airspeed
$K_1$	Constant
$K_2$	Constant
L	Lift
LHV	Lower Heating Value
M	Mach Number
$M_D$	Duct Mach Number
NAM	Nautical Air Miles
$P_{Amb}$	Ambient Pressure at Tailpipe Exit

$P_{S_2}$	Static Pressure at the Compressor Face
$P_{t_7}$	Total Pressure at Tailpipe Exit
$q$	Dynamic Pressure
$S$	Wing Area
SFC	Specific Fuel Consumption
$t$	Time
TSFC	Thrust Specific Fuel Consumption
$V_g$	Ground Speed
$V_T$	True Airspeed
$W$	Gross Weight
$\dot{W}_f$	Fuel Flow
$\alpha$	Angle of Attack
$\delta$	Ambient Pressure Ratio
$\Delta$	Increment
$\theta$	Ambient Temperature Ratio

#### FLIGHT TEST PROGRAM OVERVIEW

The test airplane was a KC-135 S/N 55-3129, on loan to NASA Dryden Flight Research Center from the 4950th Air Force Test Wing (figure 1). The external aerodynamic configuration of the basic airplane was that of a standard KC-135A, except that the refueling boom had been removed and an airspeed nose boom with angle of attack and angle of sideslip vanes had been installed. Since the goal of the testing was to determine the incremental benefit of winglets, the data reduction methods did not attempt to correct the data to a standard airplane configuration.

The flight test winglets were designed to provide for variation of winglet cant and incidence as well as for removal of the winglet to obtain baseline data. Figure 2 presents the general winglet geometry.

The performance testing was conducted at Edwards Air Force Base, Edwards, California. The testing occurred in two time segments beginning in August 1979 and July 1980, respectively.

The first series of tests were flown in the proximity of the Edwards Air Force Base complex in order that the test data could be telemetered to NASA's ground station for real time monitoring. Data were obtained for three configurations:

- Winglets on, 15° cant/-2° incidence
- Winglets on, 15° cant/-4° incidence
- Winglets off, baseline

Several attempts were made to obtain data with the winglets set at 0° cant/-4° incidence. However, the persistent fuel leaks and the discovery of the cracked wing spar chord aborted these attempts during the preliminary testing.

Data scatter and instrumentation problems were prevalent during the preliminary testing. The scatter in the fuel mileage data masked the performance increment. A review of the fuel flow data used in determining fuel mileage indicated that scanivalve operation created electrical noise and bias in the fuel flow instrumentation which resulted in erroneous fuel flow indications. Isolating the fuel flow instrumentation on separate power supplies eliminated the scanivalve interference. The fuel flow instrumentation was also modified to provide better ranging over the cruise fuel flows. During airplane down-time between the two time segments it was decided that the criteria for determining stabilized flight should be clearly specified and more strictly adhered to when flying resumed. The following criteria were decided on:

<u>Parameter</u>	<u>Maximum Allowable Change During Three-Minute Run</u>
Altitude	±80 ft
Ambient Air Temperature	±0.5°C
Mach Number (Airspeed)	±0.004 (±1.5 KCAS)
True Airspeed	±2 kts
$W/\delta$	±5,000 lb from Nominal

Testing was accomplished for three nominal  $W/\delta$ 's ( $8 \times 10^5$ ,  $9 \times 10^5$  and  $1.05 \times 10^6$  lb) throughout the range of Mach numbers from 0.70 to 0.82. Data were obtained during three minute stabilized runs at altitudes between 34,000 and 40,000 ft.

In order to find and test in stable air masses, the airplane was equipped with an onboard real time data monitoring computer. This eliminated the need for the ground station real time monitoring and allowed the airplane to leave the Edwards Air Force Base area in search of smooth stable air. The final testing was flown over the ocean, off the coast of southern California.

An inertial navigation system (INS) was installed on the airplane during the final tests and was operational from flight 31-42 to the completion of testing. The INS facilitated navigation and also furnished information on ground speed through a digital cockpit display.

Final performance data were acquired for the following configurations:

- Winglets on, 0° cant/-4° incidence
- Winglets on, 15° cant/-4° incidence
- Baseline

Table 1 lists the successful data flights and the type of performance data obtained for each flight test segment.

## RESULTS AND DISCUSSION

### Fuel Mileage

The basic parameters required to determine the cruise performance of an airplane at a given Mach number and gross weight are true airspeed ( $V_T$ ), fuel flow ( $\dot{W}_f$ ) and ambient pressure ratio ( $\delta$ ). Normalized fuel mileage (FM) is obtained by combining these parameters in the following equation:

$$FM_{Test} = \frac{V_T \times \delta \times 1000}{\dot{W}_f}$$

The FM test value for a given condition was based on the average value of these parameters over the stabilized condition time. Each parameter was sampled every second over a nominal three minute time period.

The test fuel mileage was then corrected to standard conditions so that a valid comparison could be made among configurations. Differences in drag (off  $W/\delta$  and changing energy state), fuel lower heating values and altitudes were normalized by means of correction factors applied to the test FM:

$$FM_{Corr} = FM_{Test} \times CF_{Drag} \times CF_{LHV} \times CF_{Alt}$$

The drag correction factor had two components: off,  $W/\delta$  and changing energy state.

The off  $W/\delta$  correction occurs when the data are not obtained at exactly the targeted  $W/\delta$ . This results in the airplane operating at a different  $C_L$  than desired and thus a different  $C_D$  as illustrated in figure 3. The increment of drag associated with returning to the nominal  $W/\delta$  is:

$$\left( \frac{\Delta Drag}{\delta} \right) W/\delta = 1481.4 \text{ S M}^2 \left( \Delta C_D \right)_{W/\delta}$$

The basic KC-135A drag polars (reference 9) were used to determine the  $W/\delta$  correction for all test configurations.

The changing energy state correction occurs when the airplane is in accelerated, climbing or descending flight during the test condition. At any given point in time the airplane's energy state is described by its energy altitude ( $H_e$ ) which is the sum of the airplane's geopotential altitude and its speed

converted to an equivalent geopotential altitude. An increase in  $H_e$  over the condition time indicates that the airplane is accelerating and that the engines are producing more thrust than is required to balance the drag force. A decrease in  $H_e$  indicates less thrust is being produced than that required to balance drag. Since level unaccelerated flight performance where thrust equals drag is desired, a correction for any energy state change must be applied. The time rate of change of  $H_e$  is related to drag by the following equation:

$$\left(\frac{\Delta \text{Drag}}{\delta}\right)_{H_e} = -0.592484 \times W/\delta \times \frac{1}{V_T} \times \frac{dH_e}{dt}$$

When determining  $H_e$ , the reference for the airplane speed and for the geopotential altitude should be the earth. Therefore, airplane ground speed ( $V_g$ ) is the relevant speed. However, ground speed measurements were not available until late in the program (Flight No. 31-42 and on) when an inertial navigation system was installed in the airplane. In a stable air mass with no wind or horizontal temperature gradients, changes in true airspeed are the same as changes in ground speed. Therefore, true airspeed was used in determining  $H_e$ .

On those flights where the INS was installed, an energy correction was also determined using the hand-recorded ground speed from the digital cockpit display. The energy correction was determined based on the following relationship.

$$\left(\frac{\Delta \text{Drag}}{\delta}\right)_{\text{INS}} = -0.052459 \times W/\delta \times \frac{dv_g}{dt}$$

The altitude change during a test run was minimized by the use of the altitude hold function on the autopilot. The altitude excursions experienced during the testing were negligible, and no corrections were applied in the calculation of the INS drag correction.

The relationship between the airplane drag at the nominal  $W/\delta$  in level unaccelerated flight and the drag of the airplane under the test conditions is given by the following equation:

$$\left(\frac{\text{Drag}}{\delta}\right)_{\text{Nominal}} = \left(\frac{\text{Drag}}{\delta}\right)_{\text{Test}} + \left(\frac{\Delta \text{Drag}}{\delta}\right)_{W/\delta} + \left(\frac{\Delta \text{Drag}}{\delta}\right)_{\text{Energy Changes}}$$

where

$$\left(\frac{\Delta \text{Drag}}{\delta}\right)_{\text{Energy Changes}} = \left(\frac{\Delta \text{Drag}}{\delta}\right)_{\text{INS}} \text{ or } \left(\frac{\Delta \text{Drag}}{\delta}\right)_{H_e}$$



Differences between drag for the nominal and test conditions result in different thrust requirements which may cause a change in the specific fuel consumption (TSFC/ $\sqrt{\theta}$ ). The drag correction factors applied to the test fuel mileage accounts for both the difference in thrust levels and specific fuel consumption in the following manner:

$$CF_{\text{Drag}} = \frac{\left(\frac{\text{Drag}}{\delta}\right)_{\text{Test}}}{\left(\frac{\text{Drag}}{\delta}\right)_{\text{Nominal}}} \times \frac{\left(\frac{\text{TSFC}}{\sqrt{\theta}}\right)_{\text{Test}}}{\left(\frac{\text{TSFC}}{\sqrt{\theta}}\right)_{\text{Nominal}}}$$

The variation of specific fuel consumption with thrust was obtained from the basic engine data contained in reference 10.

The energy content of JP-4 fuel, as measured by the lower heating value, can vary from flight to flight because of differences in such items as sources, shipments, contaminants and seasonal additives. Therefore, a fuel sample was obtained from the airplane fuel tanks before each flight. The samples were analyzed to determine the lower heating value. The test fuel mileage data were then corrected to a standard fuel energy level of 18,400 BTU/lb by applying the following correction factor:

$$CF_{\text{LHV}} = \frac{18,400}{\text{LHV}_{\text{Test}}}$$

Cruise performance testing was conducted between 34,000 ft and 40,000 ft pressure altitude. The specific fuel consumption for a given  $F_n/\delta$  varies with altitude in this altitude test range. For comparison purposes the cruise data were corrected to a standard altitude of 36,000 ft by applying the following correction factor:

$$CF_{\text{Alt}} = \frac{\left(\frac{\text{TSFC}}{\sqrt{\theta}}\right)_{\text{Test Altitude}}}{\left(\frac{\text{TSFC}}{\sqrt{\theta}}\right)_{36,000 \text{ ft}}}$$

The specific fuel consumption variation with altitude was obtained from the KC-135A engine data presented in reference 10.

The corrected fuel mileage was obtained by applying the three preceding correction factors to the fuel mileage measured under the test conditions:

$$FM_{\text{Corr}} = FM_{\text{Test}} \times CF_{\text{Drag}} \times CF_{\text{LHV}} \times CF_{\text{Alt}}$$

Normalized fuel mileage obtained using the airspeed/altitude method for the baseline configuration, the winglets on 15° cant/-4° incidence configuration and the winglets on 0° cant/-4° incidence configuration, are presented in figures 4, 5 and 6, respectively. These data were all obtained during the second segment of the flight test program. The cruise mileage data obtained during the preliminary testing were discarded because of extreme data scatter caused by instrumentation problems and relaxed stability criteria as previously discussed.

Figure 7 compares the faired cruise mileage performance associated with each winglet configuration. This improvement is a function of  $W/\delta$  and Mach number. Figure 8 compares the percentage improvement of both winglet configurations at 0.78 Mach number. As predicted, the 15° cant/-4° incidence winglet configuration resulted in the better performance gain.

The baseline and 0°/-4° winglet data exhibit good repeatability between flights and minimal data scatter. However, the 15°/-4° winglet data exhibits almost twice the scatter, particularly at  $9 \times 10^5$  lb  $W/\delta$ . All of these data were corrected using the airspeed/altitude energy methods discussed previously. A comparison of these energy corrections to the INS energy corrections for the same test run revealed numerous discrepancies. These discrepancies are indicative of an unstable air mass which would invalidate the assumption made in the airspeed/altitude energy method, that changes in ground speed are reflected in changes in the true airspeed. The INS energy corrected data for the baseline and 15°/-4° winglets on configurations are shown in figures 9 and 10, respectively. The scatter in the winglets on data was greatly reduced while the scatter in the baseline data was not significantly affected. Since the INS provides a more accurate measure of the energy of the airplane, these data were used in determining the 15°/-4° winglets on performance increments.

The percentage improvement in cruise mileage attributable to the flight test 15°/-4° winglet configuration is presented as a function of  $W/\delta$  and Mach number in figure 11.

### Drag

NASA-Dryden was responsible for the drag measurements. The NASA basic approach is presented in reference 11 and is only outlined in this report for the convenience of the reader. The lift and drag measurements dealt with two primary areas:

- The thrust developed by the engines.
- The acceleration experienced by the airplane.

Gross thrust was determined from engine pressures measured during the test condition, using the following relationship:

$$F_g = C_f A_j (1.259 P_{t_7} - P_{Amb})$$

Ram drag was subtracted from the gross thrust to arrive at the net thrust used in the drag calculation. The gross thrust was resolved into the flight path to be consistent with the drag direction. The relationship for ram drag is:

$$F_R = 1.4 A_D M_D^2 P_{S2} \sqrt{\frac{1 + 0.2 M_D^2}{1 + 0.2 M^2}}$$

An accelerometer package was located at approximately the airplane center of gravity to measure longitudinal and normal accelerations along the body axis. These accelerations were resolved into the flight path axis system by rotation through the angle of attack. The lift and drag were determined from these measurements as follows:

$$C_L = \frac{1}{qS} = \frac{1}{qS} \left[ W (A_Z \cos\alpha + A_X \sin\alpha) - F_g \sin\alpha \right]$$

$$C_D = \frac{D}{qS} = \frac{1}{qS} \left[ W (A_Z \sin\alpha - A_X \cos\alpha) + F_g \cos\alpha - F_R \right]$$

The drag data were then corrected to the nominal  $W/\delta$  as follows:

$$C_{D_{\text{Corr}}} = C_{D_{\text{Test}}} + \left( \Delta C_D \right)_{W/\delta}$$

This is the same drag correction discussed previously in the Fuel Mileage section which results from the test  $C_L$  being different than the desired  $C_L$  at the test Mach number. The corrected drag is presented as a function of Mach number in figures 12, 13, 14 and 15 for the baseline, 15° cant/-4° incidence, 15°/-2° incidence and 0° cant/-4° incidence configurations, respectively.

Both preliminary (solid triangles) and final (open symbols) drag data are presented in figures 12 and 13 for the baseline and 15°/-4° configurations. The preliminary data tends to exhibit higher drag levels as well as a slight counterclockwise rotation of the drag polar. Contributing factors to these differences include the limited amount of preliminary data, differing stability criteria and varying angle of attack calibrations.

The quantity of data obtained for each configuration was very limited during the preliminary tests. Only five data points per  $W/\delta$  were obtained and only one flight each was flown for the baseline and 15°/-4° configurations.

Due to excessive scatter in the preliminary fuel mileage data, the criteria for determining when the airplane was stabilized were tightened as previously noted. This minimized the size of corrections applied to the final data.

Although  $C_L$  is not sensitive to small angle of attack changes,  $C_D$  is highly sensitive to such changes. This requires that the angle of attack instrumentation provide a repeatable nonshifting calibration with a high degree of

resolution. Variations as small as 0.03 degree are significant since they result in approximately a 1 percent change in airplane drag in the cruise range. NASA's method of calibrating the angle of attack vane consisted of applying the steady state relationship:

$$\alpha_{cal} = \sin^{-1} A_X = K_1 \alpha_I + K_2$$

A random scattering of energy corrections (accelerations/decelerations) were assumed during the preliminary flight tests to determine  $K_1$  and  $K_2$ . Therefore, all of the data points were utilized in defining the linear relationship between indicated angle of attack ( $\alpha_I$ ) and  $\alpha_{cal}$ . During the final flight tests the data were screened to eliminate all points having accelerations or decelerations resulting in over a 1 percent change in airplane drag. A linear calibration was determined for each airplane configuration. Variations in calibrated angle of attack and indicated angle of attack of 0.10 degree between configurations were common as shown in figure 16. Similar variations were noted when the data were compared from flight to flight for the same configuration. Analytical studies of the influence of winglets on the flow upwash at the angle of attack vane indicated a negligible effect. No instrumentation changes were made to the angle of attack measurement system between flights. Therefore, no change was expected in the  $\alpha$  calibration. Apparently these variations are the result of limitations in instrumentation accuracies. As a result, the data from all of the final data flights were combined to arrive at a single calibration which was used to reduce the final drag data.

No reason for the shift in the  $\alpha$  calibration between the preliminary and final testing was found. Since  $C_D$  is so sensitive to changes in  $\alpha$ , the preliminary data were corrected using the final  $\alpha$  calibration to eliminate any bias. These data were also shown in figures 12, 13 and 14, (solid circles). A 2 to 3 percent drag reduction results from the  $\alpha$  calibration change. The preliminary data now tends to exhibit lower drag levels than the final data. The sensitivity of  $C_D$  to  $\alpha$  changes is obvious.

Because of the uncertainties associated with the changing stability criteria and the varying  $\alpha$  calibration, as well as the limited data, the preliminary data were not utilized in the final data analysis.

Fuel mileage improvements were determined using the drag data and engine specific fuel consumption data for each winglet configuration at 0.78 Mach number. Figure 17 compares this improvement to the measured fuel mileage benefit. The airspeed/altitude energy corrected fuel mileage data was used for both winglet configurations in this comparison since INS corrected data was not available for the 0° cant/-4° incidence data. The drag and fuel mileage data exhibited excellent agreement for the 15° cant/-4° incidence winglet configuration. The drag based benefit for the 0° cant/-4° incidence configuration showed a greater benefit than was measured by fuel mileage data. The agreement was good at  $1.05 \times 10^6$  lb W/ $\delta$  but varied by 1.3 percent at  $8 \times 10^5$  lb W/ $\delta$ .

Figure 18 compares the 15° cant/-4° incidence data to the INS corrected fuel mileage data. Again the agreement is excellent.

The INS offers an alternative data correction method to the accelerometers. The INS correction is not dependent on  $\alpha$ , which eliminates the  $\alpha$  sensitivity problem. Using the INS, the drag equation becomes:

$$C_D = \frac{1}{qS} \left[ F_g \cos \alpha - F_R + \left( \frac{\Delta \text{Drag}}{\delta} \right)_{\text{INS}} \times \delta \right]$$

The  $(\Delta \text{Drag}/\delta)_{\text{INS}}$  was obtained from the INS ground speed changes recorded during the test run as discussed in the Fuel Mileage section. INS data are available for only four of the five baseline flights and the 15° cant/-4° incidence configuration flights. The INS corrected drag is presented in figures 19 and 20.

Fuel mileage improvements were calculated based on the drag improvements obtained from the INS corrected data and SFC improvements obtained from reference 10. A comparison of this drag improvement to the directly measured fuel mileage improvement is presented in figure 21. The drag based improvement is 0.1 percent to 0.5 percent higher than that shown by the measured fuel mileage data. This is considered excellent agreement.

#### Flight Test - Wind Tunnel Data Comparison

The drag improvement determined from the flight tests was compared to wind tunnel data obtained by NASA at their Langley facilities. The flight test demonstrated benefit for winglets at 15° cant/-4° incidence was not as great as the wind tunnel data indicated. Figure 22 presents the comparison for a Mach number of 0.78 over the range of test  $W/\delta$ 's. The excellent agreement between the drag and fuel mileage test data gave confidence to the accuracy of flight test data. As a result, a careful comparison of wind tunnel and flight test pressure data was made to ensure that the winglets were developing comparable loadings in flight. Differences in winglet loading were discovered as shown in figure 23. A detailed analysis of these differences is presented in reference 7.

The winglet pressure data were affected by the "pillowing" of the winglet skin between the ribs which caused some distortions in the airfoil contour. There was also a leading edge pressure loss on the lower inboard portion of the winglet at test Mach numbers between 0.70 and 0.82 during flight testing that was not observed during wind tunnel testing. The pressure loss only occurred when the local flow in this area became supersonic. Two-dimensional transonic flow analyses were used to verify that the leading edge pressure loss was not caused by the "pillowing" of the winglet's skin. The difference is attributed to the five percent chord trip strip used on the wind tunnel model. Integration of the pressure drag differences on the winglet between wind tunnel and flight test resulted in a significant drag difference (approximately 1.5 to 2.0%) as shown in figure 24. Note that the drag data are shown plotted against the section normal force at the outboard wing station instead of the usual total airplane lift coefficient. This was done to compensate for any differences in aeroelastic twist at the wing tip between the wind-tunnel model and the flight test airplane. The relationship between airplane lift coefficient and wing tip normal force coefficient for the flight test airplane is shown

figure 25. Accounting for this difference resulted in the final flight test fuel mileage improvements shown in figure 26. The corrected flight test fuel mileage improvement is in good agreement with fuel mileage estimates obtained from the wind tunnel test data as shown in figure 27.

## CONCLUSIONS

The results of the cruise performance testing reveal a significant improvement in fuel mileage associated with the installation of winglets on the KC-135A. The 15° cant/-4 incidence winglet provided the greatest performance improvement of the three test configurations. For a 0.78 Mach number the benefit was approximately 4.4% at  $8 \times 10^5$  lb W/δ and 7.2% at  $1.05 \times 10^6$  lb W/δ.

## REFERENCES

1. Whitcomb, R. T., "A Design Approach and Selected Wind-Tunnel Results at High Subsonic Speeds for Wing-Tip Mounted Winglets", NASA TN D-8260, dated July 1976.
2. Jacobs, P. F., Flechner, S. G., Montoya, L. C., "Effect of Winglets On a First-Generation Jet Transport Wing, I - Longitudinal Aerodynamic Characteristics of a Semispan Model at Subsonic Speeds", NASA TN D-8473, dated June 1977.
3. Montoya, L. C., Flechner, S. G., Jacobs, P. F., "Effect of Winglets On a First-Generation Jet Transport Wing, II - Pressure and Spanwise Load Distributions For a Semispan Model at High Subsonic Speeds", NASA TN D-8474, dated July 1977.
4. Meyer, R. R., "Effect of Winglets On First-Generation Jet Transport Wing, V - Stability Characteristics For a Full-Span Model at Mach 0.30", NASA Technical Paper 1119, dated February 1978.
5. Flechner, S. G., "Effect of Winglets on a First-Generation Jet Transport Wing, VI - Stability Characteristics For a Full-Span Model at Subsonic Speeds", NASA Technical Paper 1330, dated October 1979.
6. Ishimitsu, K. K., VanDevender, N., Dodson, R. O., et al, "Design and Analysis of Winglets for Military Aircraft", AFFDL-TR-76-6, dated February 1976.
7. Dodson, R. O., "Comparison of Flight Measured, Predicted and Wind Tunnel Measured Winglet Characteristics on a KC-135 Aircraft", to be published in a NASA CP.
8. Dodson, R. O., Ayala, J., Shurtz, R. M., and Temanson, G., "KC-135 Winglet Flight Research and Demonstration Program", Boeing document D453-10087, to be published as an AFWAL-TR.
9. Boeing document D6-5599, "Substantiating Data Report For the KC-135A Flight Manual", dated 7 May 1964.

10. Boeing document D-16906, "Specification Engine Performance For Use in Airplane Performance Determination", dated 9 May 1955.
11. Beeler, D., Bellman, D. and Saltzman, E., "Flight Techniques for Determining Airplane Drag at High Mach Numbers", NASA TN 3821.

TABLE 1. - PERFORMANCE DATA FLIGHT TESTS

Flight No.*	Configuration	Date	Data Obtained
Preliminary Data			
10-21	15° cant/-2° incidence	8-24-79	Drag, pressure
11-22	15° cant/-2° incidence	9-19-79	Drag, pressure
12-23	15° cant/-2° incidence	9-21-79	Drag, pressure
14-25	15° cant/-4° incidence	11-02-79	Drag, pressure
16-27	Baseline	11-16-79	Drag, pressure
Final Data			
24-35	0° cant/-4° incidence	7-29-80	Fuel mileage, drag
27-38	0° cant/-4° incidence	8-08-80	Fuel mileage, drag
28-39	0° cant/-4° incidence	8-14-80	Fuel mileage, drag
30-41	Baseline	8-25-80	Fuel mileage, drag
31-42	Baseline	8-28-80	Fuel mileage, drag
32-43	Baseline	9-05-80	Fuel mileage
33-44	Baseline	9-09-80	Fuel mileage, drag
34-45	Baseline	9-11-80	Fuel mileage, drag
35-46	15° cant/-4° incidence	9-17-80	Fuel mileage, drag
36-47	15° cant/-4° incidence	9-23-80	Fuel mileage, drag
37-48	15° cant/-4° incidence	9-25-80	Fuel mileage
38-49	15° cant/-4° incidence	10-03-80	Fuel mileage, drag
40-51	15° cant/-4° incidence	12-17-80	Fuel mileage, drag, pressure
41-52	15° cant/-4° incidence	12-19-80	Fuel mileage, drag, pressure
42-53	15° cant/-4° incidence	12-23-80	Fuel mileage, drag, pressure
44-55	15° cant/-4° incidence	1-08-81	Fuel mileage, drag, pressure

\*The first two digits of the flight number refer to the number of data flights and the last two digits refer to the cumulative number of flights.



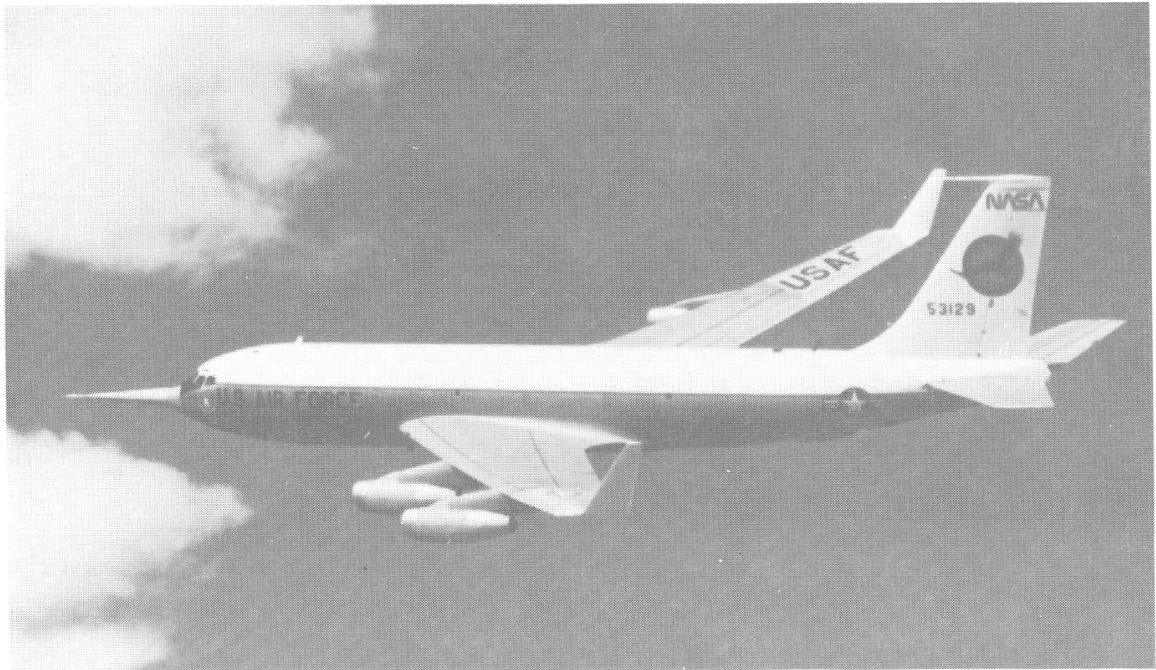


Figure 1. - Test KC-135A with winglets

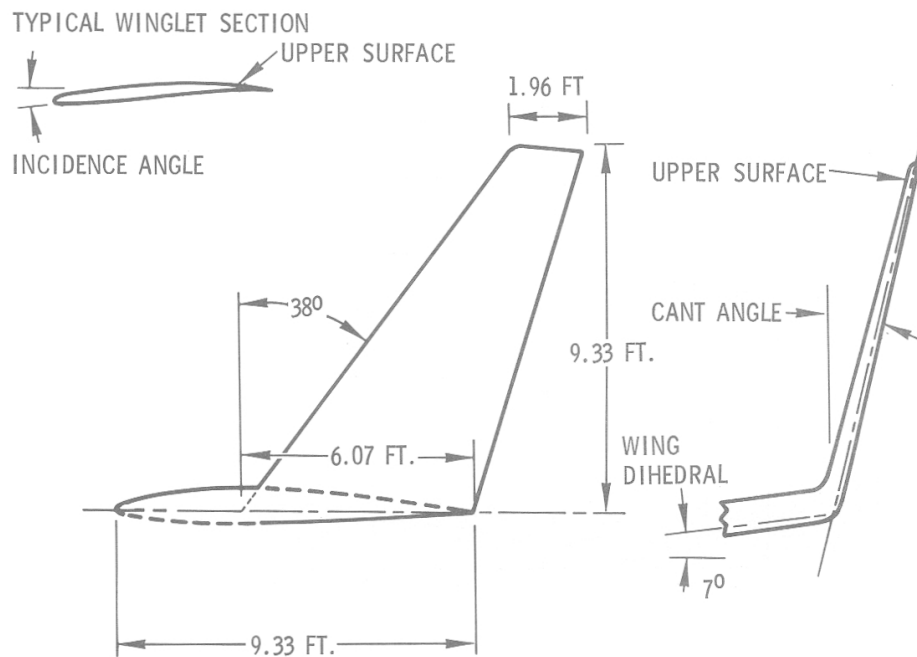


Figure 2. - Winglet geometry

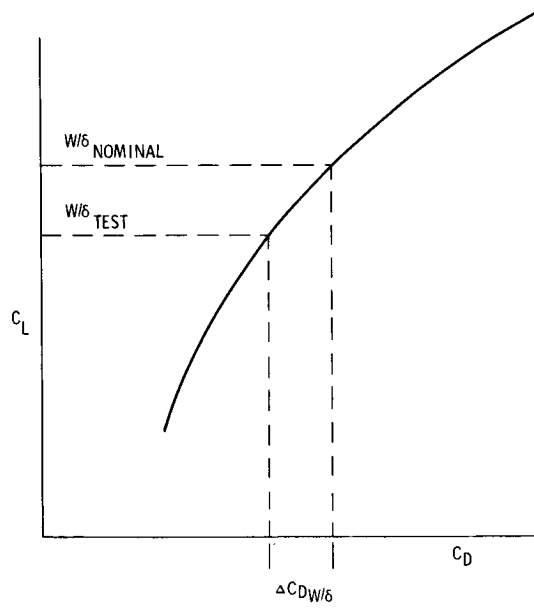


Figure 3. - Off  $W/\delta$  drag correction

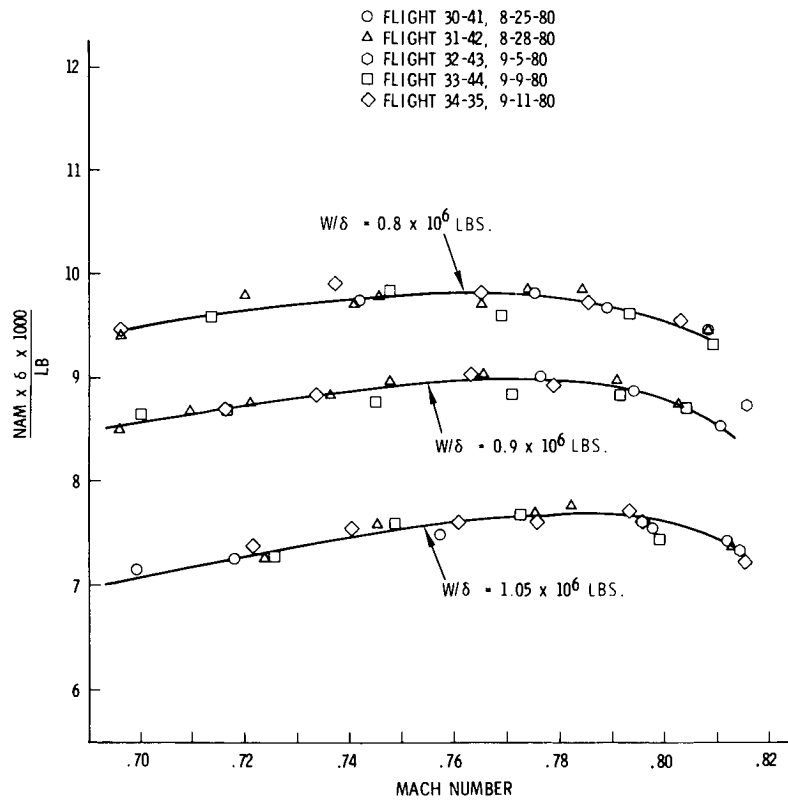


Figure 4. - KC-135 winglet flight test, baseline,  $H_p = 36,000$  feet  
airspeed/altitude energy correction

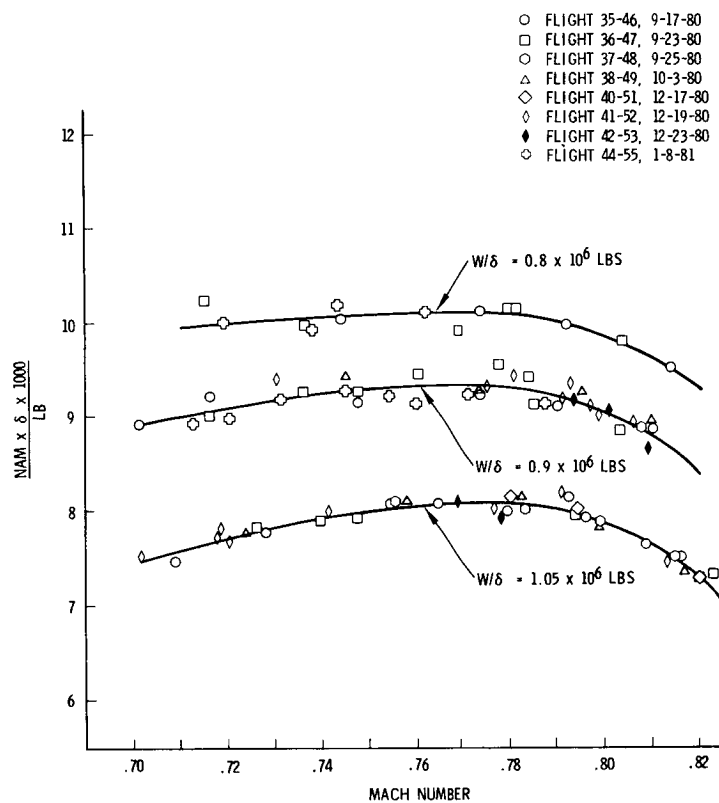


Figure 5. - KC-135 winglet flight test, 15° cant/-4° incidence,  $H_p = 36,000$  feet  
 airspeed/altitude energy correction

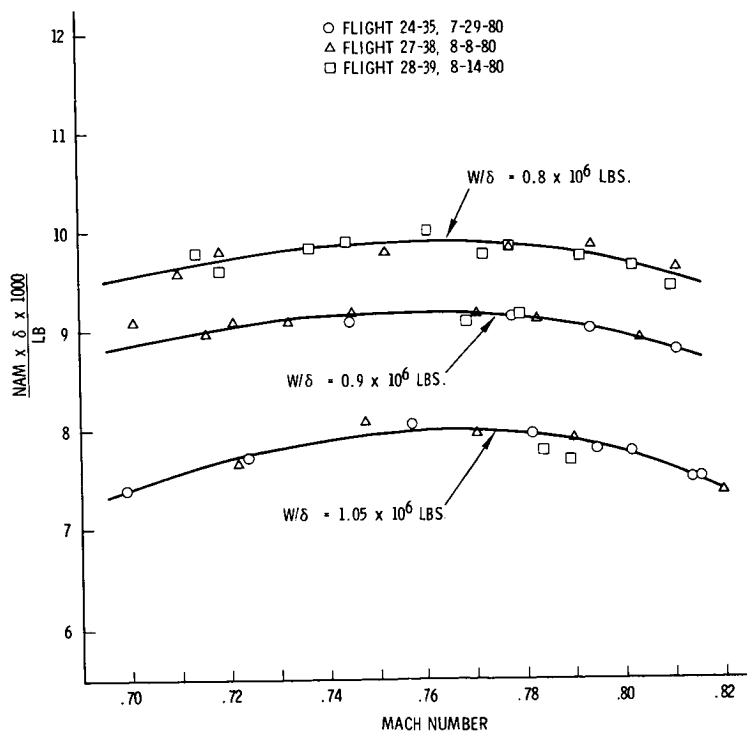


Figure 6. - KC-135 winglet flight test, 0° cant/-4° incidence,  $H_p = 36,000$  feet  
 airspeed/altitude energy correction

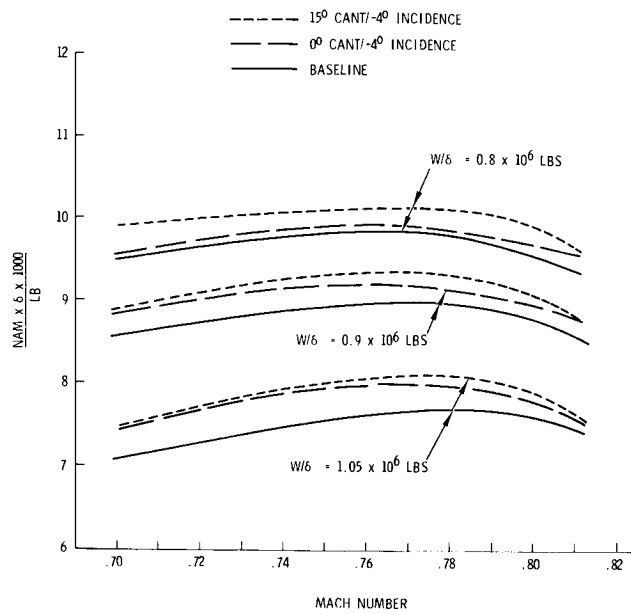


Figure 7. - KC-135 flight test data,  $H_p = 36,000$  feet  
airspeed/altitude energy correction

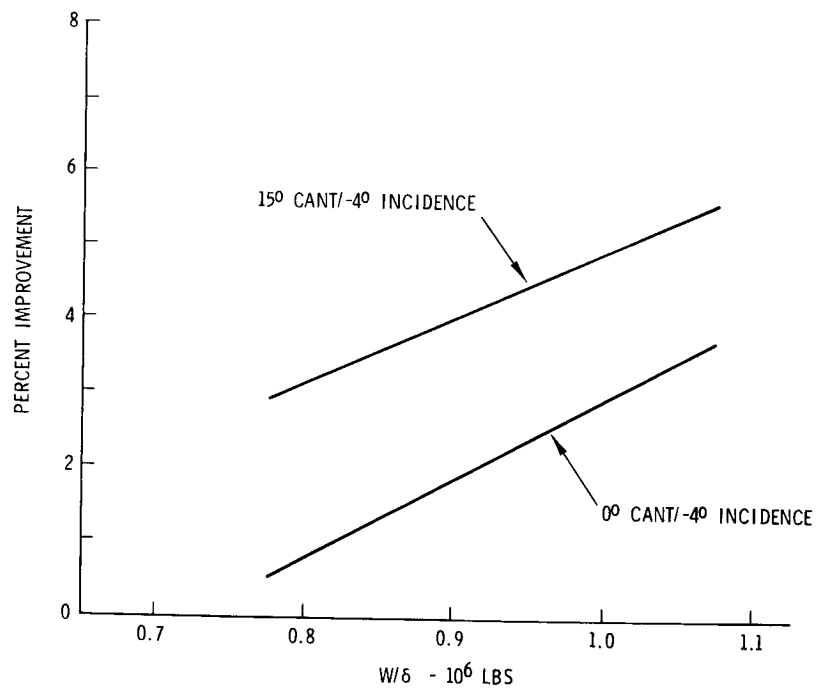


Figure 8. - KC-135A winglet flight test, cruise mileage improvement,  
airspeed/altitude energy correction mach = 0.78

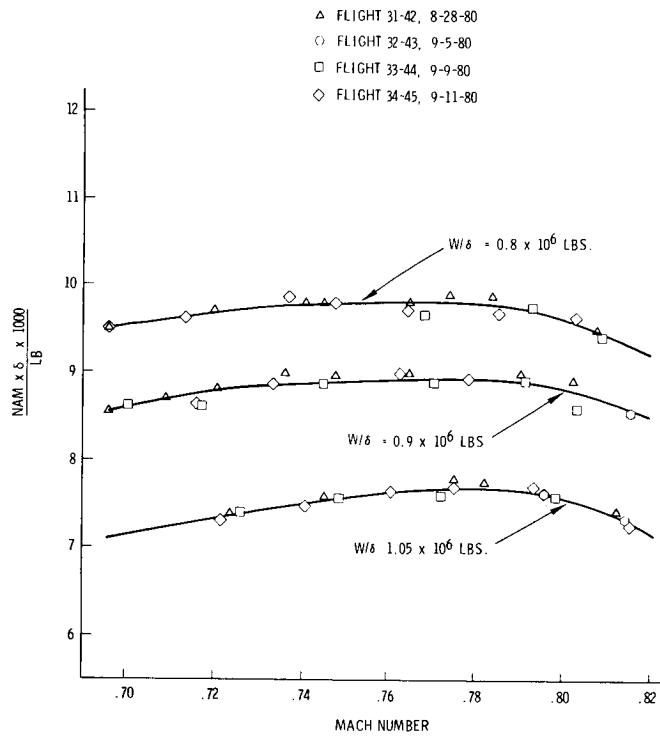


Figure 9. - KC-135A winglet flight test, baseline,  $H_p = 36,000 \text{ ft.}$ ,  
INS energy correction

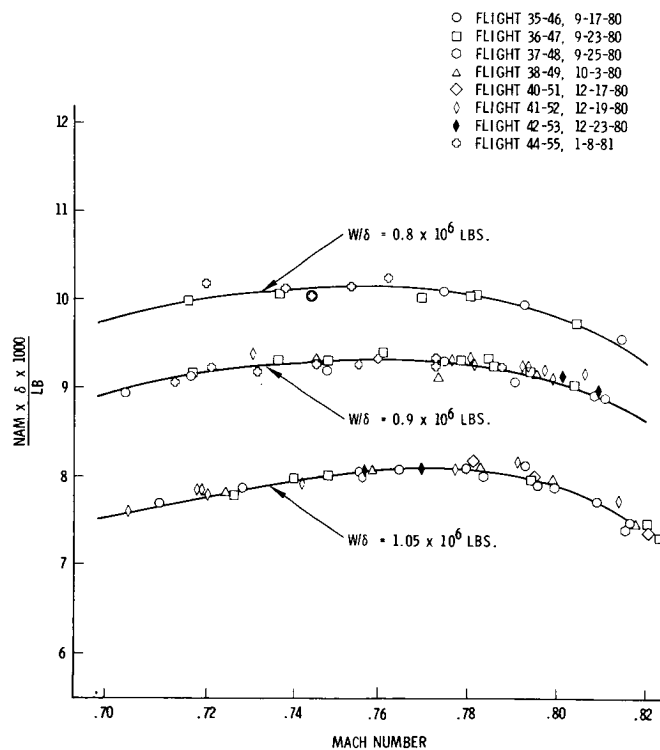


Figure 10. - KC-135A winglet flight test,  $15^\circ \text{ cant}/-4^\circ \text{ incidence}$ ,  
 $H_p = 36,000 \text{ ft.}$ , INS energy correction

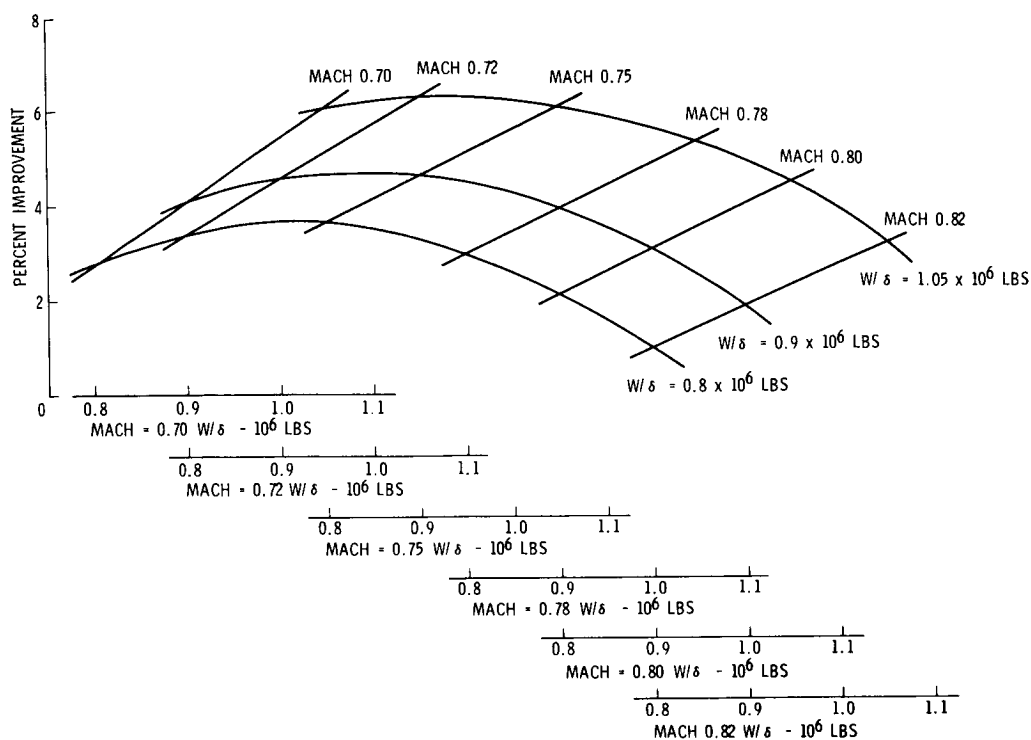


Figure 11. - KC-135A winglet flight test, cruise mileage improvement, winglet 15° cant/-4° incidence, INS energy correction

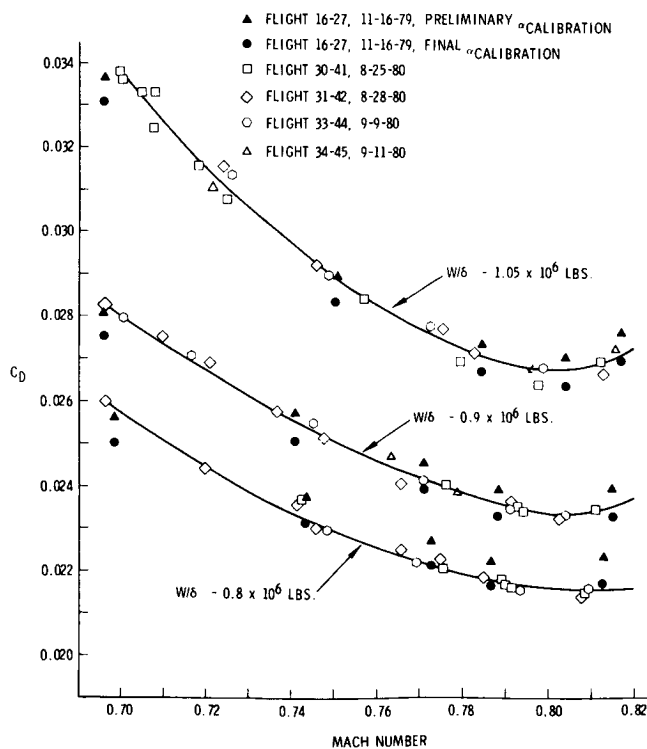


Figure 12. - KC-135A winglet flight test - baseline

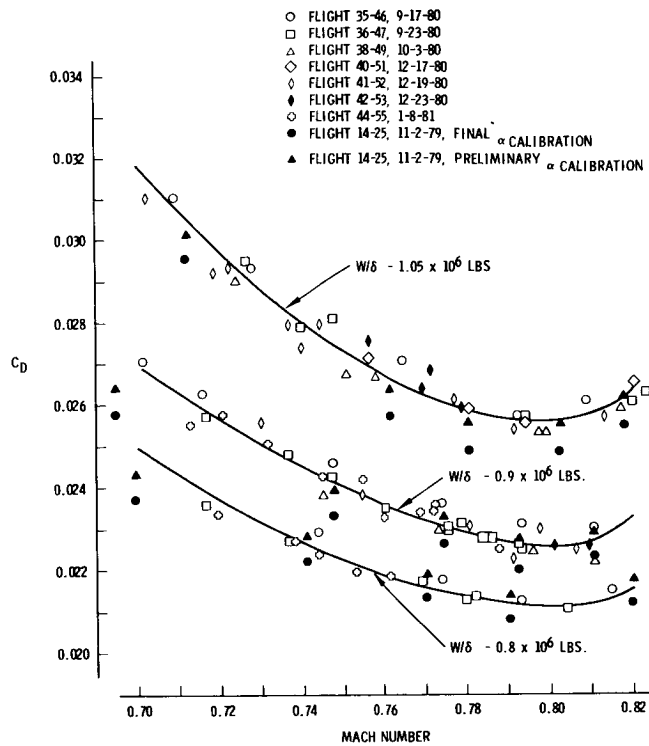


Figure 13. - KC-135A winglet flight test, 15° cant/-4° incidence

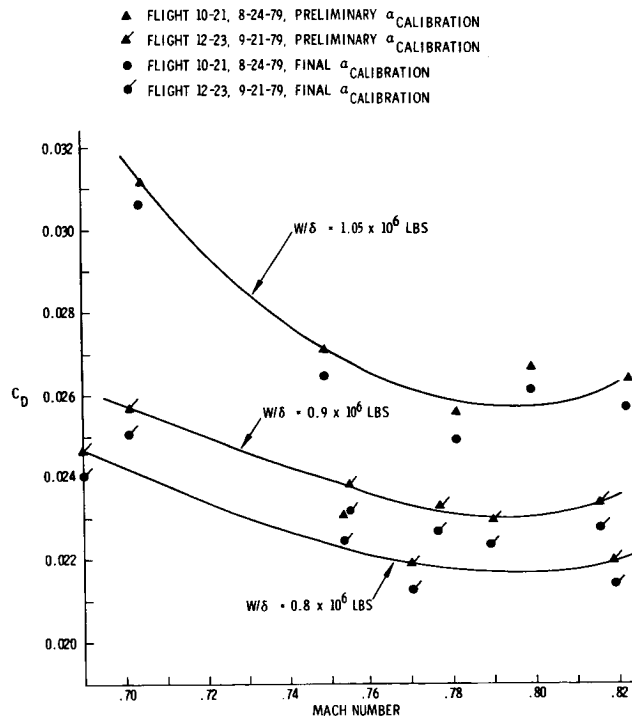


Figure 14. - KC-135A winglet flight test, 15° cant/-2° incidence

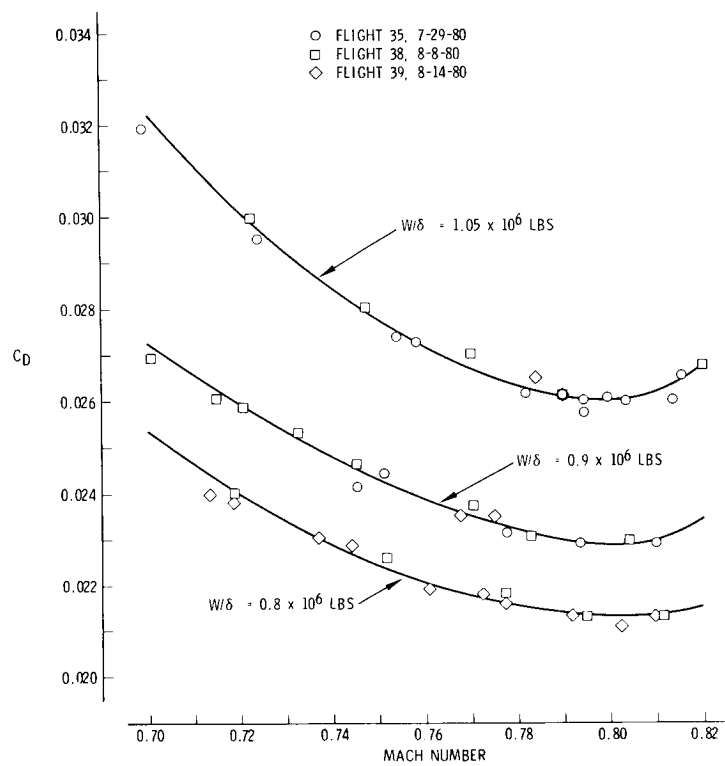


Figure 15. - KC-135A winglet flight test, 0° cant, -4° incidence

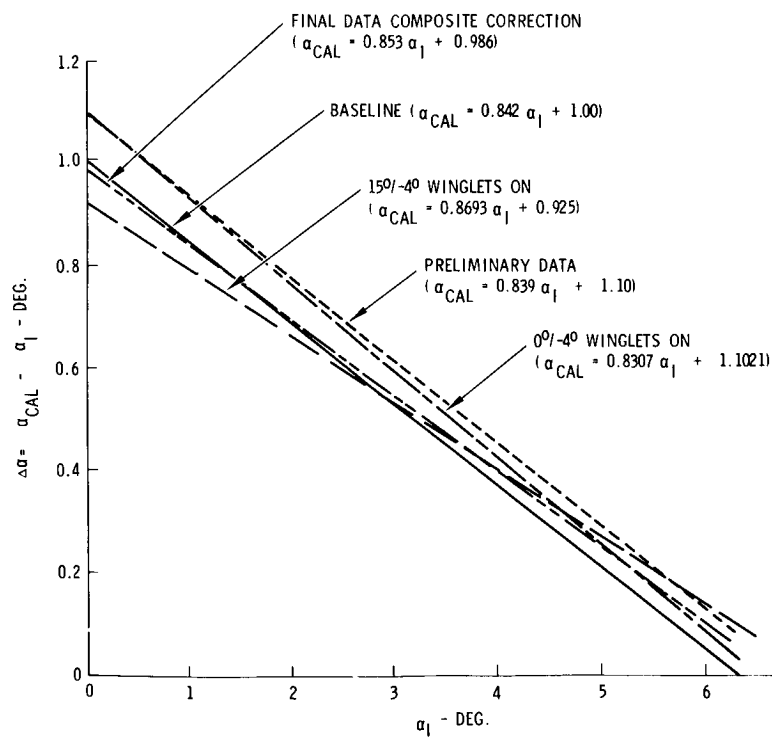


Figure 16. - Angle of attack comparison



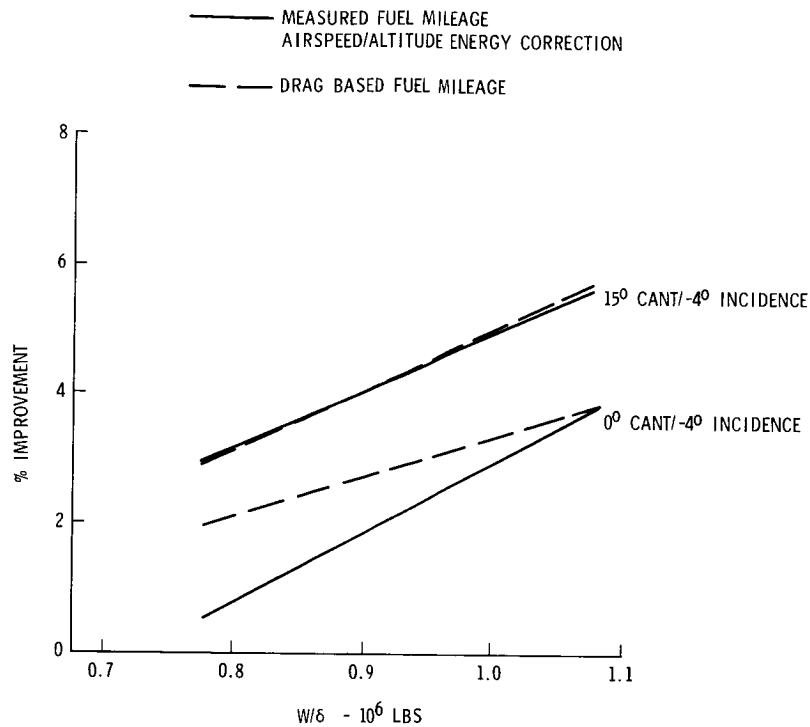


Figure 17. - KC-135A winglet flight test cruise mileage improvement, mach = 0.78

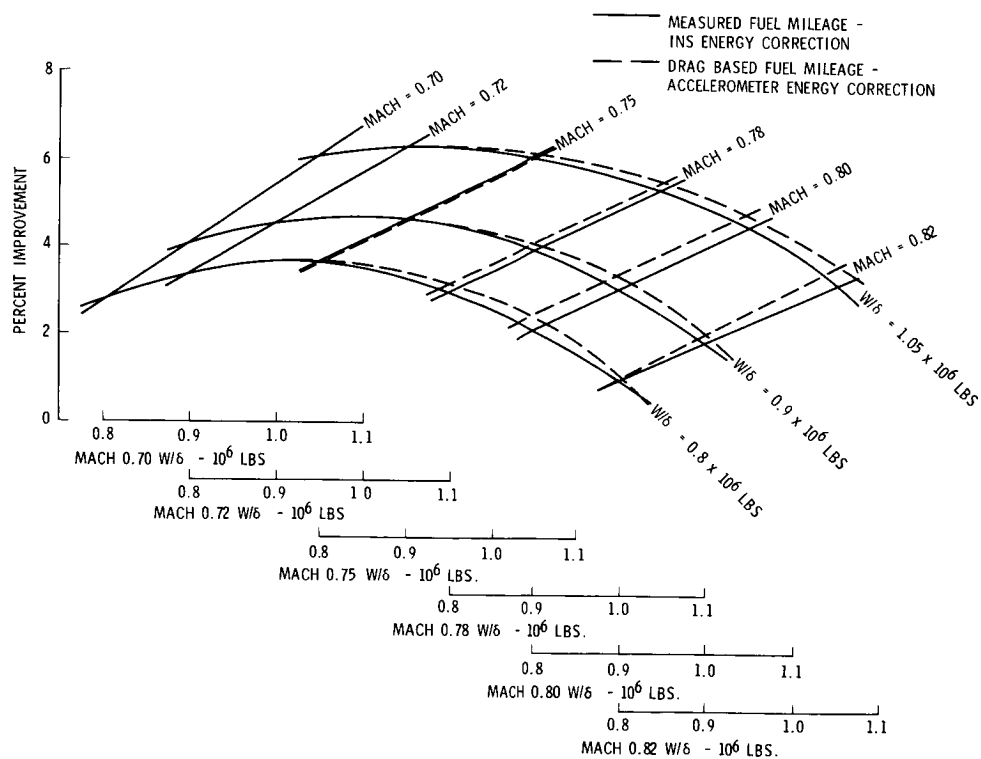


Figure 18. - KC-135A winglet flight test cruise mileage improvement, winglets 15° cant/-4° incidence

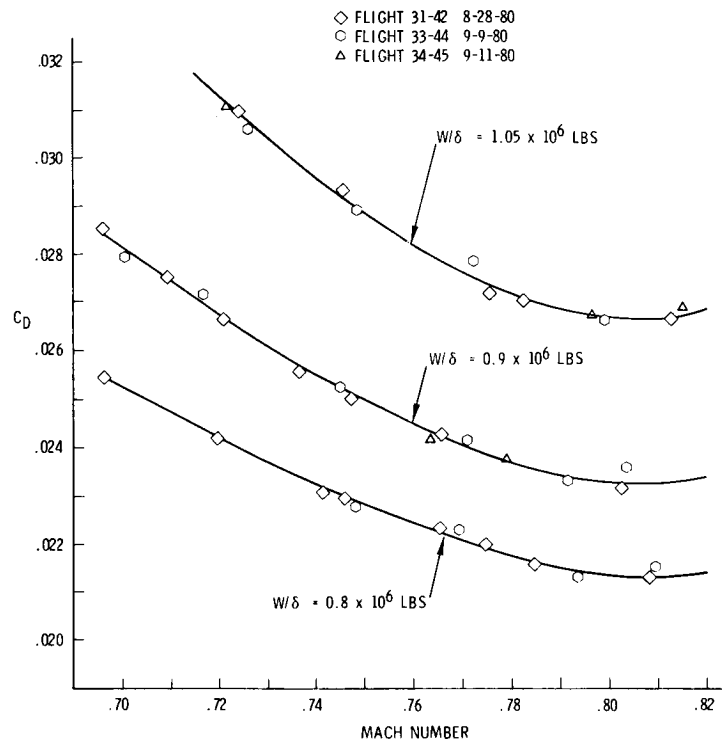


Figure 19. - KC-135A winglet flight test, baseline, INS energy correction

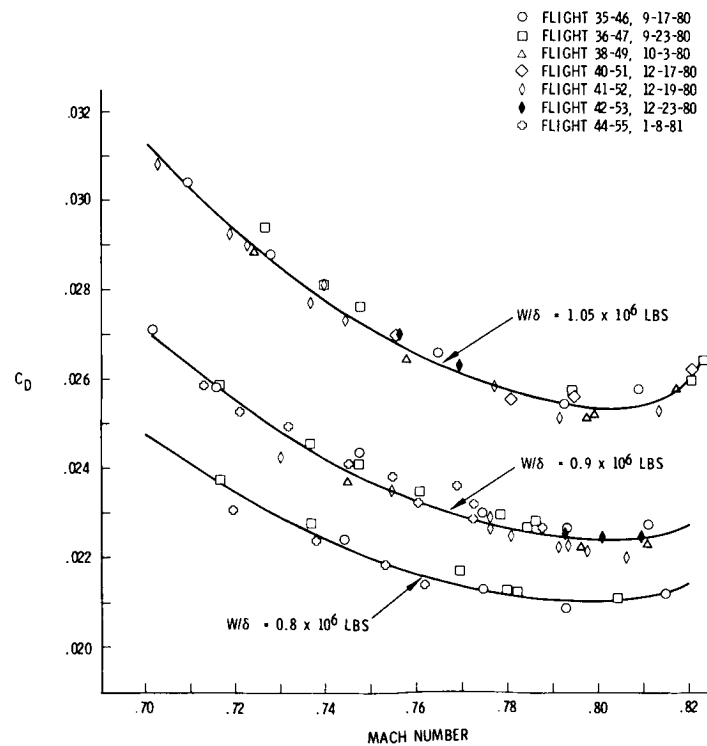


Figure 20. - KC-135A winglet flight test,  $15^\circ$  cant/ $-4^\circ$  incidence, INS energy correction

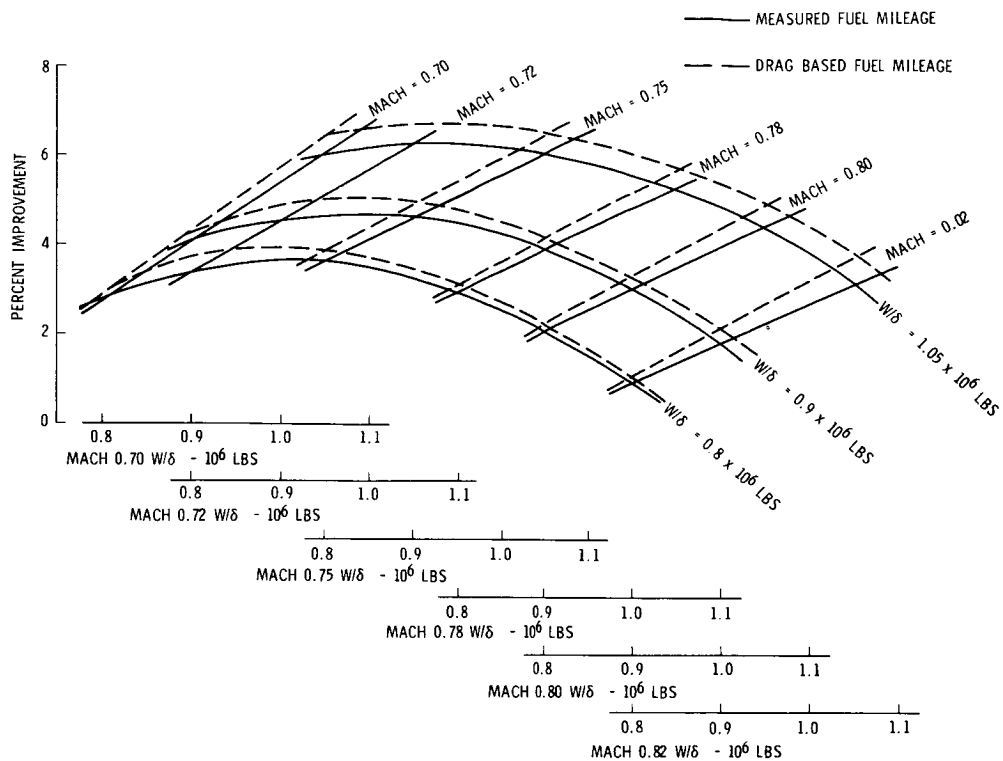


Figure 21. - KC-135A winglet flight test, cruise mileage improvement, winglet 15° cant/-4° incidence, INS energy correction

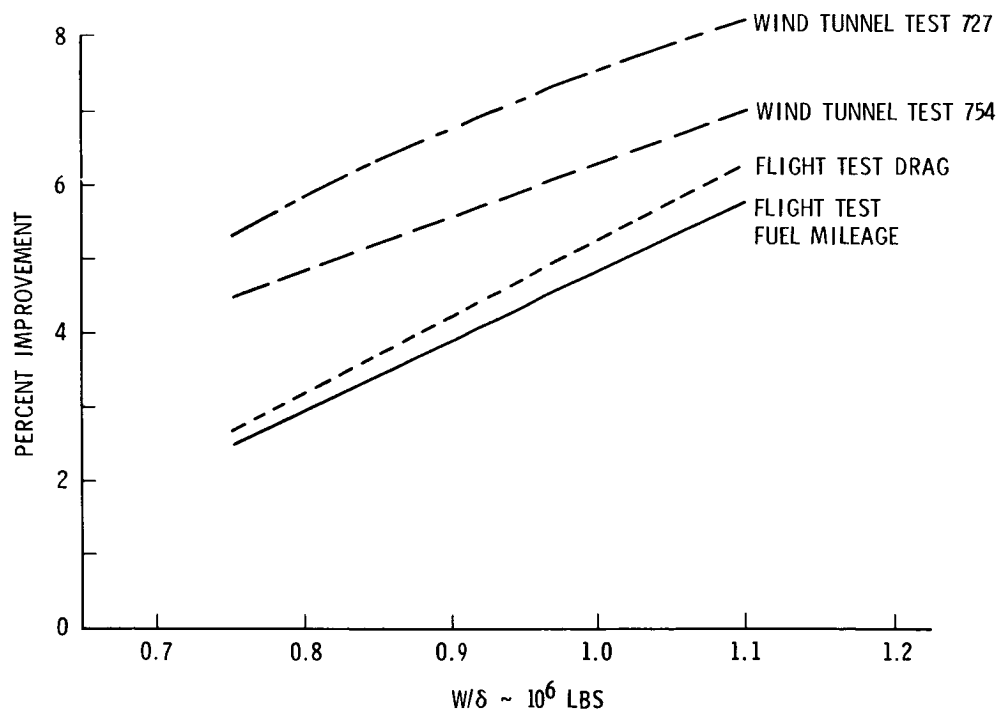


Figure 22. - KC-135A winglet flight test, cruise improvement mach = 0.78

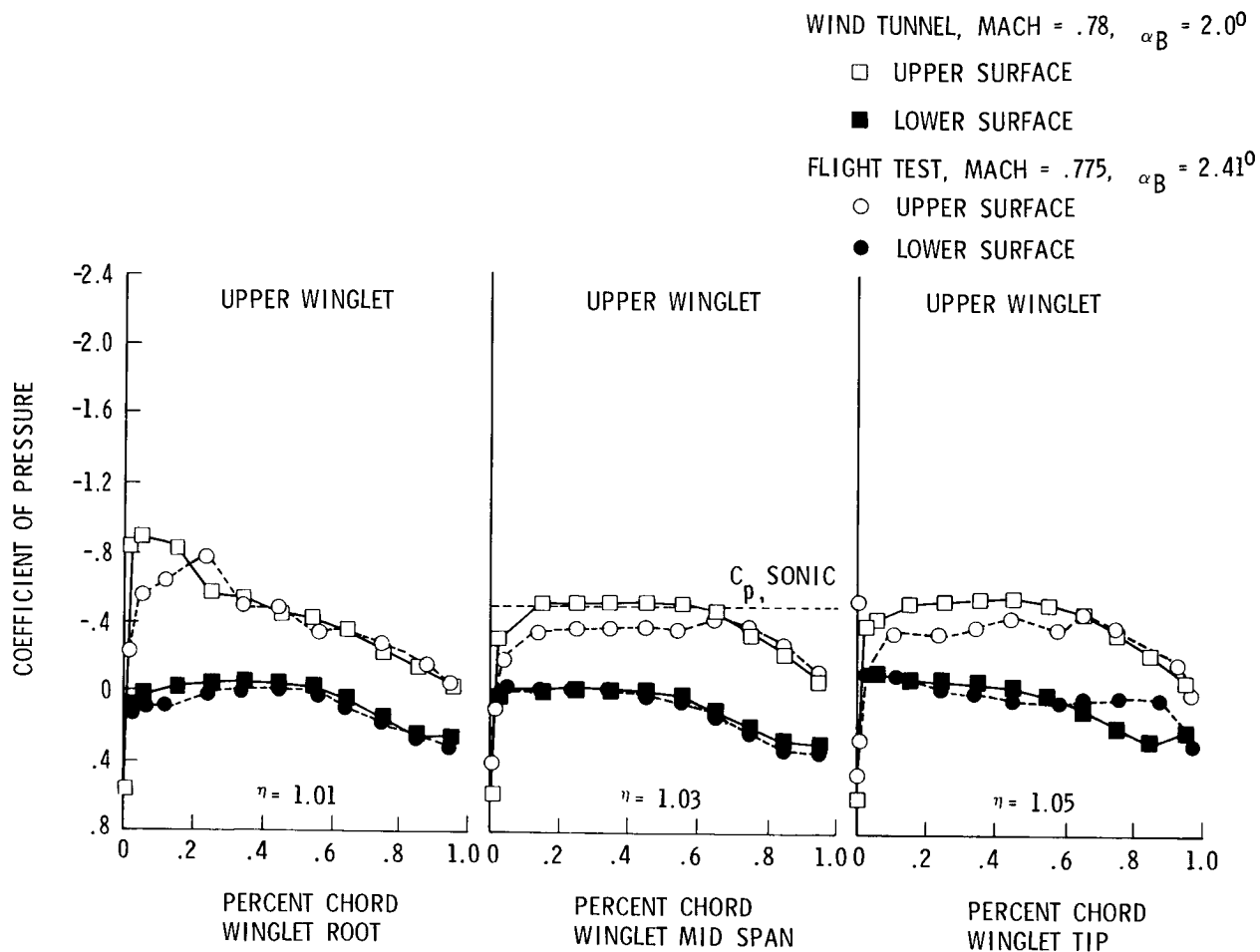


Figure 23. - KC-135 winglet program flight test and wind tunnel test winglet pressure comparison

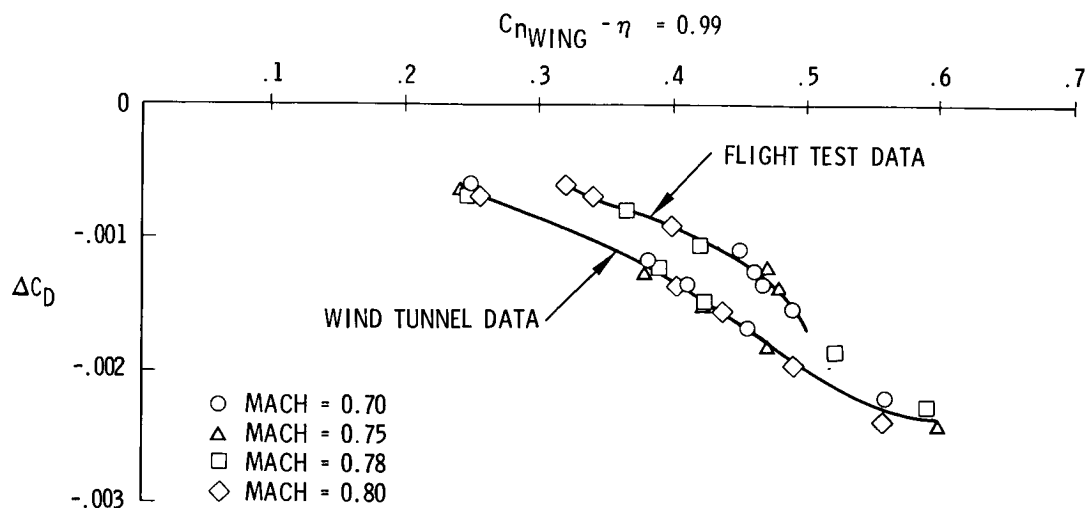


Figure 24. - Comparison of winglet flight test and wind tunnel pressure drag

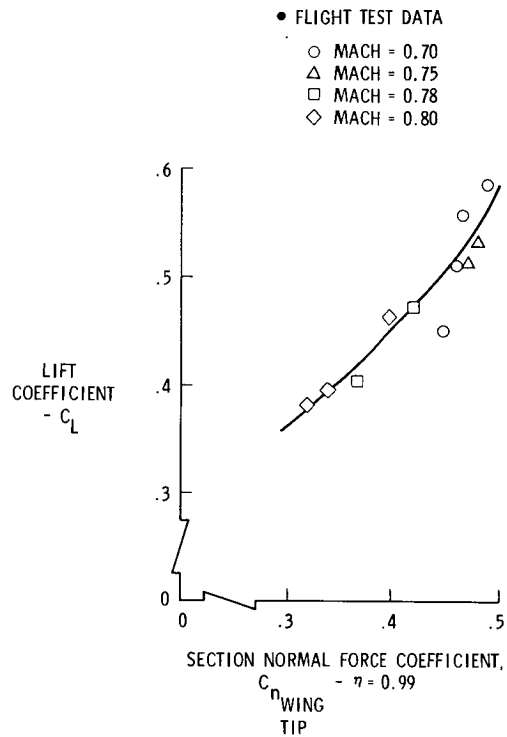


Figure 25 - Airplane lift and wing tip section normal force relationship

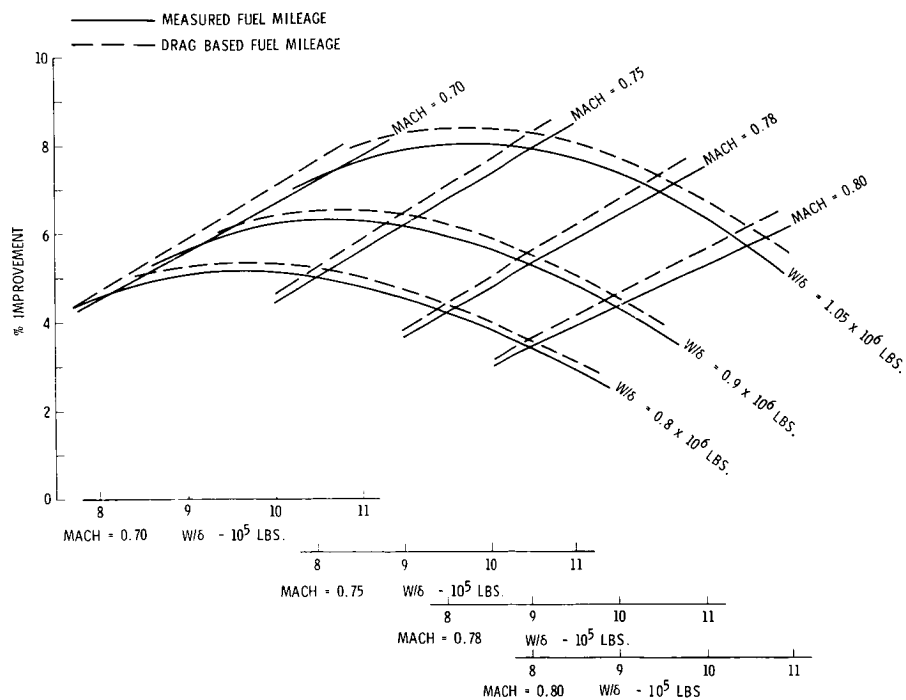


Figure 26. - KC-135A cruise mileage improvement, winglets 15° cant/-4° incidence, includes correction for pressure differences

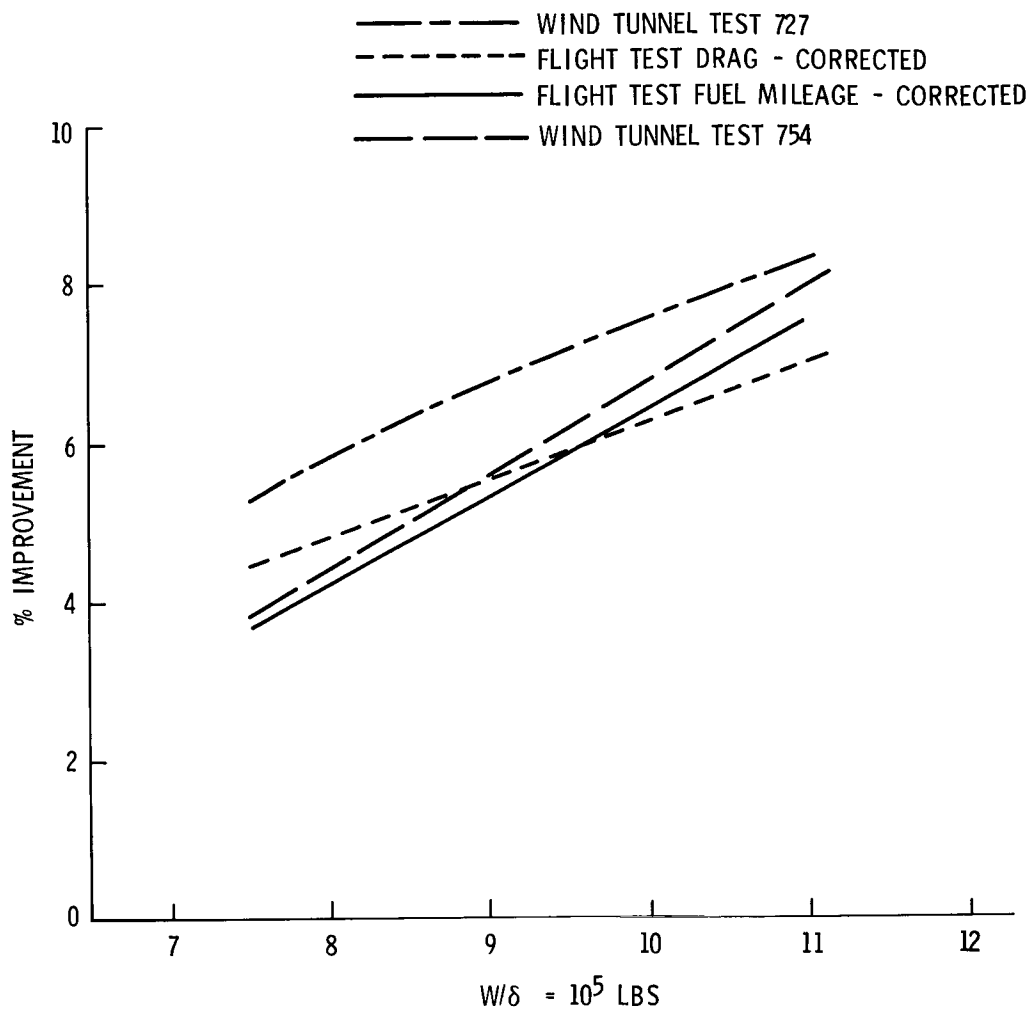


Figure 27. - KC-135A winglet flight test cruise mileage improvement, mach = 0.78

COMPARISON OF FLIGHT MEASURED, PREDICTED AND  
WIND TUNNEL MEASURED WINGLET CHARACTERISTICS  
ON A KC-135 AIRCRAFT

Robert O. Dodson, Jr.  
Boeing Military Airplane Company

SUMMARY

One of the objectives of the KC-135 Winglet Flight Research and Demonstration Program was to obtain experimental flight test data to verify the theoretical and wind tunnel winglet aerodynamic performance prediction methods. Good agreement between analytic, wind tunnel and flight test performance was obtained when the known differences between the tests and analyses were accounted for. The flight test measured fuel mileage improvements for a 0.78 Mach number was 3.1 percent at  $8 \times 10^5$  pounds  $W/\delta$  and 5.5 percent at  $1.05 \times 10^6$  pounds  $W/\delta$ . Correcting the flight measured data for surface pressure differences between wind tunnel and flight resulted in a fuel mileage improvement of 4.4 percent at  $8 \times 10^5$  pounds  $W/\delta$  and 7.2 percent at  $1.05 \times 10^6$  pounds  $W/\delta$ . The performance improvement obtained was within the wind tunnel test data obtained from two different wind tunnel models.

The buffet boundary data obtained for the baseline configuration was in good agreement with previously established data. Buffet data for the  $15^\circ$  cant/ $-4^\circ$  incidence configuration showed a slight improvement, while the  $15^\circ$  cant/ $-2^\circ$  incidence and  $0^\circ$  cant/ $-4^\circ$  incidence data showed a slight deterioration.

INTRODUCTION

Analytical and experimental investigations from the references 1 through 6 studies indicated that a significant drag reduction could be realized on large transport aircraft through the incorporation of winglets. Winglets were projected to reduce the KC-135 cruise drag between 6 and 8 percent, which translates into a significant fuel savings for the KC-135 fleet. This projected cruise performance improvement resulted in the KC-135 Winglet Flight Research and Demonstration Program. The primary objective of the program was to design, fabricate and flight test a set of winglets to prove the fuel conserving attributes of the winglet concept. A secondary objective was to obtain experimental flight test data to verify the theoretical and wind tunnel winglet aerodynamic performance prediction methods.

The Flight Research and Demonstration Program was a joint effort between the Boeing Military Airplane Company (BMAC), the U.S. Air Force and NASA.

BMAC, under contract to the Flight Dynamics Laboratory (FDL), designed, fabricated, ground tested and delivered a set of outboard wings and winglets, which were flight tested by NASA-Dryden. The wind tunnel performance data and the winglet external configuration description were provided by NASA-Langley. The BMAC role throughout the flight test program was to provide engineering

support and to promote understanding and confidence in the data being generated. A detailed discussion of the final results of the program can be found in references 7 and 8. Results presented in reference 9 discuss the analysis of flight test fuel mileage and drag measurements. This report summarizes the results of the comparisons between flight-measured, predicted and wind tunnel-measured winglet characteristics on the KC-135 aircraft.

#### SYMBOLS

ALT	Altitude
b	Wingspan
c, C	Chord Length
$C_D$	Drag Coefficient
$C_{D_i}$	Induced Drag Coefficient
$C_L$	Lift Coefficient
$C_{\ell}$	Sectional Lift Coefficient
$C_{N_A}$	Normal Force Coefficient
$C_n$	Yawing Moment Coefficient, Section Normal Force Coefficient
$C_p$	Pressure Coefficient
D	Drag
FM	Fuel Mileage
$i_w$	Winglet Incidence Angle
L	Lift
$\ell$	Winglet Height
M	Mach Number
$M_{\ell}$	Local Mach Number
MAC	Mean Aerodynamic Chord
q	Dynamic Pressure
$R_N$ , RE NO	Reynolds Number
TSFC	Thrust Specific Fuel Consumption



W, G.W.	Gross Weight
Y	Spanwise Distance Along Wing from B.L. = 0
Z	Spanwise Distance from Winglet Root Measured in Winglet Chord Plane, or Vertical Displacement
$\alpha$	Angle of Attack
$\alpha_B$	Body Angle of Attack
$\beta$	Angle of Sideslip
$\delta$	Ambient Pressure Ratio
$\Delta$	Increment
$\eta$	Nondimensional Wing Semispan
$\theta$	Ambient Temperature Ratio
$\phi$	Winglet Cant Angle

#### WIND TUNNEL TESTS AND DATA CORRECTIONS

The airplane performance wind tunnel tests were accomplished by NASA at their Langley facilities. All tests were conducted in the NASA-Langley 8-foot Transonic Pressure Tunnel except for a limited amount of low-speed flaps-down testing in the NASA-Langley 7-foot x 10-foot High Speed Tunnel to obtain high angles of sideslip. Three different wind tunnel models were used during the NASA-Langley tests. Figure 1 pictures the 0.035 scale rigid full wing span model. The wing for this model was built in a jig position. A photograph of the 0.035 scale model used for the flaps-down wind tunnel tests is shown in figure 2. The model is a rigid full wing span model with brackets for flap deflections of 30 degrees and 50 degrees and outboard aileron deflections. Figure 3 presents the 0.07 scale half model. This particular photograph shows the early upper and lower winglet configuration. The wing of this model had internal structural material removed so that the wing tip would deflect to an approximate full scale cruise position in the wind tunnel. Figure 4 shows the 0.07 scale wind tunnel model static pressure port span locations. On the 0.035 scale models the wing pressures were at the same locations and the winglet static pressure port span locations were at winglet stations 1.01 and 1.05. A summary of the KC-135A winglet wind tunnel test conducted at NASA-Langley is shown in table 1. The test number, model configuration, conditions and type of data recorded are presented.

The "flexible" wing wind tunnel half model used during the NASA-Langley test 727 had a clipped wing tip, the fuselage was not connected to the balance and the wing was built to deflect to a cruise flight position. The data from this test were based on the exposed trapezoidal wing area of the model. The

winglet on and off test data with the clipped wing, based on the exposed trapezoidal area, were corrected to the KC-135 wing area of 2,433 square feet. The incremental drag, due to the winglets, was obtained by taking the difference between the wing area-corrected clipped wing drag polars (winglet on and off) and then adjusting the drag increment to the correct lift by accounting for the fuselage lift carryover. To determine the fuselage lift contribution, the rigid and elastic effects for the KC-135A lift curves were used (reference 10) with the wind tunnel flexible model lift data. The drag increment was then corrected for trim drag and Reynolds number. The corrected incremental drag versus lift coefficient is shown in figure 5 for  $M = 0.78$ . The data points are the incremental drag from the wind tunnel corrected for wing area. The body lift correction was then applied and the combined trim drag and Reynolds number corrections were added. The resulting final corrections to the NASA test 727 data is shown by the dashed line. At  $M = 0.78$  and  $C_L = 0.45$  the drag increment was -17.5 drag counts.

The full span model used during the NASA-Langley test 754 had a rigid wing in the jig position and the winglet was at 12 degrees cant angle. A potential flow analysis was accomplished using wing and winglet geometry corrected for aeroelastic effects to determine the effect of wing aeroelastic effects on the winglet drag increment. The correction was for the cruise condition and amounted to 2.9 degrees additional wing dihedral and -2.9 degrees additional wing twist. The "flexible" wing solution reduced the winglet drag benefit compared to the rigid wing in the jig position. At a lift coefficient of 0.45 the winglet drag benefit was about 2.2 drag counts less for the "flexible" wing than the jig position wing.

From the test 727 cant angle variation there was no discernible difference in winglet drag increment between 12 and 15 degrees cant angles. The corrections for trim drag and Reynolds number were made in the same manner outlined for test 727. The winglet drag increment at  $M = 0.78$  for the NASA test 754 data is shown in figure 6. Again, the test points are noted by the symbols and the dashed line has the combined trim drag and Reynolds number correction noted on the plot.

The KC-135A winglet performance improvements predicted from the wind tunnel data are summarized in table 2. The corrected winglet drag increments obtained from both NASA wind tunnel tests 727 and 754 were added to the basic KC-135A drag polar and the cruise conditions were reoptimized for both sets of data. The performance data shown are an average from both data sets. The values shown are for a flight speed at 99 percent maximum range and the noted corrections.

#### SURFACE PRESSURE COMPARISONS AND ANALYSIS

During the winglet flight tests, chordwise static pressures were measured at four wing and three winglet span locations, as shown in figure 4. These were the same locations where pressures were obtained during the 0.07 scale half model wind tunnel tests.

Comparisons of the flight test and wind tunnel measured pressures for a typical cruise condition are shown in figures 7 and 8 for the wing and winglet, respectively. As can be seen in figure 7 the wing pressure comparison shows good agreement. On the flight test airplane the three inboard rows of wing pressures were measured using pressure belts. The outboard row of wing pressures were especially installed flush static ports. At the 0.92 wing semispan station the flight test pressures indicate some irregularities in the pressure belt contour. At the outboard wing station the flight test-measured pressure, at about 82 percent chord, indicates an ambient pressure. This was attributed to a bad pressure tap and was consistent throughout the flight test for all the flight test-measured pressures.

Figure 8 is a comparison of the flight test and wind tunnel measured pressures on the winglet for the same typical cruise condition. The overall agreement is good. However, a close look at the comparison reveals some subtle differences. First, the three flight test-measured pressures at the winglet tip on the outboard winglet surface at chord stations of about 0.65, 0.75 and 0.87 are bad pressure taps. Next, note the slight local velocity increase measured in flight, beginning at about 60 percent chord for the winglet midspan and tip locations. This effect on the flight test winglet pressures was due to the winglet pillowing causing an irregular contour change in the winglet airfoil shape at these locations. The effect of the winglet pillowing on the flight measured pressures actually begins at about 25 percent chord and a close look indicates an effect at all three span locations.

An inflight photograph of the inboard winglet surface is shown in figure 9, showing the surface contour pillowing when the winglet experiences inflight loads. The surface contour bulges inboard between the winglet ribs and spars due to the compressive stresses in the skin and the inboard suction of the local negative pressures.

The forward winglet spar is located at 15 percent chord and no pillowing effect on surface contour was noticed in flight along the leading edge. However, the inboard winglet root pressure comparison in figure 8 indicates a substantial difference between the flight test and wind tunnel measured pressures at the leading edge. At this Mach number both sets of data show a weak shock at about 25 or 30 percent chord. However, the flight test pressures do not peak to the same levels as the wind tunnel data. A close look at the flight test-measured pressures in this area at other Mach numbers revealed that as soon as the local flow went supersonic the leading edge pressure peak was affected.

The lowest Mach number that pressure data was obtained was 0.468 for the 15°/-2° winglet position. During the flight test program the first winglet position tested was the 15°/-2° position in order to clear the airplane in this configuration first for flutter. During these flights a limited amount of pressure data was taken to check out the pressure instrumentation which included a condition at a Mach number of 0.468 and an angle of attack of 2.0 degrees. To aid in determining if the winglet root leading pressure peak loss was associated with a local sonic flow condition, these flight test pressures were compared to the wind tunnel pressures. The lowest Mach number at which pressure data was recorded in the wind tunnel was 0.70, and only for the 15°/-4° winglet position. A comparison of these pressures is shown in figure 10. Since the winglet positions do not have the same incidence angle, data

at three angles of attack are shown for the wind tunnel data in order to compare the general shape of the leading edge pressures. This comparison showed that at subcritical Mach numbers the winglet root leading edge was loading the way it should. This indicated that the flight test winglet root leading edge pressure peak loss was not associated with any difference in airfoil contour between flight and wind tunnel test, but rather with a local supersonic flow condition.

In an attempt to understand the differences in the leading edge pressures and to further substantiate the effect of the winglet pillowing, a comprehensive two-dimensional transonic analysis was conducted on the winglet streamwise root airfoil section. The primary tool in the analysis was the Bauer-Garabedian-Korn-Jameson 2-D transonic viscous/inviscid analysis code (references 11 and 12). The first step in the analysis was to analyze the basic airfoil, figure 11. This figure shows that the airfoil has good characteristics that are typical of supercritical airfoils. The leading edge pressures, in general, also match the winglet root, low Mach number wind tunnel pressures in figure 8. Since the airfoil ordinates used in the analysis were the same as the ordinates used in lofting, no lofting problem was suspected. However, photographs of the winglets in flight (figure 9) reveal that there was a pillowing effect on the winglets. The rib and spar construction of the flight test article allow bulging out of the unsupported skin panels. This pillowing extends from the forward spar to the aft spar and from the aft spar to the trailing edge winglet structure between the ribs.

The skin pillowing was estimated to bulge approximately one-quarter inch on the 65 inch chord, or 0.38 percent chord at the winglet root station. The model airfoil geometry was modified to simulate the presence of this pillowing. The modified airfoil geometry was again analyzed and the results are shown in figure 12. It should be pointed out that because of the sweep of the winglet,  $M_{normal} = 0.64$  is approximately equal to  $M_{freestream} = 0.78$ . Comparing the aft 50 percent of these pressures to the aft 50 percent of the flight test pressures in figure 8 shows a very close resemblance in shapes. One cannot expect the magnitudes to match because of the three-dimensional losses from the analysis; however, the shapes of the curves should be similar.

The comparisons of the aft portions of the pressures are very similar, but the leading edge pressures do not indicate a leading edge pressure peak loss due to the skin pillowing. A close examination of the flight test photographs and conferences with the structural engineers indicated that the pillowing between the spars may not have been modeled correctly. The way the skin panel is mounted to the ribs and spar would not allow the pillowing to extend over as large a portion of the chord as originally assumed. Remodeling the airfoil, as shown at the bottom of figure 13, yielded the corresponding changes in the pressures. At slightly higher Mach numbers, the pressures seem to hold a peak at about 33 percent chord similar to the flight test pressures. However, the leading edge pressure peak was not appreciably affected.

Since the leading edge pressures were experiencing higher peaks in the analysis than in the flight test at cruise Mach numbers and the flight test pressures match wind tunnel pressures at low subcritical Mach numbers, it was concluded that a small region of separation exists on the winglet leading edge and grows with Mach number on the flight test article. The reason the separation did not show in the wind tunnel data may have been because the wind tunnel

model had a trip strip at 5 percent chord. Although the grit size was small, No. 22, it was still 3 to 4 times greater than the displacement thickness of a laminar boundary layer at this point. The grit in this case may have been doing more than forcing a transition from laminar to turbulent flow in the boundary layer. The grit may have been acting like a row of very small vortex generators which were injecting energy into the boundary layer, preventing separation.

The next step in the investigation was to define what effect the differences between flight test and wind tunnel measured winglet pressures had on winglet pressure drag. To do this, the winglet flight test and wind tunnel pressure data were transformed to suction and drag loops along the winglet span using the winglet incidence angle. This was accomplished for all Mach numbers and angles of attack for which wind tunnel and flight test pressure data existed. A typical comparison between flight test and wind tunnel data at cruise conditions is shown in figures 14 through 16 for the three winglet stations. Note the relatively large difference in the suction loop area at the winglet root station due to the flight test leading edge pressure peak loss.

A chordwise and spanwise integration on the winglet of these data yielded the incremental winglet pressure drag data shown in figure 17. Note that the drag data are shown plotted against the section normal force at the outboard wing station instead of the usual total airplane lift coefficient. This was done to compensate for any differences in aeroelastic twist at the wing tip between the wind tunnel model and the flight test airplane. The relationship between airplane lift coefficient and wing tip normal force coefficient for the flight test airplane is shown in figure 18.

Referring back to the incremental pressure drag plot in figure 17 indicates that at typical cruise conditions the difference between the flight test and wind tunnel measured drag data would be about 4 drag counts, which is about 1.5 to 2 percent when transformed to a cruise fuel mileage benefit. This difference reveals the importance of the aerodynamic pressure loading on the winglet in order to obtain the expected winglet performance benefit.

In order to obtain a feel for the amount of the drag difference obtained between flight test and wind tunnel data that can be attributed to the winglet root leading edge suction loss and the winglet pillowing effect, the winglet root suction/drag loop for the flight test was assumed to be exactly equal to the wind tunnel data. Performing a similar integration over the winglet revealed the drag differences shown in figure 19. The drag differences shown here between the flight test and wind tunnel data are approximately the differences that can be attributed to the winglet pillowing effect. About one-third of the total difference shown in figure 17 can be attributed to winglet pillowing and two-thirds to the winglet root leading edge suction loss obtained in flight.

#### COMPARISONS OF WIND TUNNEL AND THEORETICAL PREDICTION TO FLIGHT TEST DATA

One of the objectives of the KC-135 Winglet Flight Research and Demonstration Program was to obtain experimental flight test data to verify the theoretical and wind tunnel winglet performance prediction methods.

Theoretical surface pressures and drag increments due to the winglets were compared to wind tunnel and flight test data for selected conditions. The following discussion presents the results of these comparisons.

A comparison of theoretical potential flow, wind tunnel and flight test pressure distributions on the wing tip and winglet are presented in figure 20. The comparison is at a Mach number of 0.70. The overall comparison is good. The potential flow wing geometry had an aeroelastic twist distribution representative of typical lg cruise conditions. Also note in figure 20 the loss of the leading edge pressure peak at the winglet root obtained from the flight test data.

Integrating the wind tunnel and flight test pressure data to obtain the section normal force results in the typical comparison shown in figure 21. The 15° cant/-4° incidence angle data compared well. At the winglet midspan and tip positions the flight test data may be slightly lower compared to the wind tunnel data. The 15° cant/-2° incidence data show the winglet carrying more load as expected.

Flight test incremental drag results are compared to wind tunnel and theoretical predicted drag increments in figures 22 through 24. The flight test data shown in the figures have the pressure drag increment correction included. The wind tunnel drag increments have been corrected for Reynolds number and trim drag.

The data shown in figure 20 compares the test data to a predicted theoretical drag increment at a Mach number of 0.70. The theoretical drag increment was obtained using the same potential flow geometry model with aeroelastic twist that was discussed before. The wing and winglet potential flow span loading solution was again used as input to a Trefftz plane analysis computer program to compute the induced drag. The induced drag was then corrected for skin friction and trim drag. As can be seen in figure 22, the comparison was good between theory, wind tunnel and flight test. Since the theoretical potential flow method was a subcritical flow method, only a comparison at a Mach number of 0.70 is shown. At the higher Mach numbers shock waves begin to appear on the surface and the method is no longer valid.

Wind tunnel predicted and flight test incremental drag comparisons at higher Mach numbers are shown in figures 23 and 24. In each case the comparison was good except at a Mach number of 0.82. The flight test drag increment shows less improvement than predicted from wind tunnel data at this Mach number. This was attributed to the winglet root leading edge pressure peak loss in flight and the surface pillowing problems becoming more aggravated at this higher Mach number, as previously discussed.

The KC-135A performance improvements based on these incremental drag data are shown in table 3. The winglet drag increment was added to the basic KC-135A Flight Manual drag polar and cruise conditions were reoptimized. The wind tunnel-predicted fuel mileage improvement value previous to the flight test was 6.3 percent (table 2) and, using the flight test obtained drag increment, the fuel mileage improvement was 6.5 percent. These percentages were obtained by ratioing the winglet on and off fuel mileage at the optimum  $W/\delta$  of each configuration.

Figure 25 presents the performance benefit for winglets obtained from flight test fuel mileage and drag data compared to the wind tunnel predicted improvement at  $M = 0.78$ . The percent improvement shown has been corrected to account for the winglet surface pressure discrepancies. Good agreement was obtained between the corrected flight test data and the corrected full model wind tunnel data.

Buffet boundaries were established during the flight test program using wing tip mounted accelerometer data. Data were obtained for the winglets on configurations as well as for the baseline configuration, as shown in figure 26. The buffet boundary data obtained for the baseline configuration was in good agreement with the previously established data. The buffet data for the  $15^\circ$  cant/ $-4^\circ$  incidence configuration shows a slight improvement over the baseline. The  $15^\circ$  cant/ $-2^\circ$  incidence configuration showed a slight deterioration to the baseline configuration again indicating that the additional winglet loading was causing an earlier flow separation. The  $0^\circ$  cant/ $-4^\circ$  incidence configuration exhibited buffet characteristics similar to the  $15^\circ$  cant/ $-2^\circ$  incidence configuration. The decrease in buffet boundary for the  $0^\circ$  cant/ $-4^\circ$  incidence configuration is in agreement with the performance data that showed a lower than predicted performance increase, possibly due to flow separation between the wing tip and winglet root.

#### CONCLUSIONS

Results of the KC-135 winglet flight test have verified that the performance improvement can be predicted using conventional analytic and wind tunnel testing techniques. The data show that winglet retrofit would provide a six percent performance improvement for the KC-135 at the optimum cruise condition.

Particular attention should be paid to the design of the wing tip and winglet intersection. Since the drag differences obtained between flight test and wind tunnel data were significant, the implications for a production winglet design are important. First a production winglet should be constructed so that no winglet pillowing could occur, possibly by using composite material or reinforced honeycomb techniques. Second, a production winglet should be designed so that the highly sensitive winglet root leading edge area does not experience a peak pressure loss during flight conditions that result in locally supersonic flow in this area. A row of vortex generators to prevent a separation bubble or a winglet root leading edge fairing to prevent local supersonic flow conditions are two possible solutions.

#### REFERENCES

1. Whitcomb, R. T., "A Design Approach and Selected Wing-Tunnel Results at High Subsonic Speeds for Wing-Tip Mounted Winglets," NASA TN D-8260, dated July 1976.

2. Jacobs, P. F., Flechner, S. G., Montoya, L. C., "Effect of Winglets on a First-Generation Jet Transport Wing, I - Longitudinal Aerodynamic Characteristics of a Semispan Model at Subsonic Speeds," NASA TN D-8473, dated June 1977.
3. Montoya, L. C., Flechner, S. G., Jacobs, P. F., "Effects of Winglets on a First-Generation Jet Transport Wing, II - Pressure and Spanwise Load Distributions For a Semispan Model at High Subsonic Speeds," NASA TN D-8474, dated July 1977.
4. Meyer, R. R., "Effect of Winglets on a First-Generation Jet Transport Wing, IV - Stability Characteristics For a Full-Span Model at Mach 0.30," NASA Technical Paper 1119, dated February 1978.
5. Flechner, S. G., "Effect of Winglets on a First-Generation Jet Transport Wing, VI - Stability Characteristics For a Full-Span Model at Subsonic Speeds," NASA Technical Paper 1330, dated October 1979.
6. Ishimitsu, K. K., VanDevender, N., Dodson, R. O., et al., "Design and Analysis of Winglets For Military Aircraft," AFFDL-TR-76-6, dated February 1976.
7. Dodson, R. O., Ayala, J., Shurtz, R. M., et al., "KC-135 Winglet Flight Research and Demonstration Program - Trade Study Results," AFWAL-TR-81-3031, dated May 1981.
8. Dodson, R. O., Ayala, J., Shurtz, R. M. and Temanson, G., "KC-135 Winglet Flight Research and Demonstration Program," Boeing document D453-10087, to be published as an AFWAL-TR.
9. Temanson, G., "Measurements of the Fuel Mileage of a KC-135 Aircraft With and Without Winglets," to be published in a NASA CP.
10. Boeing document D3-9090, "Summary of the Stability, Control and Flying Qualities Information for All the -135 Series Airplanes," dated October 1973.
11. Bauer, F., Garabedian, P., Korn, D., "Supercritical Wing Sections," Lecture Notes in Economics and Mathematical System 66, 1972.
12. Bauer, F., Garabedian, P., Korn, D., Jameson, A., "Supercritical Wing Sections II," Lecture Notes in Economics and Mathematical Systems 108, 1975.



TABLE 1. -- KC-135A WINGLET WIND TUNNEL TESTS

Test	Fuselage	Wing	Winglet	Tail		$\alpha$ Range (deg)	$\beta$ (deg)	Mach								Data				
				Hor.	Vert.			0.30	0.50	0.70	0.75	0.78	0.80	0.82	0.85	0.90	0.95	Force & moment	Pressure	
																			Wing	Winglet
727	A	D	OFF/ON	OFF	OFF	-1/7	0			X	X	X					X	X	X	
						4/12	0	X									X	X	X	
	B	E	OFF/ON	OFF	OFF	-2/5	0, $\pm 5$		X	X	X	X	X	X	X	X	X			
	C	F	OFF/ON	G	ON	-6/14	0, $\pm 5$	X									X			
766	B	E	OFF/ON	OFF	OFF	-8/14	0, $\pm 5$			X		X				X	X	X		
767	C	F	ON	-10°	ON	-8/16	0, $\pm 5$	X								X		X		
772	C	E	OFF/ON	G	ON	-6/16	0, $\pm 5$	X	X	X			X			X	X	X		
7 x 10 75 20	C	F	ON	-10°	ON	-6/16	0, $\pm 5$ $\pm 8, \pm 12$	X								X		X		

Fuselage codes: A - Semispan 0.070 scale KC-135A

B - Full span cylindrical body of revolution

C - Full span 0.035 scale KC-135A

D - Semispan 0.07 scale KC-135A

E - Full span 0.035 scale KC-135A; right hand panel has orifice rows

F - Full span 0.035 scale KC-135A; provisions for flaps and ailerons

Hor. tail code: G - OFF, 0°, -4°, -10°

TABLE 2. — KC-135A WINGLET PERFORMANCE BENEFITS PREDICTED

FROM WIND TUNNEL DATA

- Flight speed for 99% maximum range
- Climb cruise corrected
- 5% service tolerance (fuel flow increase per MIL-C-5011B)
- Bleed and power extraction included (1.25%)

	W/ $\delta$ ** (lbs)	Mach	L/D*	M (L/D) *	TSFC*/ $\sqrt{\theta}$ (lb/hr-lb)	Fuel* Mileage (nm/lb)	Range** Factor (nm)
KC-135A (basic)	882,300	0.79	17.4	13.8	1.1151	0.0407	8084
KC-135A with winglets	933,000	0.79	18.4	14.6	1.1106	0.0433	8597
Percent change relative to KC-135A			5.7%	5.8%	0.4%	6.3%	6.3%

\*200,000 lbs gross weight

\*\*Average over gross weight range (includes owe change for winglets)

TABLE 3. — KC-135A WINGLET PERFORMANCE BENEFITS PREDICTED

## FROM FLIGHT TEST DATA

- Flight speed for 99% maximum range
- Climb cruise corrected
- 5% service tolerance (fuel flow increase per MIL-C-5011B)
- Bleed and power extraction included (1.25%)

	W/ $\delta$ ** (lbs)	Mach	L/D*	M(L/D) *	TSFC*/ $\sqrt{\theta}$ (lb/hr-lb)	Fuel* Mileage (nm/lb)	Range** Factor (nm)
KC-135A (basic)	882,300	0.79	17.4	13.8	1.1151	0.0407	8084
KC-135A with winglets	942,000	0.79	18.43	14.63	1.1114	0.04335	8611
Percent change relative to KC-135A			5.9%	6.0%	0.33%	6.5%	6.5%

\*200,000 lbs gross weight

\*\*Average over gross weight range (includes owe change for winglets)

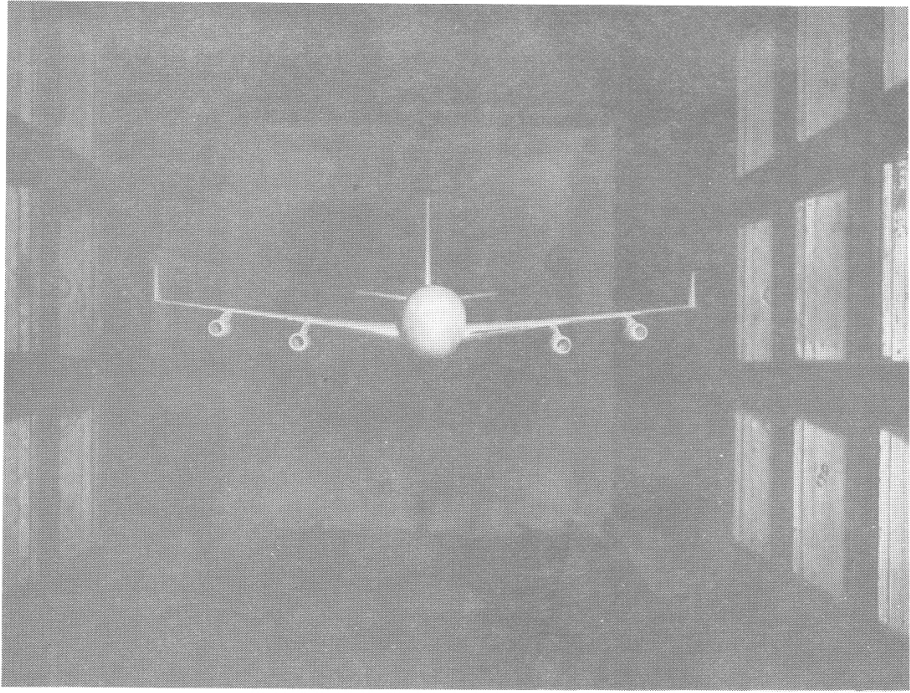


Figure 1. - Rigid wind tunnel model - 0.035 scale

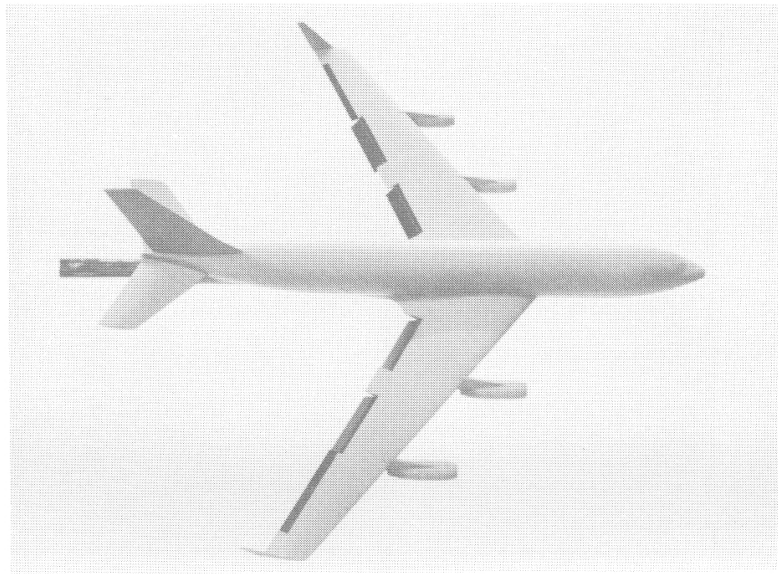


Figure 2. - Flaps down wind tunnel model - 0.035 scale

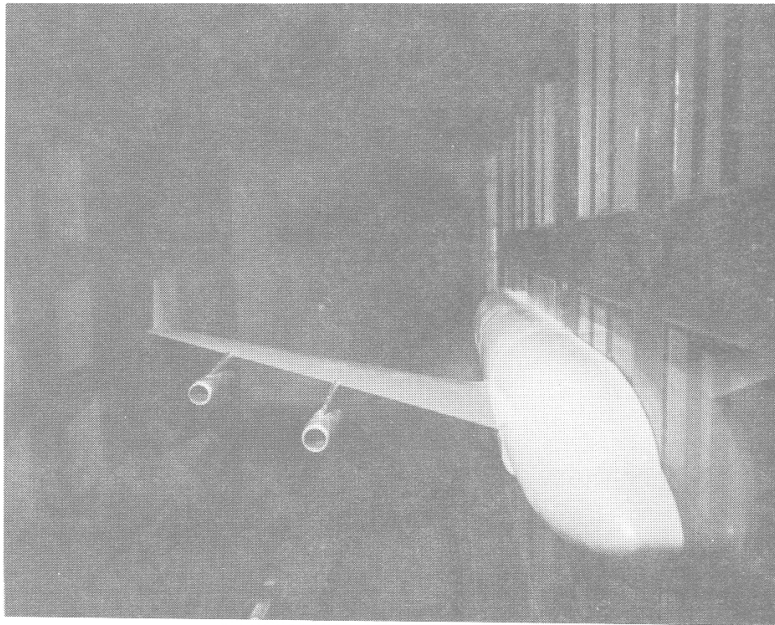


Figure 3. - Wind tunnel half-model - 0.07 scale

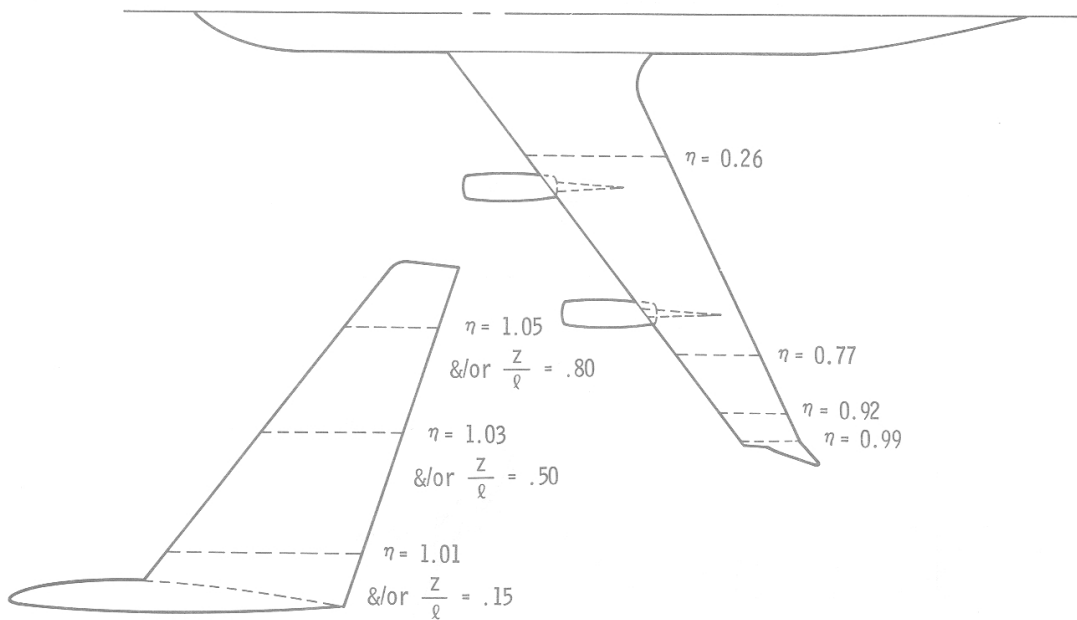


Figure 4. - Wing and winglet static pressure span locations

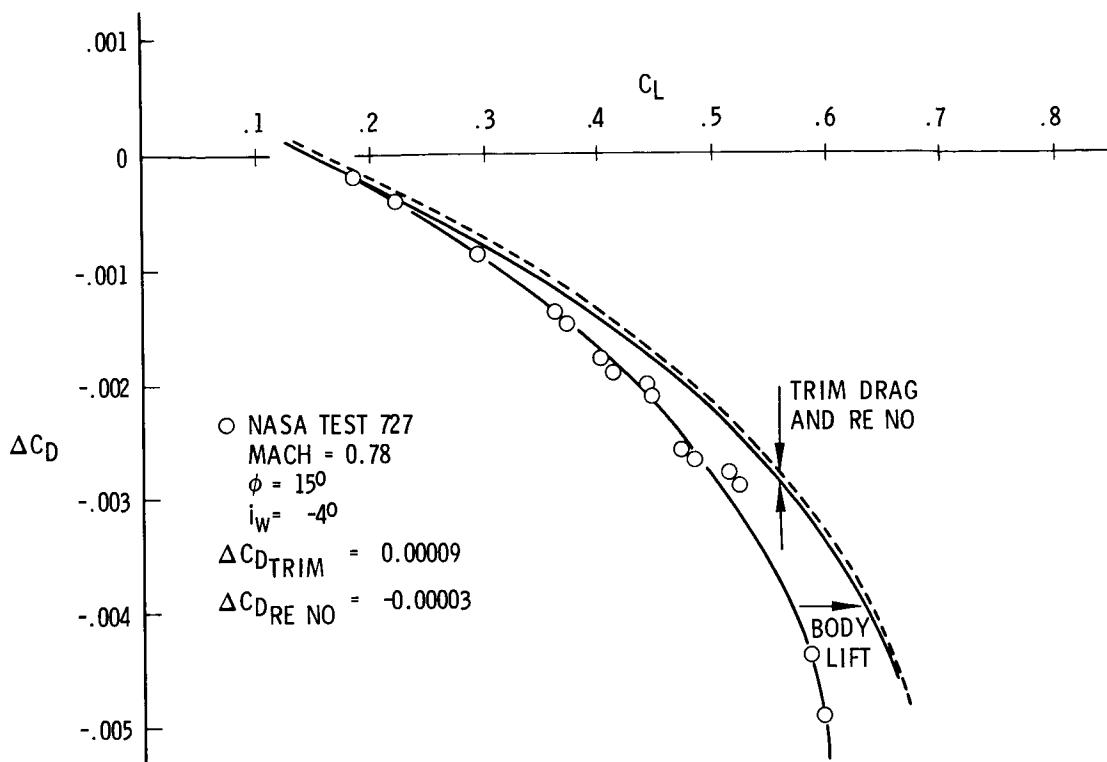


Figure 5. - Winglet drag increment wind tunnel data corrections, 0.07 scale flexible wing half model

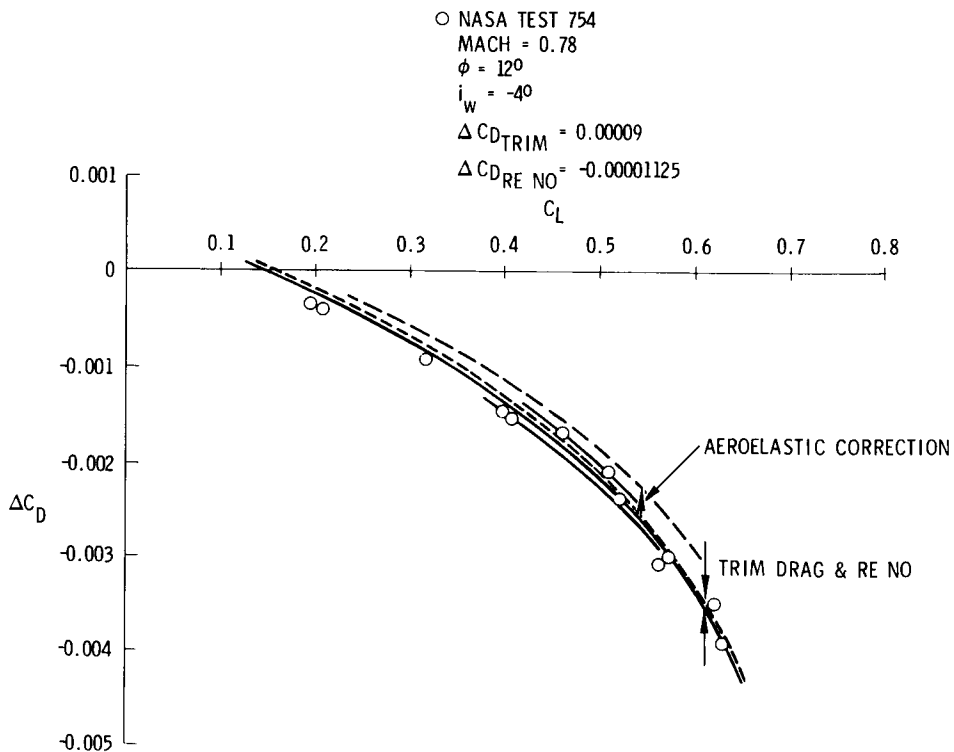


Figure 6. - KC-135 winglet drag increment - wind tunnel data corrections, 0.035 scale rigid full model

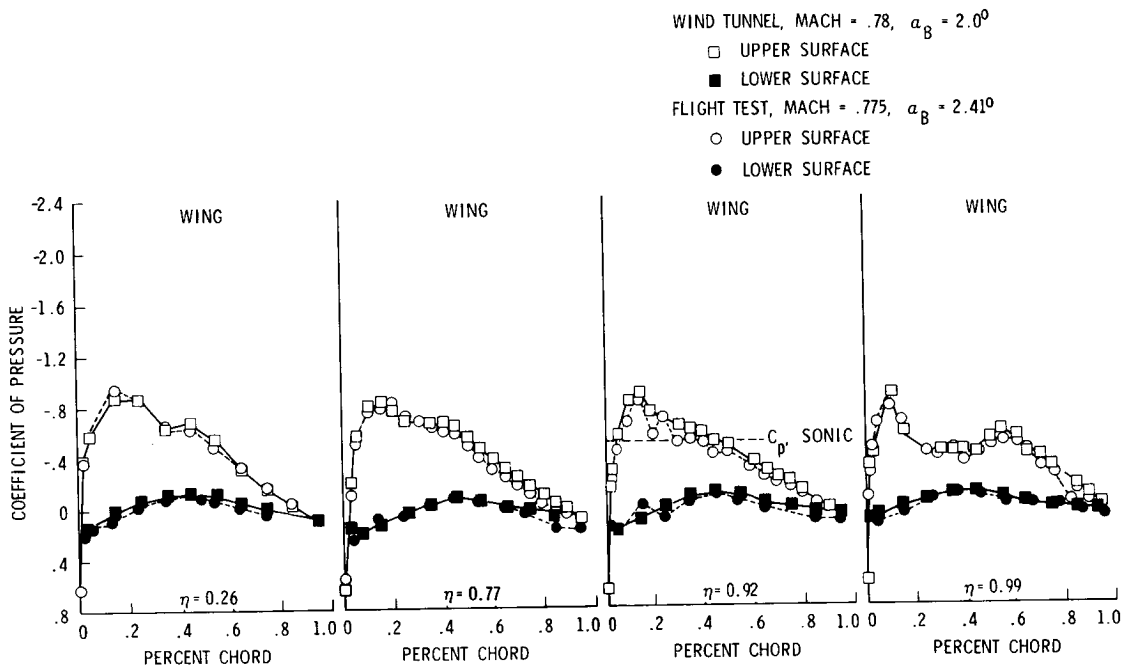


Figure 7. - KC-135 winglet program - flight test and wind tunnel test wing pressure comparison

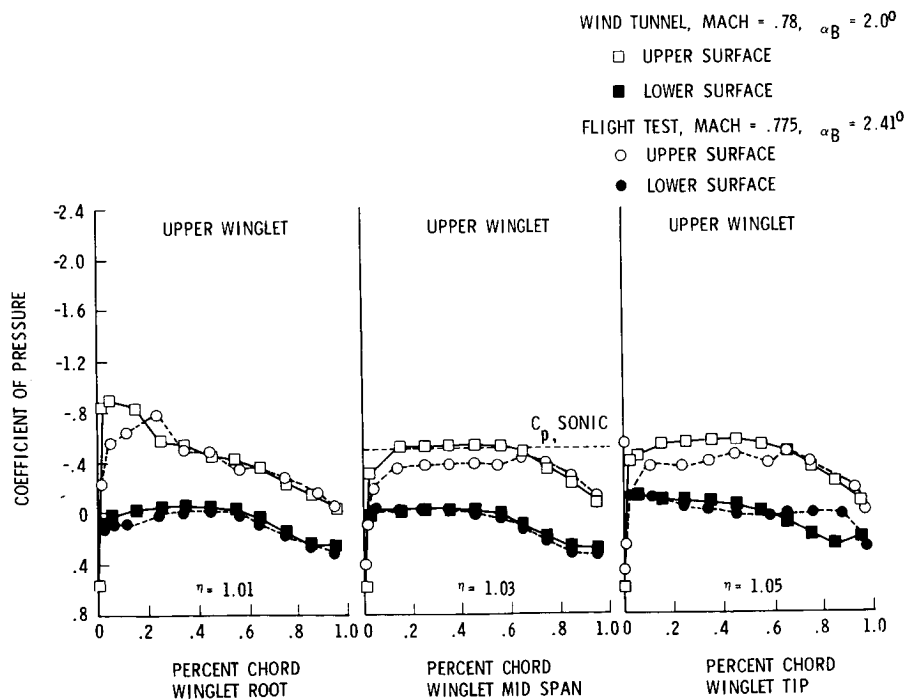


Figure 8. - KC-135 winglet program - flight test and wind tunnel test winglet pressure comparison

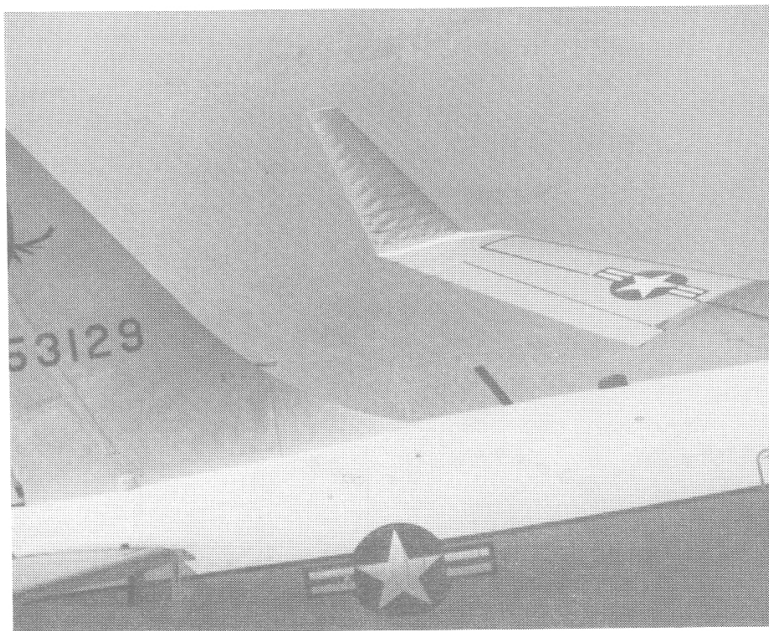


Figure 9. - Winglet in flight with skin "pillowing"

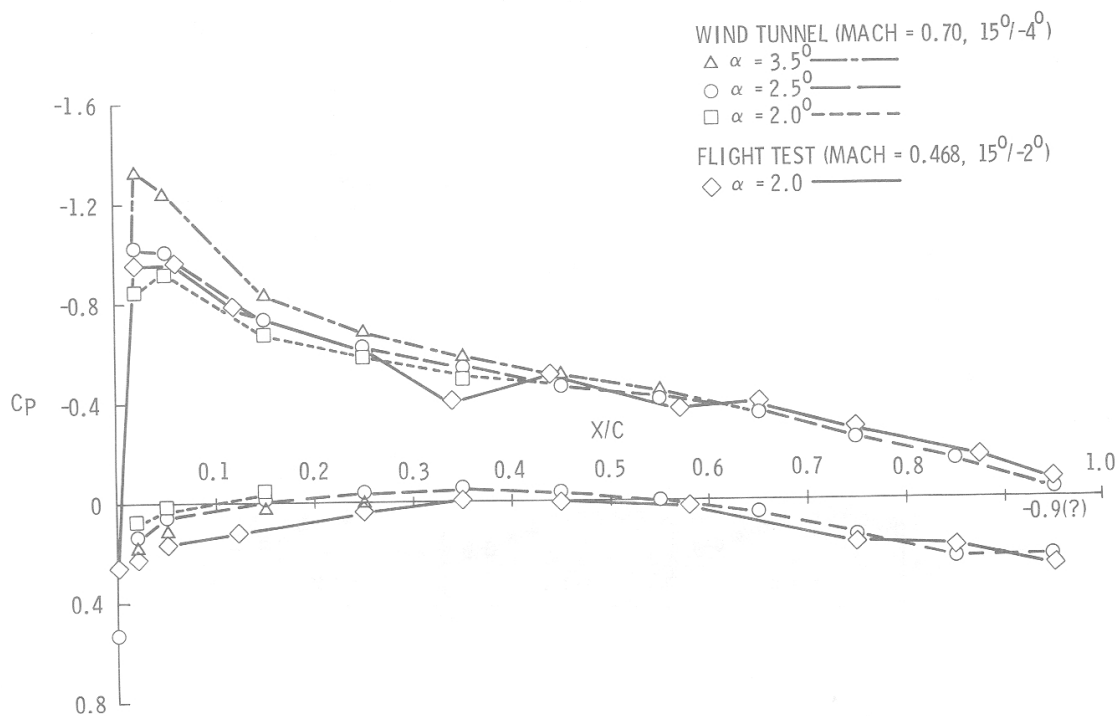


Figure 10. - Pressure comparisons near winglet root,  $\eta = 1.01$  and/or  $Z/\ell = 0.15$



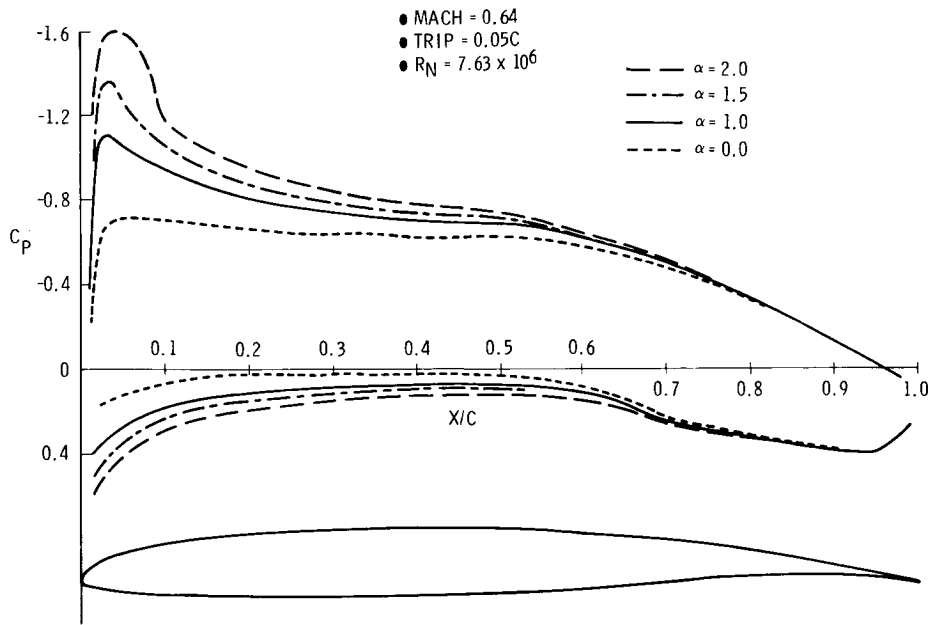


Figure 11. - Bauer-Garabedian-Korn-Jameson 2-D transonic airfoil analysis (smooth airfoil)

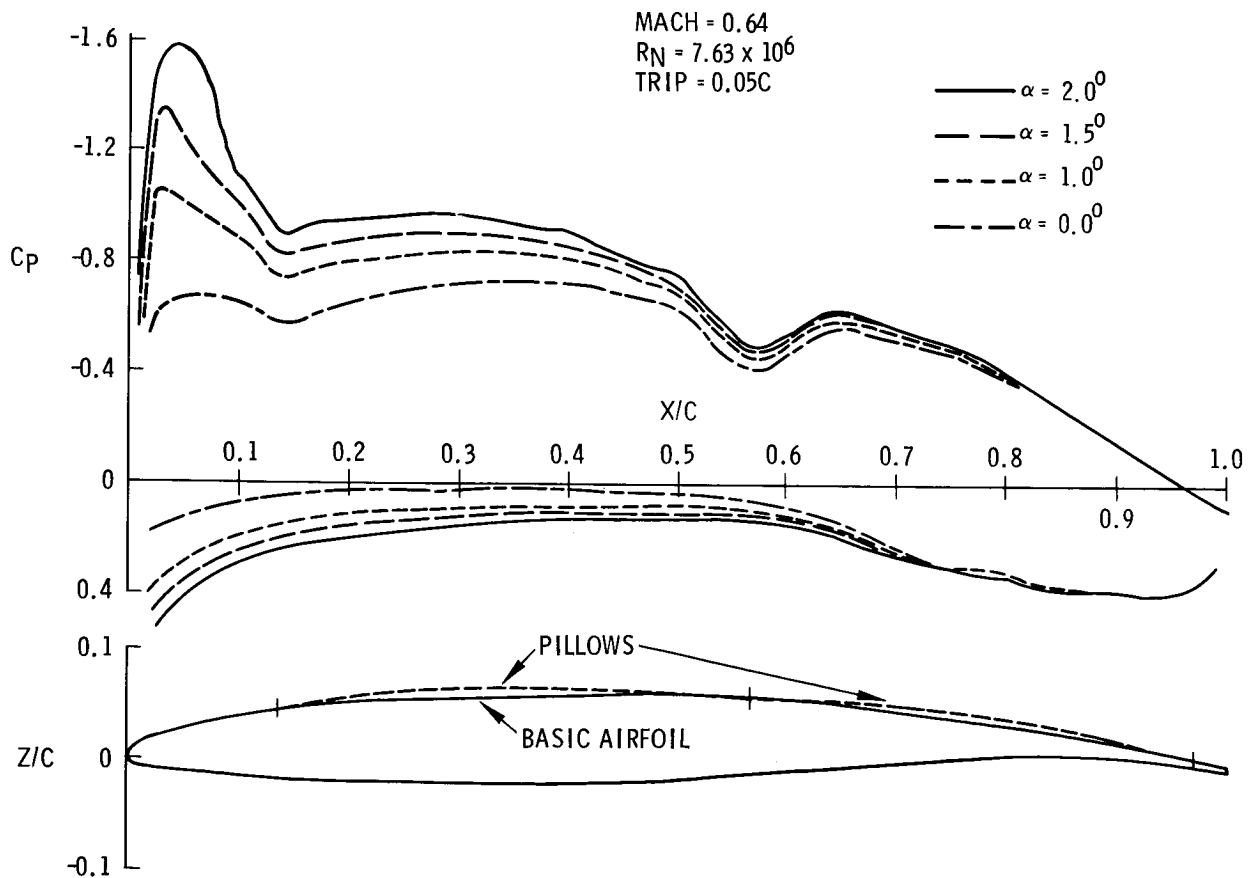


Figure 12. - Bauer-Garabedian-Korn-Jameson 2-D transonic airfoil analysis with 0.004C pillows

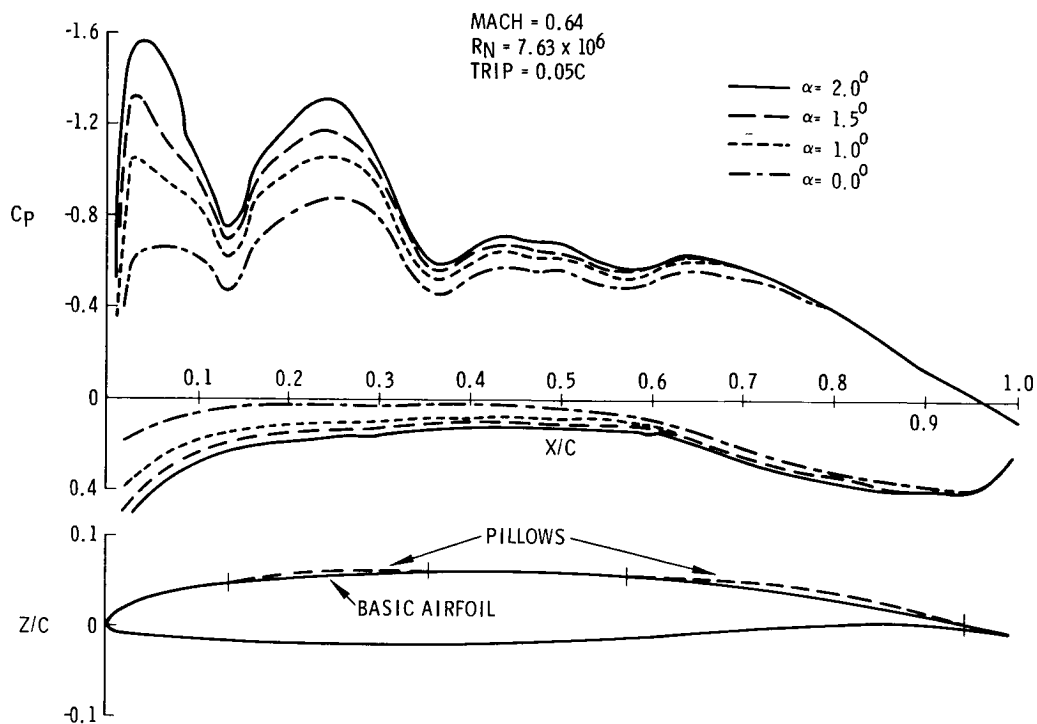


Figure 13. - Bauer-Garabedian-Korn-Jameson 2-D transonic airfoil analysis with 0,004C pillows

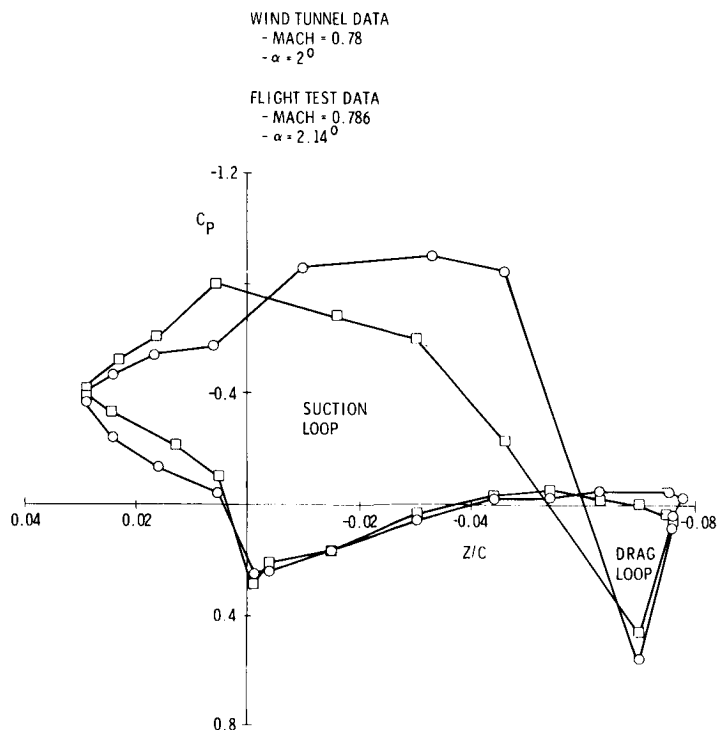


Figure 14. - Sectional drag comparison,  $\eta = 1.01$

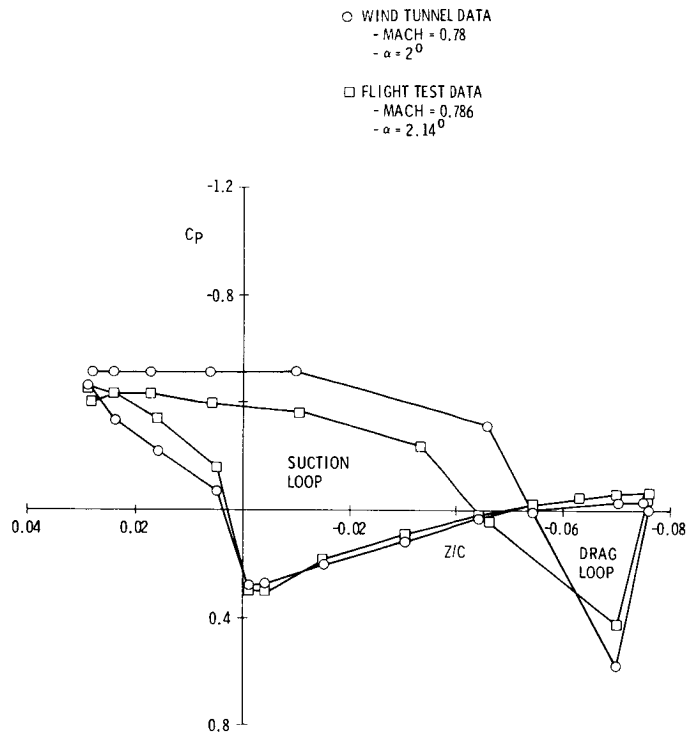


Figure 15. - Sectional drag comparison,  $\eta = 1.03$

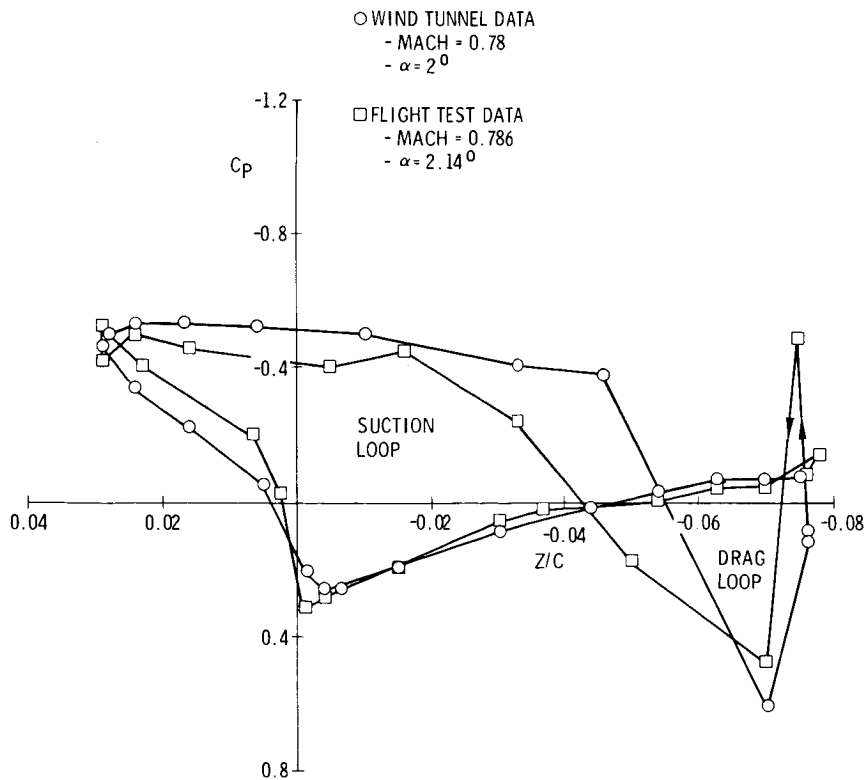


Figure 16. - Sectional drag comparison,  $\eta = 1.05$

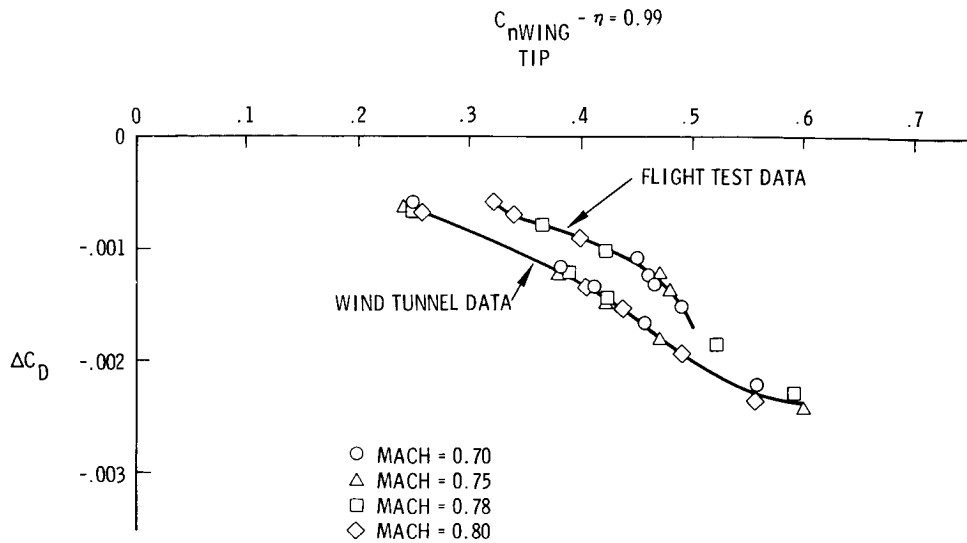


Figure 17. - Comparison of winglet flight test and wind tunnel pressure drag

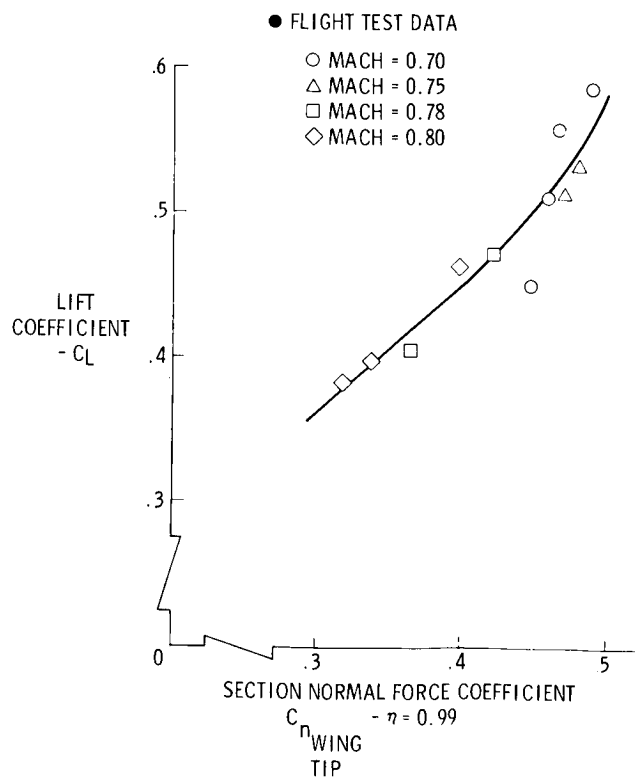


Figure 18. - Airplane lift and wing tip section normal force relationship

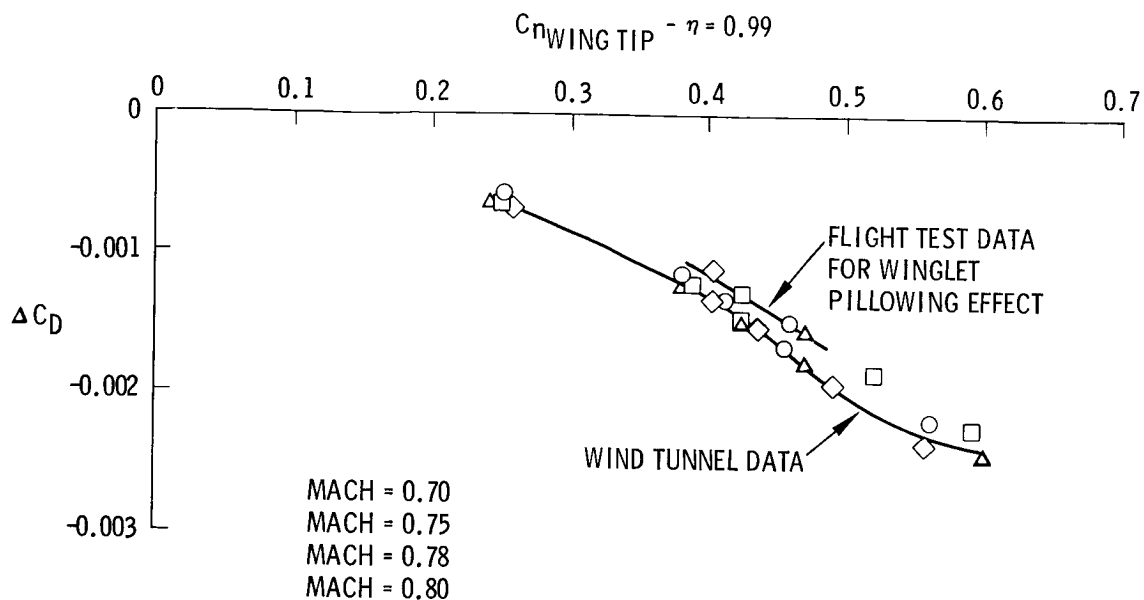


Figure 19. - Comparison of winglet flight test and wind tunnel pressure drag

- MACH = 0.78
- WIND TUNNEL DATA TEST 727 "FLEXIBLE" WING MODEL, 15° CANT, -4° INCIDENCE
- FLIGHT TEST DATA, 15° CANT, -4° INCIDENCE
- △ FLIGHT TEST DATA, 15° CANT, -2° INCIDENCE

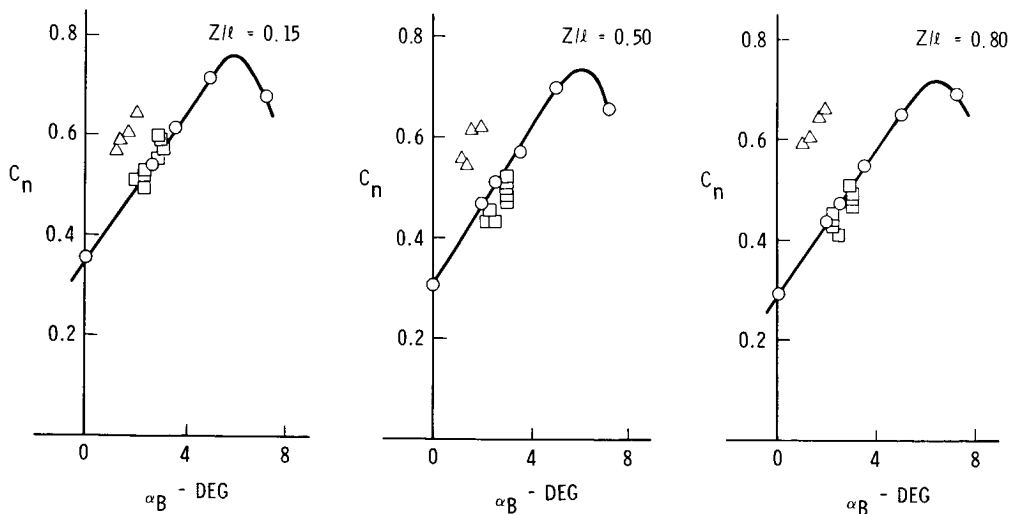


Figure 20. - Comparison of theory, wind tunnel and flight test KC-135 winglets and wing tip pressures, mach = 0.70,  $\phi = 15^\circ$ ,  $i_w = -4^\circ$

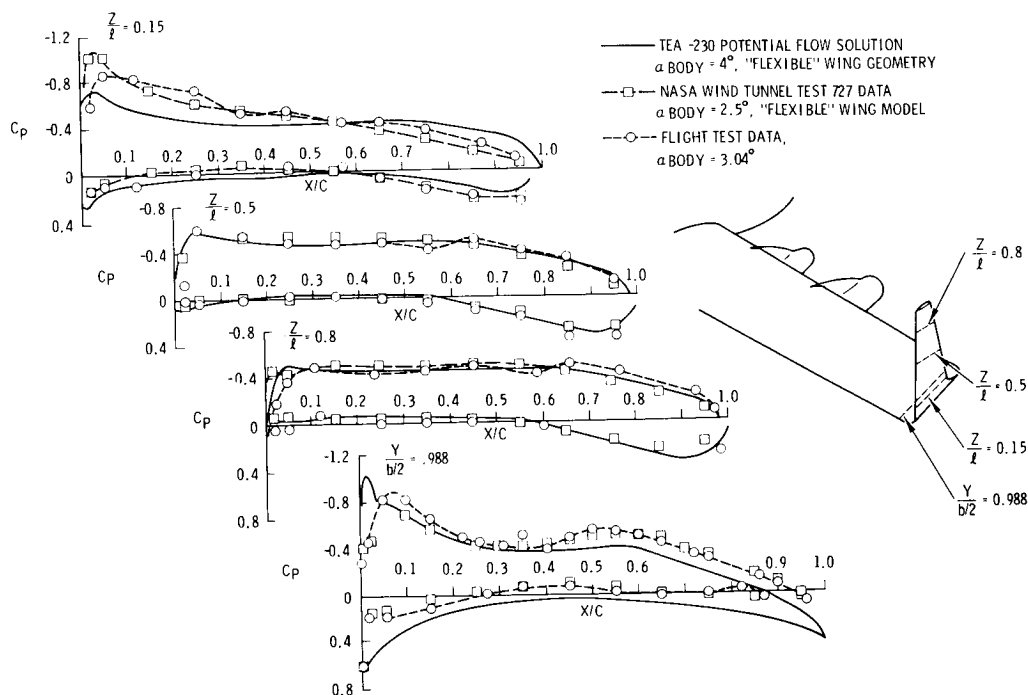


Figure 21. - KC-135 winglet section normal force comparison of wind tunnel to flight test data

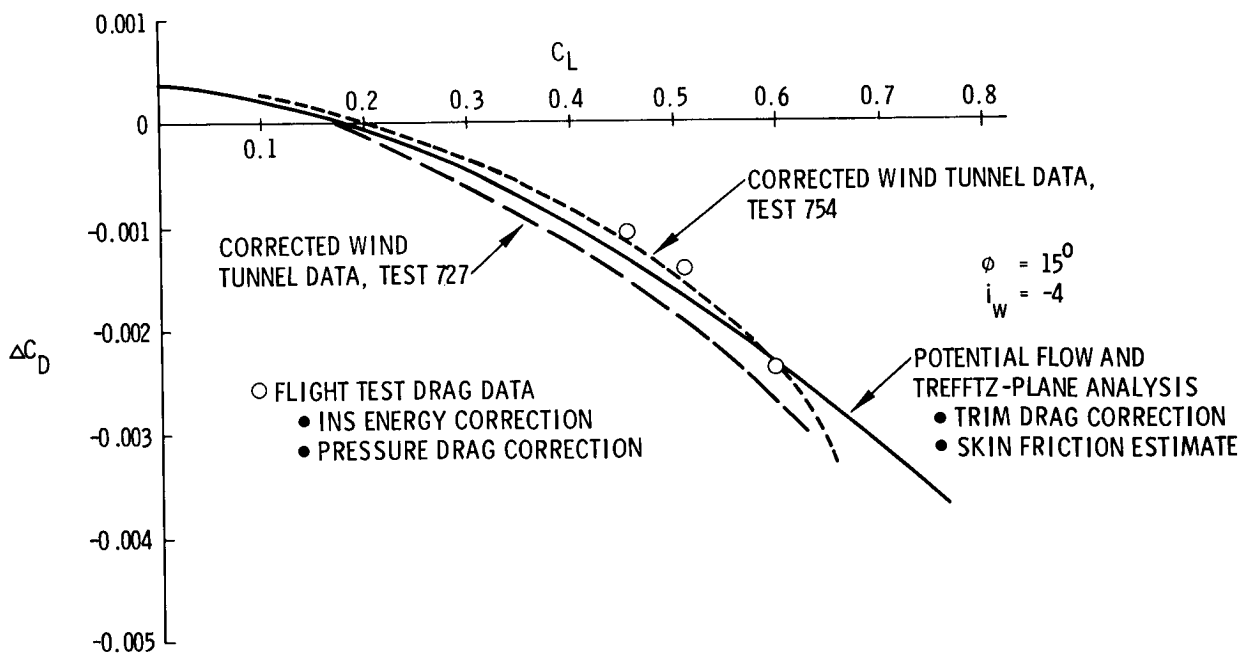


Figure 22. - Comparison of flight measured, theoretical and wind tunnel predicted incremental drag due to winglets, mach = 0.70

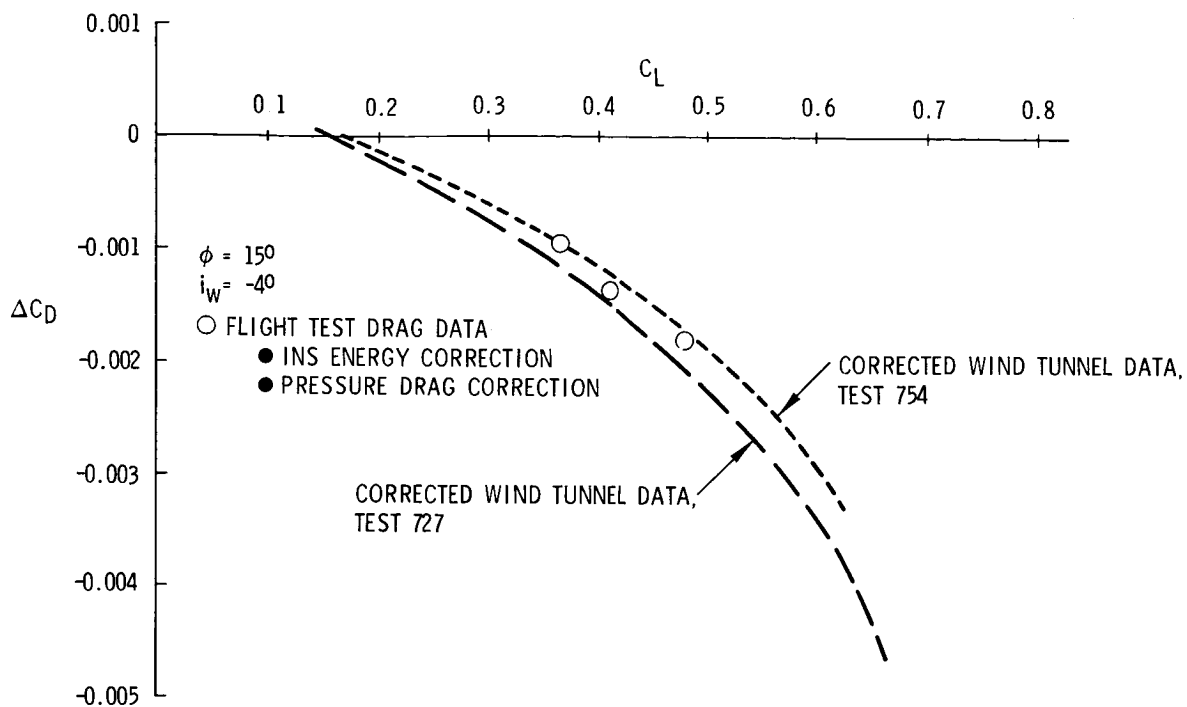


Figure 23. - Comparison of flight measured and wind tunnel predicted incremental drag due to winglets, mach = 0.78

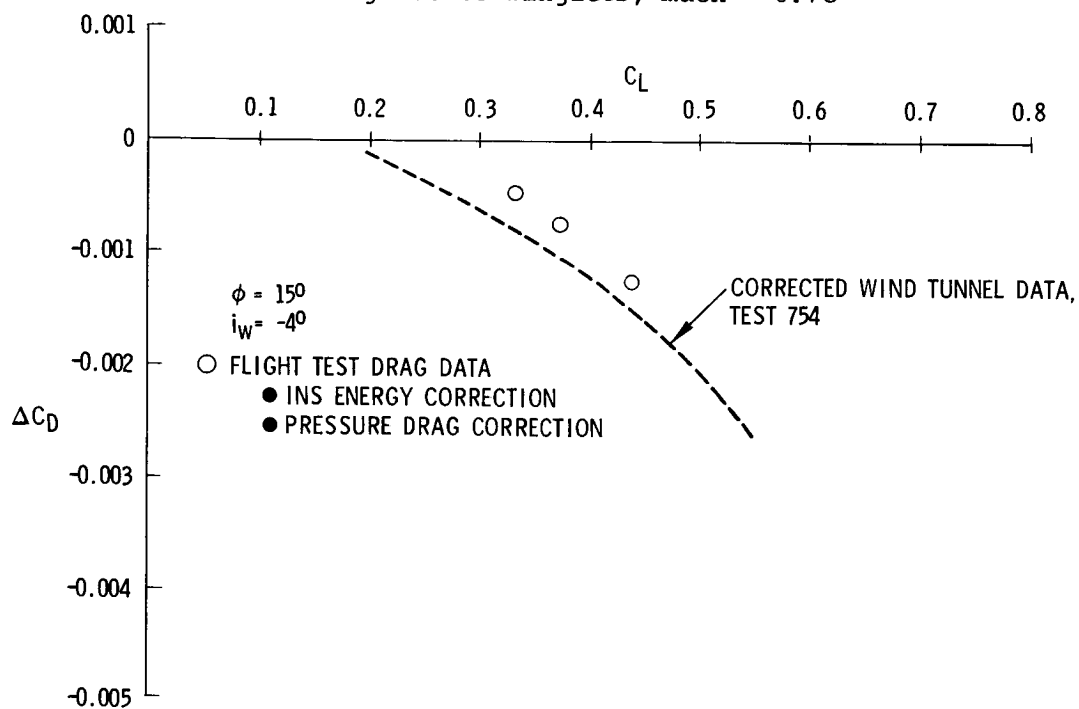


Figure 24. - Comparison of flight measured and wind tunnel predicted incremental drag due to winglets, mach = 0.82

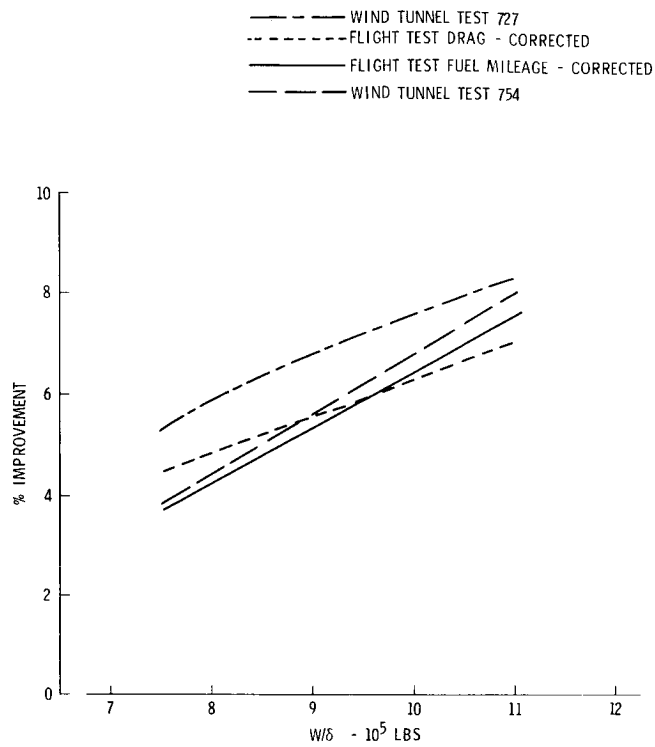


Figure 25. - KC-135A winglet flight test cruise mileage improvement, mach = 0.78

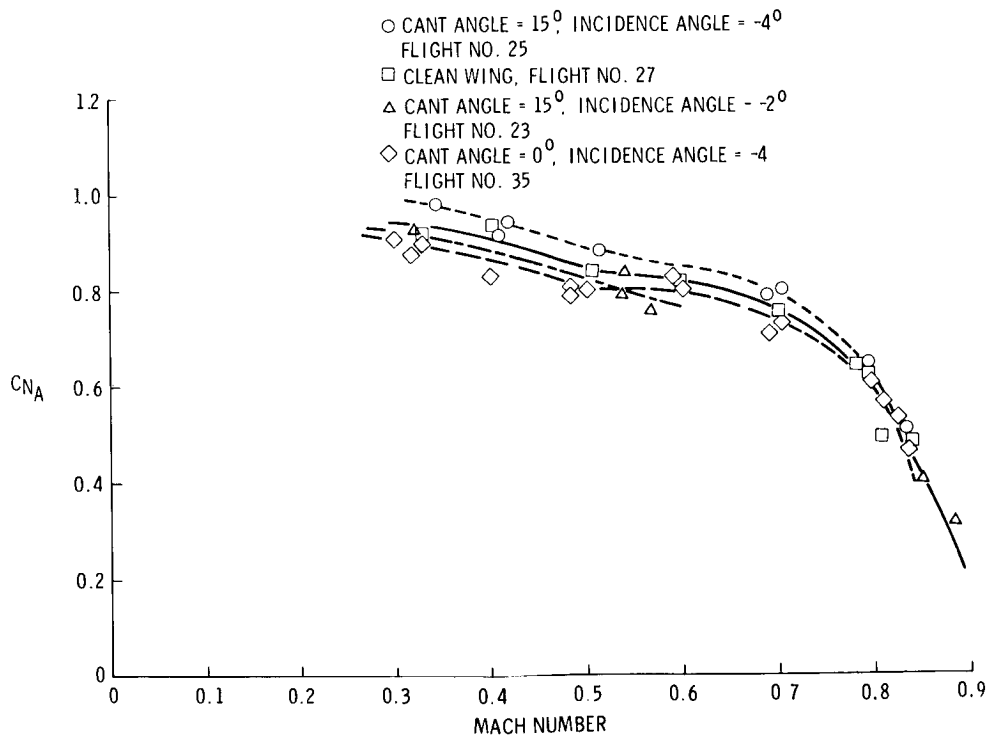


Figure 26. - KC-135 buffet boundaries



## KC-135A WINGLET FLIGHT FLUTTER PROGRAM

Michael W. Kehoe  
NASA Dryden Flight Research Center

### SUMMARY

This paper discusses the evaluation techniques, results and conclusions for the flight flutter testing conducted on a KC-135A airplane configured with and without winglets. Test results are presented for the critical symmetric and antisymmetric modes for a fuel distribution that consisted of 10,000 pounds in each wing main tank and empty reserve tanks. The results indicated that a lightly damped oscillation was experienced for a winglet configuration of  $0^\circ$  cant and  $-4^\circ$  incidence. The effects of cant and incidence angle variation on the critical modes are also discussed. Lightly damped oscillations were not encountered for any other winglet cant and incidence angles tested.

### INTRODUCTION

A KC-135A aircraft was modified with winglets for use in a flight research and demonstration program to evaluate the effects of winglets on the performance of the airplane. Due to the addition of the winglet and the structural modifications necessary for the attachment to the wing, flight flutter testing of the airplane was required. The methods used to clear the KC-135A with winglets for flutter were:

1. A low speed wind tunnel flutter model test (reference 1).
2. A ground vibration test (GVT) of a cantilevered outer wing panel with the winglet attached (reference 2).
3. A predictive flutter analysis (reference 3).
4. A flight flutter test (reference 4).

The concept used for this program was to compare flight test data for the airplane with winglets off (baseline) versus winglets on to determine the effects of winglets on the basic airplane. The winglets on data were comprised of data for different winglet cant and incident angle configurations.

The objectives of the program were:

1. To provide a flutter clearance for the KC-135A winglet airplane to allow performance and loads testing on the baseline and selected winglet configurations.
2. To obtain frequency and damping information for critical structural modes of vibration.

## ABBREVIATIONS

ALT	Altitude
CONF	Configuration
F	Frequency
$\bar{g}$	Damping Coefficient
G	Modal Damping same as $\bar{g}$
GVT	Ground Vibration Test
KCAS	Knots Calibrated Airspeed
KEAS	Knots Equivalent Airspeed
LE	Leading Edge
L/H	Left Hand
R/H	Right Hand
S/N	Serial Number
TE	Trailing Edge
$V_D$	Limit Dive Speed

## WINGLET AND FUEL CONFIGURATIONS TESTED

Flutter testing of the KC-135A winglet airplane was originally planned to be accomplished at an altitude of 21,500 feet for the winglet off (baseline) configuration and for the following winglet cant and incidence configurations:

- 15° cant/-2° incidence.
- 15° cant/-6° incidence.
- 0° cant/-2° incidence.
- 0° cant/-6° incidence.
- USAF selected optimum (later determined to be 15° cant/-4° incidence).

The USAF selected optimum winglet configuration was also to be tested at an altitude of 35,000 feet. Flight testing these configurations would clear all other winglet configurations for flutter.

The flutter speed was dependent on the airplane fuel distribution. The lowest flutter speed for the critical symmetric mode was predicted by analysis and exhibited in the wind tunnel to occur when the wing fuel tanks were nearly empty (light wing fuel loading). The critical antisymmetric mode was predicted to yield the lowest flutter speed with the wing tanks full (heavy wing fuel loading). In order to verify wind tunnel test data and the predictive flutter

analysis, the first winglet configuration ( $15^\circ$  cant/ $-2^\circ$  incidence) was to be tested with the first five different fuel configurations presented in table 1.

Due to program constraints fuel configuration 2 was eliminated. The locations of the fuel tanks in the airplane are illustrated in figure 1. The winglet off and all other winglet on configurations were to be flight tested in the heavy and light wing fuel configurations. For the flight test program, fuel configurations 5 and 6 were the light and heavy wing loading, respectively.

The test data for the  $15^\circ$  cant/ $-2^\circ$  incidence winglet configuration indicated that the lowest damping exhibited for the antisymmetric mode was with fuel configuration 4. The lowest damped symmetric mode was exhibited with fuel configuration 5 but there was not a significant change in damping trend or level between configurations 4 and 5. The antisymmetric mode appeared to be the most critical so it was decided to test all other winglet configurations with fuel configurations 4 and 6 instead of 5 and 6.

During the first flutter flight, significant skin wrinkling was noticed on the winglets. Due to uncertainty of the effect of the wrinkling on the performance of the winglets, program engineers chose to deviate from the flight test plan and to test the  $15^\circ$  cant/ $-4^\circ$  incidence winglet configuration next. It was at this configuration that the majority of wind tunnel pressure distribution data had been acquired. Subsequently, a decision was made not to test all four corners of the winglet configuration matrix (figure 2) for flutter, but to limit the remaining configurations to those specifically needed to be cleared for performance testing.

#### ENVELOPE EXPANSION

Flutter testing was accomplished at an altitude of 21,500 feet. A maximum Mach number of 0.91 and airspeed of 395 knots equivalent airspeed (KEAS) were attainable at this altitude. Each flutter flight consisted of a constant altitude, incremental airspeed flight envelope expansion. Aircraft dives were required for test points above 390 knots calibrated airspeed (KCAS). The incremental airspeed test points are illustrated in figure 3. The yaw damper was off and the rudder boost power was on for all these test points.

Test points at 300, 350 and 390 KCAS were repeated with the autopilot turned on to evaluate the effect of the autopilot on the flutter characteristics of the airplane.

#### INSTRUMENTATION

Flutter instrumentation onboard the airplane consisted of accelerometers and control surface position indicators as listed in table 2. Locations of the instrumentation on the airplane are shown in figure 4. The airspeed and altitude were measured from a nose boom installed on the test airplane.

## EXCITATION

The structure was excited at each test point by pilot induced control surface pulses. The excitation consisted of nose-up and nose-down elevator pulses, left and right rudder pulses and left and right aileron pulses for all straight and level test points. For test points that required dives, only a nose-up elevator pulse, a left rudder pulse and left aileron pulse were accomplished.

Random atmospheric turbulence was used to excite the structural modes of vibration which were not excited by control surface pulses. Typically, two minutes of random data were collected at the test points of interest.

## TEST RESULTS

Eight symmetric and five antisymmetric modes were tracked during the program for each winglet configuration tested. The velocity/frequency and velocity/damping plots for each winglet configuration tested are contained in reference 4.

Significant skin wrinkling was present on the winglets during all flights. The depth of the wrinkles appeared to increase with an increase in dynamic pressure. A review of pressure distributions and modal frequency data indicated that the winglet skin wrinkling did not have a significant effect on the flutter characteristics of the winglet.

The damping values calculated for autopilot-on test points were similar to data calculated for autopilot-off test points. The autopilot-on data did not reveal any significant changes in structural damping for all winglet configurations tested.

The winglet structural modes were monitored during data analysis. The pilot induced pulses did not excite the winglet modes because of the low frequency content of the pulses. Random data were acquired at selected test points to analyze the winglets modes. The damping levels of the winglet were satisfactory from a flutter standpoint.

## SUMMARY OF TEST RESULTS FOR ELEVATOR EXCITATION

The critical mode excited by elevator pulses was approximately 4.5 Hz. The flight test data indicated the 4.5 Hz mode consistently exhibited a flat damping trend with damping values generally lower than other modes excited by elevator pulses. Flight test results also indicated the damping to be the lowest for this mode in fuel configuration 5 (2,500 pounds in each wing main tank, reserve tanks empty). The response of this mode was most clearly indicated by the wing tip longitudinal accelerometer.

Predictive flutter analysis indicated that a 4.6 Hz symmetric mode exhibited the lowest flutter speed for a fuel configuration which included empty body and center wing tanks, empty outboard main and reserve tanks, and inboard main tanks 46 percent full. The analysis predicted a 35 percent

margin of safety. Wind tunnel testing indicated the frequency of the critical symmetric mode to be 4.5 to 4.8 Hz for the same fuel configuration.

A comparison of the frequency and damping trends between the baseline and winglets on configurations is presented in figures 5 and 6 for the 4.5 Hz mode. The fuel loading was configuration 4. The data points were faired so that the general data trends can be followed. The baseline frequency (4.9 Hz) was greater than the frequencies for the winglets on configurations ( $\approx 4.5$  Hz).

The comparison of the cant angle variation results (figure 5) yielded:

1. The baseline configuration exhibited the highest damping values.
2. As the cant angle was decreased from  $15^\circ$  to  $0^\circ$ , the damping increased.
3. The damping trends were fairly flat.
4. The winglets on frequency trends exhibited a small increase in frequency as airspeed was increased.

The comparison of the incidence angle variation (figure 6) results yielded:

1. The baseline configuration exhibited the highest damping values.
2. As the incidence angle was increased from  $-2^\circ$  to  $-4^\circ$ , the damping decreased.
3. The damping trends were fairly flat.
4. The winglets on frequency trends revealed a small increase in frequency as airspeed was increased.

#### SUMMARY OF TEST RESULTS FOR AILERON AND RUDDER EXCITATION

The critical mode excited by aileron and rudder pulses was a 3.0 Hz anti-symmetric mode. A damping of  $\bar{g} = 0.015$  was obtained for this mode at 370 KEAS with fuel configuration 4 (10,000 pounds in each wing main tank, empty reserves) for the  $0^\circ$  cant/ $-4^\circ$  incidence winglet configuration. Wind tunnel test data indicated that a 2.8 Hz mode was the critical antisymmetric mode. However, the critical wind tunnel fuel configuration was with wing main and reserve fuel tanks full.

A 4.3 Hz antisymmetric mode was analytically predicted to have the lowest flutter speed. The fuel configuration in the analysis was:

<u>Tank</u>	<u>Percent Full</u>
Forward Body	90.2
Center Wing	47.3
Aft Body	100
Upper Deck	42.8
Wing Inboard Main	100
Wing Outboard Main	100
Reserve	100

The predicted flutter speed margin of safety for this antisymmetric mode was greater than the margin for the critical symmetric mode (4.6 Hz).

A comparison of the frequency and damping trends between the baseline and winglets on configurations is presented in figures 7 and 8 for the 3.0 Hz mode. The fuel loading was configuration 4. The frequency of the baseline configuration was lower than the frequency of the winglets on configurations in spite of the increased wing tip mass. The difference is most likely due to the aerodynamic effects of the winglets on the wing structure.

A comparison of the cant angle variation results (figure 7) yielded:

1. At airspeeds below 330 KEAS, the damping level was about equal for the baseline and winglets on configurations.
2. At airspeeds above 330 KEAS, the baseline configuration had the highest level of damping.
3. At airspeeds above 360 KEAS, the damping decreased as the cant angle decreased from 15° to 0°. Testing was terminated at 370 KEAS for the 0° cant configuration.
4. The baseline and the 15° cant configuration frequency trends exhibited an increase in frequency as the airspeed was increased above 340 KEAS.
5. The 0° cant configuration exhibited a fairly flat frequency trend.

A comparison of the incidence angle variation (figure 8) revealed:

1. At airspeeds above 360 KEAS, the baseline configuration exhibited the highest damping.
2. The -2° and -4° incidence angle data exhibited similar damping trends.
3. At airspeeds above 340 KEAS, the frequency trends for the baseline and winglets on configurations increased in frequency as airspeed was increased.

Testing was terminated at 370 KEAS with fuel configuration 4 due to a lightly damped 3.0 Hz antisymmetric oscillation in the 0° cant/-4° incidence winglet configuration. The damping exhibited at termination was  $\bar{g} = 0.015$ . The 3.0 Hz mode was best excited by aileron pulses. The time history traces of several accelerometers responding to an aileron pulse at 370 KEAS are presented in figure 9. The inflight mode shape of this 3.0 Hz oscillation is presented in table 3. The frequency and damping trends for a 2.6 Hz mode and 3.0 Hz mode are presented in figure 10. The data exhibited a constant increase in frequency for the 2.6 Hz mode while the 3.0 Hz mode frequency trend remained flat. Both modes exhibited wing bending and wing torsion at all airspeeds. It appeared that the coalescence of these two modes was the cause of the oscillation for this flight configuration. The coalescence of the 2.6 Hz and 3.0 Hz modes did not occur in other winglet configurations that were flight flutter tested. The damping trends for both modes exhibit a constant decrease in damping starting at 330 KEAS. The modes could no longer be separated at airspeeds above 355 KEAS. There were no adverse damping trends exhibited for the 0° cant/-4° incidence winglet configuration with fuel configuration 6. Testing was terminated at 382 KEAS due to the onset of Mach buffet. It was thought that keeping the airplane out of buffet would help reduce the number of fuel leaks

that were occurring in the airplane. There was no indication from the flutter data obtained that the testing could not have continued to 395 KEAS.

#### CORRELATION WITH ANALYSIS

A comparison of flight test data with analysis for the 3.0 Hz antisymmetric mode is presented in figure 11. The winglet configuration was 0° cant/-4° incidence. The fuel loading was fuel configuration 4. This analysis (figure 11) was accomplished after the flight test data was obtained. The exact fuel distribution was incorporated in the analysis. The flight test damping exhibited a steep slope toward zero damping around 500 knots true airspeed (KTAS). The analysis does not predict a flutter speed with either 0.85 or 0.95 Mach number aerodynamics. There is no explanation at this time for the lack of correlation between the flight test data and the analysis.

#### CONCLUDING REMARKS

Flight flutter testing was accomplished for the KC-135A winglet airplane in the baseline (modified wing tips - no winglets) configuration to a maximum airspeed of 397 KEAS at an altitude of 21,500 feet with the wing main and reserve tanks full of fuel. The aircraft was also tested to a maximum airspeed of 395 KEAS at an altitude of 21,500 feet with 10,000 pounds of fuel in each wing main tank and reserve tanks empty. The results showed satisfactory damping and damping trends for all structural modes.

Flutter testing was also accomplished for the KC-135A winglet airplane configured in the following conditions:

Cant (degrees)	Incidence (degrees)	Maximum Airspeed (KEAS) Tested	Fuel
15	-2	393	Wing Main Tanks Full, Reserve Tanks Full, Minimum Body Fuel
15	-2	399	10,000 lbs in Main Tanks 1,300 lbs in Reserve Tanks
15	-2	392	10,000 lbs in Main Tanks Empty Reserve Tanks
15	-2	399	2,500 lbs in Main Tanks Empty Reserve Tanks
15	-4	398	Wing Main Tanks Full Reserve Tanks Full
15	-4	395	10,000 lbs in Main Tanks Empty Reserve Tanks
0	-4	370	10,000 lbs in Main Tanks Empty Reserve Tanks
0	-4	382	Wing Main Tanks Full Reserve Tanks Full

The results revealed satisfactory damping for all winglet configurations tested except the  $0^\circ$  cant/ $-4^\circ$  incidence configuration. Testing was terminated in this winglet configuration at 370 KEAS at an altitude of 21,500 feet due to a lightly damped ( $\bar{g} = 0.015$ ), 3.0 Hz antisymmetric oscillation. The fuel distribution at this condition was 10,000 pounds in each wing main tank and empty wing reserve tanks.

As the cant angle was decreased from  $15^\circ$  to  $0^\circ$ , the damping of the critical symmetric mode increased. As the incidence angle was increased from  $-2^\circ$  to  $-4^\circ$ , the damping decreased. The critical symmetric mode exhibited the highest damping in the baseline configuration.

The critical antisymmetric mode exhibited the highest damping in the baseline configuration. At airspeeds above 330 KEAS, the damping level decreased with winglets installed on the airplane regardless of cant or incidence angle configuration. The  $-2^\circ$  and  $-4^\circ$  incidence angle data exhibited similar damping trends. At airspeeds above 360 KEAS, the damping decreased as the cant angle decreased from  $15^\circ$  to  $0^\circ$ .

#### REFERENCES

1. Schneider, F. C., and Shoup, G. S.: "KC-135A Winglet Flutter Model Test," Boeing Document D3-11353-1, Boeing Wichita Company, Wichita, Kansas, May 5, 1978.
2. Shoup, G. S.: "KC-135 Winglet Ground Vibration Test Report," Boeing Document D3-11591-1, Boeing Wichita Company, Wichita, Kansas, June 12, 1979.
3. French, H. S., and Shoup, G. S.: "KC-135 Winglet Flutter Analysis and Test," Boeing Document D3-11437-1, Boeing Wichita Company, Wichita, Kansas, January 5, 1979.
4. Kehoe, M. W.: "KC-135A Winglet Flight Flutter Test Program," AFFTC-TR-81-4, Air Force Flight Test Center, Edwards Air Force Base, California, June 1981.



TABLE 1. - PLANNED TEST FUEL CONFIGURATIONS

Fuel Configuration Number	Center Wing and Body Fuel	Wing Fuel - Pounds Per Tank	
		Main Tanks	Reserves
1	Note 1	Full	Full
2	Note 3	Full	Full
3	Note 2	10,000	1,300
4	Note 2	10,000	0
5	Note 2	2,500	0
6	Note 2	Full	Full

## Notes

1. As required to complete condition with minimum body fuel.
2. As required to accomplish testing.
3. As required to maintain a gross weight above 230,000 pounds at end of test condition.

TABLE 2. - AIRCRAFT FLUTTER INSTRUMENTATION

Item No.	Parameter Identification
1	R/H Wing Tip LE Normal Acceleration
2	R/H Wing Tip TE Normal Acceleration
3	R/H Wing Tip LE Longitudinal Acceleration
4	R/H Winglet LE Normal Acceleration
5	R/H Winglet TE Normal Acceleration
6	R/H Winglet LE Longitudinal Acceleration
7	L/H Wing Tip LE Normal Acceleration
8	L/H Winglet LE Normal Acceleration
9	L/H Winglet LE Longitudinal Acceleration
10	R/H Otbd Nacelle Normal Acceleration
11	R/H Otbd Nacelle Lateral Acceleration
12	Aft Body Normal Acceleration
13	Aft Body Lateral Acceleration
14	R/H Horizontal Stabilizer Acceleration
15	Vertical Fin Lateral Acceleration
16	L/H Inbd Aileron Position
17	R/H Inbd Aileron Position
18	L/H Otbd Aileron Position
19	R/H Otbd Aileron Position
20	L/H Elevator Position
21	R/H Elevator Position
22	Rudder Position
23	Lower Wing Skin Panel Acceleration

See Figure 4 for locations

TABLE 3. - 3.0 Hz LIGHTLY DAMPED OSCILLATION MODE SHAPE  
Reference: R/H Fwd Wing Tip Normal Accelerometer  
Flight Conditions: 370 KEAS, 21,500 ft.,  
Fuel Configuration 4

Accelerometer	Phase (Degrees)	Direction of Motion	Normalized Amplitude
R/H Fwd Wingtip Normal	---	Up	1.0
R/H Rear Wingtip Normal	0	Up	1.16
R/H Wingtip Longitudinal	180	Rear	0.29
R/H Fwd Winglet Normal	0	Inboard	0.29
R/H Winglet Longitudinal	0	Fwd (R/H Wing LE Down)	1.19
L/H Fwd Wingtip Normal	180	Outboard	0.19
Aft Body Lateral	0	Right	0.16
Vertical Fin Lateral	0	Right	0.48
R/H Horizontal Stabilizer	180	Down	0.5

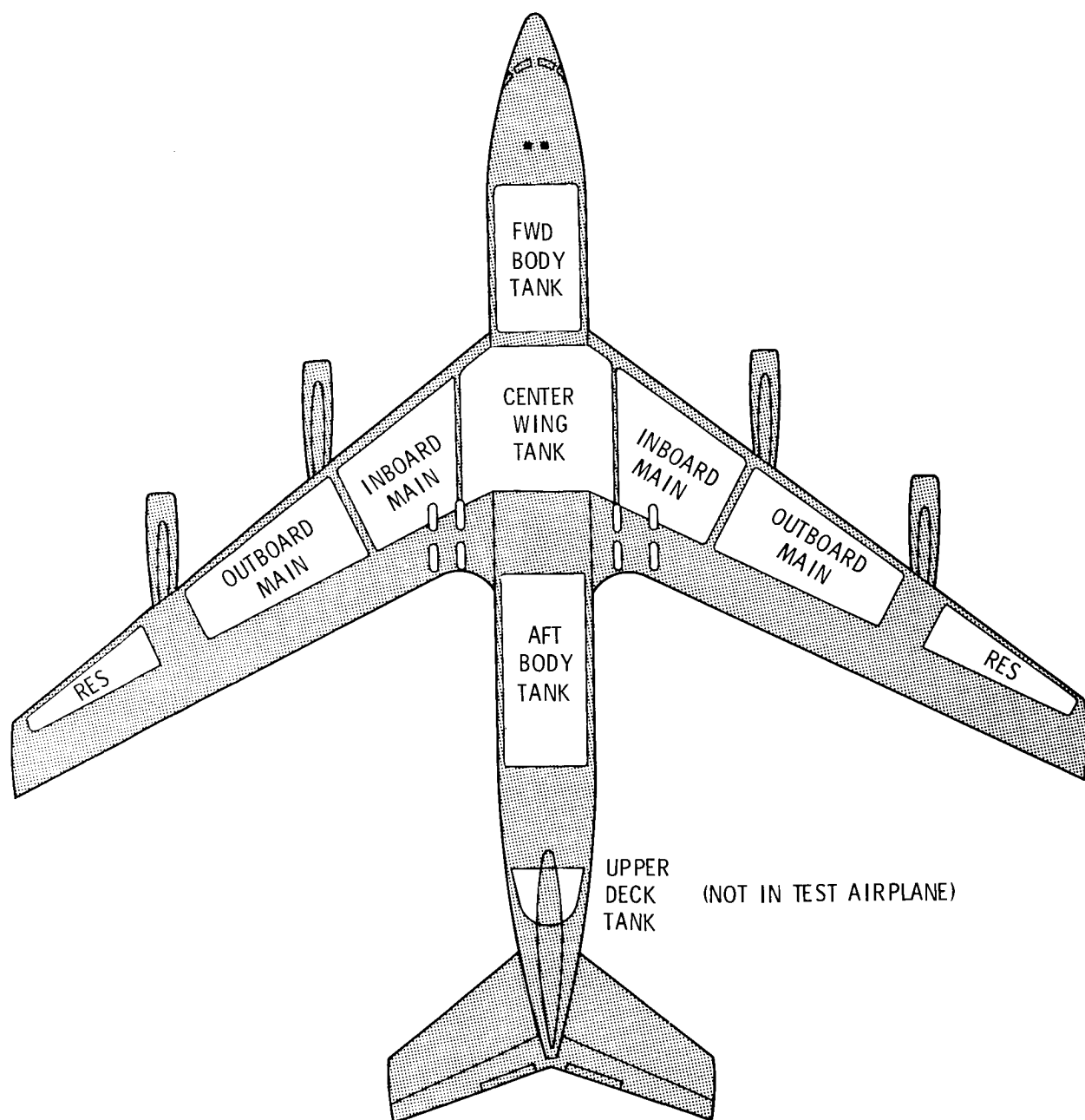


Figure 1. - Airplane fuel tank locations

ORIGINAL PLAN				
WINGLET CANT ANGLE				
		0	7.5	15
W I N G L E T  I N C I D E N C E	-2	FUEL CONF. 5 FUEL CONF. 6		FUEL CONF. 1 FUEL CONF. 2 FUEL CONF. 3 FUEL CONF. 4 FUEL CONF. 5
	-4			
	-6	FUEL CONF. 5 FUEL CONF. 6		FUEL CONF. 5 FUEL CONF. 6

FLIGHT TESTED				
WINGLET CANT ANGLE				
		0	7.5	15
W I N G L E T  I N C I D E N C E	-2			FUEL CONF. 1 FUEL CONF. 3 FUEL CONF. 4 FUEL CONF. 5
	-4	FUEL CONF. 4 FUEL CONF. 6		FUEL CONF. 4 FUEL CONF. 6
	-6			

Figure 2. - Winglet configuration matrix

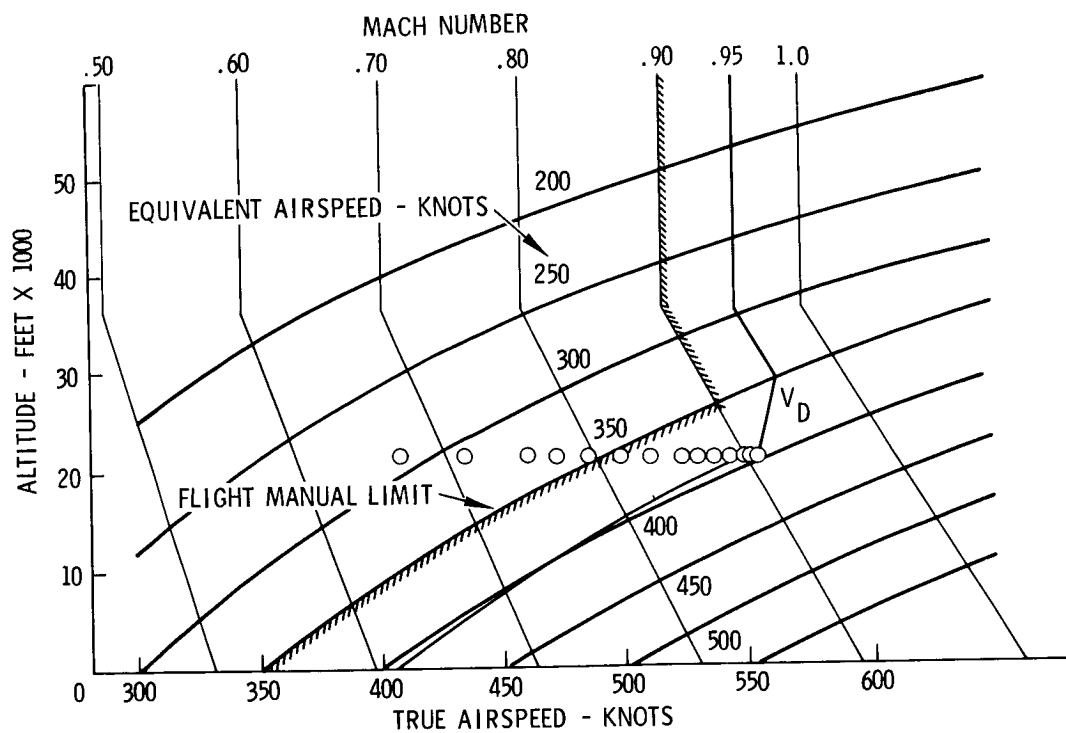


Figure 3. - Flight test envelope

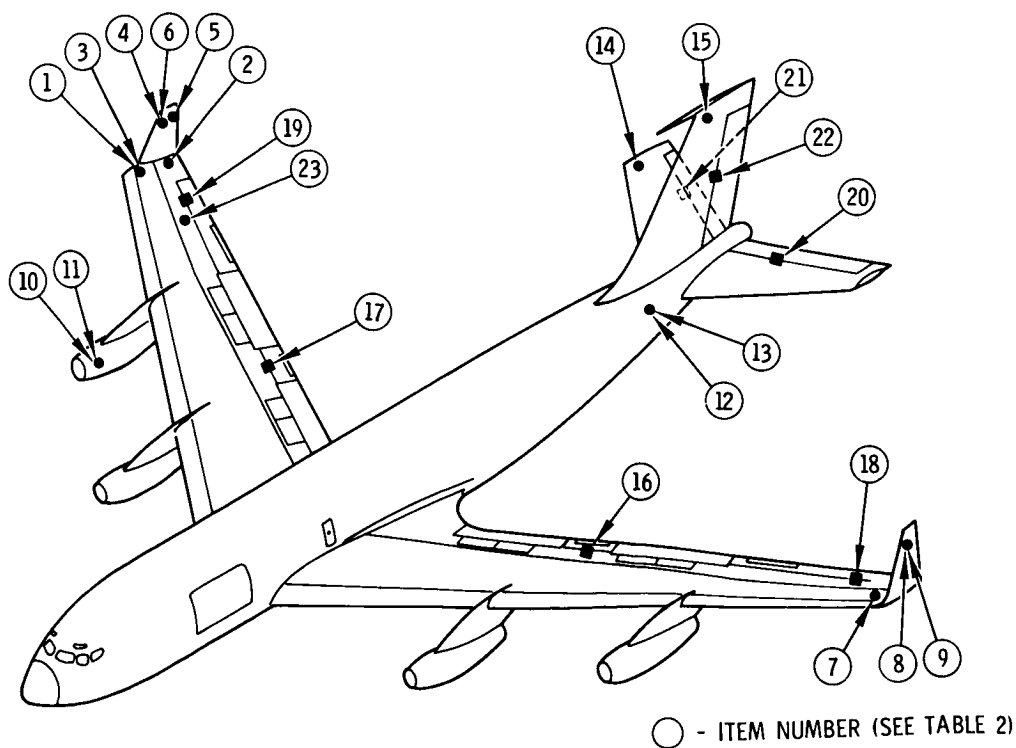


Figure 4. - Airplane instrumentation locations

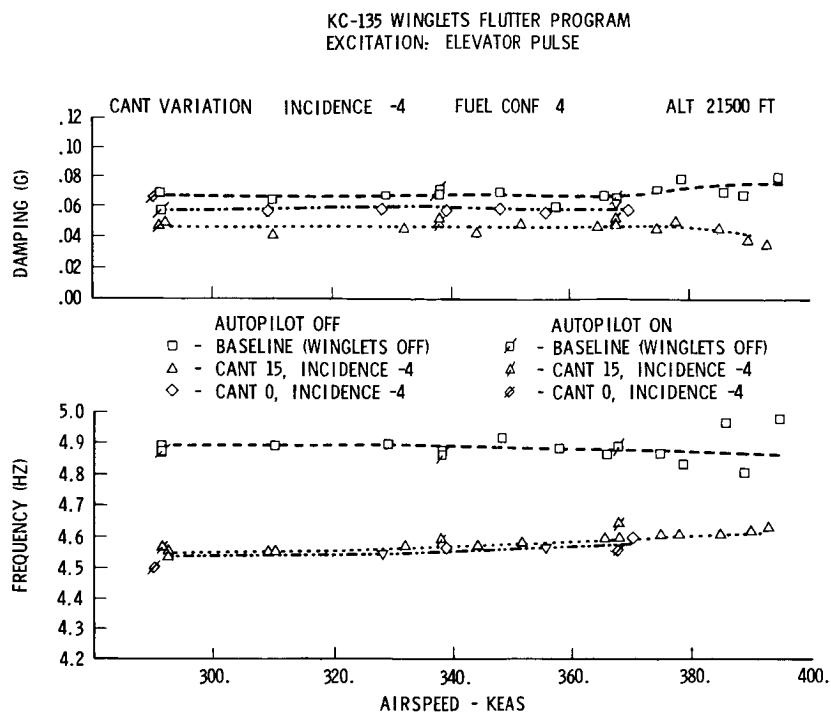


Figure 5. - Cant angle variation for elevator excitation

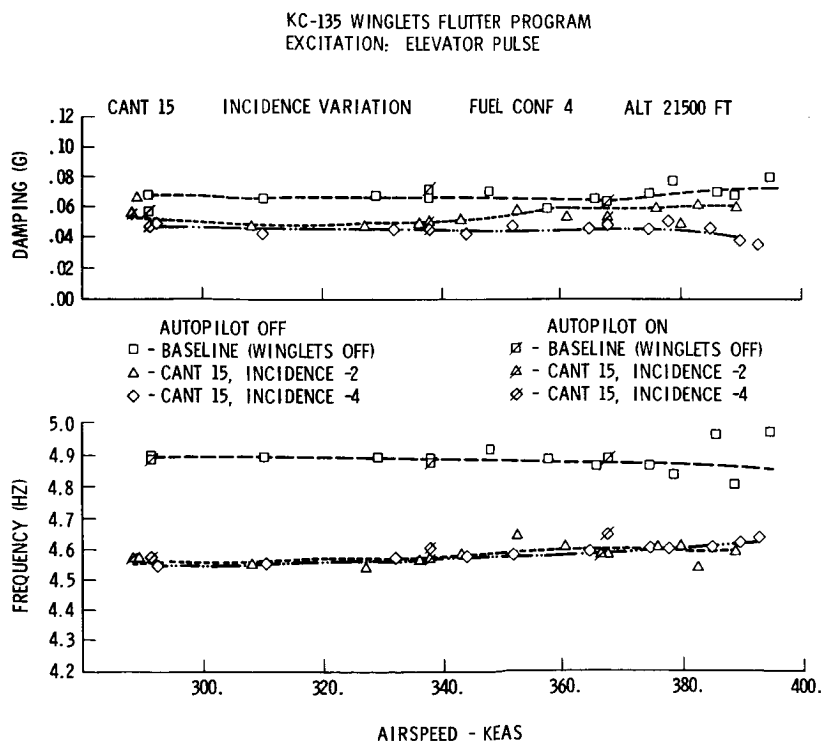


Figure 5. - Incidence angle variation for elevator excitation

KC-135 WINGLETS FLUTTER PROGRAM  
EXCITATION: AILERON AND RUDDER PULSE

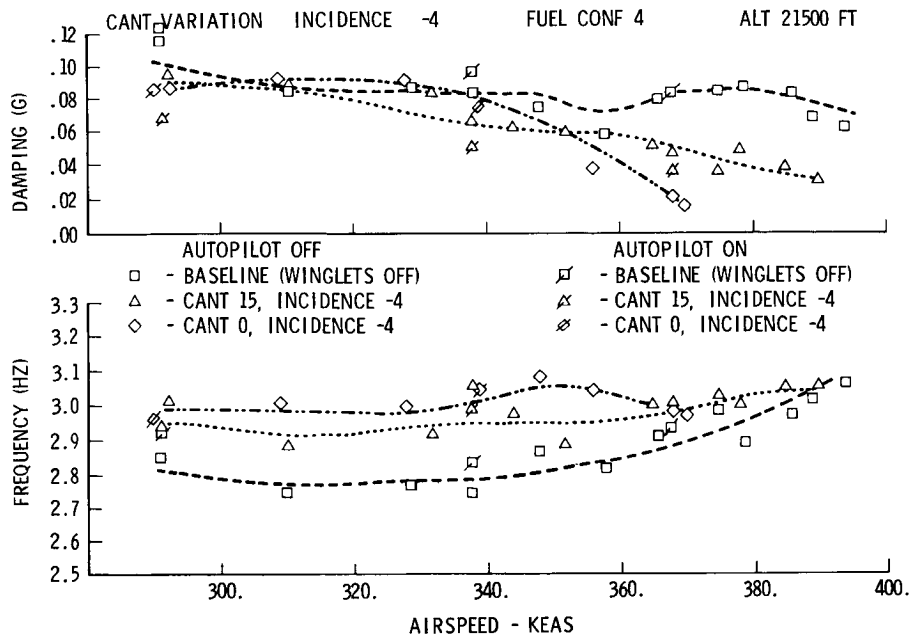


Figure 7. - Cant angle variation for aileron and rudder excitation

KC-135 WINGLETS FLUTTER PROGRAM  
EXCITATION: AILERON AND RUDDER PULSE

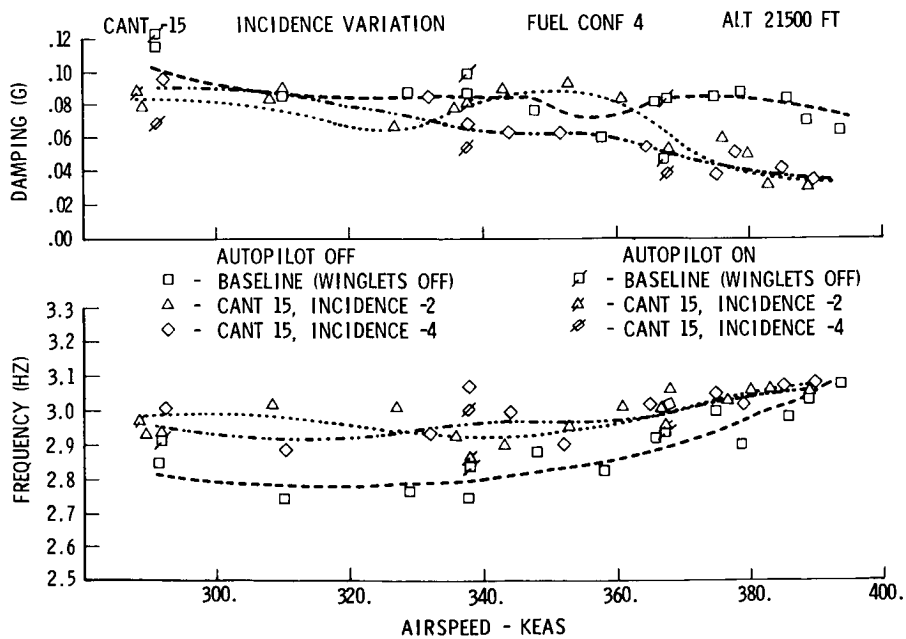


Figure 8. - Incidence angle variation for aileron and rudder excitation



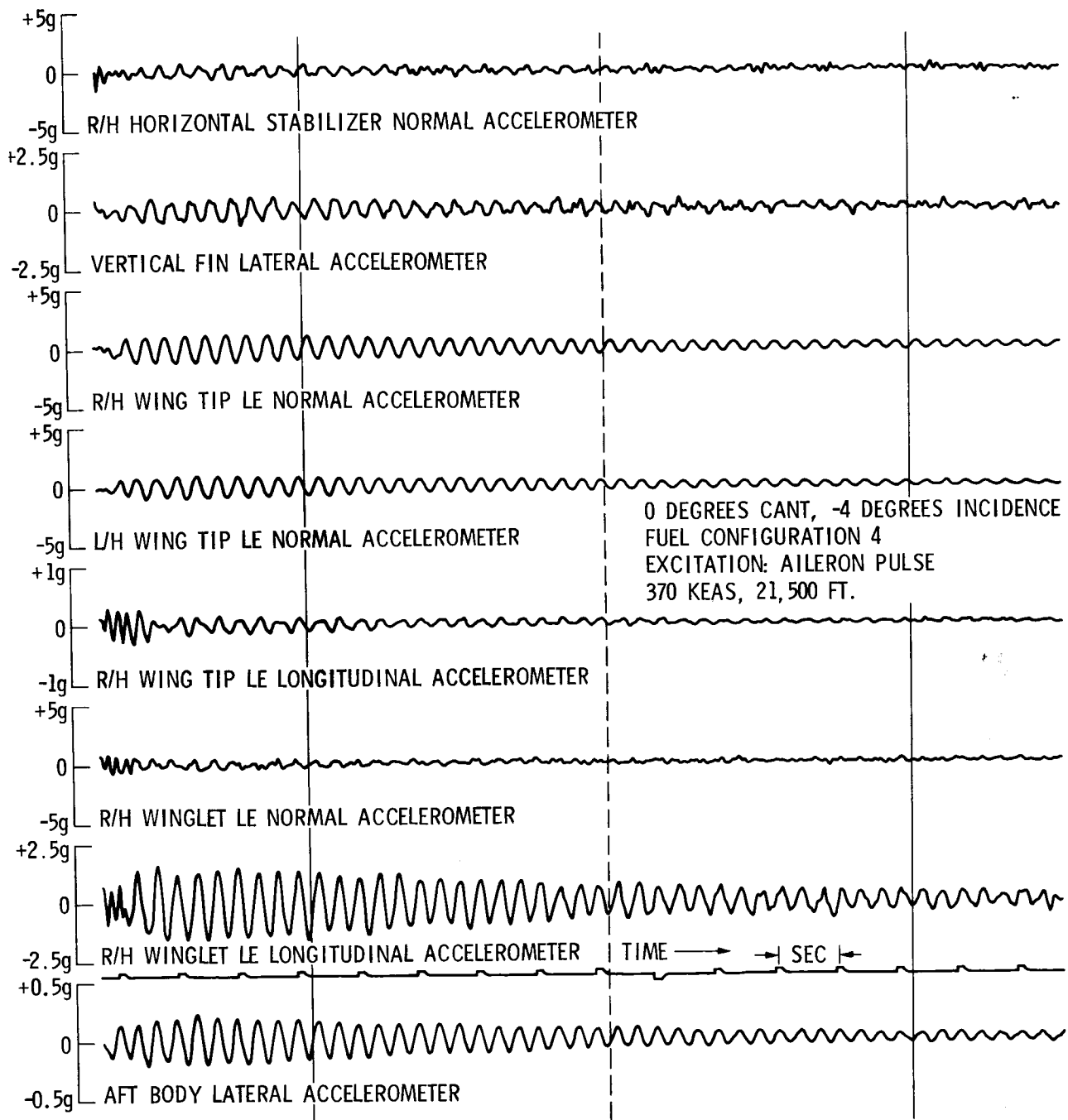


Figure 9. - Time history of 3.0 Hz antisymmetric oscillation

KC-135 WINGLETS FLUTTER PROGRAM  
EXCITATION: AILERON AND RUDDER PULSE

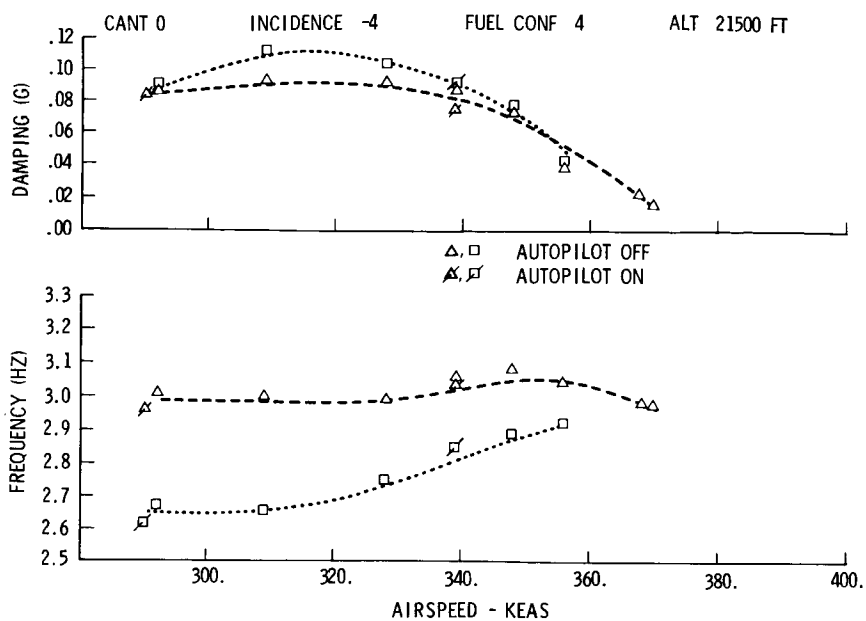


Figure 10. - Frequency and damping versus airspeed

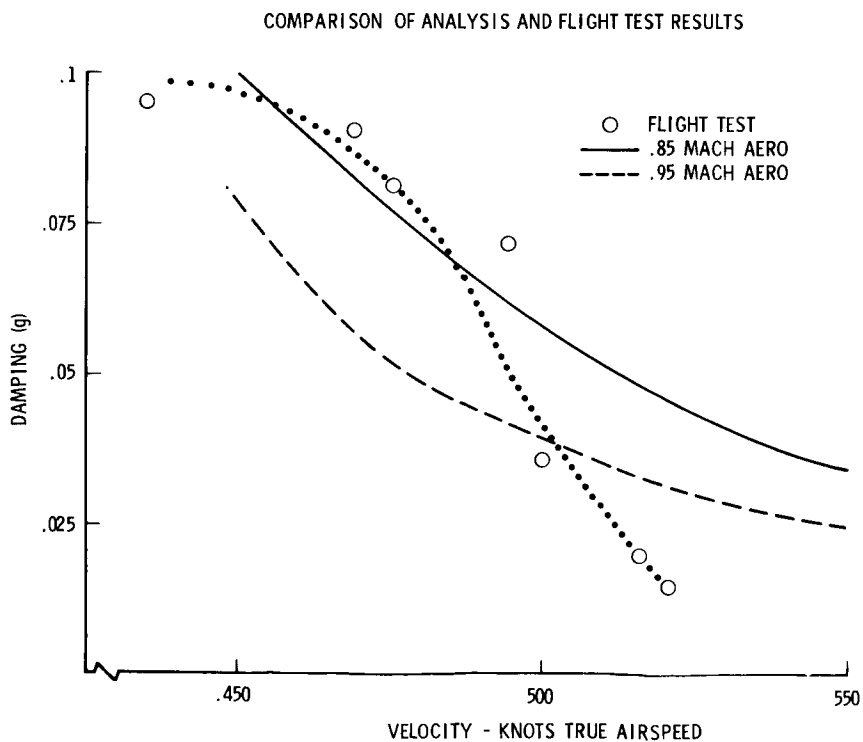


Figure 11. - Comparison of analysis and flight test results

1. Report No. NASA CP-2211		2. Government Accession No.		3. Recipient's Catalog No.	
4. Title and Subtitle  KC-135 WINGLET PROGRAM REVIEW				5. Report Date January 1982	
				6. Performing Organization Code 534-02-14	
7. Author(s)				8. Performing Organization Report No. H-1165	
				10. Work Unit No.	
9. Performing Organization Name and Address Ames Research Center Dryden Flight Research Facility P.O. Box 273 Edwards, CA 93523				11. Contract or Grant No.	
				13. Type of Report and Period Covered Conference Publication	
12. Sponsoring Agency Name and Address National Aeronautics and Space Administration Washington, D.C. 20546				14. Sponsoring Agency Code	
15. Supplementary Notes					
16. Abstract					
<p>A review of the results of a joint NASA/USAF program to develop and flight test winglets on a KC-135 aircraft was held at the Dryden Flight Research Center on September 16, 1981. This publication is a compilation of the results presented. The winglet development from concept through wind tunnel and flight tests is discussed. Predicted, wind tunnel, and flight test results are compared for the performance loads and flutter characteristics of the winglets. The flight test winglets had a variable winglet cant and incidence angle capability which enabled a limited evaluation of the effects of these geometry changes.</p>					
17. Key Words (Suggested by Author(s)) Winglets KC-135 aircraft Aerodynamics Loads Flutter Fuel mileage				18. Distribution Statement  FEDD distribution  Subject category 02	
19. Security Classif. (of this report) Unclassified		20. Security Classif. (of this page) Unclassified		21. No. of Pages 192	
				22. Price	

Available: NASA's Industrial Applications Centers